NASA CR-66125

BOEING

[redacted]

Distribution of this report is provided in the interest of information exchange. Responsibility for the contents resides in the author or organization that prepared it.

AIRPLANE DIVISION

REV LTR

THE BOEING COMPANY

AIRPLANE DIVISION
P.O. BOX 707
RENTON, WASHINGTON 98055

CODE IDENT. NO. 81205

NUMBER D6-10743

TITLE: SIMULATION OF THREE SUPERSONIC TRANSPORT CONFIGURATIONS WITH THE BOEING 367-80 IN-FLIGHT DYNAMIC SIMULATION AIRPLANE

FOR LIMITATIONS IMPOSED ON THE USE OF THE INFORMATION CONTAINED IN THIS DOCUMENT AND ON THE DISTRIBUTION OF THIS DOCUMENT, SEE LIMITATIONS SHEET.

Submitted in partial fulfillment of NASA

MODEL ______ CONTRACT NASI-4096

ISSUE NO. ______ ISSUED TO: ______

PREPARED BY William Eldridge
W. M. Eldridge

PREPARED BY
P. M. Condit

PREPARED BY
R. C. Schwanz

PREPARED BY C. R. Taylor
C. R. Taylor

SUPERVISED BY H. C. Higgins
H. C. Higgins

APPROVED BY J. K. Wimpress 12/29/65
J. K. Wimpress

APPROVED BY ______ (DATE)

THE BOEING COMPANY

ACTIVE SHEET RECORD

		ADDED SHEETS						ADDED SHEETS			
SHEET NUMBER	REV LTR	SHEET NUMBER	REV LTR	SHEET NUMBER	REV LTR	SHEET NUMBER	REV LTR	SHEET NUMBER	REV LTR	SHEET NUMBER	REV LTR
Title Page						43					
i	B					44					
ii	B					45					
iii	B					46					
iv	B					47					
2						48					
3						49	A				
4		4a				50	B				
5						51	B				
6						52	A				
7						53	A				
8						54	A				
9						55					
10						56					
11						57					
12						58					
13						59					
14						60					
15						61					
16						62					
17						63					
18						64					
19						65					
20						66					
21						67					
22						68					
23						69					
24						70	A				
25						71	B				
26						72	B				
27						73	A				
28						74	A				
29						75	A				
30						76					
31						77					
32						78					
33						79					
34						80					
35						81					
36						82					
37						83					
38						84					
39						85					
40	A					86					
41						87					
42						88					

LIST OF ACTIVE PAGES

SECTION	PAGE NUMBER	REV SYM	ADDED PAGES: PAGE NUMBER	REV SYM	PAGE NUMBER	REV SYM	PAGE NUMBER	REV SYM
	89							
	90							
	91							
	92	A						
	93	A						
	94							
	95							
	96							
	97							
	98							
	99							
	100							
	101							
	102							
	103							
	104							
	105							
	106							
	107							
	108							
	109							
	110	B						
	111	B						
	112	A						
	113	A						
	114	A						
	115							
	116							
	117							
	118							
	119							
	120							
	121							
	122							
	123							
	124							
	125							
	126							
	127							
	128							
	129							
	130	C	133A	C				
	131	C	133B	C				
	133	C	134A	C				
	134	C	134B	C				

SECTION	PAGE NUMBER	REV SYM	ADDED PAGES: PAGE NUMBER	REV SYM	PAGE NUMBER	REV SYM	PAGE NUMBER	REV SYM
	135							
	136	C						
	137	C						
	138	C						
	139							
	140							
	141							
	142							
	143							
	144							
	145							
	146							
	147							
	148							
	149							
	150							
	151							
	152							
	153							
	154							
	155							
	156							
	157							
	158							
	159							
	160							
	161							
	162							
	163							
	164							
	165							
	166							
	167							
	168							
	169							
	170							
	171							
	172							
	173							
	174							
	175							
	176							
	177							
	178							
	179							
	180							

LIST OF ACTIVE PAGES

SECTION	PAGE NUMBER	REV SYM	ADDED PAGES PAGE NUMBER	REV SYM	PAGE NUMBER	REV SYM	PAGE NUMBER	REV SYM	SECTION	PAGE NUMBER	REV SYM	ADDED PAGES PAGE NUMBER	REV SYM	PAGE NUMBER	REV SYM	PAGE NUMBER	REV SYM
	181																
	182																
	183		183A	C													
	184																
	185																
	186		186A	C													
	187																
	188	A															
	189	B															
	190	B															
	191	B															
	192																
	193	B															
	194	B															
	195	A															
	196	A															
	197	B	197A	C													
	198																
	199																
	200																
	201																
	202																

R E V I S I O N S

REV SYM	DESCRIPTION	DATE	APPROVAL
A	Miscellaneous Pages	2/4/66	W. M. E.
B	Miscellaneous Pages	2/11/66	W. M. E.
C	Miscellaneous Pages	4/29/66	W. M. E.

TABLE OF CONTENTS

SUMMARY

Three supersonic transport configurations were evaluated with the Boeing 367-80 in-flight dynamic simulation airplane. Typical variable geometry and delta SST configurations in landing approach configuration were simulated and evaluated in detail. In addition a variable geometry airplane in an emergency wings back configuration (72° sweep) was briefly evaluated.

In this program the basic SST configurations were evaluated and systems of longitudinal and lateral-directional stability augmentation were developed and evaluated. (The 72° sweep was tested in the basic configuration only). The effect of center of gravity position was evaluated with and without longitudinal stability augmentation. Configurations with degraded lateral-directional stability were evaluated to anticipate the possible variations with SST configuration changes or inaccuracies in estimating the stability derivatives. The test configurations are summarized in the table on page 4A.

The 367-80 simulation is mechanized using the response feedback technique, in which the pilot's control inputs are modified by the simulation computer to match the dynamics of the simulated airplane control system. The 367-80 stability characteristics are modified by the computer which feeds back the measured motions of the 367-80 to the controls so that the 367-80 equations of motion match those of the theoretical SST configuration.

The initial flight check-out is performed by measuring the airplane response to pulse inputs of each of the controls. The 367-80 flight response is compared to the theoretical SST response, and if the response is not correct, the gains of the computer are re-adjusted in flight.

In addition to the control pulses, a number of maneuvers were performed by the evaluation pilots to document each configuration. These are listed below:

Manuever	To Document
Airspeed changes	Lift, Drag, Static Stability
Wind-up turn	Manuevering characteristics - stick force, deflection, and angle of attack per "g"
Cross-control sideslip	Lateral-Directional static stability and control
Step wheel input	Roll response and damping
Roll reversal	Lateral control power and sensitivity

The simulation documentation data are presented in this document. Overall, the quality and fiedlity of simulation was very good. Some difficulty was encountered in setting up test configurations which had low longitudinal static stability. This was caused by the small errors in calibrating the basic 367-80 characteristics and the pitching moment of the thrust reversers and speed brakes. These configurations required a lot of "cut and try" set-up time, but they were simulated well. There were also some problems in simulating the delta and 72° sweep configurations because of the high cross-product-of-inertia. A transformation was performed between stability and body axes which gave approximately correct stability and control response.

The documentation of the 367-80 aerodynamic characteristics for the test configurations flown is given in Appendix 1.

The theoretical SST configurations and supplementary test configurations are listed in Appendix 2. The theoretical calculation methods are also given for reference.

TEST CONFIGURATIONS

Airplane Configuration	Augmentation or Change	Page
Variable Geometry Basic (9.75% static margin)	Unaugmented	16
Augmented	Longitudinal - response augmentation $\delta E = \left[\frac{\delta E}{\delta_{col}}\right]_{BASIC} \times 2\,\delta_{col} + 1.46\,\dot{\theta}$ Lateral-Directional - yaw damper $\delta R = -1\,\dot{\beta}$	35
$(\dot{\theta} + \Delta\alpha)$ Longitudinal Augmentation	$\delta E = \left[\frac{\delta E}{\delta_{col}}\right]_{BASIC} \times 4\,\delta_{col} + 1.46\,\dot{\theta} + 1.5\,\Delta\alpha$	48
Aft C. G.	3% Static Margin	59
Aft C. G. $(\dot{\theta} + \Delta\alpha)$ Augmentation	Same augmentation as above	70
Degraded Lateral-Directional	$N_{\dot{\phi}} = -.1$ Dutch roll damping ratio = .05	80
Delta Basic (2.5% static margin)	Unaugmented	85
Augmented	Longitudinal - response augmentation $\delta E = \left[\frac{\delta E}{\delta_{col}}\right]_{BASIC} \times 4\,\delta_{col} + 1.46\,\dot{\theta} + 1\,\Delta\alpha$ Lateral-Directional - roll damper $\delta_{WH} = -.45\,\dot{\phi}$	108
Forward C. G.	7% static margin Unaugmented	119
Degraded Lateral-Directional	$N_{\dot{\phi}} = -.1$ Duth roll damping ratio = .05	126
Variable Geometry with wings aft	Unaugmented	130

REFERENCES

1. D6-6618 A Feasibility Study of Using the 707 Prototype Airplane for Evaluation of the Approach and Landing Characteristics of Supersonic Transports (Confidential).

2. D6-3590 Use of the 707 Prototype Aircraft for In-Flight Dynamic Simulation of Supersonic Transport Configurations.

3. D6-8574 A Program to Develop Slow Speed Flight for High Speed Jet Transports.

4. D6-6627 Aerodynamic Characteristics of the 367-80B Airplane Equipped with Boundary Layer Control Trailing Edge Flaps.

5. D6-10720 Stability and Control Characteristics of the 367-80 Airplane with BLC Flaps and Hydraulic Powered Controls.

6. D6-10719 A Simulator and Flight Test Program to Develop Low Speed Flight Controls for Swept-Wing Jet Transports.

7. D6-19856 Boeing 367-80 Variable Stability Simulation System.

LIST OF ILLUSTRATIONS

LIST OF SYMBOLS

α	angle-of-attack
β	sideslip angle
θ	pitch angle
ϕ	bank angle
ψ	yaw angle
V_e	equivalent air speed
V_t, V	true air speed
δcol	control column deflection
δwh	control wheel deflection
δp	rudder pedal deflection
δE, δe	elevator deflection
δSB	speed brake deflection
δR	rudder deflection
TH, T	engine thrust
δC	thrust modulator clamshell door angle
Δ_{FRL}	stabilizer trim angle
F_s	control column force
F_{wh}	control wheel force
F_p	rudder pedal force
C_L	lift coefficient
C_D	drag coefficient
C_M	pitching moment coefficient
C_ℓ	rolling moment coefficient
C_n	yawing moment coefficient
C_y	side force coefficient
C_u	BLC blowing coefficient

S	wing area
b	wing span
$\bar{C}$	mean aerodynamic chord
N_z	normal acceleration
g, n	load factor
F	axial force
τ	time constant
W_n	undamped natural frequency
ζ	damping ratio
ρ	air density

INTRODUCTION

The configurations of the supersonic transport (SST) presently proposed are different from any existing military or commercial airplanes. The SST will be a large gross weight, high inertia airplane. The yaw/roll inertia ratio will be very high compared to present large airplanes. Preliminary studies by NASA and Boeing indicated that the SST may encounter control problems because of its large size and new configurations. These studies showed that there was a need to conduct a comprehensive evaluation of SST flying qualities prior to prototype construction to evaluate the current SST configuration concepts as well as some degradations of the airplane characteristics that may develop in future designs.

Ground-based analog flight simulators are well suited to evaluating the problems of cruise and instrument flight. At the present time they are not completely satisfactory for evaluating the problems of low speed approach and landing because here the pilot relies on a complex combination of airplane motion and visual cues which cannot be simulated accurately. The simulator also lacks the psychological environment of danger that a pilot has in flight which forces him to perform the landing well. The best means of evaluating the problems of the SST low speed approach and landing is the in-flight dynamic simulator which gives the pilot a real flight experience with the airplane configuration under study.

Boeing conducted a feasibility study in 1963, under NASA contract, which indicated that the Boeing 367-80 airplane could be modified for in-flight dynamic simulation of the SST. The results of this study are given in reference 1 and 2. The airplane equipment for this simulation was designed and installed in the airplane in 1964-1965.

The 367-80, shown in Fig. 1, is the prototype of the C/KC-135 jet transport/tanker airplanes and the 707 series of airplanes. The 367-80 is entirely company owned and has been used as a development test bed for improved flap systems, autopilot devices, and other airplane equipment. At the present time, the 367-80 is equipped with a set of boundary layer control (BLC) flaps, installed during the high lift development program. These are large chord flaps with single pivot hinges and have high pressure engine bleed air blown over their upper surface through ejector nozzles. The wing leading edge has 727 type slats and Krueger flaps for maximum high lift development. A detailed description of the BLC flap system and the airplane aerodynamic characteristics are given in references 3 and 4.

The 367-80 is equipped with a complete hydraulic powered control system. This was installed because the original servo tab control system did not give adequate control response and resolution at the extreme low speeds possible with the BLC flaps. A comprehensive roll and yaw axis stability augmentation system was installed as a part of the powered control system design in order to provide good flying qualities at low speeds. The design characteristics of the 367-80 powered control system and the results of a low speed flight research program are given in references 5 and 6.

The 367-80 has been equipped with an up-to-date cockpit instrument system similar to that of the Boeing 727. These instruments include:

Collins FD-108 Flight Director and Integrated Instrument System

Heading, bank, pitch attitude instrumentation

Slip indicator

VOR/ILS capture and tracking

Altitude and heading hold

SR3 Gyro Compass

Radio Compass, ADF, and VOR

Fin Tip Airspeed System and Normal Ship's System

Barometric and Radar Altitude

Angle of Attack

Sideslip Angle

Normal Acceleration

Control Deflections and Forces

The 367-80 in-flight dynamic simulation is mechanized in five-degrees-of-freedom. The pitch, roll, and yaw equations are simulated by control inputs to the elevator, lateral control, and rudder. Lift is simulated by inputs to the wing spoiler type speed brakes and drag by the engine thrust modulators. There is no simulation of the side force equation, but both the analytical and flight evaluation have shown that the side force characteristics of the 367-80 are similar to the airplanes being simulated.

The simulation uses the response feedback technique in which the airplane motions are measured and the signals introduced to the controls to change the stability derivatives of the 367-80 to match these of the simulated airplane. The simulation computer mechanizes the feedback circuits and also simulates the dynamics and authority limits of the airplane control system and engines. The simulation equations and computer functions are described in detail in reference 7.

The simulation evaluation pilot is located in the right hand seat of the 367-80. The control column and wheel are identical to these of the left hand seat except that they have been disconnected from the airplane control system and are connected to electrical position transducers. The control forces are provided by artificial feel systems. The wheel has a spring and centering detent with two pounds break-out and .133 lbs/deg gradient. This centering spring can be quickly changed to provide several different wheel force characteristics. The column has a 4 1/2 pounds break-out force and a variable force gradient from a hydraulic spring. The evaluation pilot has a single throttle handle which drives the thrust modulators through the computer. The evaluation pilot uses the actual 367-80 rudder control system, and the simulation signals are superimposed on the pilot inputs by means of the series yaw damper.

MODEL 367-80 CHARACTERISTICS

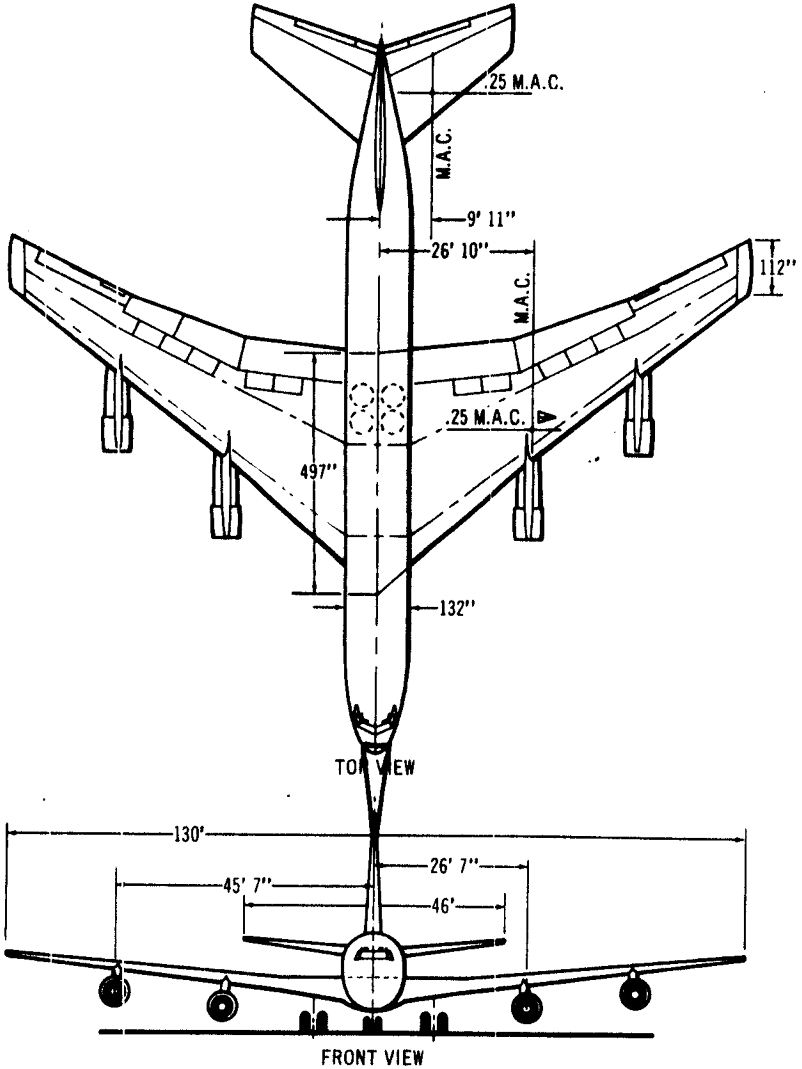

WING

Area	2,821.36 Ft^2
Aspect Ratio	6.00
Sweep (.25C)	35°
Dihedral	7°
Incidence	2°
M.A.C.	20.05 Ft

POWER PLANT

Four Pratt & Whitney
Model JT3D-1 Turbofan
Jet Engines

HORIZONTAL TAIL

Area (Increased to)	625 Ft^2
Aspect Ratio	3.37
Taper Ratio	.421
Sweep (.25C)	35°
Dihedral	7°

VERTICAL TAIL

Area(excl.dorsal)	312 Ft^2
Aspect Ratio (excl.doral)	1.46
Taper Ratio (excl.dorsal)	.45
Sweep .25C	31°

Maximum Gross Weight = 180,000 Pounds

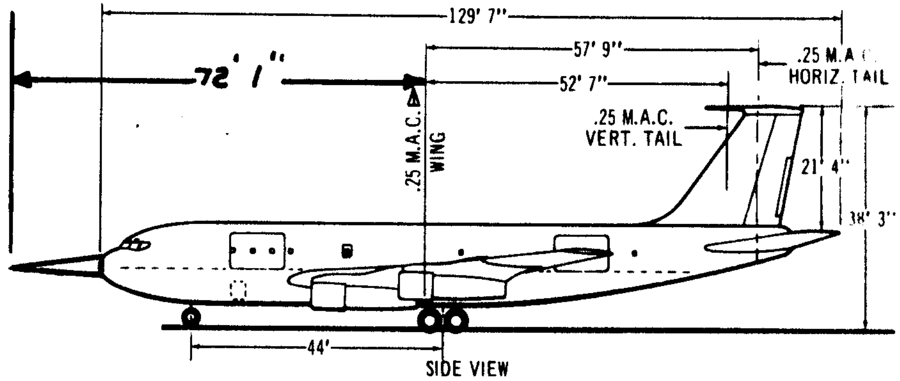

FIG. 1

FLIGHT TESTING PERFORMED

Because of the mechanization of the response feedback technique of simulation depends on an accurate knowledge of the basic airplane characteristics, the 367-80 test configurations were documented carefully. The longitudinal static characteristics and speed brake effectiveness were documented by speed stability tests in which the airplane was restabilized at speeds above and below the trim speed. The longitudinal control response and short period dynamics were documented by elevator step inputs, and the phugoid was excited and measured. The lateral-directional static stability and control characteristics were documented by cross-control sideslips. The roll response and damping were documented by applying step wheel inputs and measuring the steady-state roll rate. The Dutch roll and spiral stability were excited and measured. The thrust modulators were calibrated by flying a series of stabilized conditions at different thrust settings. The data from these tests are presented in Appendix I.

The simulation configurations were set up on the computer and checked out by measuring the airplane response to pulses of the elevator, rudder, lateral control, and thrust modulators. These pulses were compared to theoretical calculations performed by a digital computer. This technique is described in detail in reference 7.

After the simulation configurations had been checked out by the computer, the airplane characteristics were documented. The longitudinal static characteristics were documented by speed stability tests and the maneuvering characteristics by a wind-up turn. The short period was documented by elevator steps and the longitudinal control response characteristics were measured by pitch reversals in which a control pulse was applied in one direction, followed by a step in the other. The phugoid oscillation was excited and measured. The lateral static characteristics were documented by cross-control sideslips. The roll response and damping were measured by step wheel inputs and the roll control power and sensitivity were documented by roll reversals similar to the pitch reversals. The Dutch roll and spiral stability modes were excited and measured.

SIMULATION OF THE NASA 20

The NASA 20 configuration simulated by the 367-80 is an advanced version of the SCAT-15 variable sweep SST with increased aspect ratio. This configuration has the wings forward at 20 degrees sweep (leading edge sweep), a landing weight of 280,000 pounds, and a 135 knots approach speed. The details of the configuration and stability derivatives are listed in Appendix 2.

The flight test data of the simulation documentation maneuvers are shown in Fig. 2 to 19, compared with the theoretical NASA 20 characteristics. The data for the speed stability tests are shown in Fig. 2 and 3. The 367-80 has an accurate simulation of the NASA 20 speed stability and stick force per knot. The wind-up turn data are shown in Fig. 4 to 6. The 367-80 simulates the normal acceleration versus angle of attack characteristics, $N_{z\alpha}$ and the stick deflection and force per "g" accurately. The pitch reversal data are shown in Fig. 7. The simulation of the longitudinal control power and sensitivity is very good. The lateral static stability characteristics are shown in Fig. 8. The 367-80 closely matches the pedal and wheel deflection required to hold sideslip and also the bank angle-sideslip relationship, which shows that the 367-80 simulation is correct even though the side force equation is not simulated. The flight data from the wheel steps and reversals are shown in Fig. 8 to 10. The 367-80 matches the roll response and damping of the NASA 20 very well. The airplane response to an elevator pulse is shown in Fig. 11 to 13 and the response to a rudder pulse in Fig. 14, 15 and 16. These pulse responses show a good simulation of the NASA 20 control response and dynamic stability characteristics. The measured 367-80 control force characteristics used in the NASA 20 simulation are shown in Fig. 17 to 19.

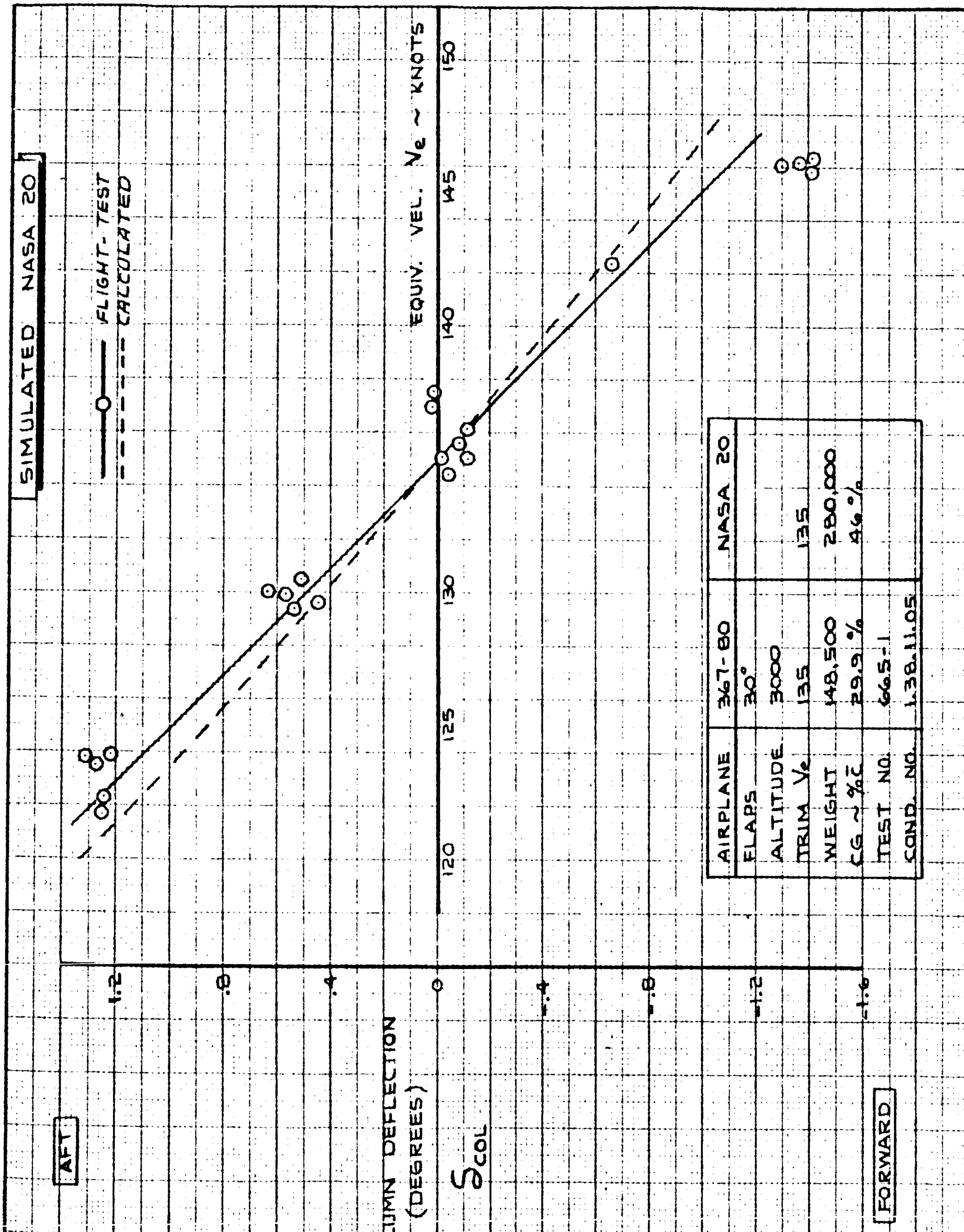

AIRPLANE	367-80	NASA 20
FLAPS	30°	
ALTITUDE	3000	
TRIM V_e	135	135
WEIGHT	148,500	280,000
CG ~ %c̄	29.9 %	46 %
TEST NO.	665-1	
COND. NO.	1.38.11.05	

FIG. 2

			REVISED	DATE		
CALC	TAYLOR				COLUMN VS SPEED CHARACTERISTICS	BASIC NASA 20
CHECK						D6-10743
APR						
APR					THE BOEING COMPANY	PAGE 17

TD 461 C-R4

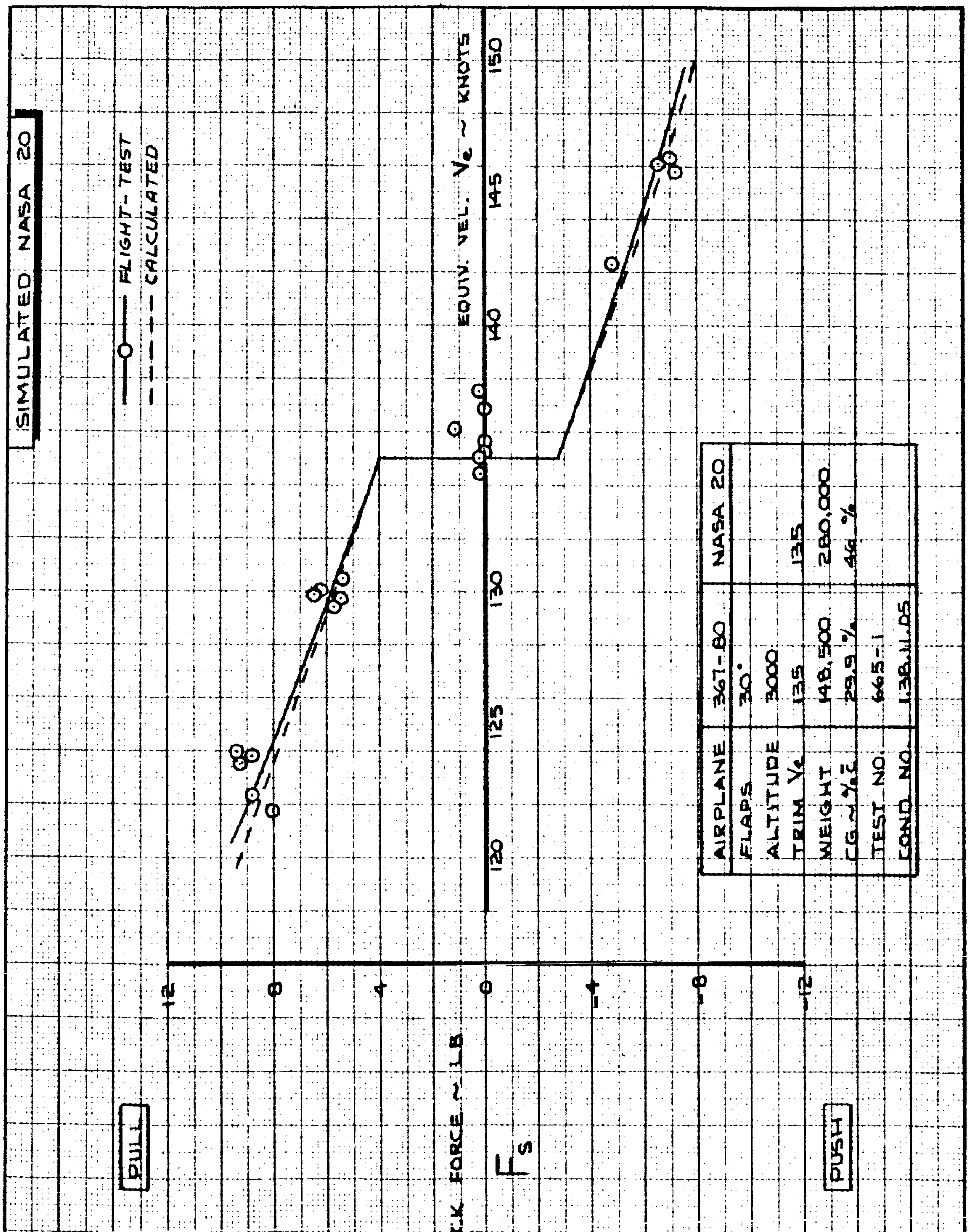

FIG. 3

CALC	TAYLOR		REVISED	DATE
CHECK				
APR				
APR				

SPEED STABILITY
STICK FORCE VS SPEED

THE BOEING COMPANY

BASIC NASA 20

D6-10743

TD 441 C-R4

SIMULATED NASA 20

AIRPLANE	367-80	NASA 20
FLAPS	30°	
ALTITUDE	5600	
TRIM V_e	134	135
WEIGHT	150,000	280,000
CG ~ % $\bar{c}$	29.3 %	46 %
TEST NO.	664-3	
COND. NO.	1.22.04.2	

DATA FROM WIND-UP TURN

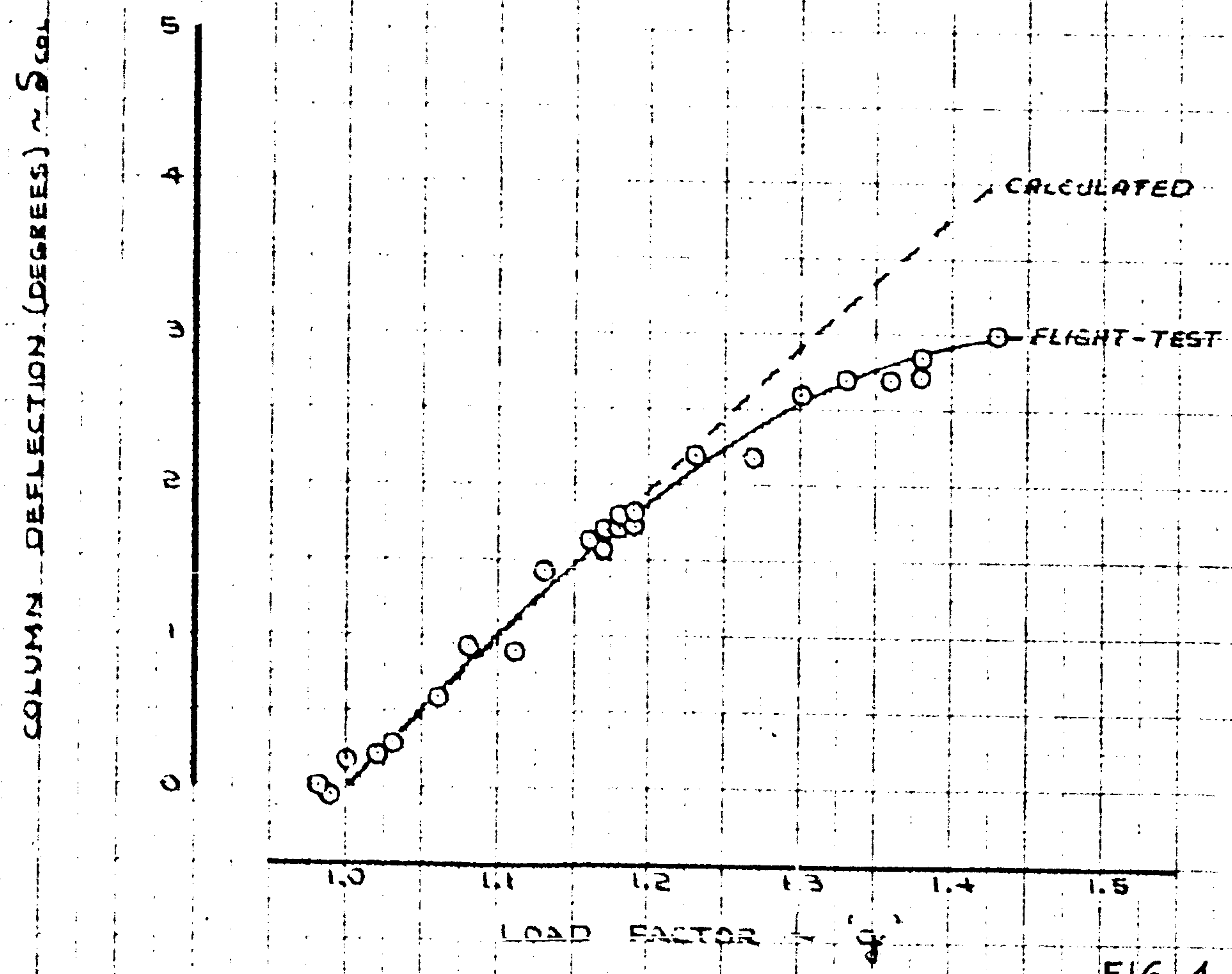

FIG. 4

CALC	TAYLOR	REVISED	DATE	NORMAL ACCELERATION VS COLUMN CHARACTERISTICS	BASIC NASA 20
CHECK					
APR					D6-10743
APR				THE BOEING COMPANY	

SIMULATED NASA 20

AIRPLANE	367-80	NASA 20
FLAPS	30°	
ALTITUDE	5600	
TRIM V_e	134	135
WEIGHT	150,000	280,000
CG ~ %$\bar{c}$	25.3 %	46.0 %
TEST NO.	664-3	
COND. NO.	1.22.04.2	

DATA FROM WIND-UP TURN

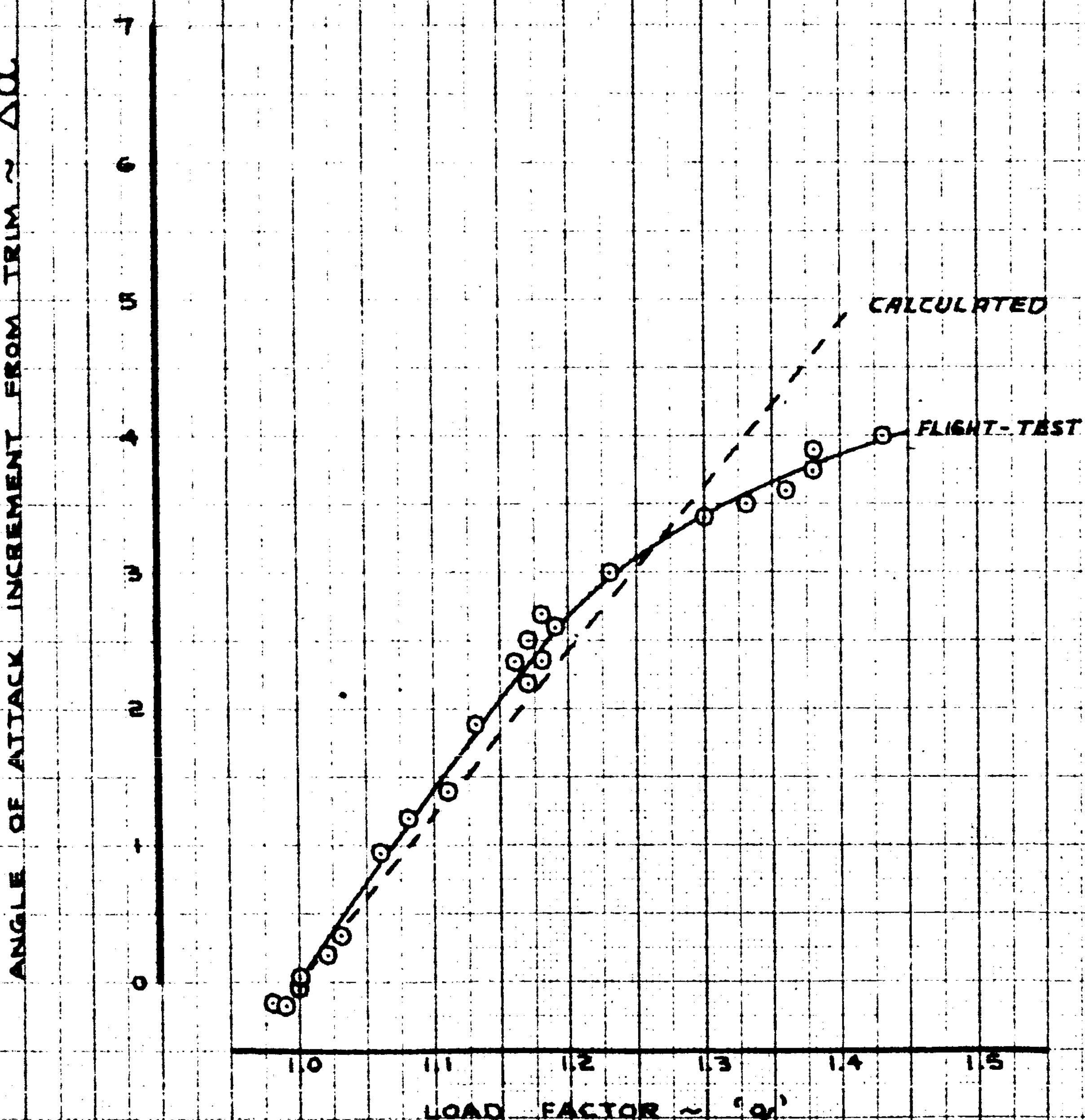

FIG. 5

CALC	TAYLOR	REVISED	DATE	NORMAL ACCELERATION VS. ANGLE OF ATTACK	BASIC NASA 20
CHECK					D6-10743
APR				THE BOEING COMPANY	PAGE 20
APR					

SIMULATED NASA 20

AIRPLANE	367-80	NASA 20
FLAPS	30°	
ALTITUDE	5600	
TRIM Ve	134	135
WEIGHT	150,000	280,000
CG ~ %c̄	29.3 %	46 %
TEST NO.	664-3	
COND. NO.	1.22.04.2	

DATA FROM WIND-UP TURN

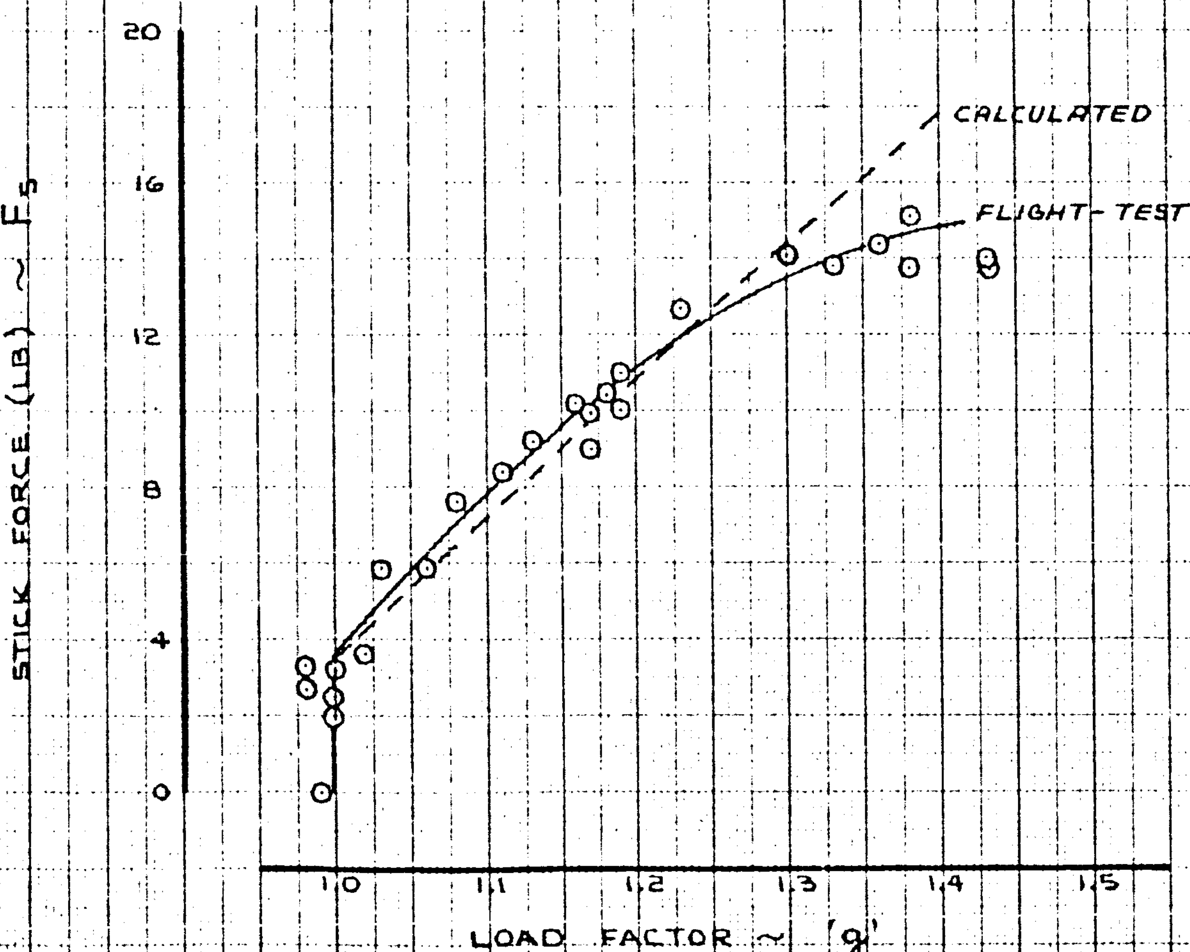

FIG. 6

CALC	Taylor		REVISED	DATE	NORMAL ACCELERATION VS. FORCE CHARACTERISTICS	BASIC NASA 20
CHECK						D6-10743
APR						
APR					THE BOEING COMPANY	PAGE 21

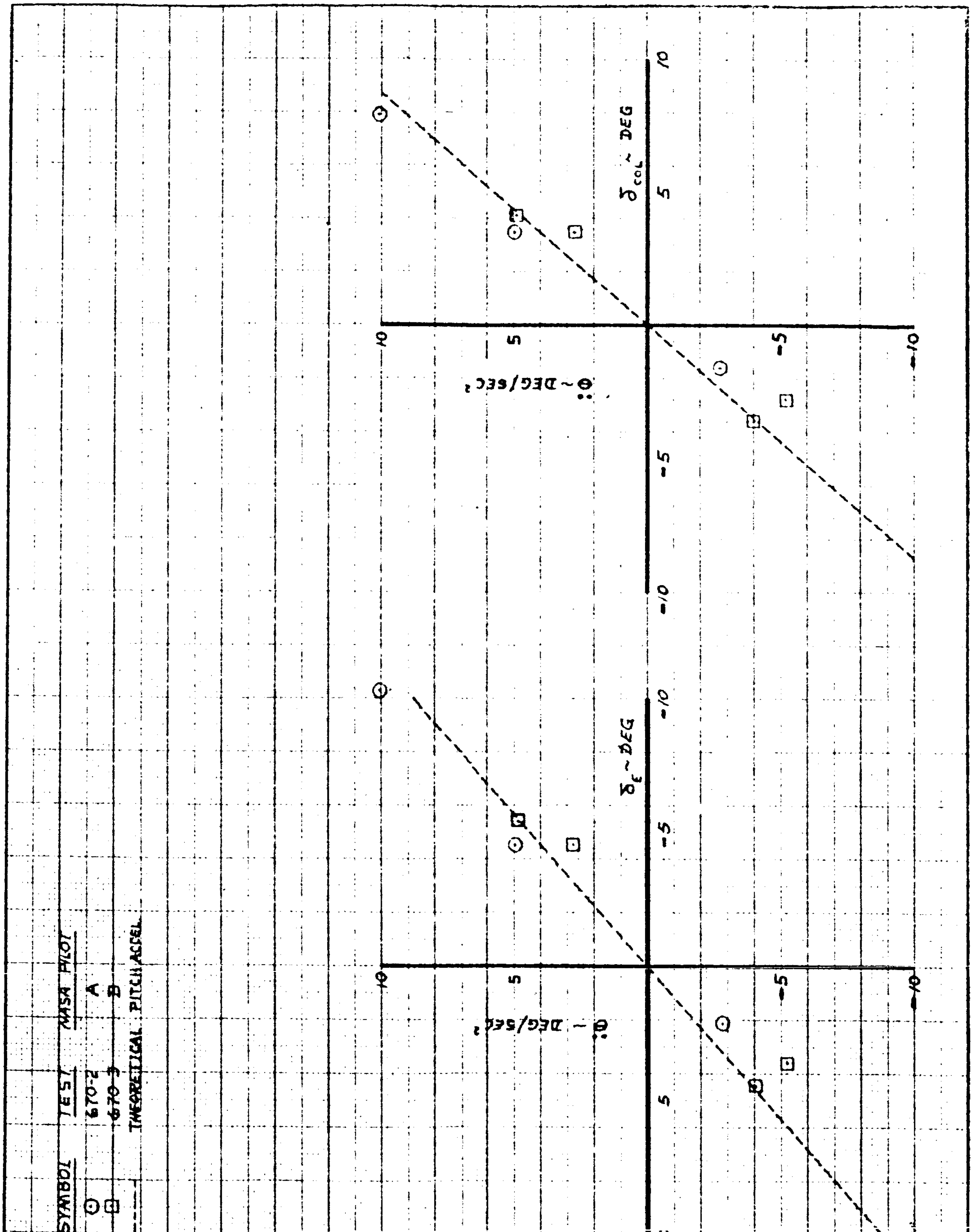

FIG. 7

CALC	D J BECK	11-18-65	REVISED	DATE
CHECK				
APR				
APR				

PITCH ACCELERATION OF THE NASA 20 SST (BASIC CG ~ NO SAS)

D6-10743

THE BOEING COMPANY

TD 461 C R4

	367-80	NASA-20
FLAPS	30°	
SPEED BRAKES	6°	
Ve	135 KTS.	135 KTS.
ALTITUDE	5800 FT.	
G.W.	147,500 LBS	280,000 LBS
C.G.	28.8 % MAC	46 % MAC
TEST NO.	664-3	

SIMULATED NASA-20

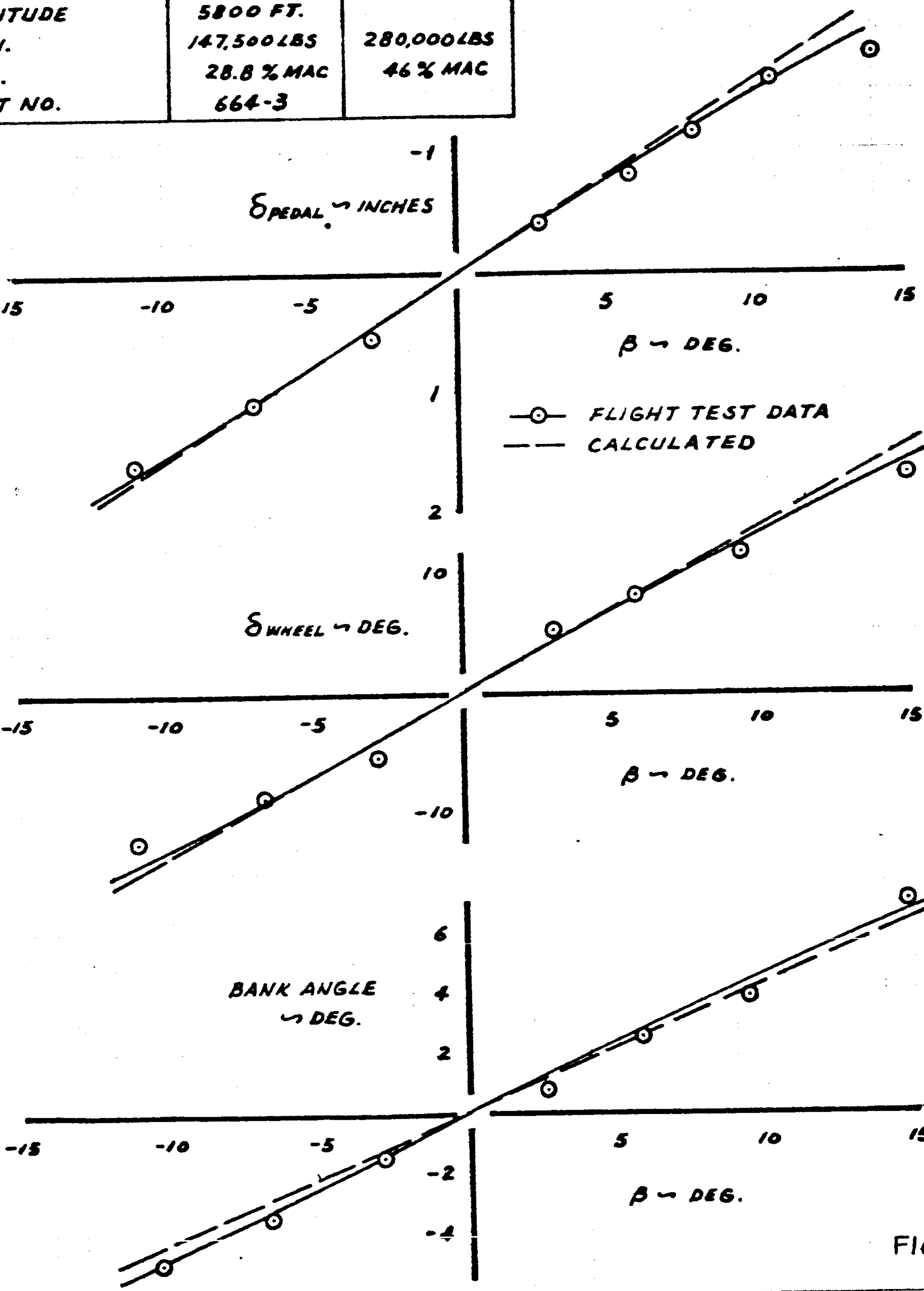

FIG. 8

CALC			REVISED	DATE	LATERAL - DIRECTIONAL STATIC STABILITY	SIMULATED NASA-20
CHECK						D6-10743
APR					THE BOEING COMPANY	PAGE 23
APR						

	B6T-80	NASA - 20
FLAPS	30°	
SPEED BRAKES	6°	
V_e	135 KTS	135 KTS
ALTITUDE	5800. FT.	
G.W.	150,000 LBS.	280,000 LBS.
C.G.	28.7 %MAC	46.0 %MAC
TEST NO.	664-3	

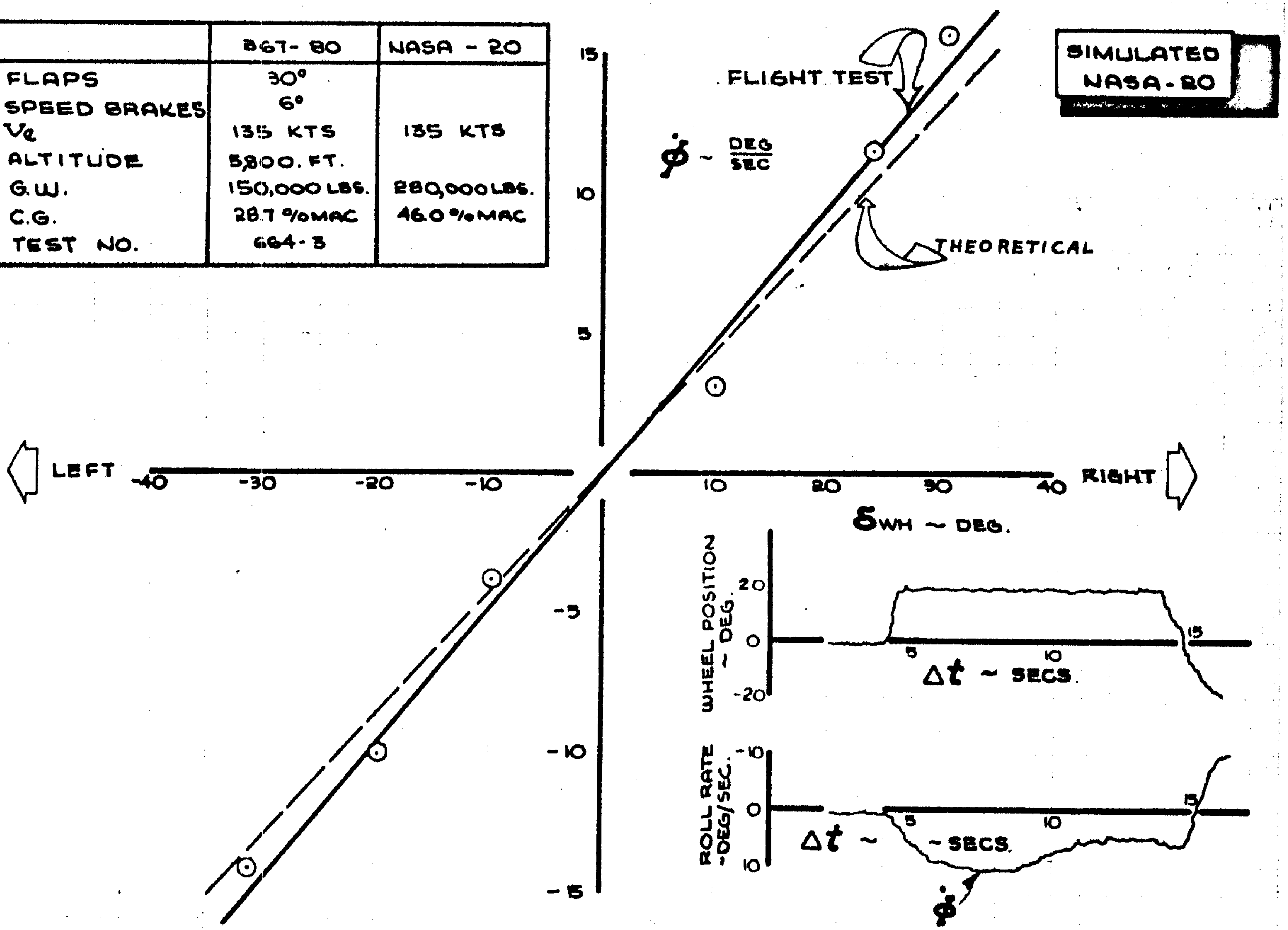

FIG. 9

			REVISED	DATE
CALC				
CHECK				
APR				
APR				

LATERAL CONTROL RESPONSE
STEADY STATE ROLL RATES

THE BOEING COMPANY

SIMULATED NASA-20
D6-10743
PAGE 24

SIMULATED NASA-20

	367 - 80	NASA - 20
FLAPS	30°	
SPEED BRAKES	6°	
Ve	135 KTS	135 KTS
ALTITUDE	4,250 FT.	
G.W.	163,000 LBS.	280,000 LBS.
C.G.	31.2 % MAC	46.0 % MAC
TEST NO.	664-4	

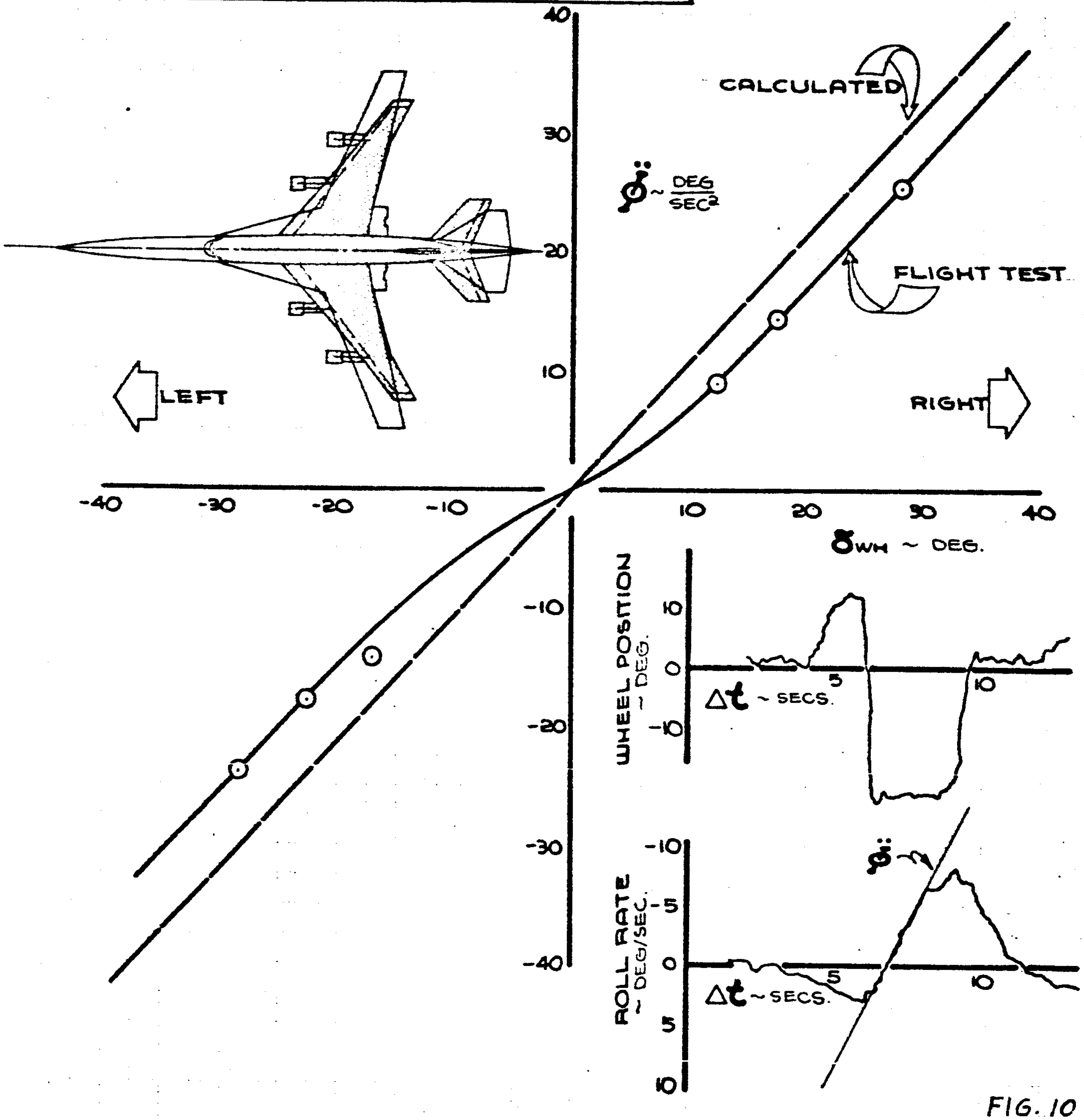

FIG. 10

CALC	PS	6-65	REVISED	DATE	ROLL ACCELERATION CHARACTERISTICS	SIMULATED NASA-20
CHECK						D6-10743
APR					THE BOEING COMPANY	PAGE 25
APR						

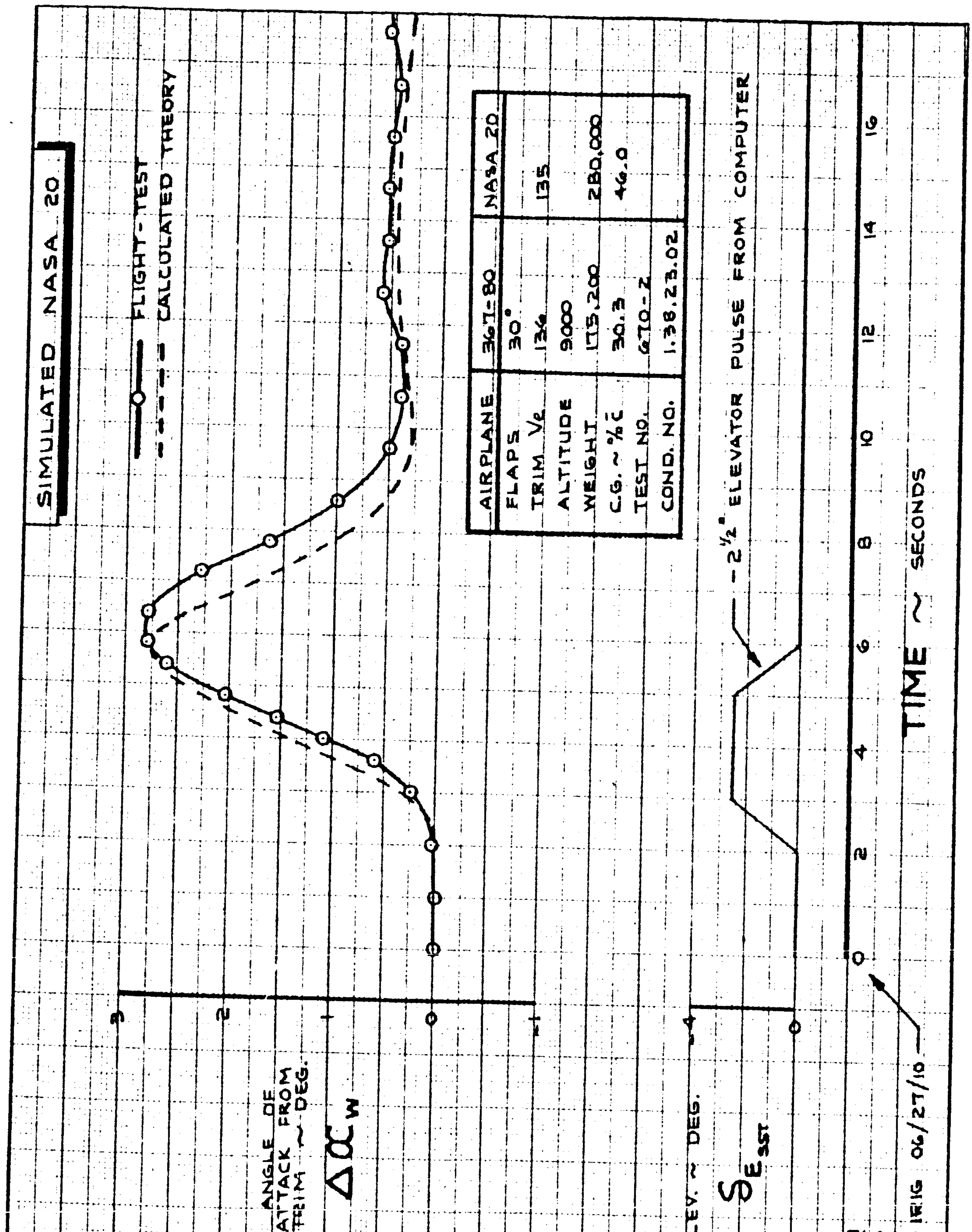

AIRPLANE	367-80	NASA 20
FLAPS	30°	
TRIM V_2	136	135
ALTITUDE	9000	
WEIGHT	175,200	280,000
C.G. ~ %c̄	30.3	46.0
TEST NO.	670-Z	
COND. NO.	1.38.23.02	

FIG. 11

CALC	TAYLOR	REVISED	DATE	SHORT PERIOD CHARACTERISTICS	BASIC NASA 20
CHECK					
APR					D6-10743
APR				THE BOEING COMPANY	PAGE 26

TD 46 C R4

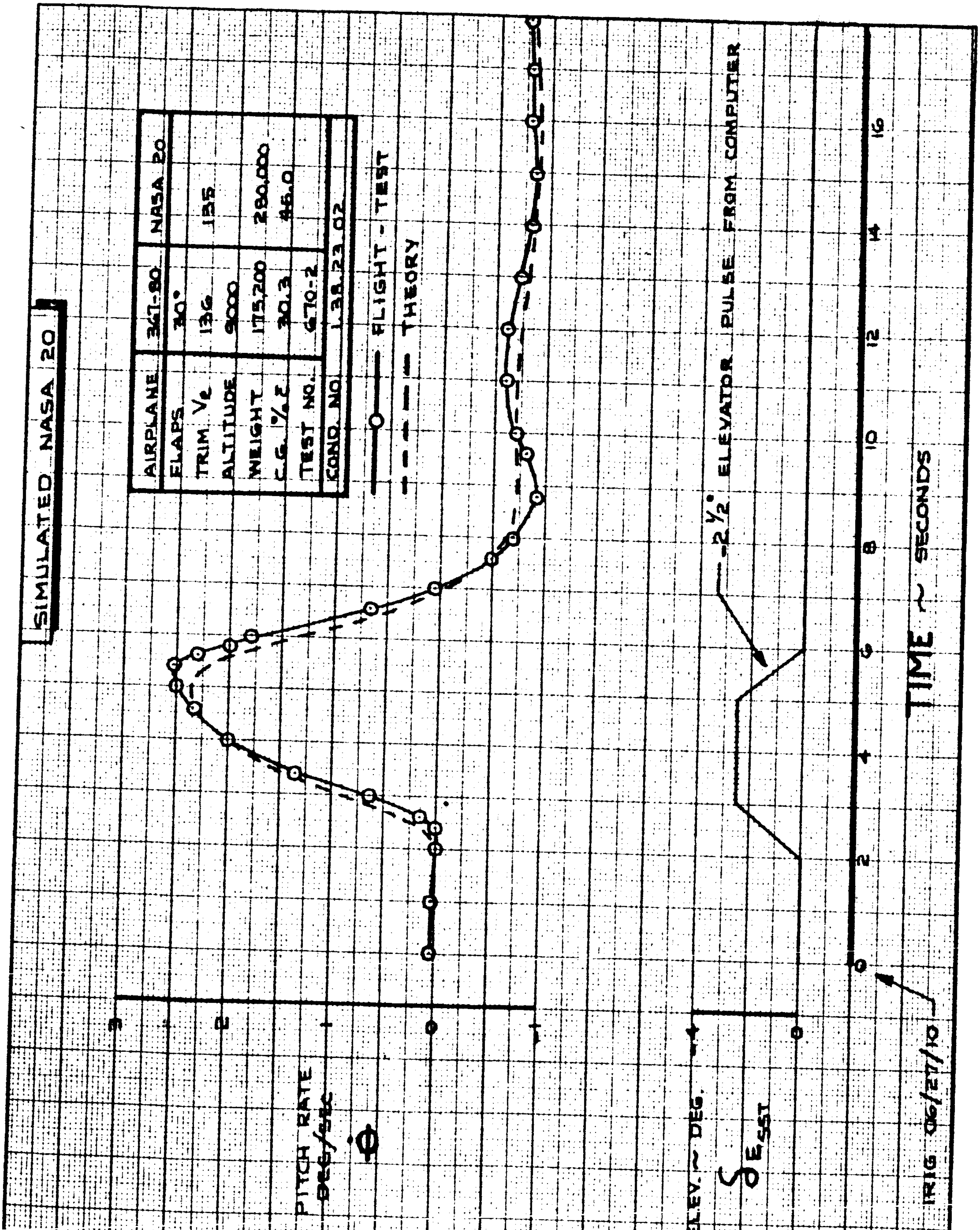

FIG. 12

CALC	TAYLOR		REVISED	DATE	SHORT PERIOD CHARACTERISTICS	BASIC NASA 20
CHECK						D6-10743
APR					THE BOEING COMPANY	PAGE 27
APR						

TD 461 C-R4

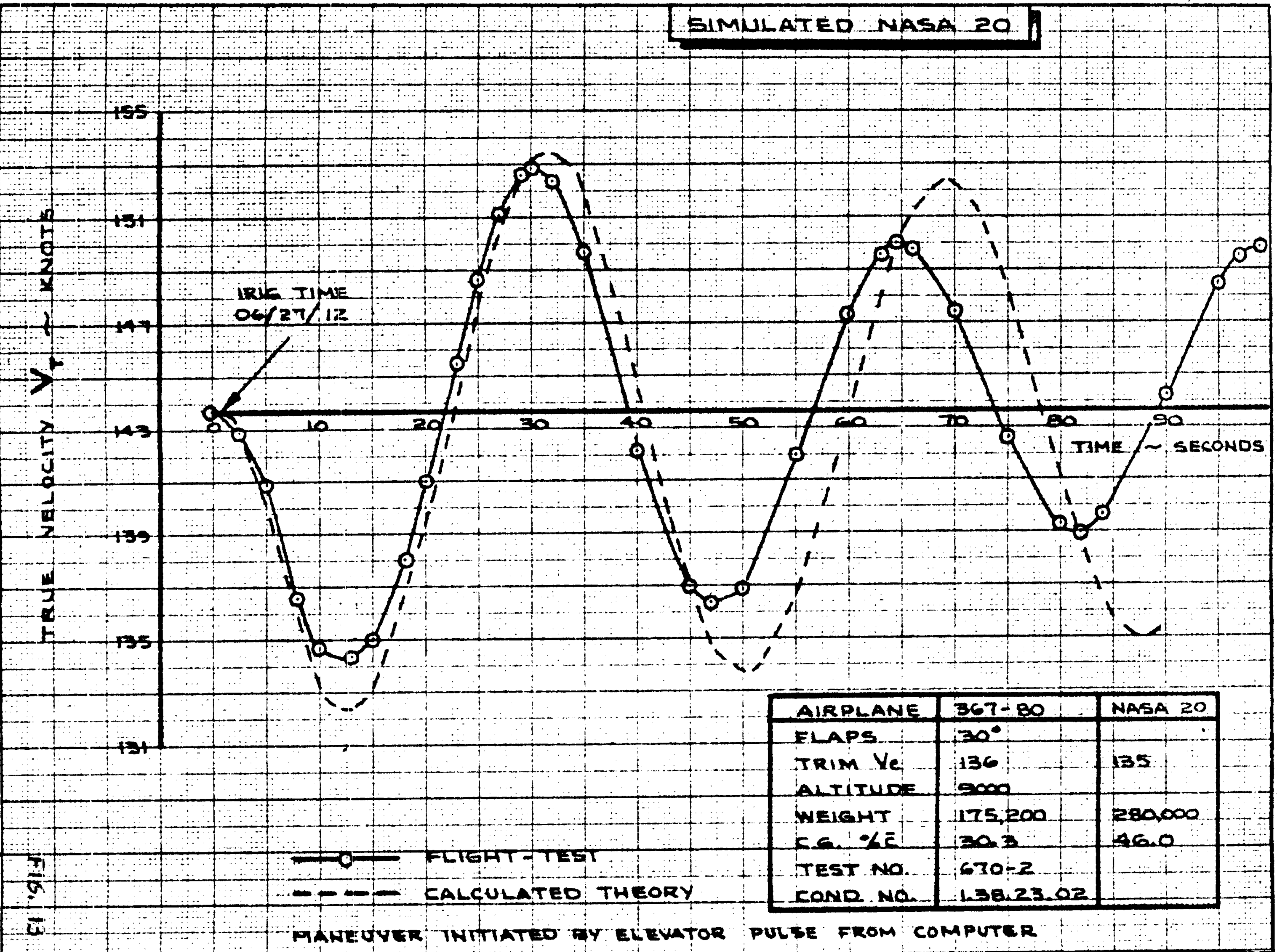

AIRPLANE	367-80	NASA 20
FLAPS	30°	
TRIM Ve	136	135
ALTITUDE	9000	
WEIGHT	175,200	280,000
C.G. %c̄	30.3	46.0
TEST NO.	670-2	
COND. NO.	1.38.23.02	

FIG. 13

CALC	TAYLOR	REVISED	DATE	PHUGOID CHARACTERISTICS	BASIC NASA 20
CHECK					D6-10743
APR					
APR				THE BOEING COMPANY	PAGE 28

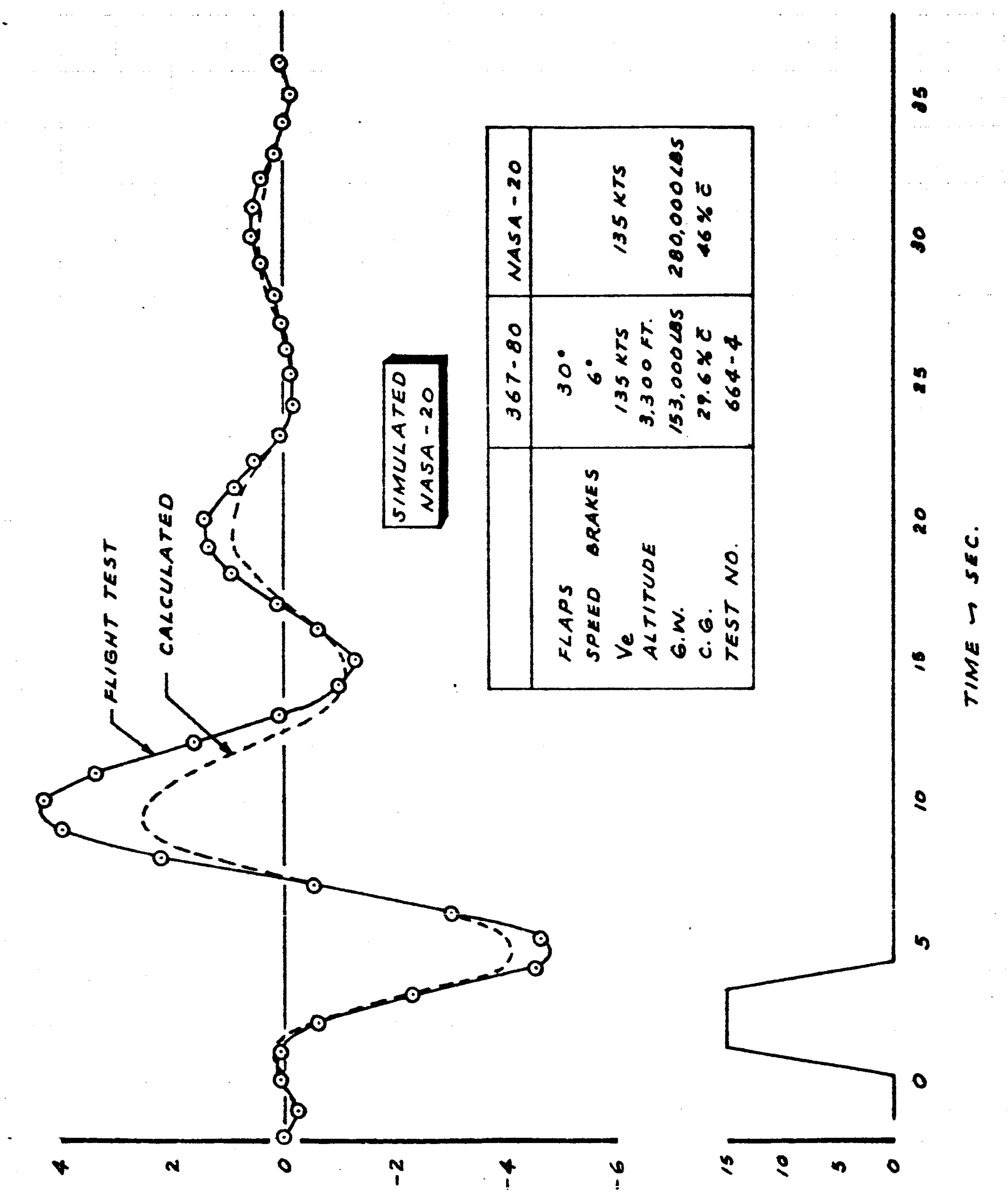

FIG. 14

CALC	RCS	6/29/65	REVISED	DATE	LATERAL - DIRECTIONAL DYNAMICS	SIMULATED NASA-20
CHECK						D6-10743
APR					THE BOEING COMPANY	PAGE 29
APR						

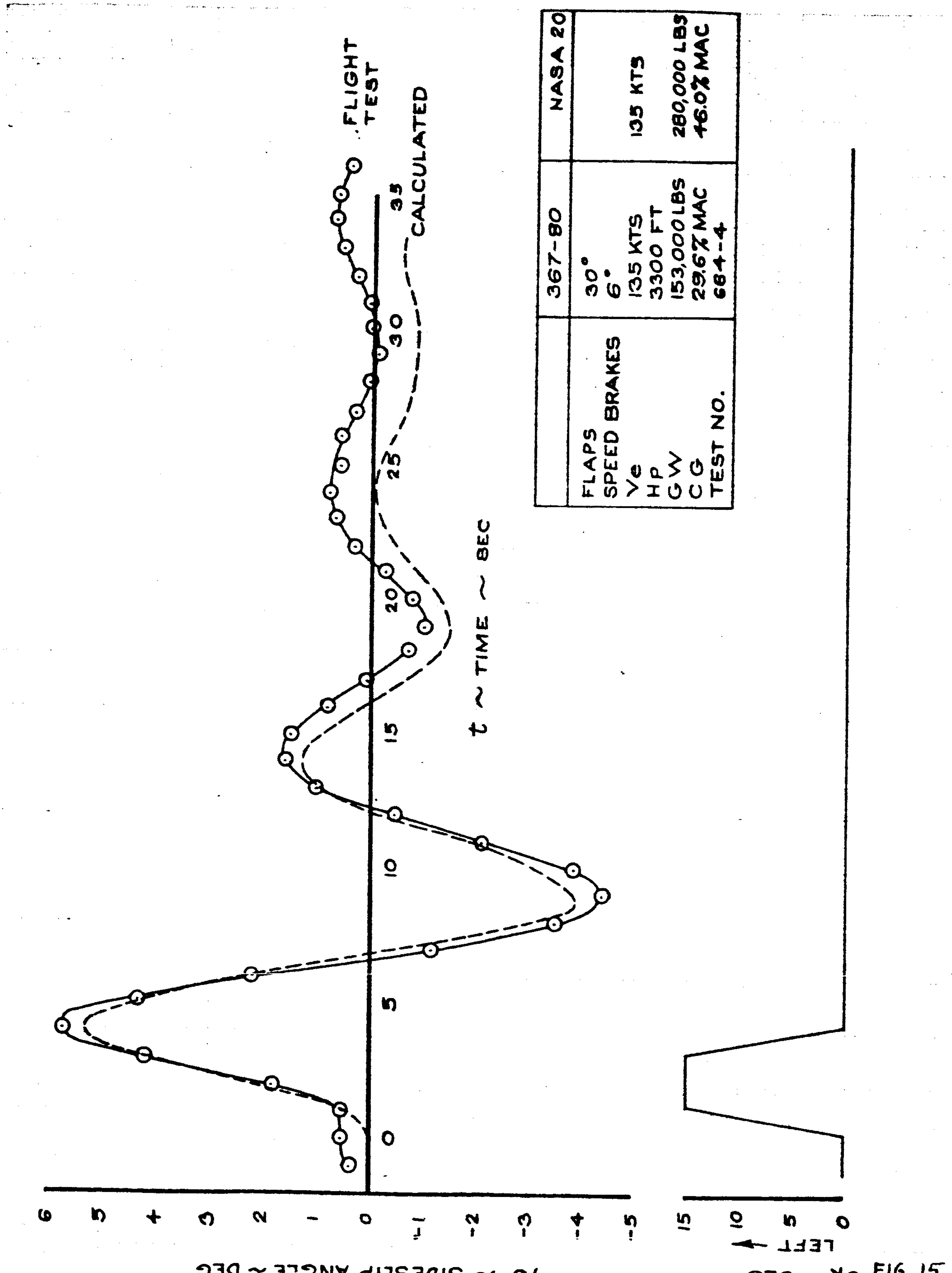

	367-80	NASA 20
FLAPS	30°	
SPEED BRAKES	6°	
Ve	135 KTS	135 KTS
Hp	3300 FT	
GW	153,000 LBS	280,000 LBS
CG	29.6% MAC	46.0% MAC
TEST NO.	684-4	

FIG. 15

CALC			REVISED	DATE	LATERAL - DIRECTIONAL DYNAMICS	SIMULATED NASA20
CHECK						
APR					1.38.18.38	D6-10743
APR					THE BOEING COMPANY	PAGE 30

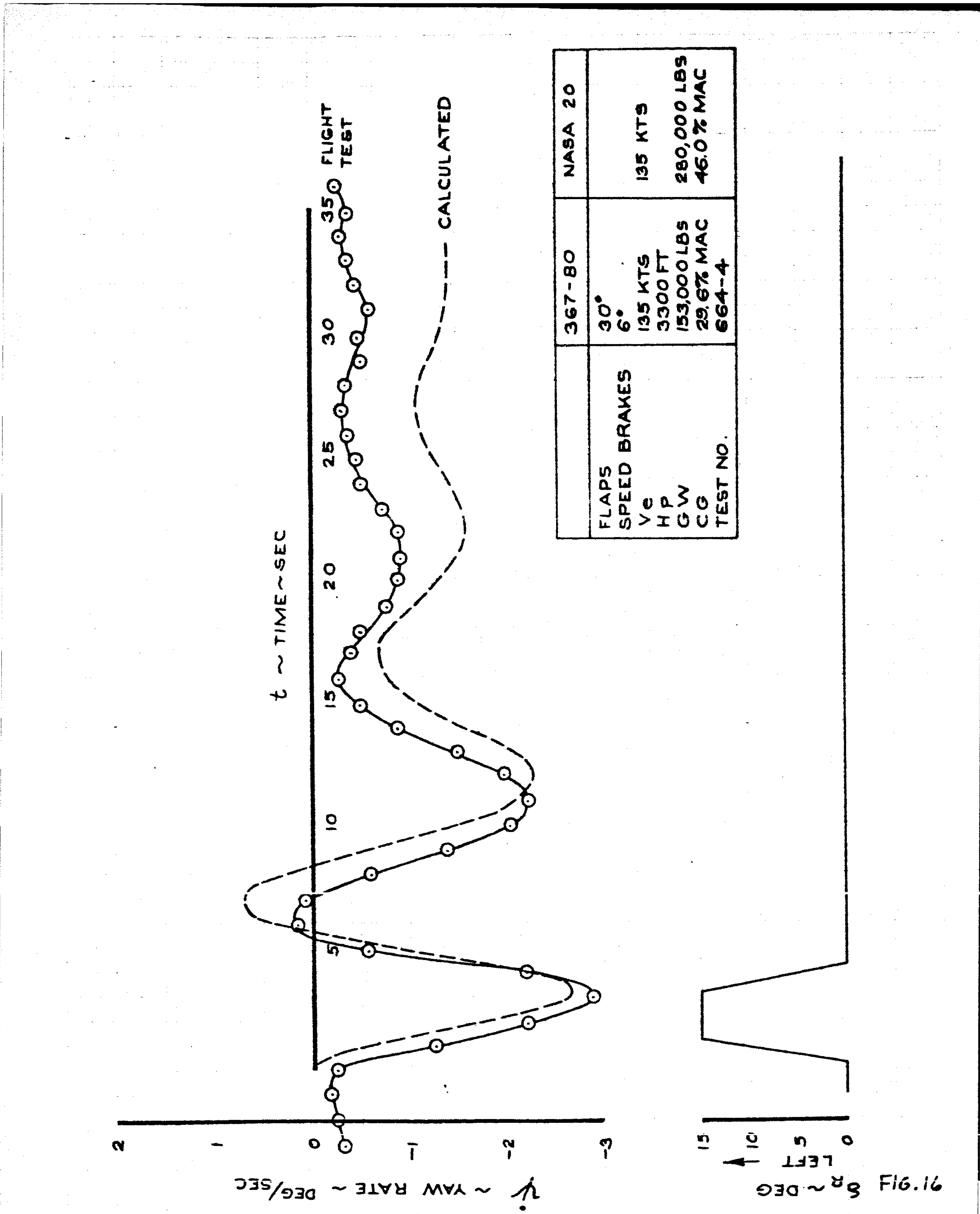

FIG. 16

CALC			REVISED	DATE	LATERAL-DIRECTIONAL DYNAMICS
CHECK					
APR					
APR					THE BOEING COMPANY

SIMULATED NASA-20

D6-10743

SIMULATED
NASA - 20

	367-80	NASA-20
FLAPS	30°	
SPEED BRAKES	6°	
Ve	135 KTS	135 KTS
ALTITUDE	3,800 FT.	
G.W.	150,700 LBS	280,000 LBS
C.G.	28.7% $\bar{c}$	46% $\bar{c}$
TEST NO.	664-3	

DATA FROM WIND UP TURN MANEUVERS

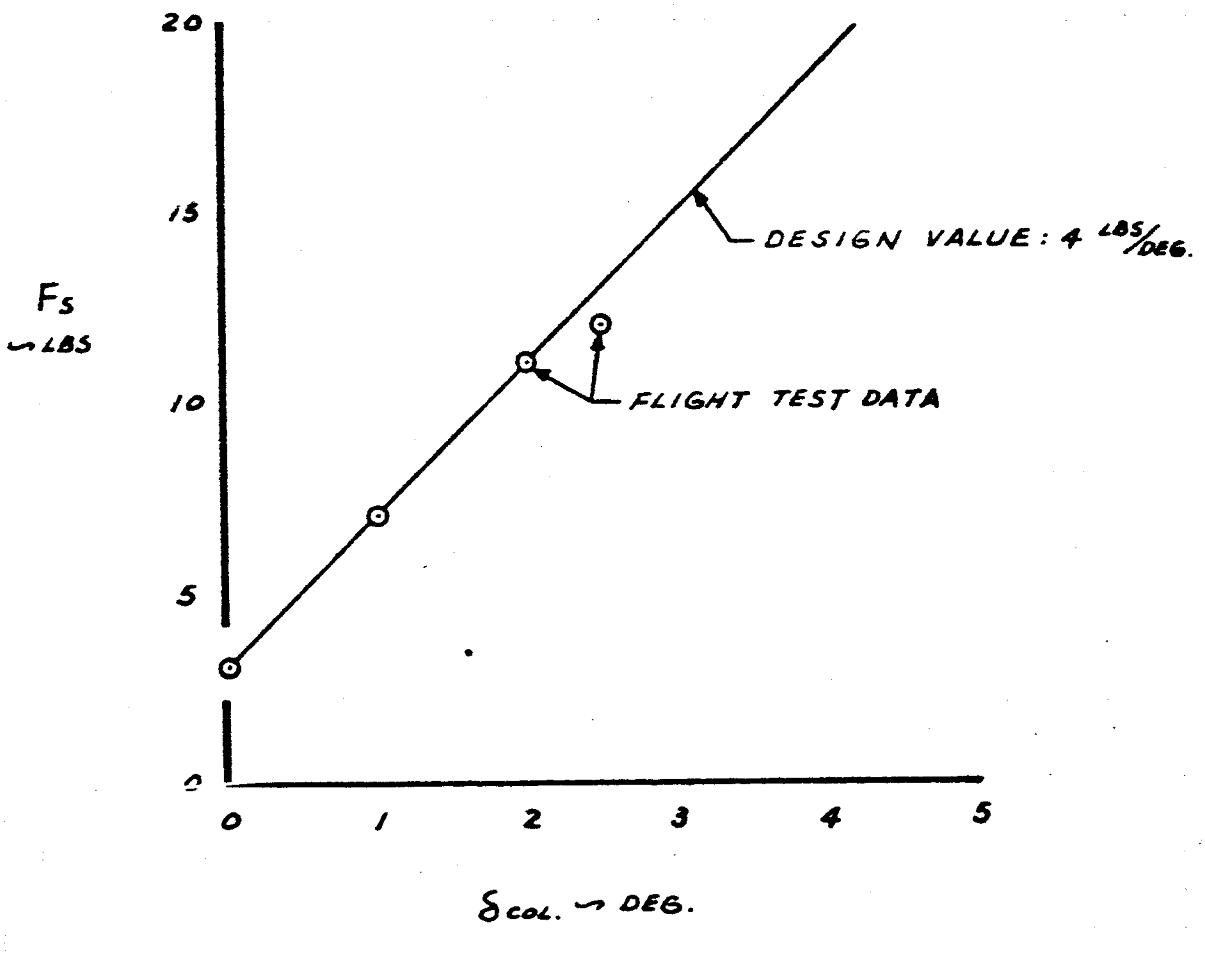

FIG. 17

			REVISED	DATE		
CALC					STICK FORCE VS. COLUMN DEFLECTION CHARACTERISTICS	SIMULATED NASA-20
CHECK						D6-10743
APR					THE BOEING COMPANY	PAGE 32
APR						

SIMULATED NASA-20

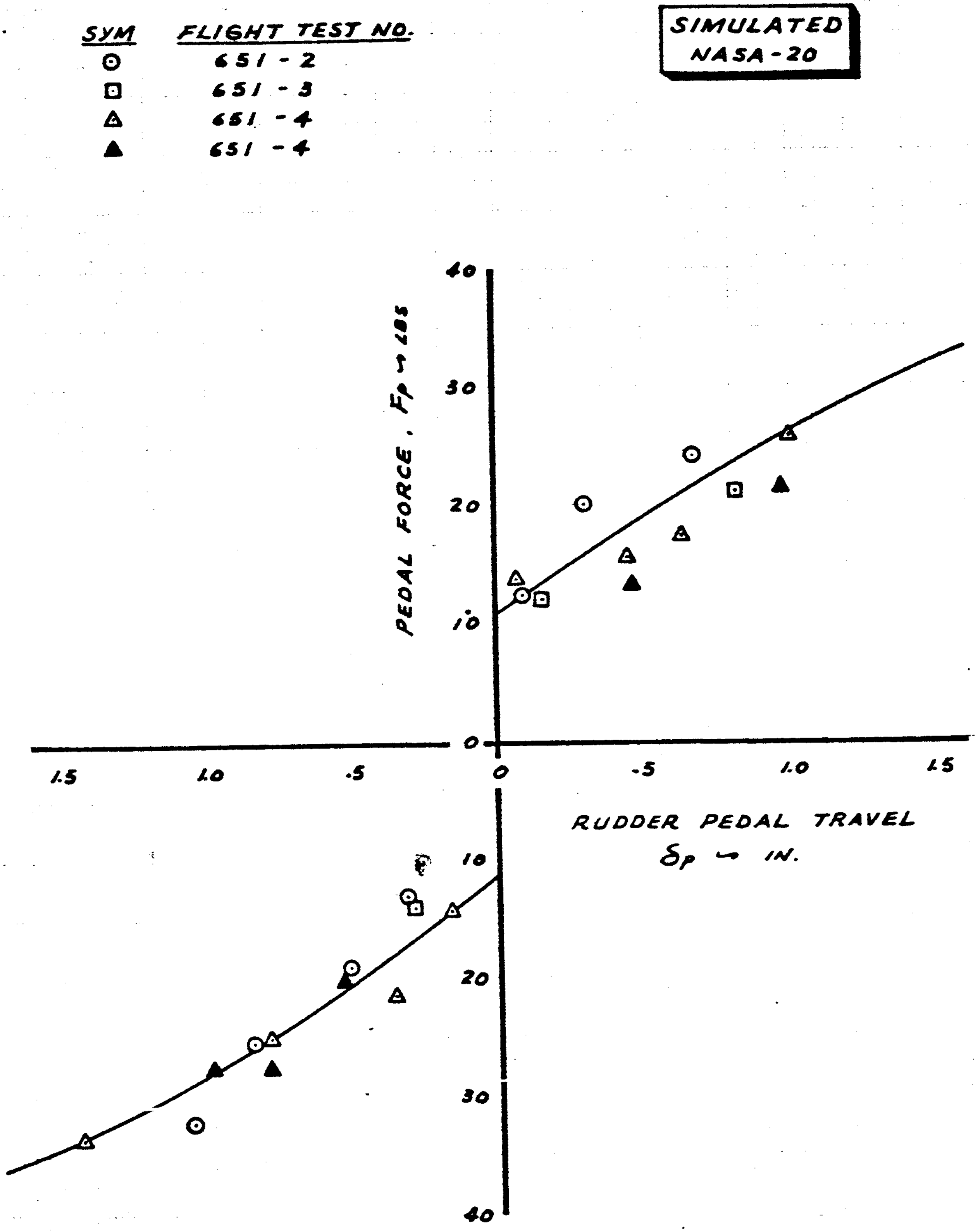

FIG. 18

CALC	P S	4/11/65	REVISED	DATE	RUDDER PEDAL FORCE CHARAC. (RIGHT HAND SEAT)	SIMULATED NASA-20
CHECK			HUANG	7-26-65		D6-10743
APR						PAGE 33
APR					THE BOEING COMPANY	

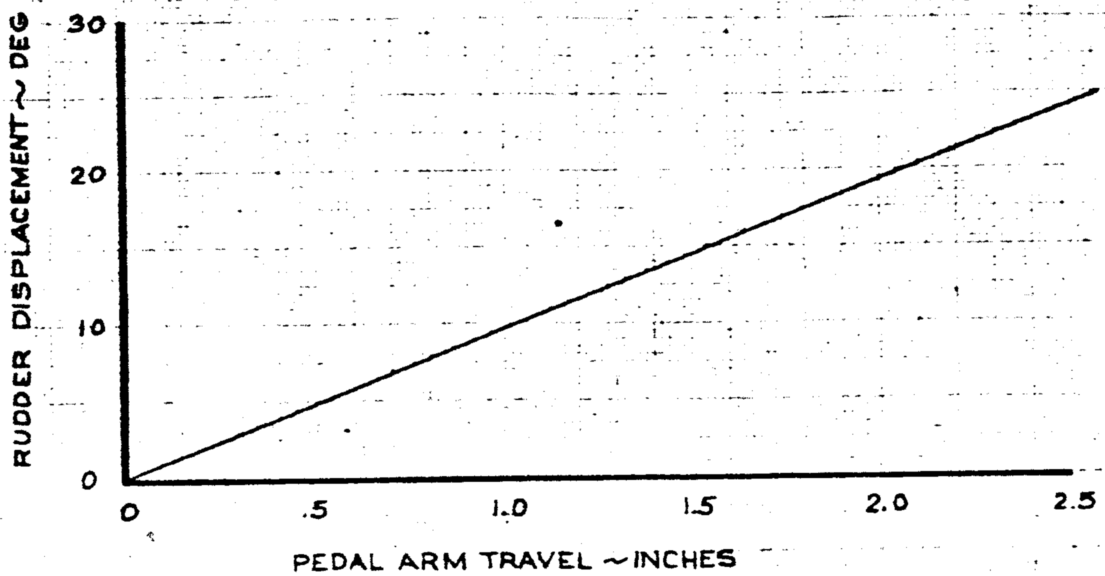

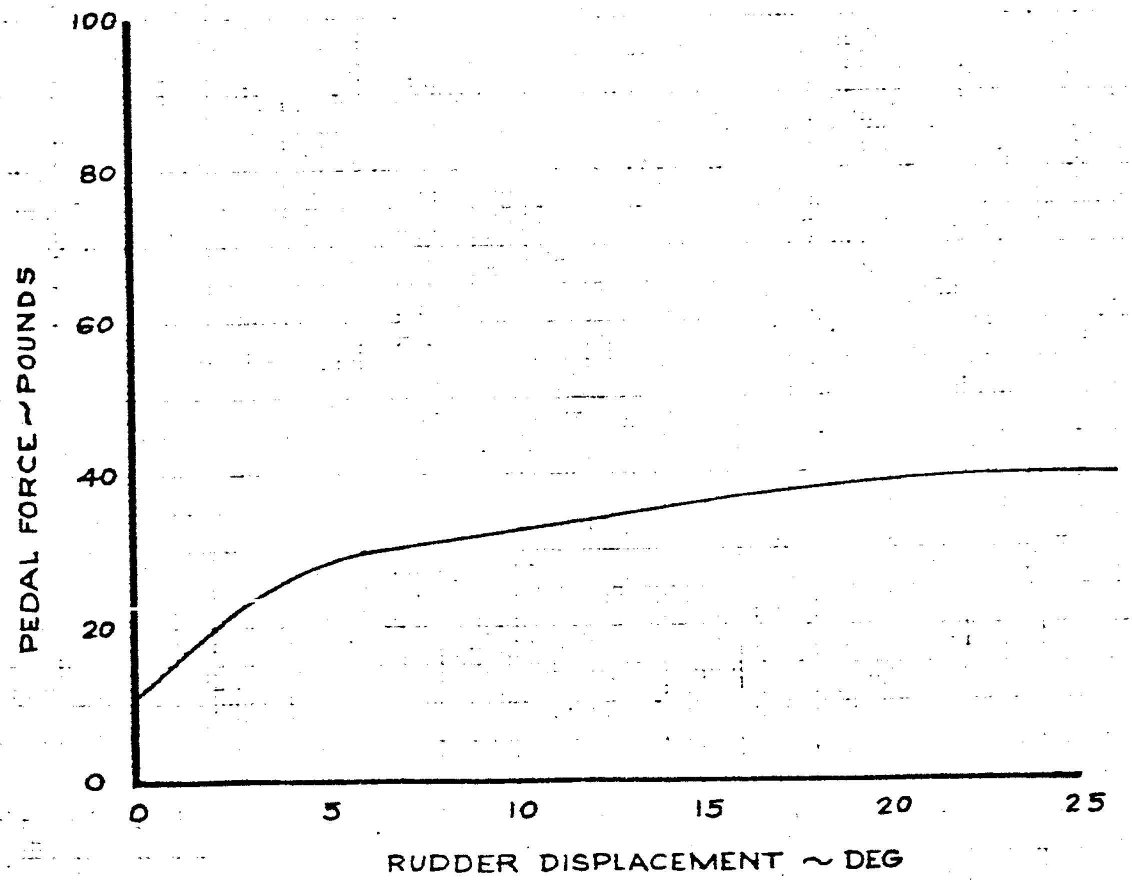

FIG. 19

			REVISED	DATE		
CALC					CALCULATED RUDDER PEDAL FORCES (SYSTEM FRICTION NOT INCLUDED.)	SIMULATED NASA-20
CHECK						D6-10743
APR						
APR					THE BOEING COMPANY	PAGE 34

SIMULATION OF THE NASA 20A

The NASA 20A is the NASA 20 SST configuration with the longitudinal and lateral-directional stability augmentation. The longitudinal stability augmentation consists of a pitch rate damper and a column-to-elevator gearing increase as shown below:

$$\delta E = \left[\frac{\delta E}{\delta \text{ column}} \right]_{\text{Basic}} \times 2\, \delta_{col} + 1.46\, \dot{\theta}$$

The pitch rate feedback increases the short period frequency and damping to quicken the longitudinal control response. The increase in stick gearing compensates for the artificially increased airplane maneuver margin and keeps the stick force and deflection per "g" approximately constant.

The lateral-directional stability augmentation consists of a sideslip rate yaw damper to increase the Dutch roll damping ratio. The path-axis sideslip rate is computed and this signal is introduced to the rudder, as shown below:

$$\dot{\beta}_{\text{Path}} = \frac{g}{V} \phi - \dot{\psi}$$

$$\delta R = -1\, \dot{\beta}_{\text{Path}}$$

This damper increased the Dutch roll damping ratio from .2 to .3.

Simulation Documentation:

The data from the NASA 20A documentation flight testing are shown in Fig.20 to 30 . Fig. 20 and 21 show the speed stability testing. There is a good simulation of the stick force and deflection per knot. Fig. 22, 23 and 24 show the wind-up turn data. The stick force per "g" is simulated well, but there is a slight mismatch in the stick deflection and angle of attack per "g" above 1.15 "g's". Data from the pitch reversal are shown in Fig. 25 . The simulation of the NASA 20A control power and sensitivity was very accurate. Fig. 26 shows the data from the wheel step inputs. The roll rate-wheel characteristic is simulated very well. Figs. 27 and 28 show the airplane response to an elevator pulse. The theoretical response is matched well. Fig. 29 shows the phugoid oscillation. Both the period and damping ratio are simulated well. Fig. 30 shows the airplane response to a rudder pulse. The airplane control response and the Dutch roll period and damping are simulated well.

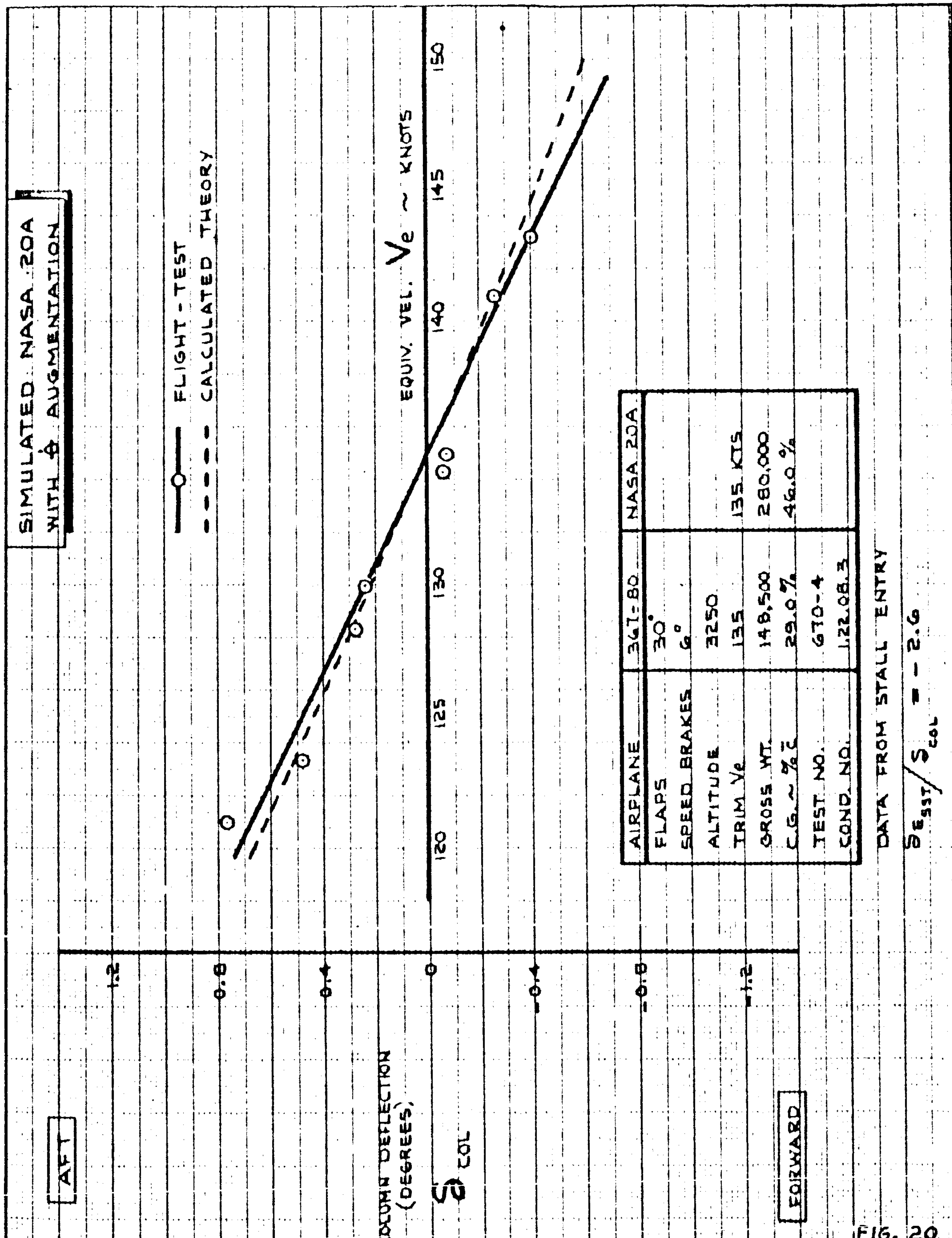

AIRPLANE	367-80	NASA 20A
FLAPS	30°	
SPEED BRAKES	6°	
ALTITUDE	3250	
TRIM Ve	135	135 KTS
GROSS WT.	148,500	280,000
C.G. ~ %c̄	29.0%	46.0%
TEST NO.	670-4	
COND. NO.	122.08.3	

DATA FROM STALL ENTRY

$\delta_{E_{SST}} / \delta_{COL} = -2.6$

FIG. 20

CALC	TAYLOR		REVISED	DATE	COLUMN VS SPEED CHARACTERISTICS	NASA 20A
CHECK						D6-10743
APR					THE BOEING COMPANY	PAGE 37
APR						

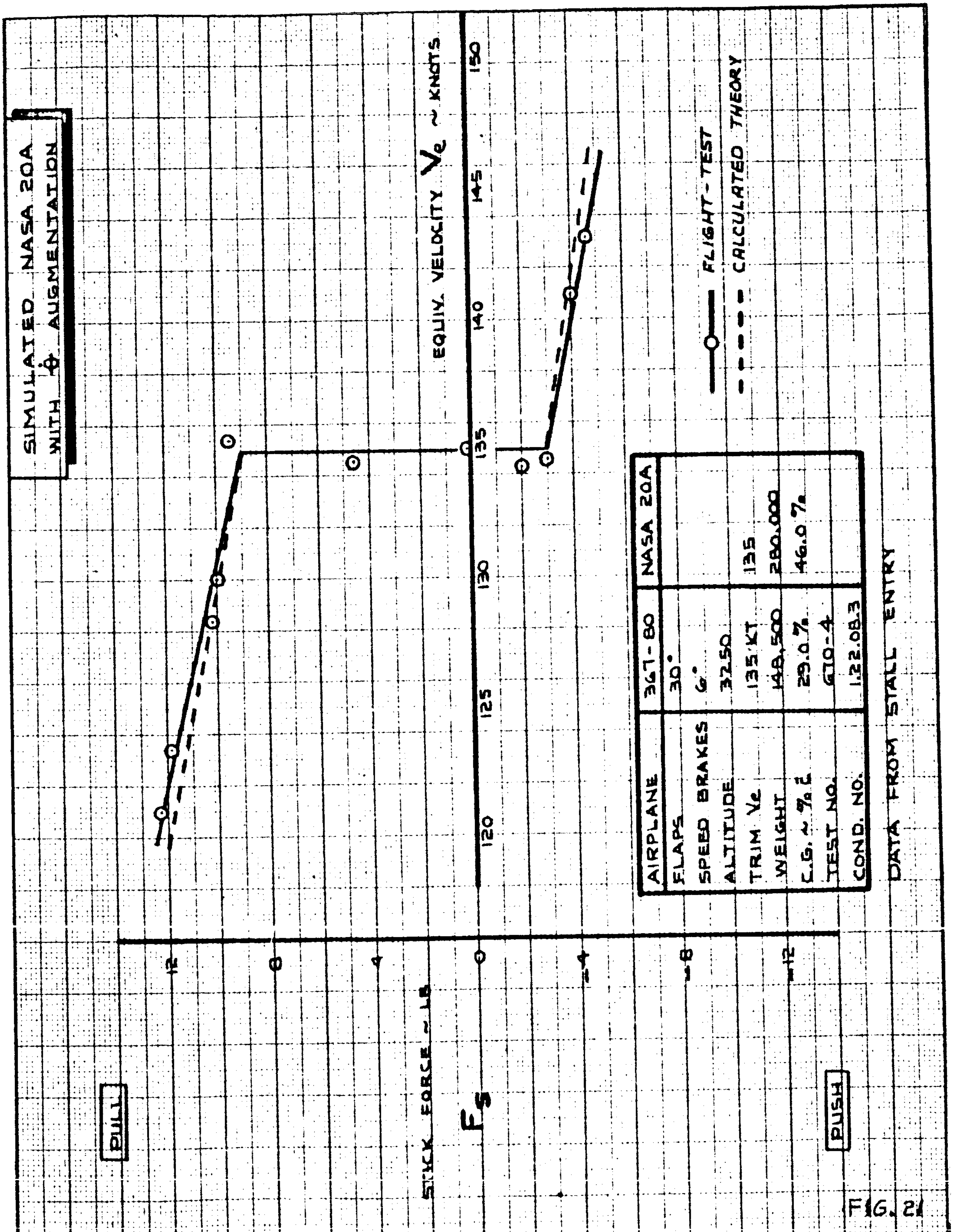

AIRPLANE	367-80	NASA 20A
FLAPS	30°	
SPEED BRAKES	6°	
ALTITUDE	3250	
TRIM V_e	135 KT	135
WEIGHT	148,500	280,000
C.G. ~ % $\bar{c}$	29.0 %	46.0 %
TEST NO.	670-4	
COND. NO.	1.22.08.3	

FIG. 21

CALC	TAYLOR	REVISED	DATE
CHECK			
APR			
APR			

SPEED STABILITY
STICK FORCE VS SPEED

THE BOEING COMPANY

NASA 20A

D6-10743

SIMULATED NASA 20A
WITH $\dot{\theta}$ AUGMENTATION

AIRPLANE	367-80	NASA 20A
FLAPS	30°	
SPEED BRAKES	6°	
EQUIV. VEL. Ve	135	135 KTS.
GROSS WT.	150,500	280,000
C.G. ~ % $\bar{c}$	28.9 %	46.0 %
ALTITUDE	3400	
TEST NO.	670-4	
COND. NO.	1.22.08.4	

DATA FROM WIND-UP TURN MANEUVER

$\delta_{E_{SST}}/\delta_{COL} = -2.6$

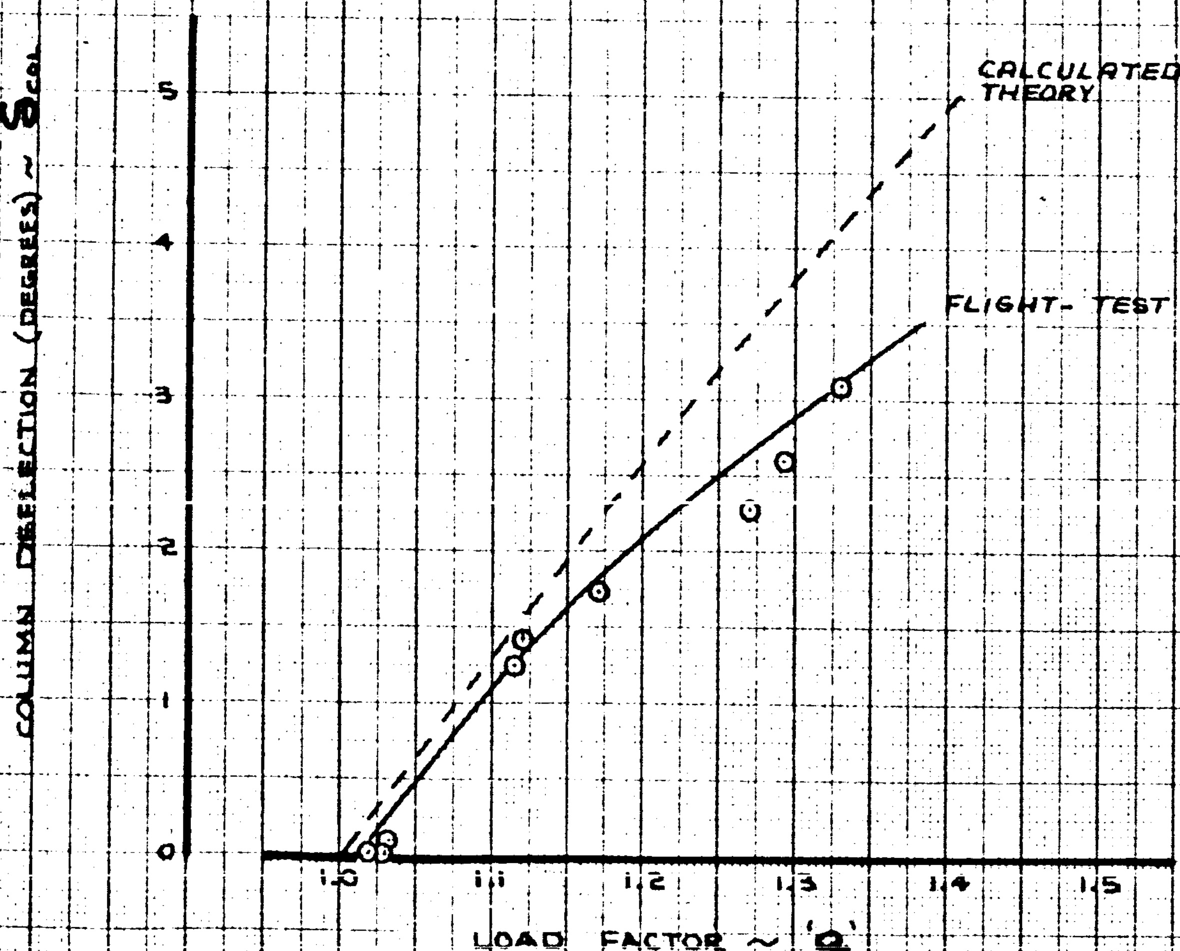

FIG. 22

CALC	TAYLOR		REVISED	DATE	NORMAL ACCELERATION VS. COLUMN CHARACTERISTICS	NASA 20A
CHECK						D6-10743
APR					THE BOEING COMPANY	PAGE 39
APR						

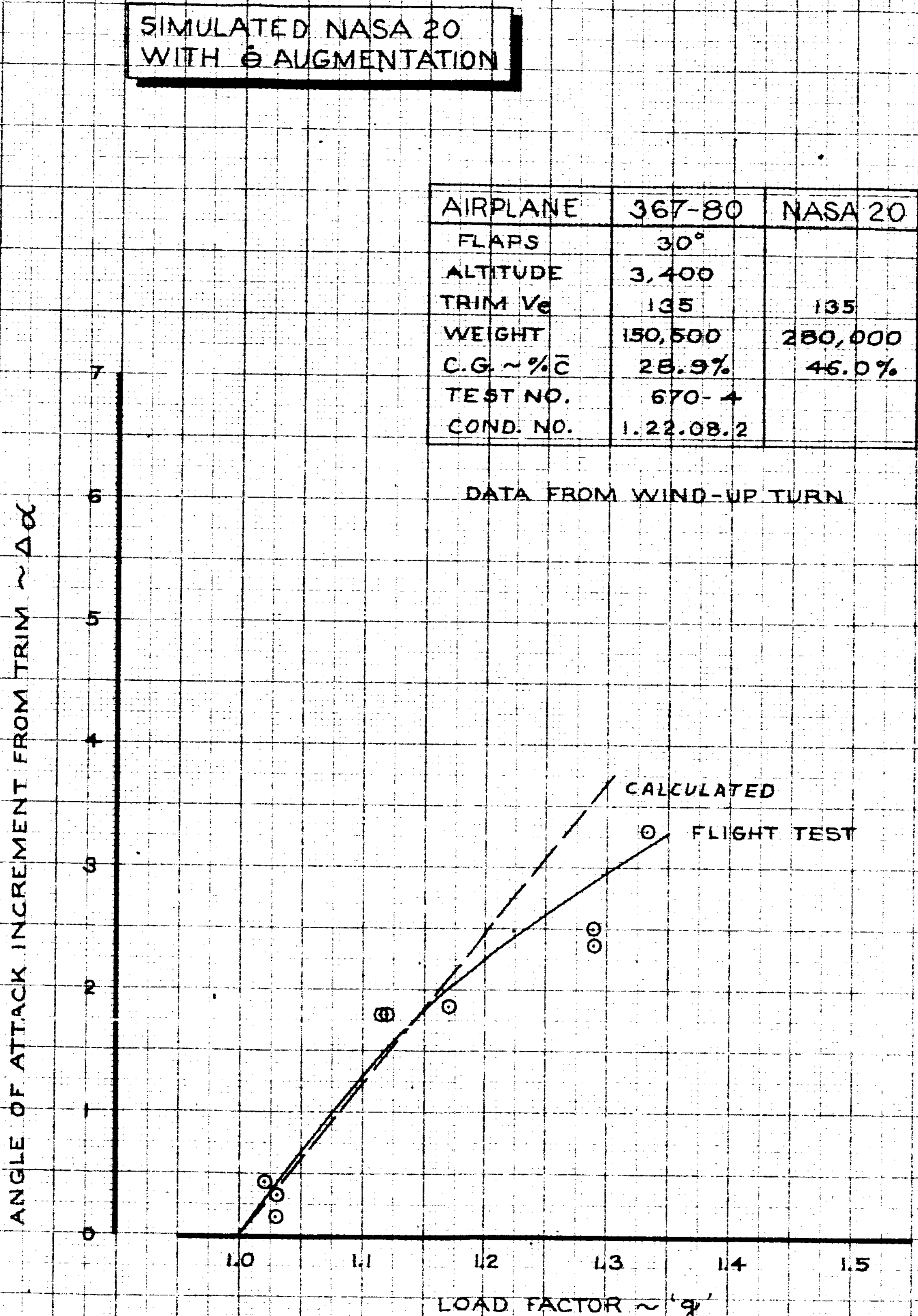

FIG. 23

CALC	TAYLOR	REVISED	DATE	NORMAL ACCELERATION Vs. ANGLE OF ATTACK	NASA 20A
CHECK		STEMWELL	1-28-66		D6-10743
APR					
APR				THE BOEING COMPANY	PAGE 40

TD 461 C-R4

SIMULATED NASA 20A WITH $\dot{\theta}$ AUGMENTATION

AIRPLANE	367-80	NASA 20A
FLAPS	30°	
SPEED BRAKES	6°	
ALTITUDE	3400	
TRIM Ve	135 KT	135 KT
WEIGHT	150,500	280,000
C.G. ~ % $\bar{c}$	28.9 %	46 %
TEST NO.	670-4	
COND. NO.	1.22.08.2	

DATA FROM WIND-UP TURN MANEUVER

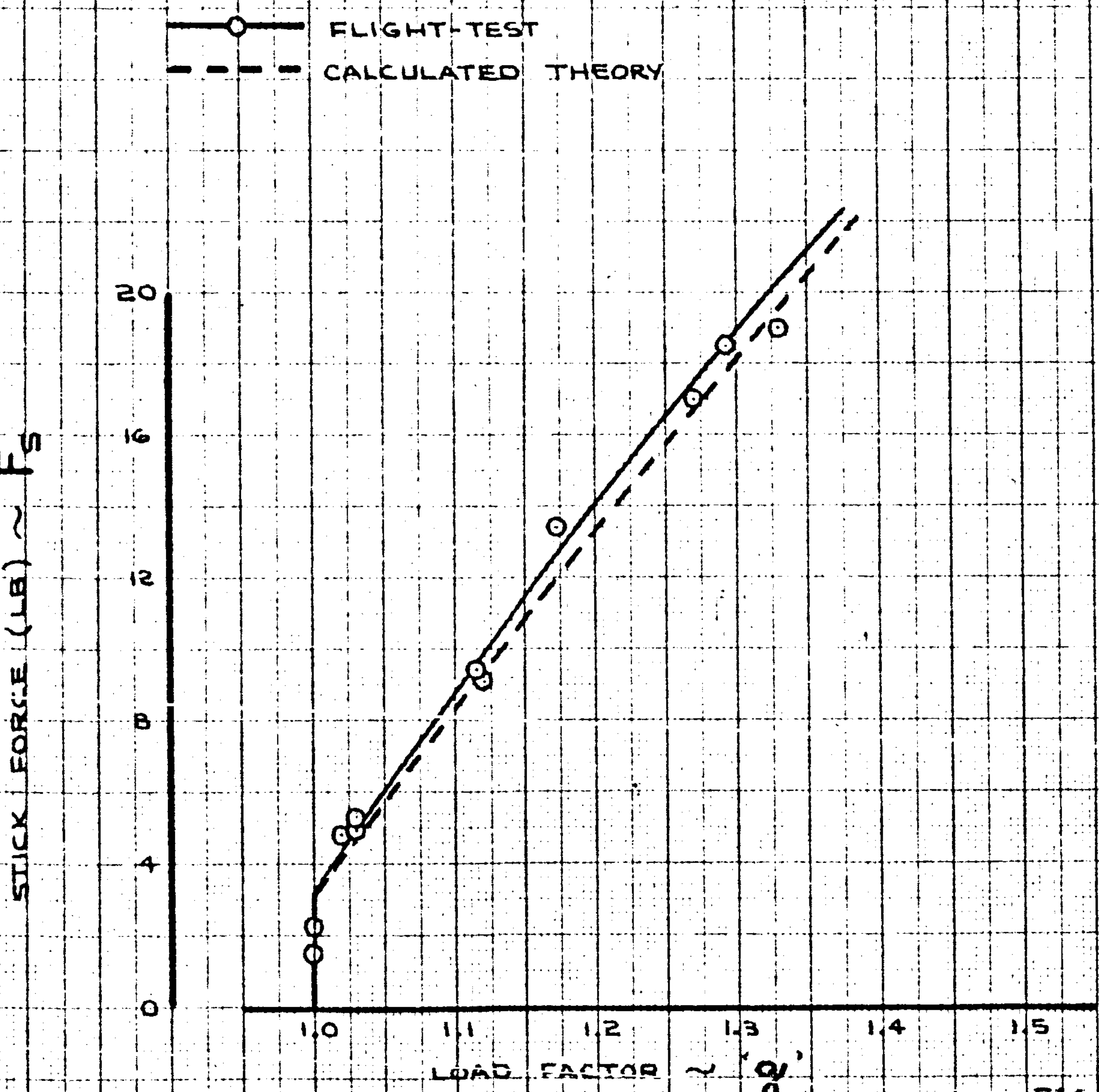

FIG. 24

CALC	TAYLOR		REVISED	DATE
CHECK				
APR				
APR				

NORMAL ACCELERATION VS. FORCE CHARACTERISTICS

NASA 20A

D6-10743

THE BOEING COMPANY

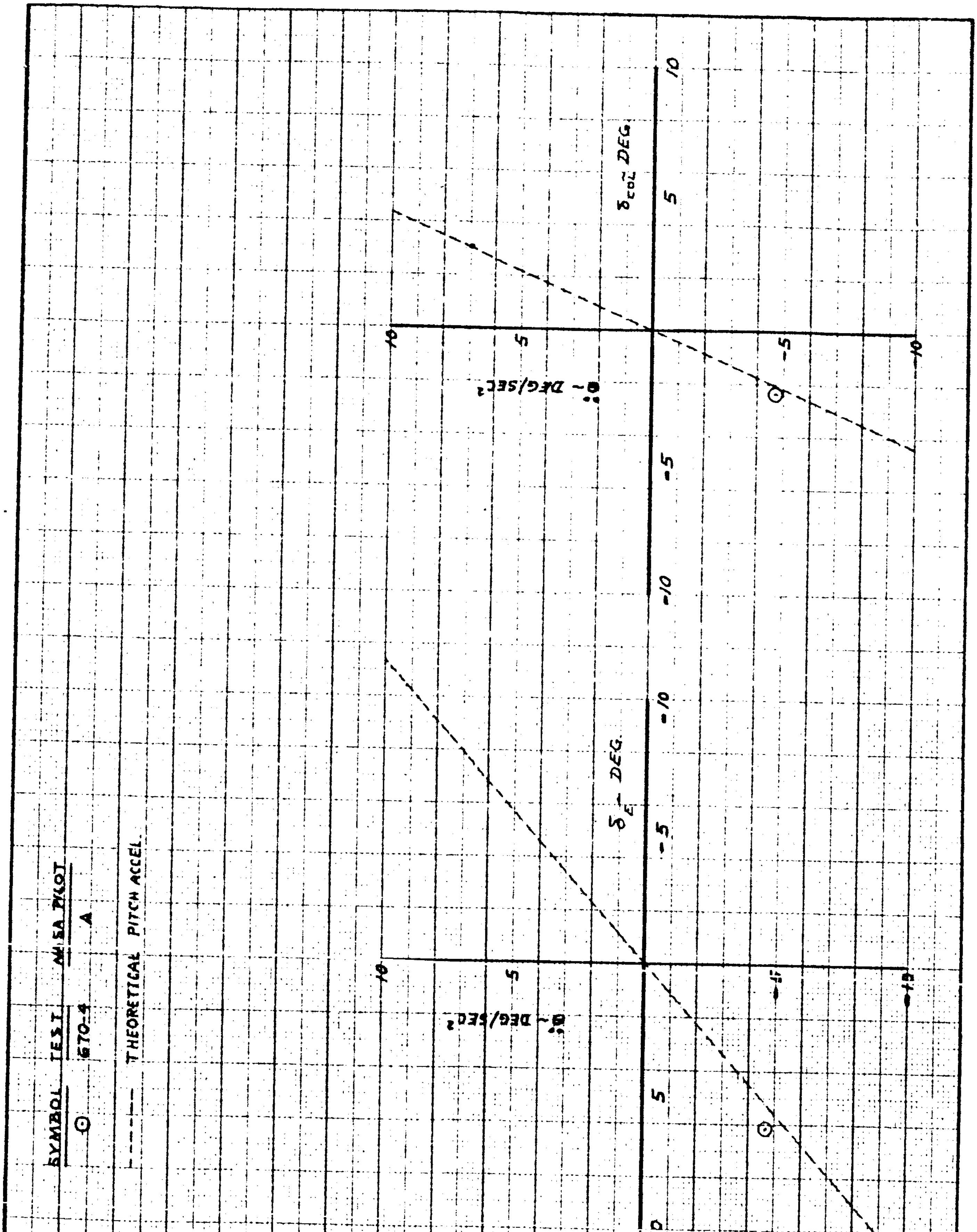

FIG. 25

CALC	D J BECK	11-18-65	REVISED	DATE
CHECK				
APR				
APR				

PITCH ACCELERATION OF THE NASA 20A SST (BASIC CG ~ $\dot{\theta}$ SAS)

D6-10743

THE BOEING COMPANY

TD 461 C-R4

	367-80	NASA 20A
FLAPS	30°	
SPEED BRAKES	6°	
V_e	135 KTS	135 KTS
H_p	2960 FT	
GW	141,700 LBS	280,000 LBS
CG	29.4% MAC	46.0% MAC
TEST NO	670-4	

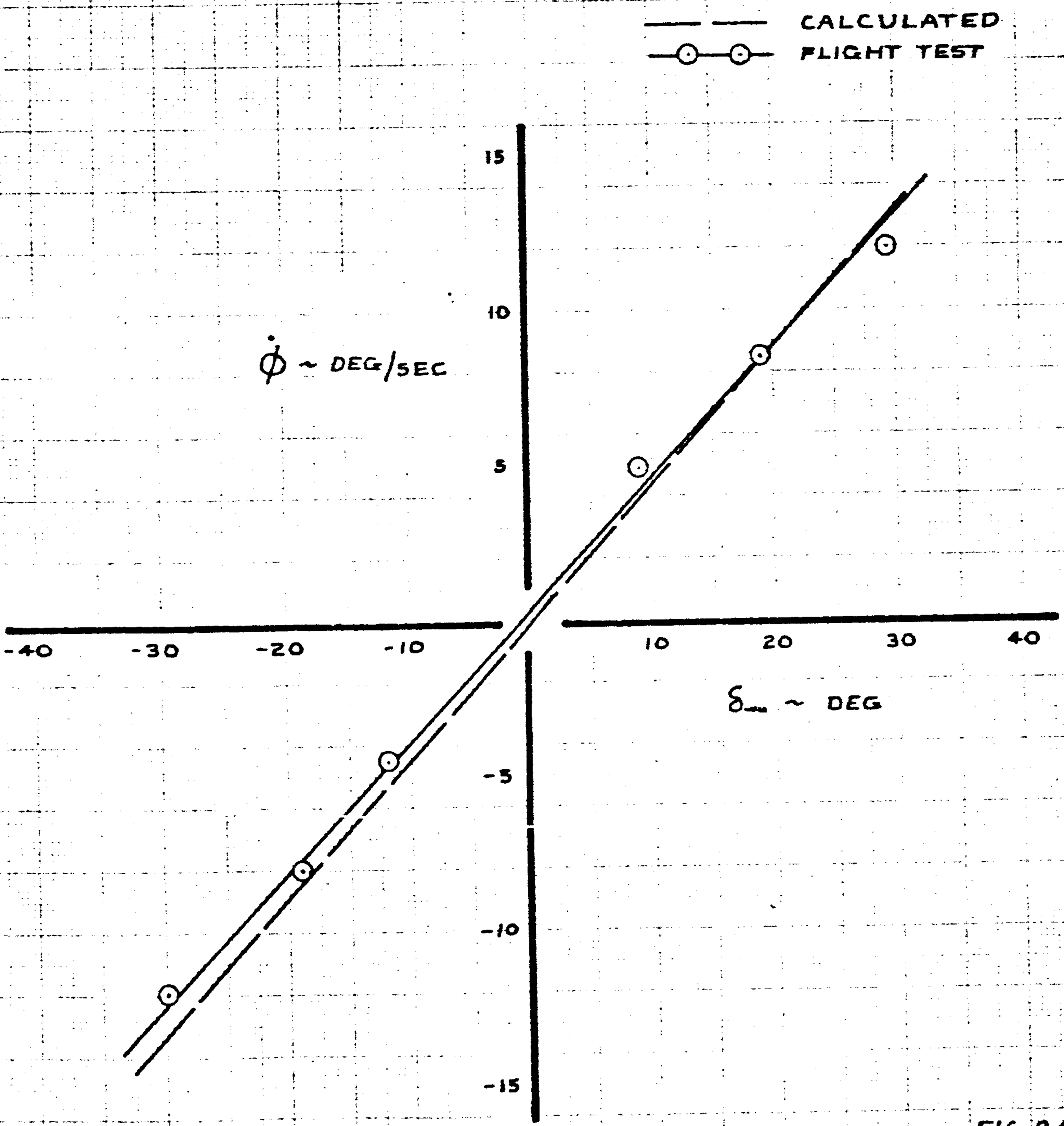

FIG. 26

CALC	RCS	8/11/65	REVISED	DATE	LATERAL CONTROL RESPONSE	SIMULATED NASA 20A
CHECK			RCS	9/27/65	STEADY STATE ROLL RATES	D6-10743
APR						
APR					THE BOEING COMPANY	PAGE 43

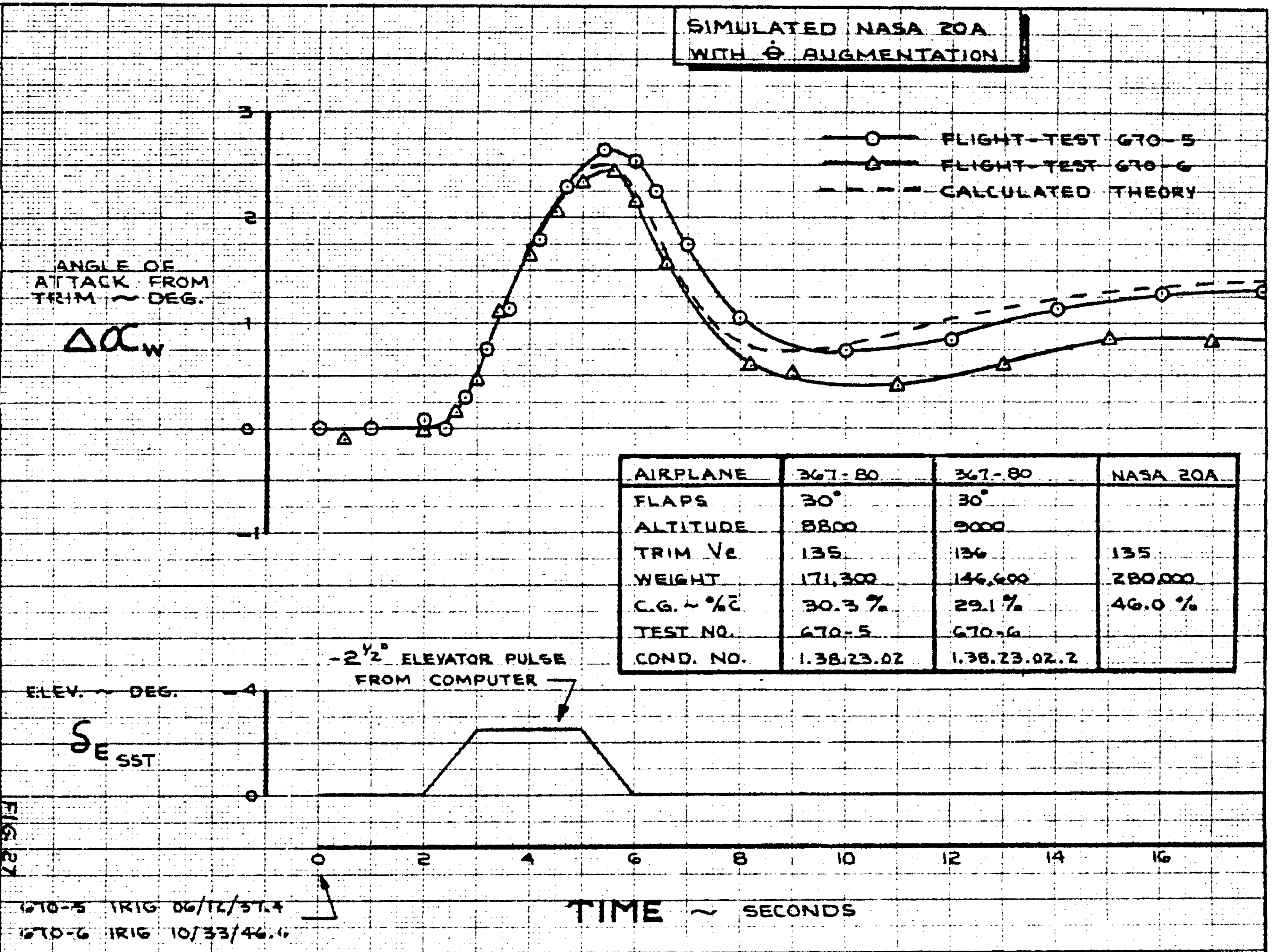

AIRPLANE	367-80	367-80	NASA 20A
FLAPS	30°	30°	
ALTITUDE	8800	9000	
TRIM V_e	135	136	135
WEIGHT	171,300	146,600	280,000
C.G. ~ %$\bar{c}$	30.3 %	29.1 %	46.0 %
TEST NO.	670-5	670-6	
COND. NO.	1.38.23.02	1.38.23.02.2	

FIG. 27

CALC	TAYLOR	REVISED	DATE
CHECK			
APR			
APR			

SHORT PERIOD CHARACTERISTICS

THE BOEING COMPANY

NASA 20A

D6-10743

TD 461 C-R4

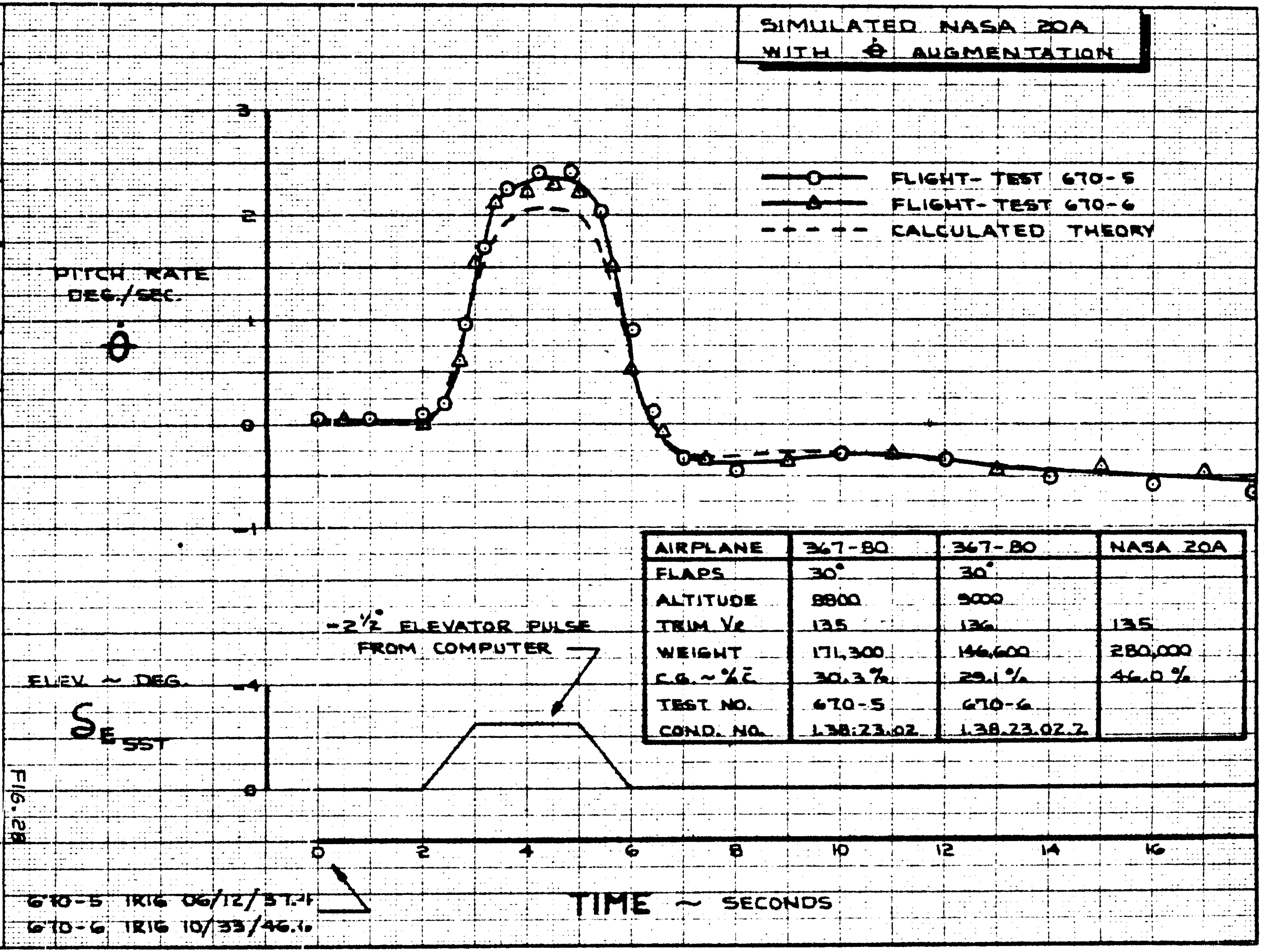

AIRPLANE	367-80	367-80	NASA 20A
FLAPS	30°	30°	
ALTITUDE	8800	9000	
TRIM V_e	135	136	135
WEIGHT	171,300	146,600	280,000
C.G. ~ %$\bar{c}$	30.3%	29.1%	46.0%
TEST NO.	670-5	670-6	
COND. NO.	1.38:23.02	1.38.23.02.2	

FIG. 28

CALC	TAYLOR	REVISED	DATE
CHECK			
APR			
APR			

SHORT PERIOD CHARACTERISTICS

THE BOEING COMPANY

NASA 20A

D6-10743

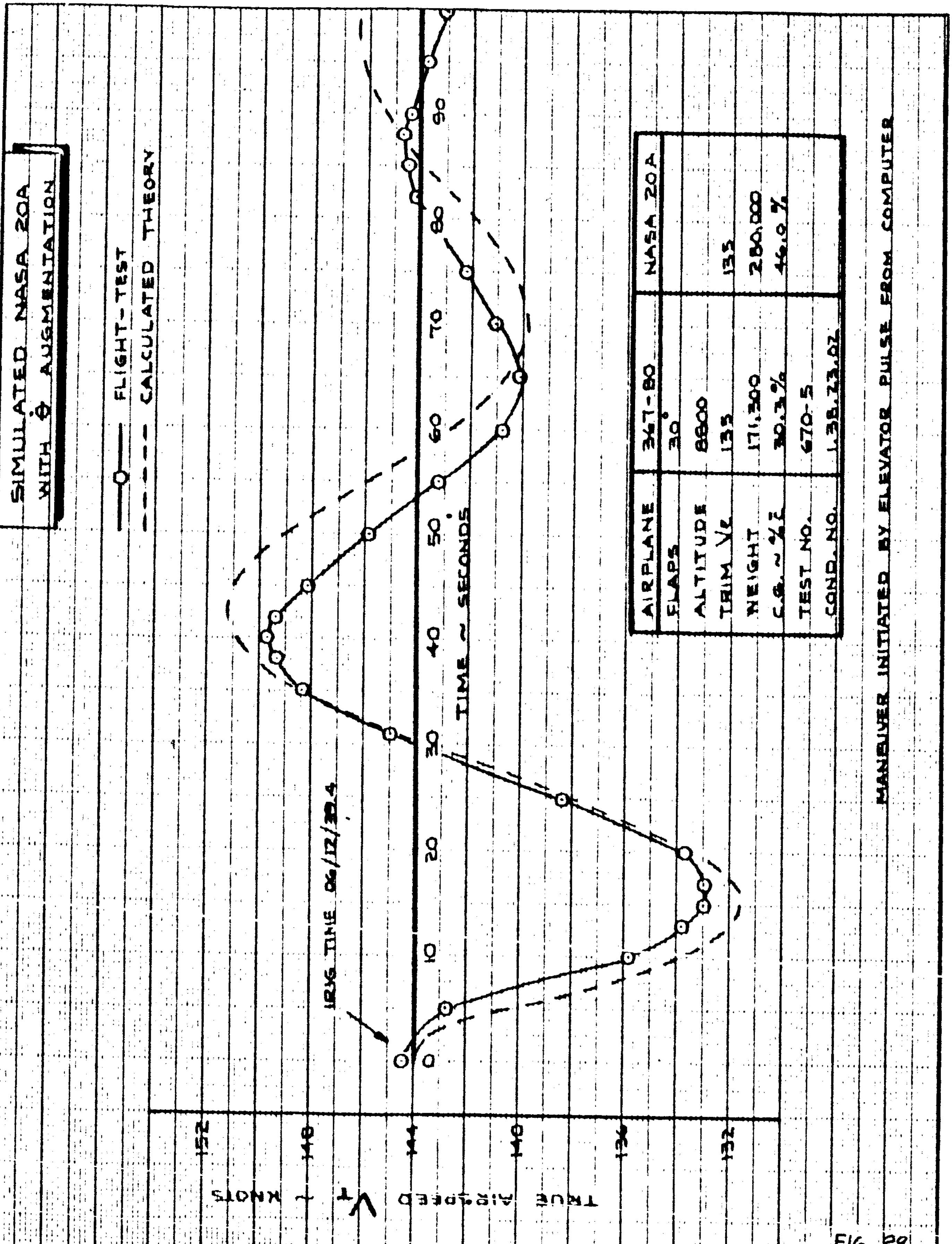

FIG. 29

CALC	TAYLOR	REVISED	DATE	PHUGOID CHARACTERISTICS	NASA 20A
CHECK					
APR					D6-10743
APR				THE BOEING COMPANY	PAGE 46

DUTCH ROLL NASA 20A

LAT.-DIR. SAS : $\dot{\beta}$ DAMPER
LONG. SAS : $\dot{\theta}$ FEEDBACK

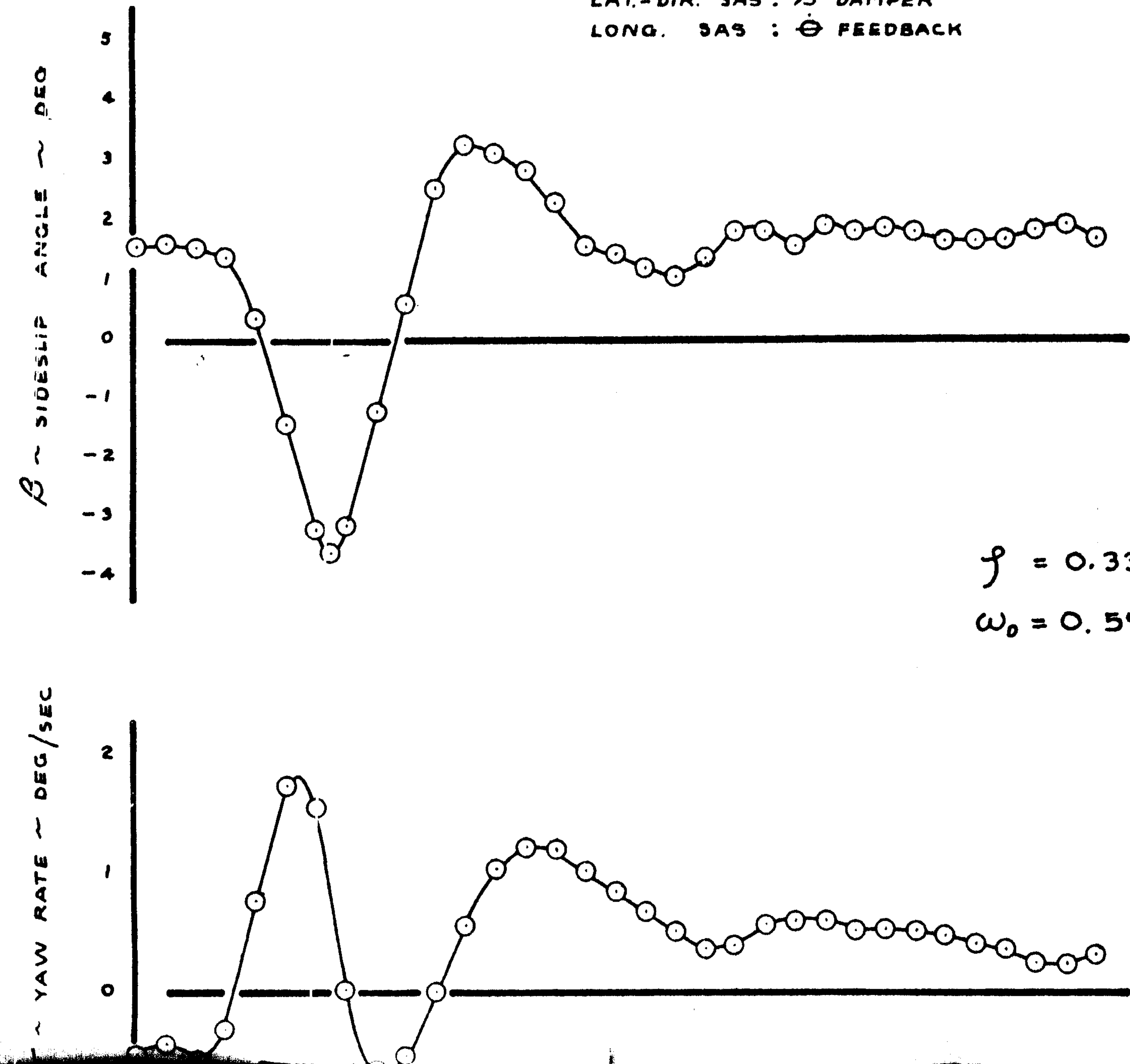

$\zeta = 0.33$

$\omega_0 = 0.593$ RAD/SEC

407-1

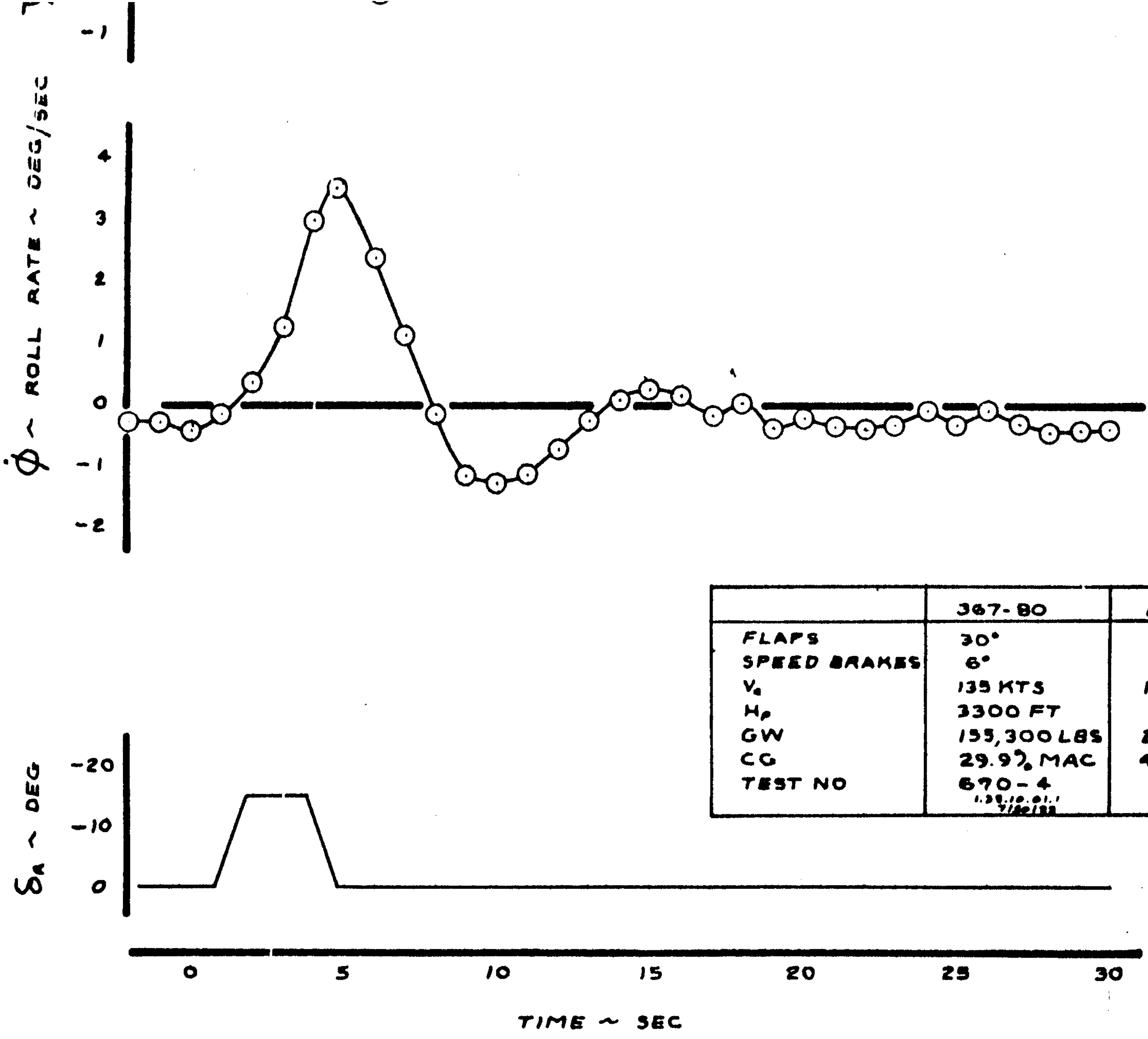

	367-80	NASA 20A
FLAPS	30°	
SPEED BRAKES	6°	
V_e	135 KTS	135 KTS
H_p	3300 FT	
GW	155,300 LBS	280,000 LBS
CG	29.9% MAC	46.0% MAC
TEST NO	670-4	

SAM 9/1/65
Rc 9/22/65

FIG. 30

SUPPLEMENTARY TEST CONFIGURATIONS - NASA 20

$(\dot{\theta} + \Delta\alpha)$ Longitudinal Augmentation

The pitch rate feedback of the NASA 20 A configuration causes the short period to have a high damping ratio (.938) in addition to the desired increased frequency. This heavy damping appears to the pilot as a slight sluggishness in the airplane response and as low static stability, as the airplane is slow in returning to trim when displaced. The increase in stick gearing reduces the stick force per knot to one-half of its basic value, which also appears to the pilot as reduced static stability.

In order to overcome these shortcomings of the basic pitch rate longitudinal augmentation, an angle of attack feedback was added. With the $(\dot{\theta} + \Delta\alpha)$ combination, the short period was quickened, but the damping ratio was held near .7, which is the optimum for quick control response without appreciable overshoot. The stick gearing was increased to hold the stick deflection and force per "g" constant. The elevator equation is:

$$\delta E = \left[\frac{\delta E}{\delta col}\right]_{Basic} \times 4\delta_{col} + 1.46\dot{\theta} + 1.5\,\Delta\alpha$$

This augmentation system is not necessarily the optimum for the NASA-20 configuration. The $\Delta\alpha$ feedback was added to the existing $\dot{\theta}$ feedback in order to show the improvement possible, and as a result the control sensitivity is very high.

Simulation Documentation

The flight test data from the $(\dot{\theta} + \Delta\alpha)$ longitudinal augmentation system documentation are shown in **Fig. 31 to 39**, compared with the theoretical characteristics. Fig. 31 and 32 show the speed stability testing. Both the column deflection and stick force per knot are simulated very prdcisely. These characteristics are close to those of the basic NASA-20 configuration, as was desired. Figs. 33 to 35 show the wind-up turn data. The simulation is good up to 1.25 load factor, but the 367-80 load factor falls off slightly from the theoretical above this point. Data from the pitch reversal are shown in Fig. 36. The longitudinal control response was simulated well.

The airplane response to an elevator pulse is shown in Figs. 37 to 39. The airplane response and the short period and phugoid modes are simulated very accurately.

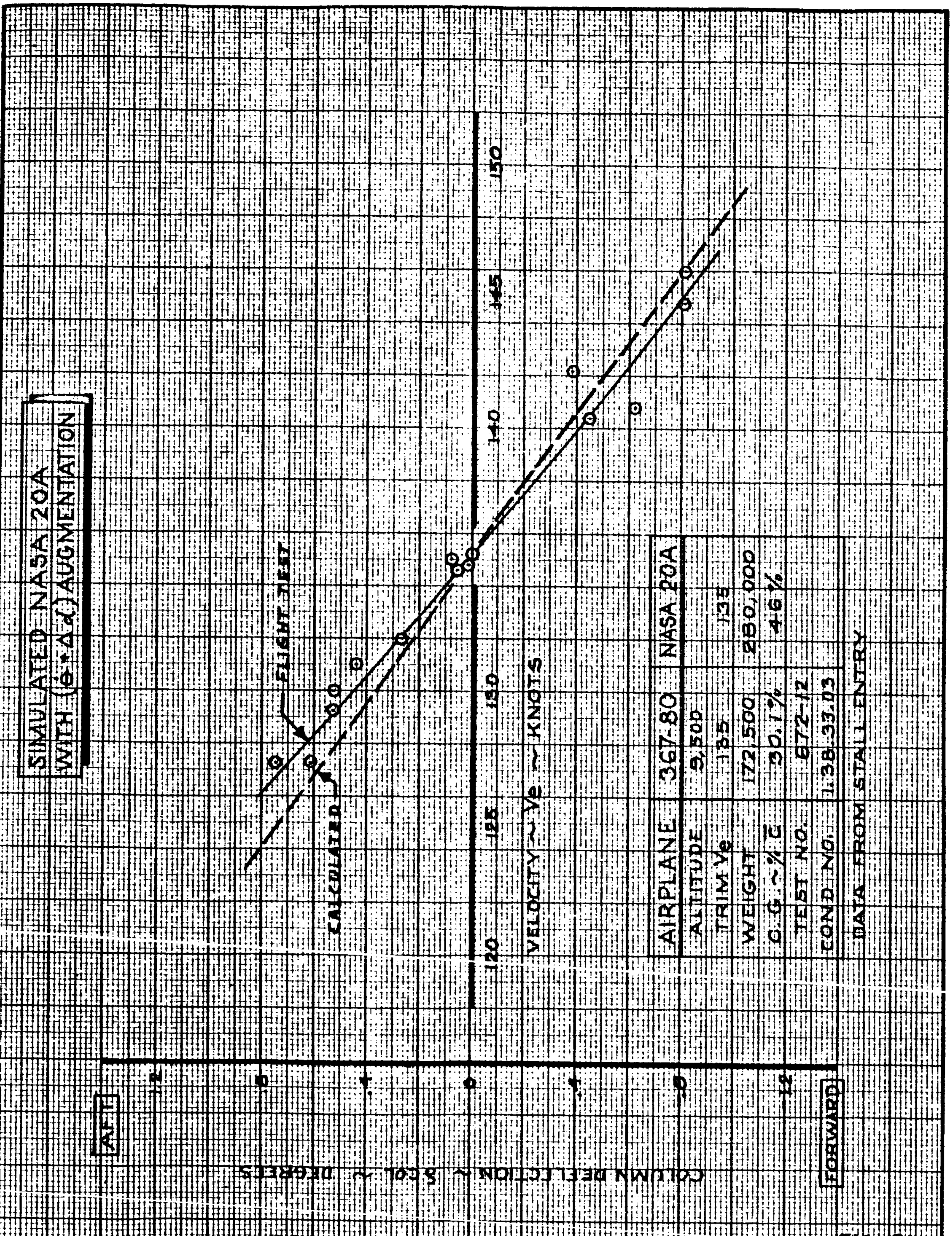

FIG. 31

CALC	TAYLOR		REVISED	DATE	COLUMN Vs. SPEED CHARACTERISTICS	NASA 20A
CHECK			R S	2-10-66		D6-10743
APR						
APR					THE BOEING COMPANY	PAGE 50 B

TD 461 C-R4

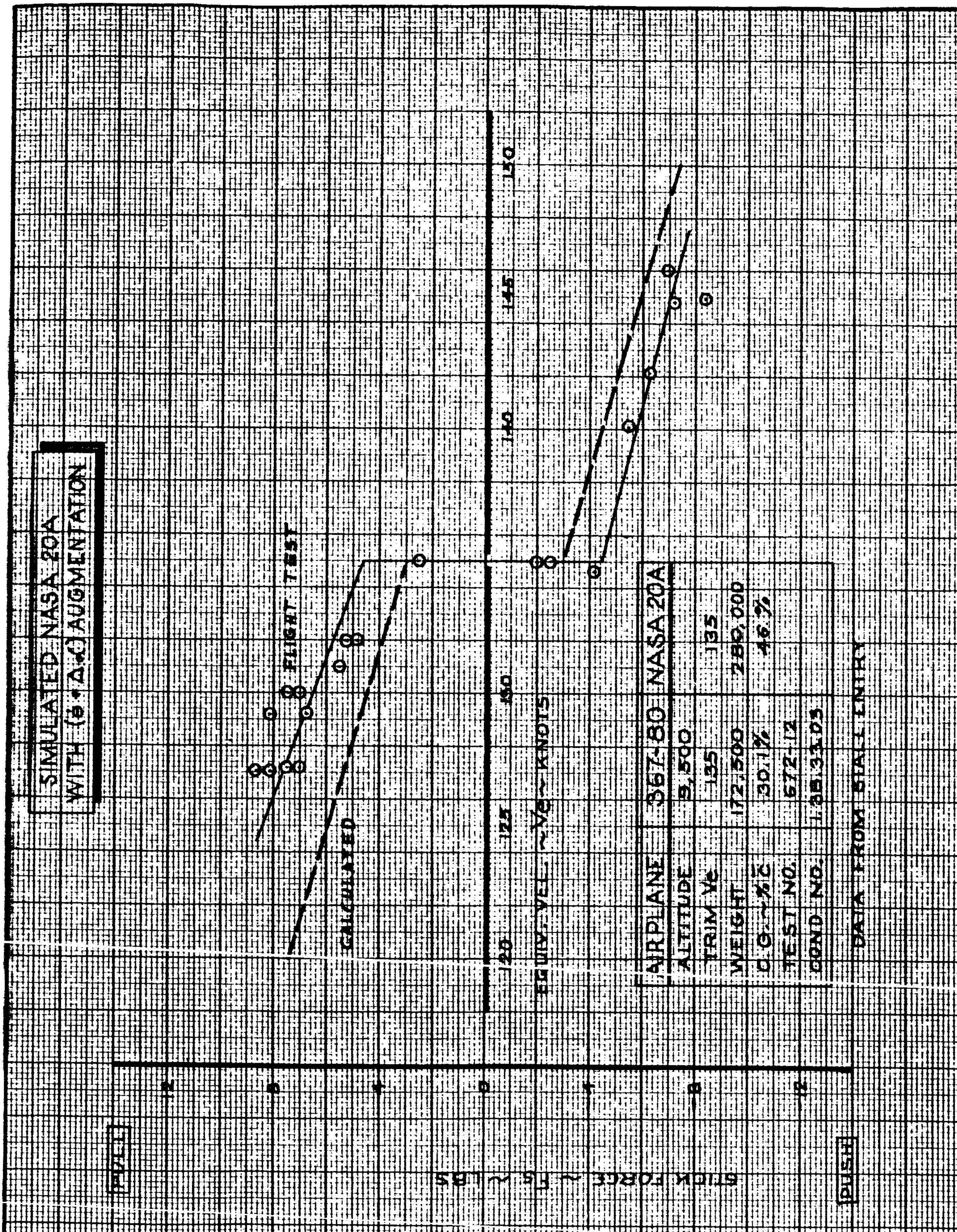

FIG. 32

CALC	TAYLOR		REVISED	DATE	SPEED STABILITY STICK FORCE Vs. SPEED	NASA 20A
CHECK			STEMWELL	2-10-66		D6-10743
APR						
APR					THE BOEING COMPANY	PAGE 51 B

TD 461 C-R4

SIMULATED NASA 20A
WITH ($\dot{\theta}+\Delta_{\alpha}$) AUGMENTATION

AIRPLANE	367-80	NASA 20A
FLAPS	30°	
TRIM Ve	135	135
WEIGHT	169,700	280,000
C.G. ~ % $\bar{c}$	30.3%	46.0%
TEST NO.	672-12	
COND. NO.	1.38.33.02	

DATA FROM WIND-UP TURN MANEUVER

$\delta_{E_{SST}}/\delta_{COL} = -5.2$

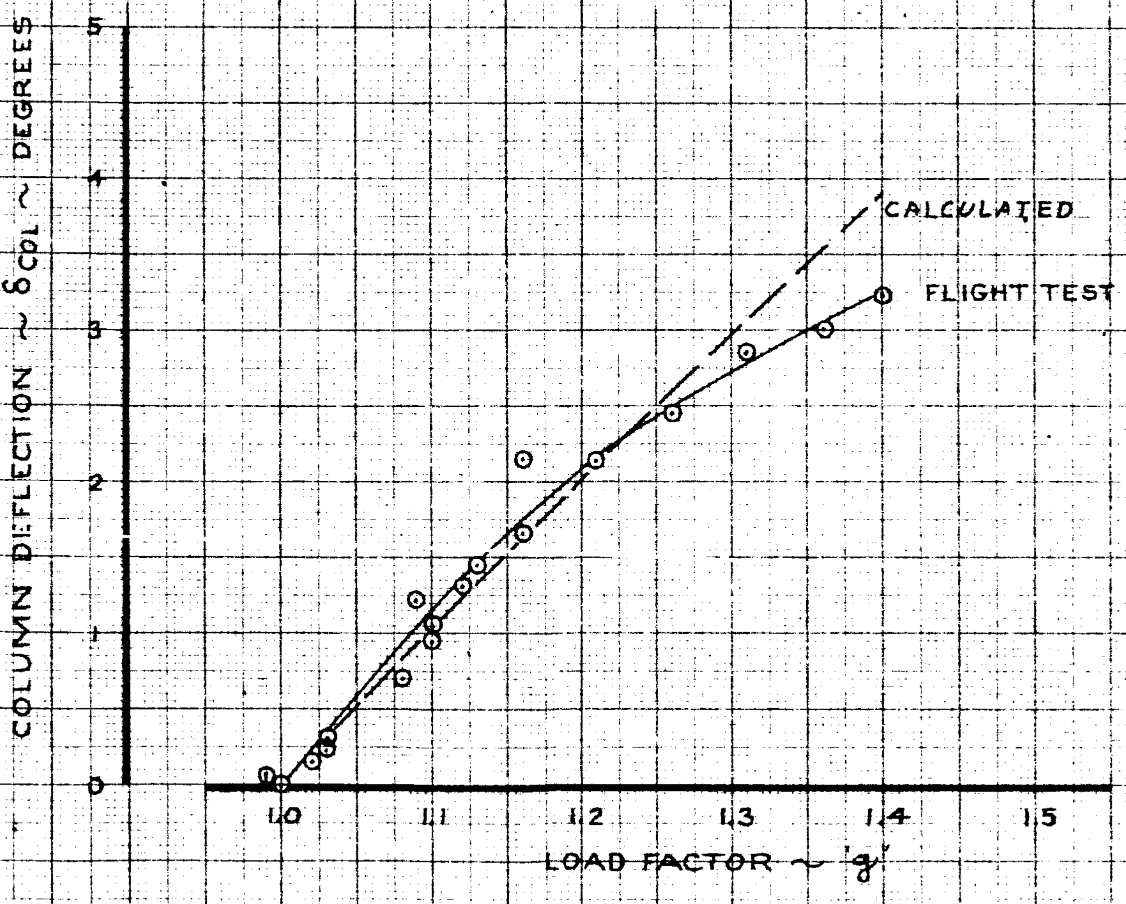

FIG. 33

			REVISED	DATE		
CALC	TAYLOR				NORMAL ACCELERATION Vs. COLUMN CHARACTERISTICS	NASA 20A
CHECK			STEMWELL	1-28-66		D6-10743
APR					THE BOEING COMPANY	PAGE 52
APR						

SIMULATED NASA 20A WITH ($\dot{\theta} + \Delta\alpha$) AUGMENTATION

AIRPLANE	367-80	NASA 20A
FLAPS	30°	
ALTITUDE	2,600	
TRIM Ve	135	135
WEIGHT	169,700	280,000
C.G. ~ % $\bar{c}$	30.3%	46.0%
TEST NO.	672-12	
COND. NO.	1.38, 33.02	

DATA FROM WIND-UP TURN

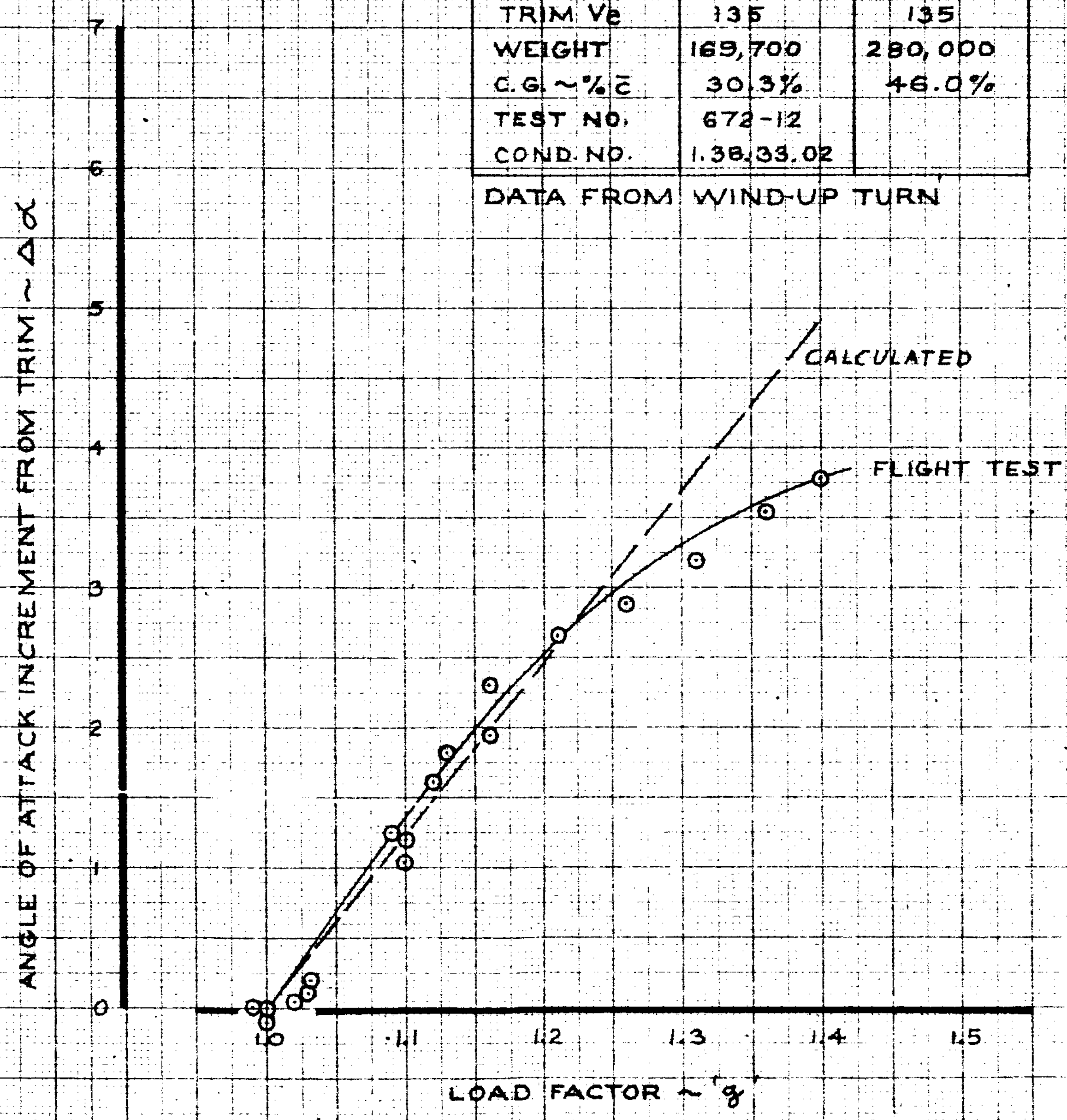

FIG. 34

CALC	TAYLOR	REVISED	DATE
CHECK		STEMWELL	1-31-66
APR			
APR			

NORMAL ACCELERATION Vs. ANGLE OF ATTACK

THE BOEING COMPANY

NASA 20A

D6-10743

TD 461 C-R4

SIMULATED NASA 20A
WITH ($\dot{\theta} + \Delta\alpha$) AUGMENTATION

AIRPLANE	367-80	NASA 20A
FLAPS	30°	
ALTITUDE	2,600	
TRIM Ve	135	135
WEIGHT	169,700	280,000
C.G. ~ % $\bar{c}$	30.3%	46.0%
TEST NO.	672-12	
COND. NO.	1.38.33.02	

DATA FROM WIND-UP TURN MANEUVER

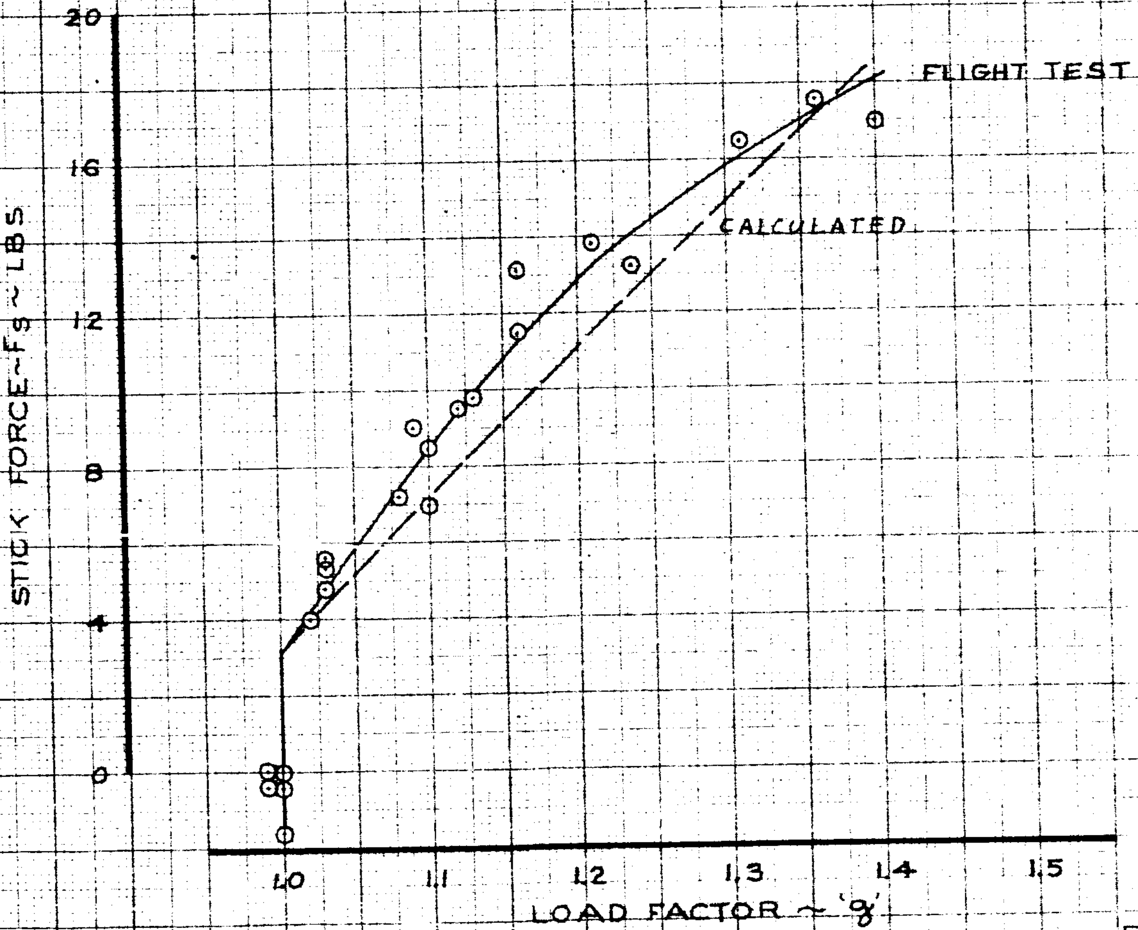

FIG. 35

CALC	TAYLOR		REVISED	DATE	NORMAL ACCELERATION Vs FORCE CHARACTERISTICS	NASA 20A
CHECK			STEMWELL	1-31-66		D6-10743
APR					THE BOEING COMPANY	PAGE 54
APR						

TD 461 C-R4

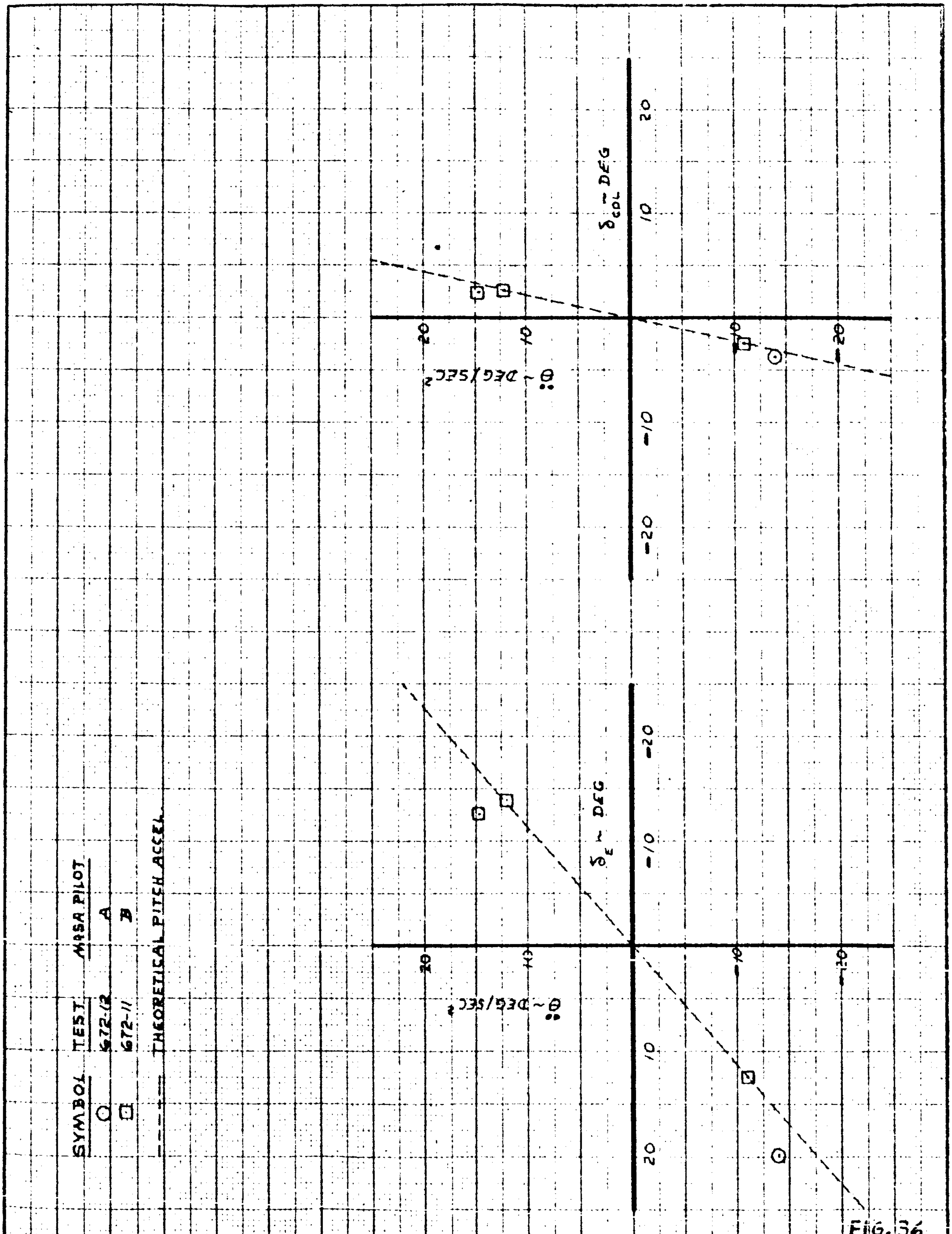

FIG. 36

CALC	DJ BECK	11-18-65	REVISED	DATE
CHECK				
APR				
APR				

PITCH ACCELERATION OF THE
NASA 20A SST (BASIC CG ~ $\dot{\theta}+\alpha$ SAS)

D6-10743

THE BOEING COMPANY

TD 461 C R4

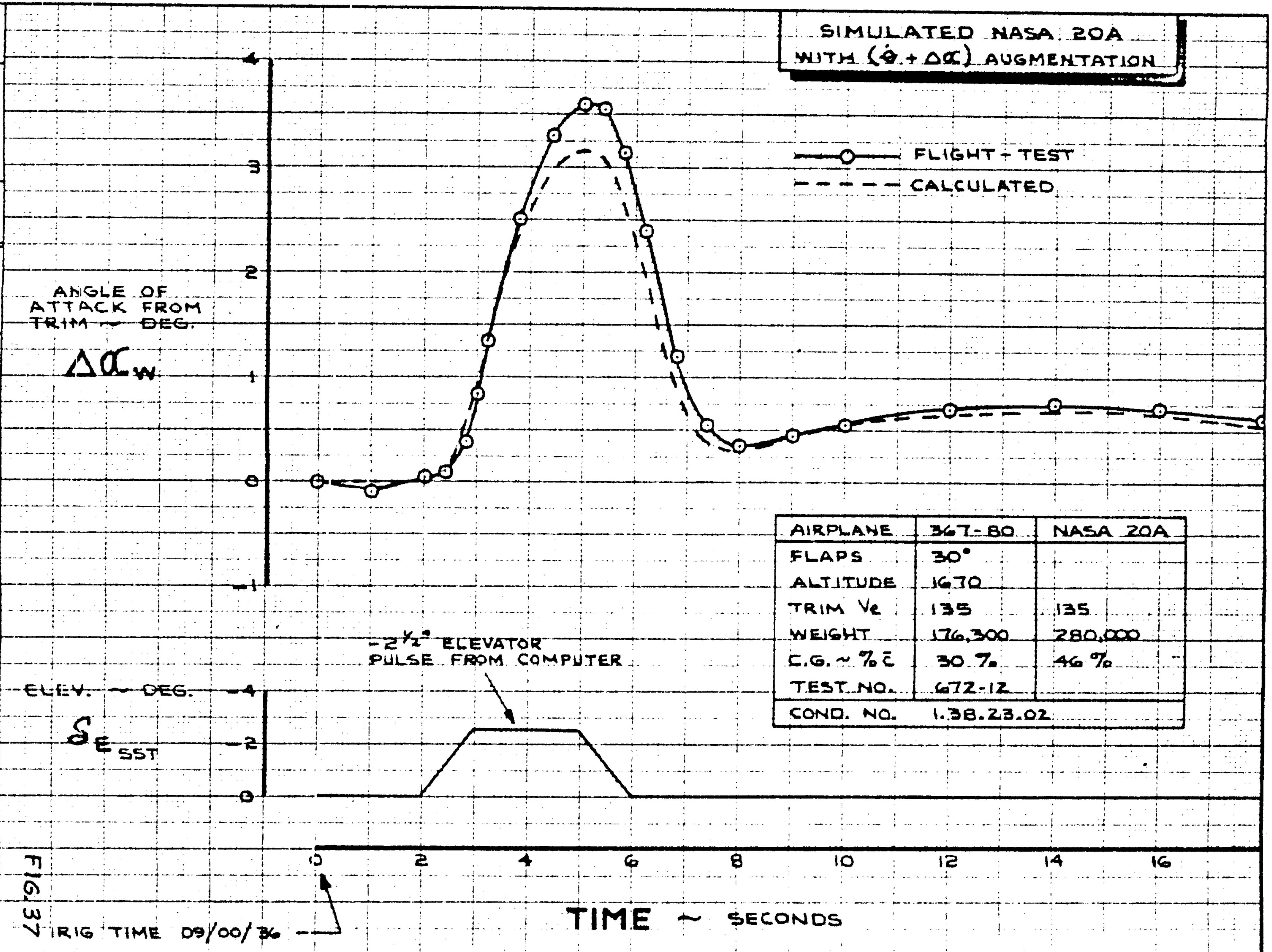

AIRPLANE	367-80	NASA 20A
FLAPS	30°	
ALTITUDE	1670	
TRIM Ve	135	135
WEIGHT	176,300	280,000
C.G. ~ % $\bar{c}$	30 %	46 %
TEST NO.	672-12	
COND. NO.	1.38.23.02	

FIG. 37

CALC	TAYLOR	REVISED	DATE
CHECK			
APR			
APR			

SHORT PERIOD CHARACTERISTICS

NASA 20A

D6-10743

THE BOEING COMPA

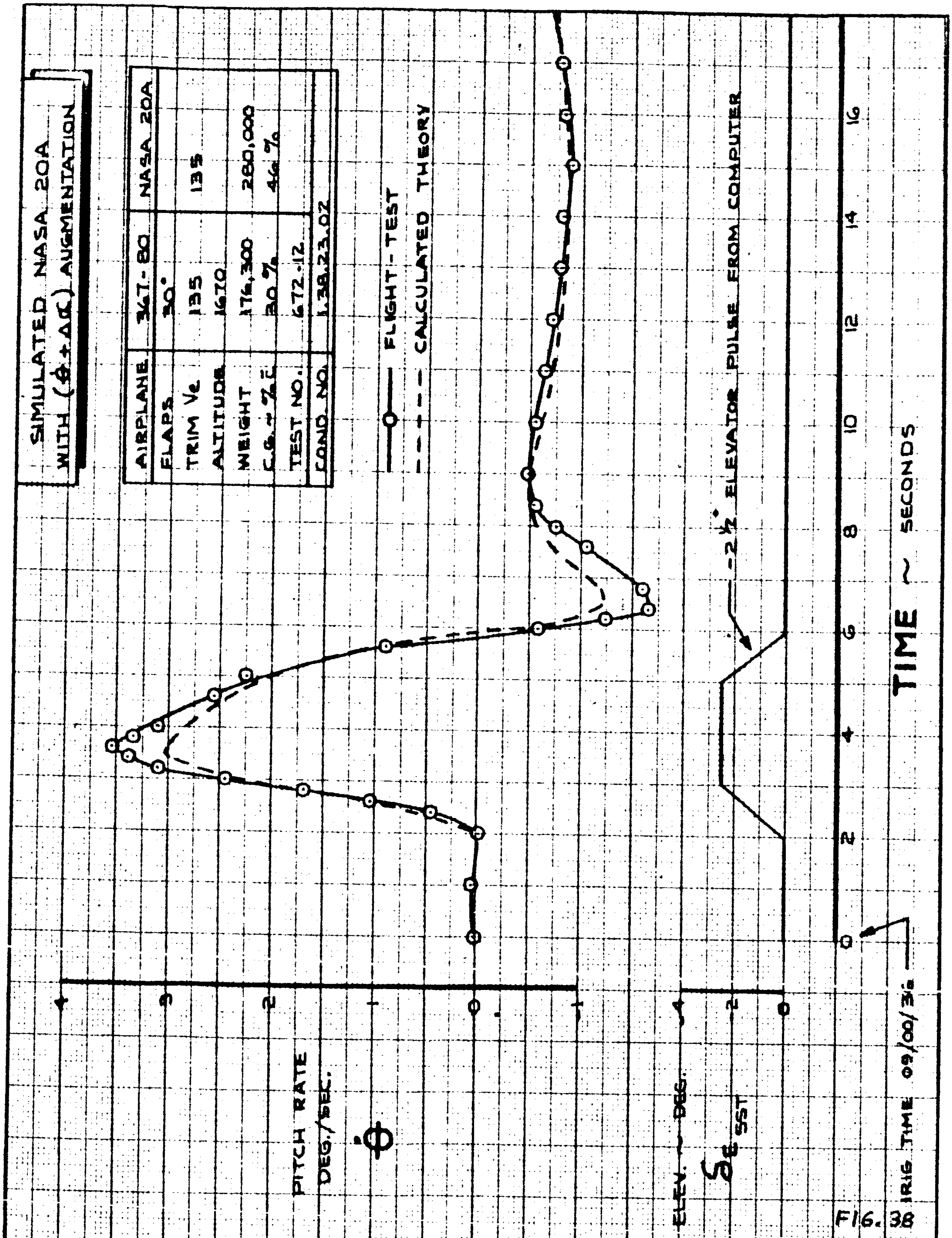

FIG. 38

CALC	TAYLOR		REVISED	DATE	SHORT PERIOD CHARACTERISTICS	NASA 20A
CHECK						
APR						D6-10743
APR						

...ING COMPANY

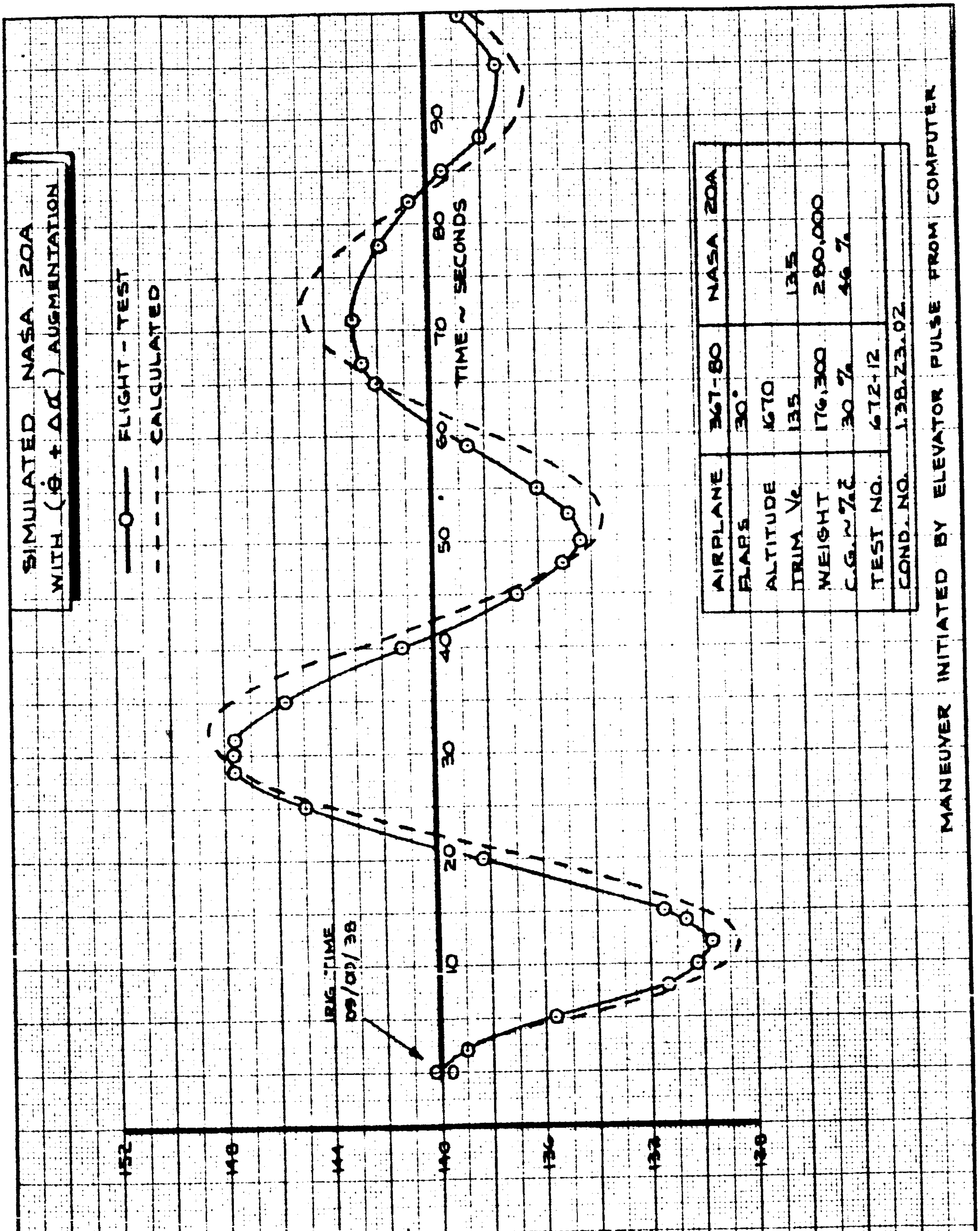

FIG. 39

CALC	TAYLOR		REVISED	DATE	PHUGOID CHARACTERISTICS	NASA 20A
CHECK						D6-10743
APR						

THE BOEING CO

Aft C. G.

An aft C. G. configuration was evaluated with the static margin reduced to 3%. (Basic NASA-20 static margin = 9.75%). This was implemented by reducing the value of C_{m_α} from -.458 to -.141. No other derivatives were changed. The stick gearing and force characteristics were not changed, which reduced the maneuvering stick force from 31 to 14 lbs/g.

The flight test data from the simulation documentation maneuvers are shown in Figs. 40 to 48, compared with the theoretical characteristics. The speed stability tests are shown in Figs. 40 and 41. The 367-80 trim speed for these tests was 3 kts high. The slopes of the column-velocity and stick force-velocity curves are slightly different from the predicted characteristics. This was caused by the errors in C_{m_α}, caused by the speed brakes, thrust reversers, and errors in the calibration of the basic 367-80 characteristics, which cause difficulty in simulating low static margin configurations. The data from a wind-up turn are shown in Figs. 42 to 44. There is an offset in the column-load factor curve caused by the fact that pilot had trouble trimming this configuration and was using a 1.5° column deflection to hold trim speed. The slope of this curve is accurate, however. The angle-of-attack to maneuver is shown in Fig. 43. This simulation is accurate up to a load factor of 1.2 g's. The stick force per "g" is shown in Fig. 44. There is a slight difference in the slope of the two curves, caused by the static stability error, but the simulation quality is good. The pitch reversal data are shown in Fig. 45. The simulation of the longitudinal control power and sensitivity was accurate. The airplane response to an elevator pulse, introduced by the computer, is shown in Figs. 46 and 47. The initial angle-of-attack response is precise, but there is an error between the two after the pulse. This was caused by the 367-80 static stability being higher than that of the NASA-20 aft C. G. The pitch rate response is accurate for the entire pulse. The phugoid characteristics are shown in Fig. 48. The 367-80 has approximately the correct phugoid frequency and damping, but the airspeed changed because the airplane was not in trim at the start of the pulse.

There were no lateral-directional documentation maneuvers done for this configuration, as it was identical to the NASA 20A configuration.

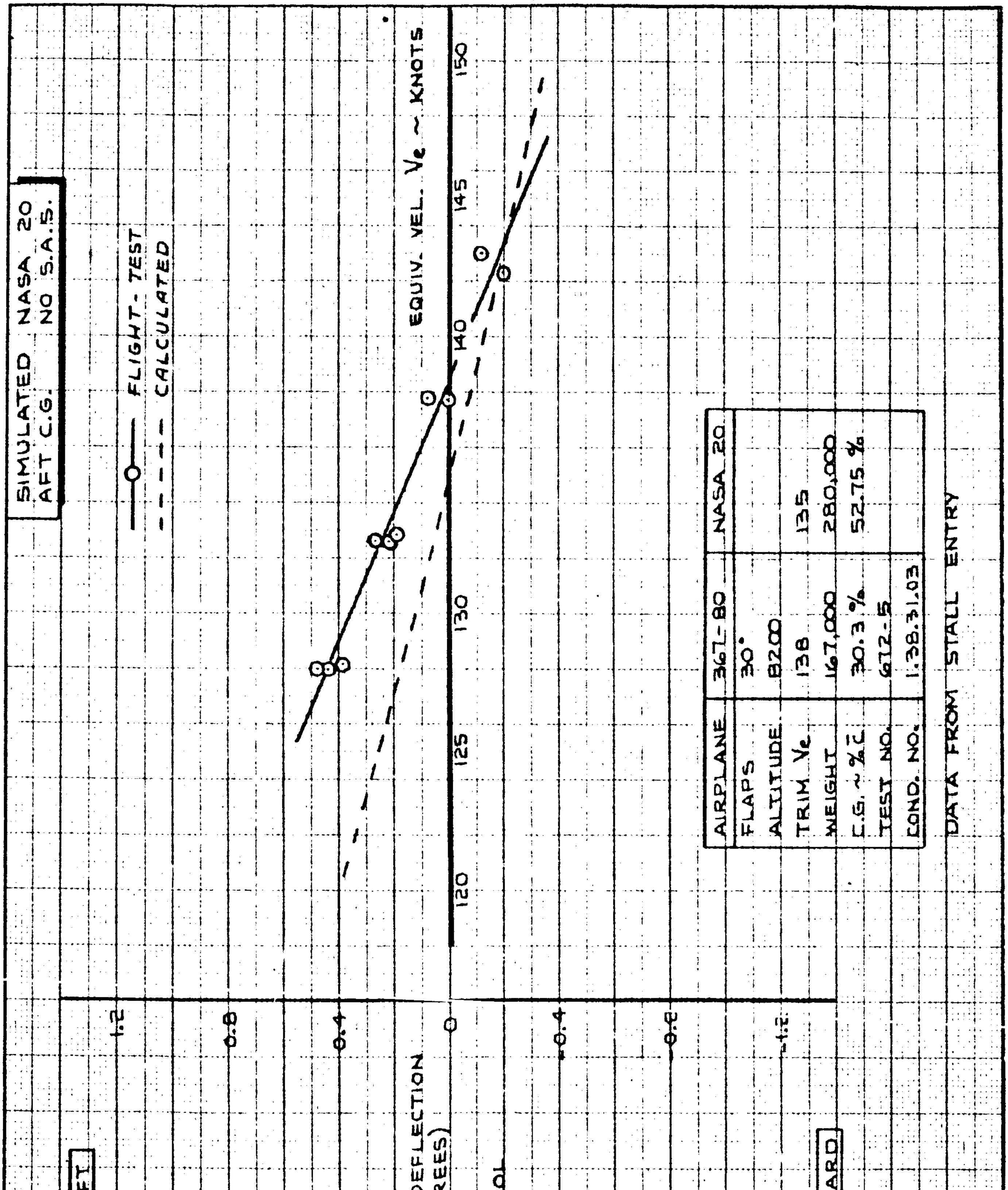

AIRPLANE	367-80	NASA 20
FLAPS	30°	
ALTITUDE	8200	
TRIM V_e	138	135
WEIGHT	167,000	280,000
C.G. ~ %$\bar{C}$	30.3 %	52.75 %
TEST NO.	672-5	
COND. NO.	1.38.31.03	

FIG. 40

CALC	TAYLOR	REVISED	DATE	COLUMN VS SPEED CHARACTERISTICS	NASA 20 AFT C.G.
CHECK					D6-10743
APR					
APR				THE BOEING COMPANY	PAGE 61

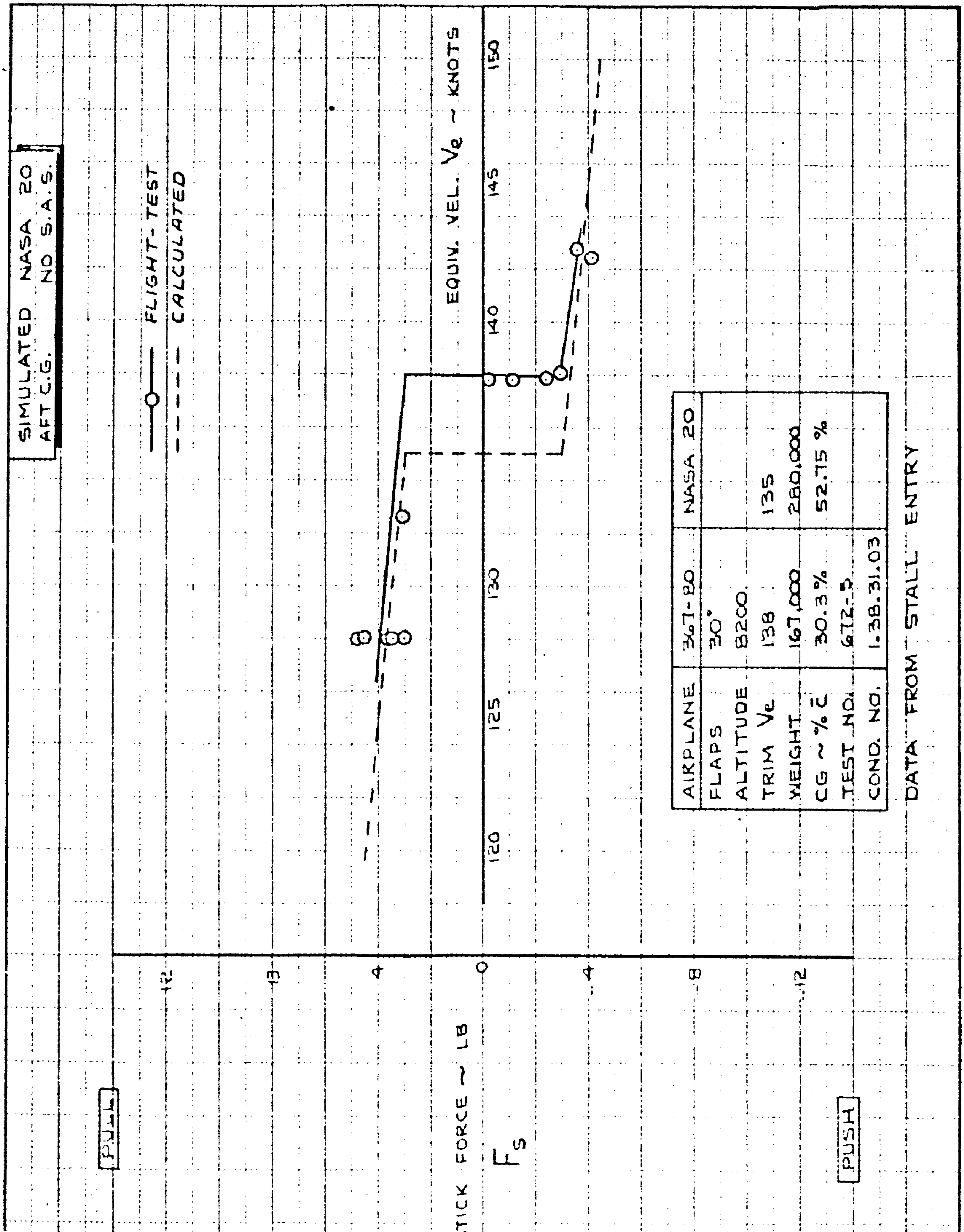

FIG. 41

CALC	TAYLOR	REVISED	DATE	SPEED STABILITY STICK FORCE VS SPEED	NASA 20 AFT C.G.
CHECK					D6-10743
APR				THE BOEING COMPANY	62
APR					

SIMULATED	NASA 20
AFT C.G.	NO S.A.S.

AIRPLANE	367-80	NASA 20
FLAPS	30°	
ALTITUDE	9250	
TRIM Ve	138	135
WEIGHT	157,500	280,000
CG ~ % $\bar{c}$	29.1 %	52.75 %
TEST NO.	672-4	
COND. NO.	1.38.31.02.1	

DATA FROM WIND-UP TURN

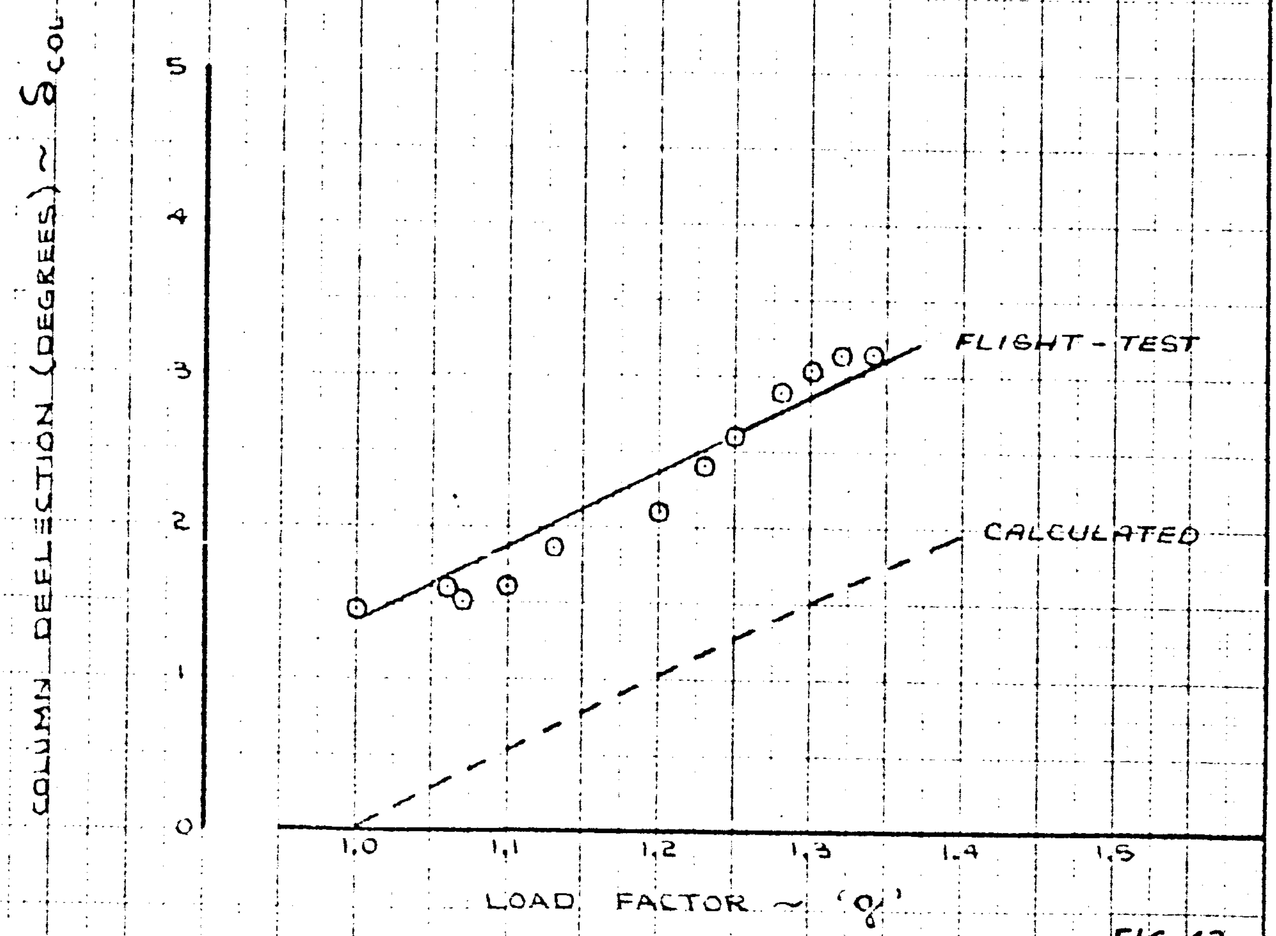

FIG. 42

CALC	TAYLOR	REVISED	DATE	NORMAL ACCELERATION VS. COLUMN CHARACTERISTICS	NASA 20 AFT C.G.
CHECK					D6-10743
APR				THE BOEING COMPANY	PAGE 63
APR					

SIMULATED AFT C.G.	NASA 20 NO S.A.S

AIRPLANE	367-80	NASA 20
FLAPS	30°	
ALTITUDE	9250	
TRIM Ve	138	135
WEIGHT	157,500	280,000
CG ~ % c̄	29.1 %	52.75 %
TEST NO	672-4	
COND. NO.	1.38.31.02.1	

DATA FROM WIND-UP TURN

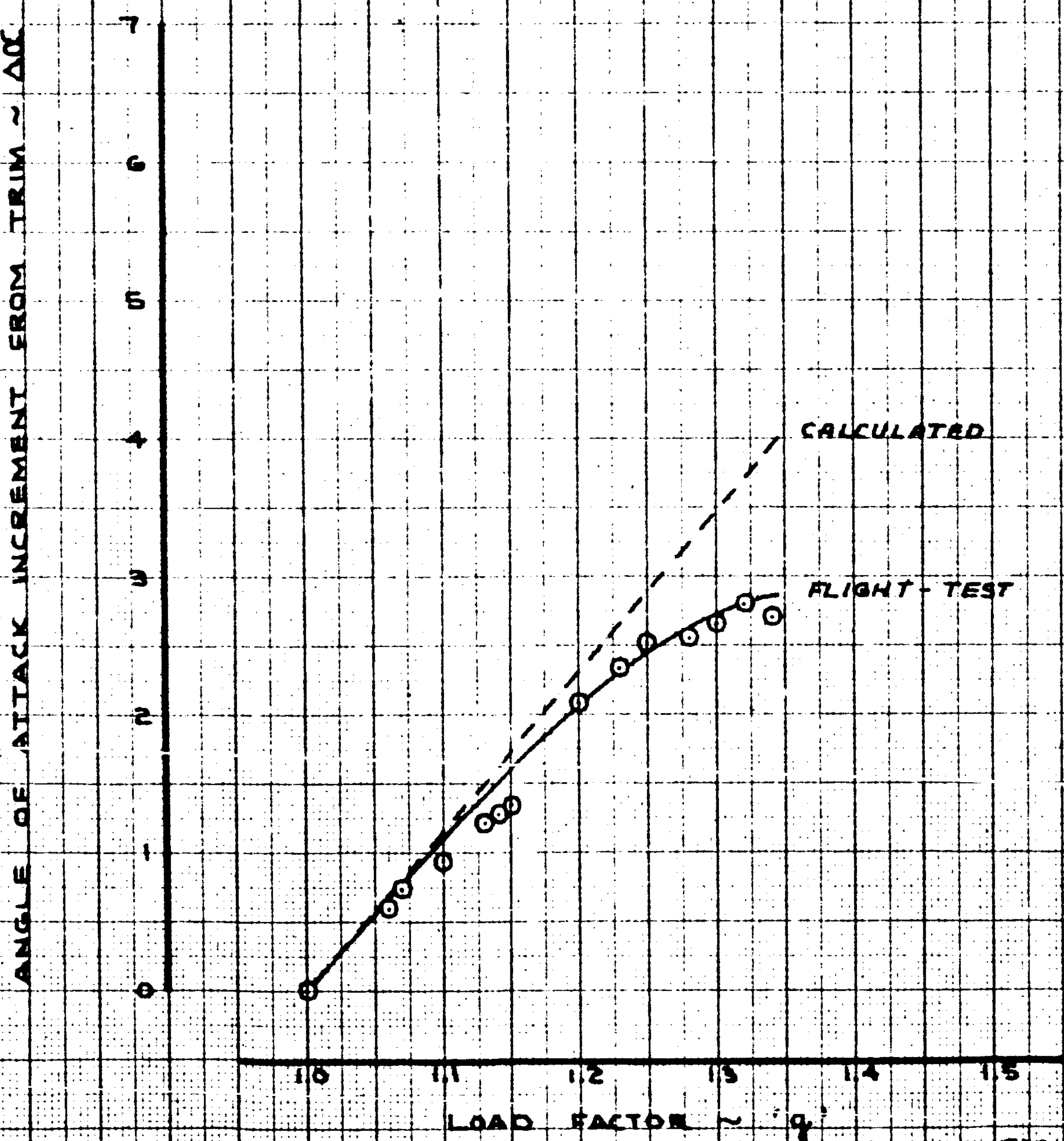

FIG. 43

CALC	TAYLOR		REVISED	DATE	NORMAL ACCELERATION VS. ANGLE OF ATTACK	NASA 20 AFT C.G.
CHECK						D6-10743
APR					THE BOEING COMPANY	PAGE 64
APR						

SIMULATED AFT C.G.	NASA 20 NO S.A.S.

AIRPLANE	367-80	NASA 20
FLAPS	30°	
ALTITUDE	9250	
TRIM Ve	138	135
WEIGHT	157,500	280,000
CG ~ % c̄	29.1 %	52.75 %
TEST NO.	672-4	
COND. NO.	1.38.31.02.1	

DATA FROM WIND-UP TURN

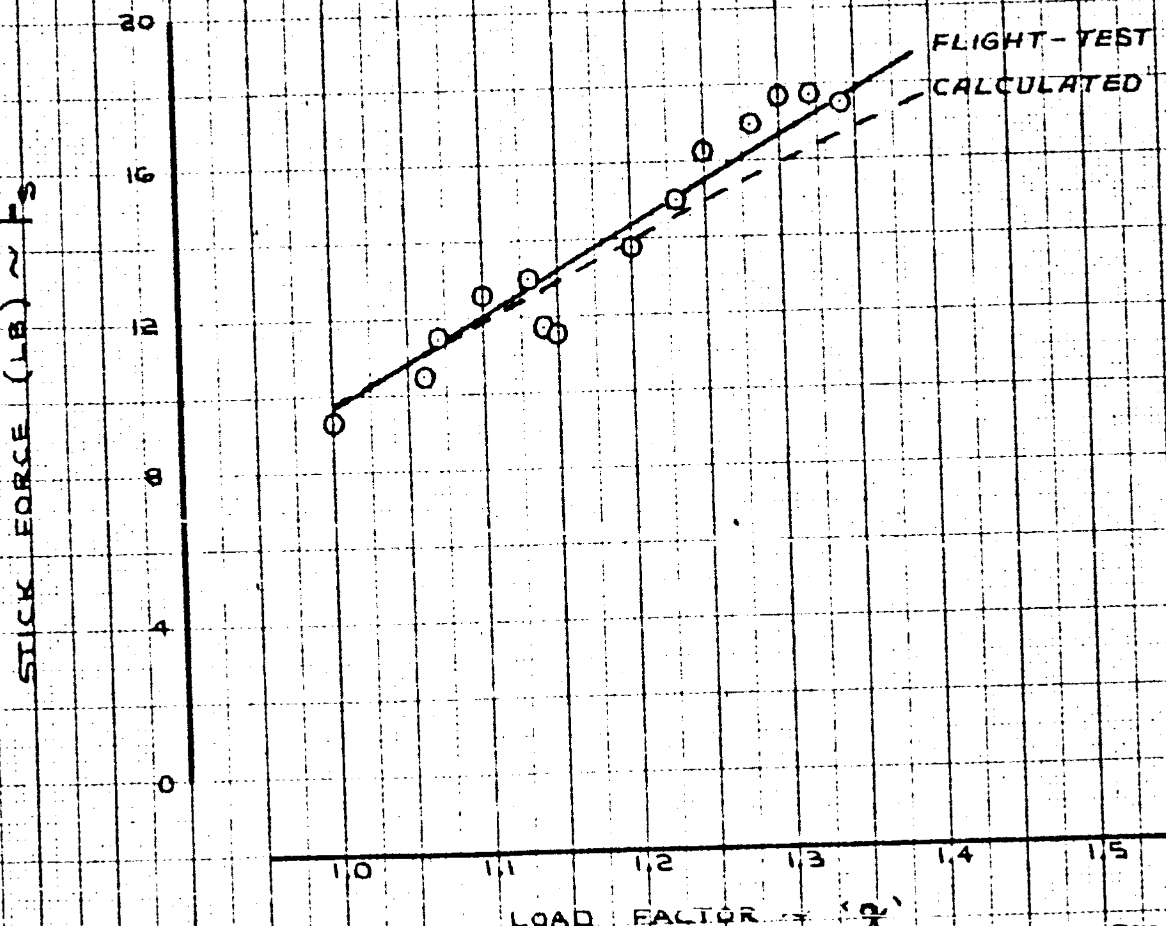

FIG. 44

		REVISED	DATE		
CALC	TAYLOR			NORMAL ACCELERATION VS FORCE CHARACTERISTICS	NASA 20 AFT C.G.
CHECK					D6-10743
APR					
APR				THE BOEING COMPANY	PAGE 65

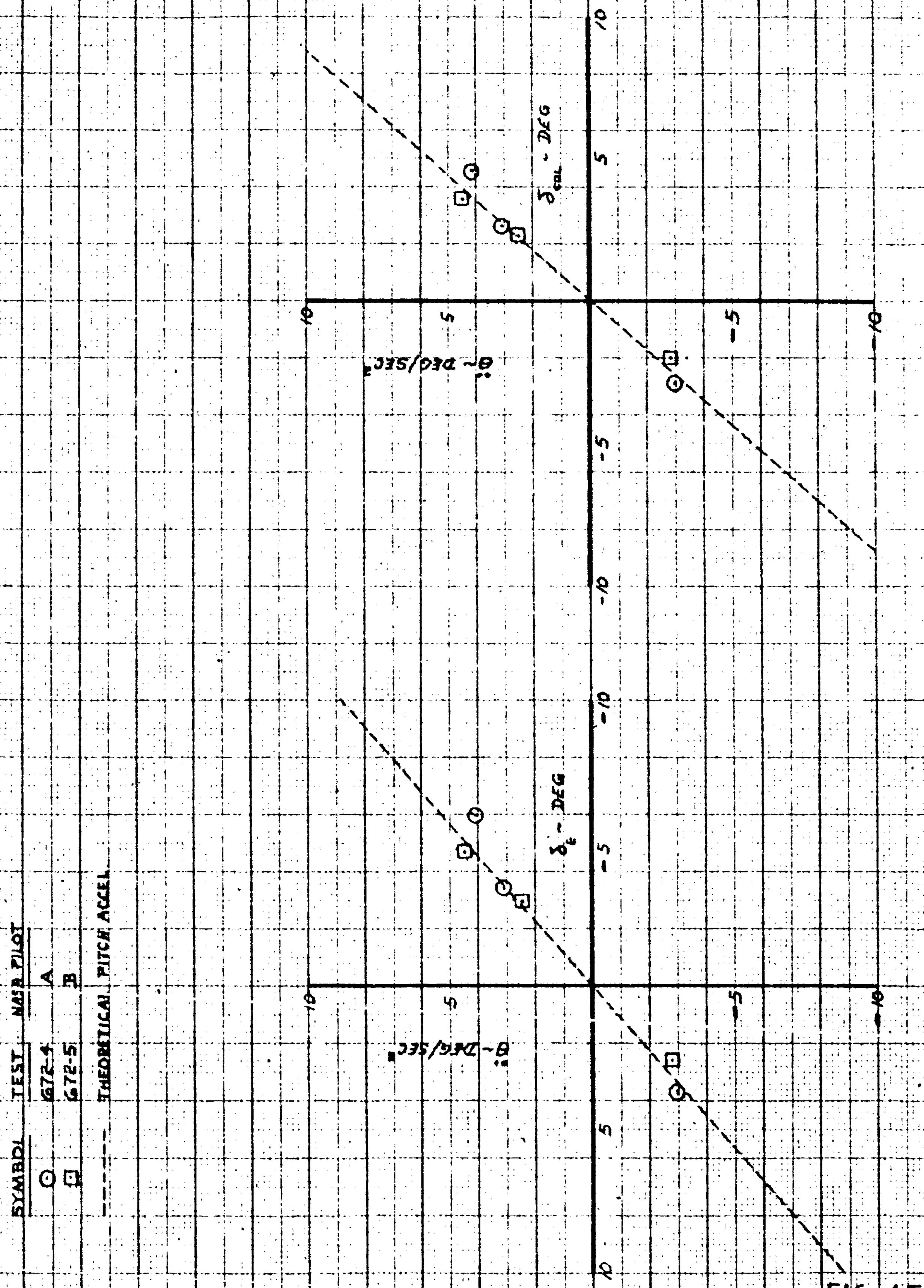

FIG. 45

CALC	D J BECK	11-18-65	REVISED	DATE	PITCH ACCELERATION OF THE NASA 20 SST (AFT CG ~ NO SAS)	D6-10743
CHECK						
APR						
APR					THE BOEING COMPANY	PAGE 66

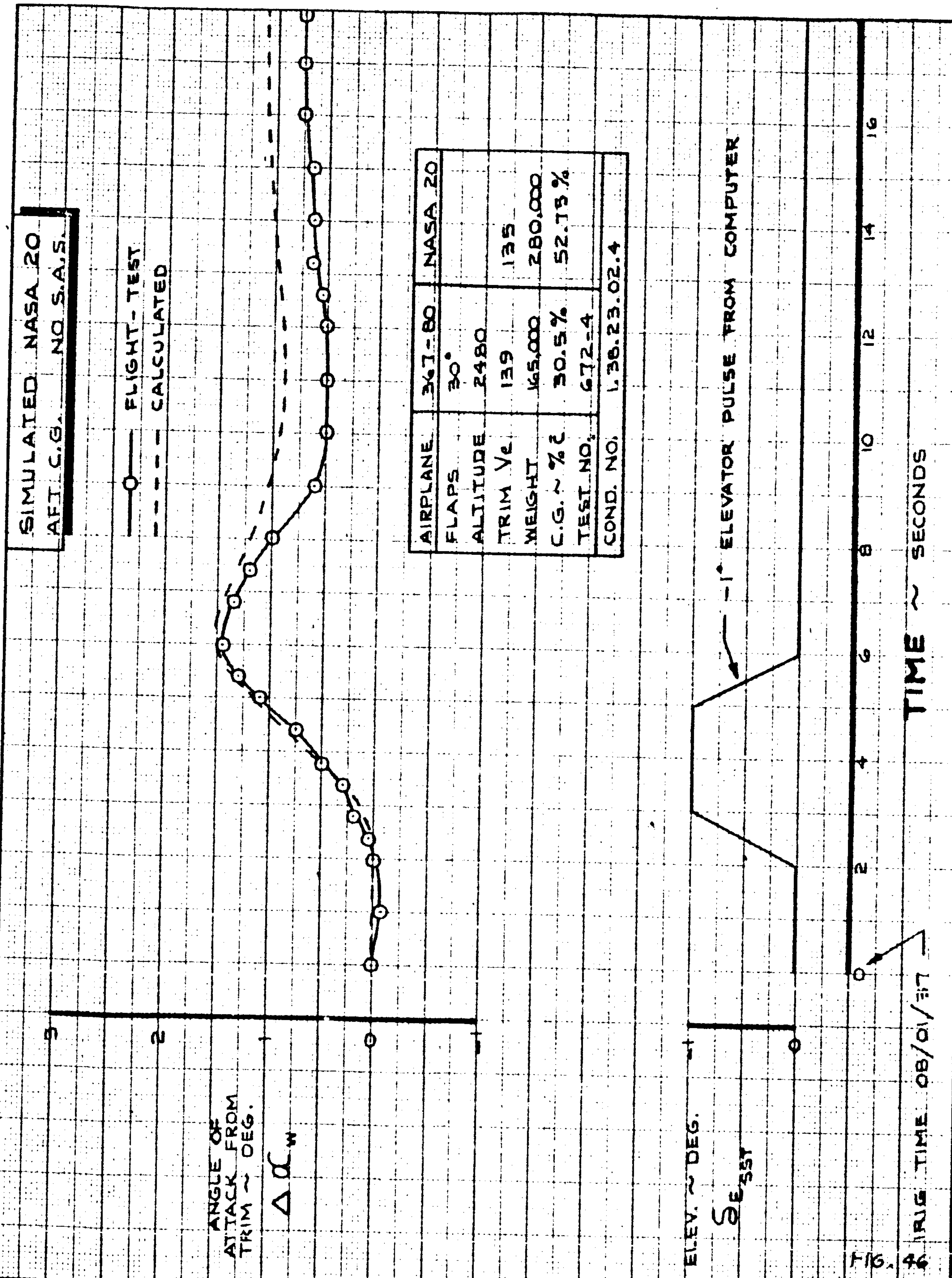

FIG. 46

CALC	TAYLOR	REVISED	DATE
CHECK			
APR			
APR			

SHORT PERIOD CHARACTERISTICS

THE BOEING COMPANY

NASA 20 AFT C.G.

D6-10743

TD 461 C-R4

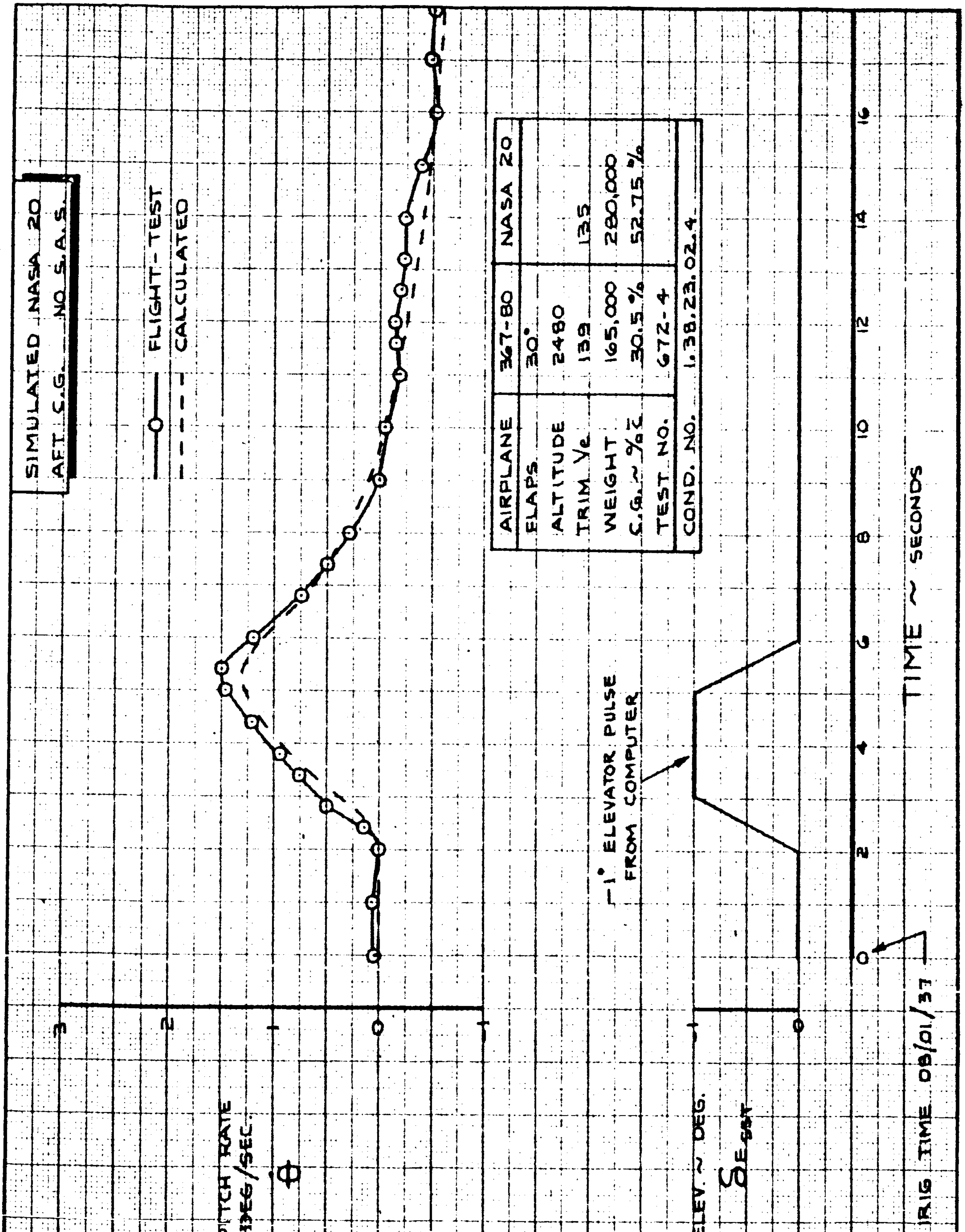

FIG. 47

CALC	TAYLOR		REVISED	DATE	SHORT PERIOD CHARACTERISTICS
CHECK					
APR					
APR					
					THE BOEING COMPANY

NASA 20 AFT C.G.

D6-10743

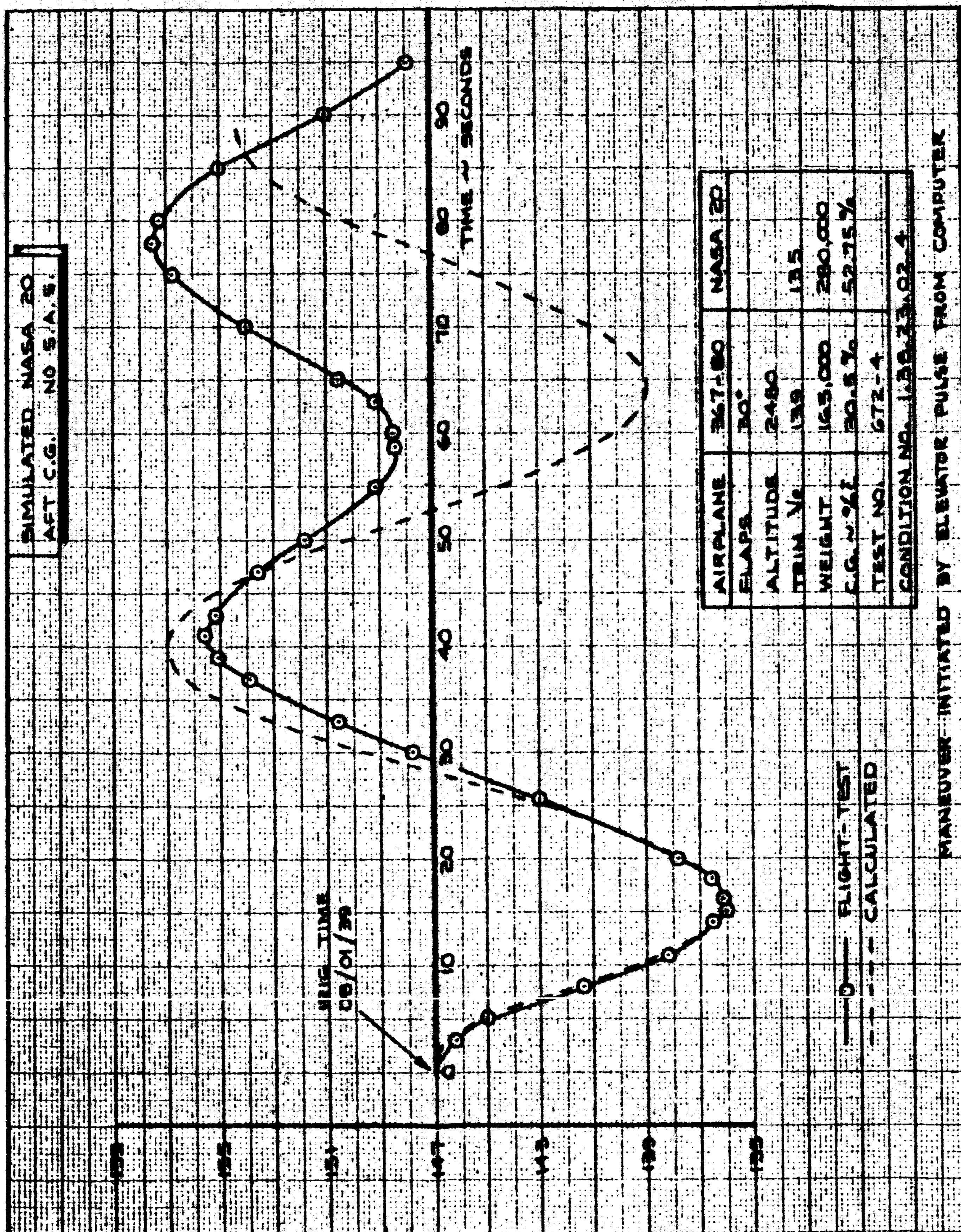

FIG. 48

CALC	TAYLOR	REVISED	DATE	PHUGOID CHARACTERISTICS	NASA 20 AFT C.G.
CHK					D6-10743
APR				THE BOEING COMPANY	PAGE 69

Aft C. G. - ($\dot{\theta} + \Delta\alpha$) Longitudinal Augmentation

The ($\dot{\theta} + \Delta\alpha$) longitudinal augmentation was mechanized with the aft C. G. configuration to improve the long period and poor control response caused by the low static margin. With augmentation, the maneuvering stick force was 30 lbs/g, which is very close to the basic NASA-20 configuration. Because this augmentation system introduces strong artificial static stability, it greatly reduces the natural effect of C. G. position.

The flight test data from the simulation documentation maneuvers are shown in Figs. 49 to 57. The speed stability tests are shown in Figs. 49 and 50. The 367-80 was trimmed off speed, but the slopes of the column-velocity and stick force-velocity curves are very accurate. The wind-up turn data are shown in Figs. 51 to 53. This simulation is good, but the flight test data does not coincide with the calculated values because of the initial mis-trim. The data for the pitch reversal are shown in Fig. 54. The simulation of longitudinal control power and sensitivity is accurate. The response to an elevator pulse is shown in Figs. 55 and 56. The 367-80 response matches the theoretical SST characteristics well. The phugoid characteristics are shown in Fig. 57. The 367-80 matches the damping ratio, but the period is about two seconds long.

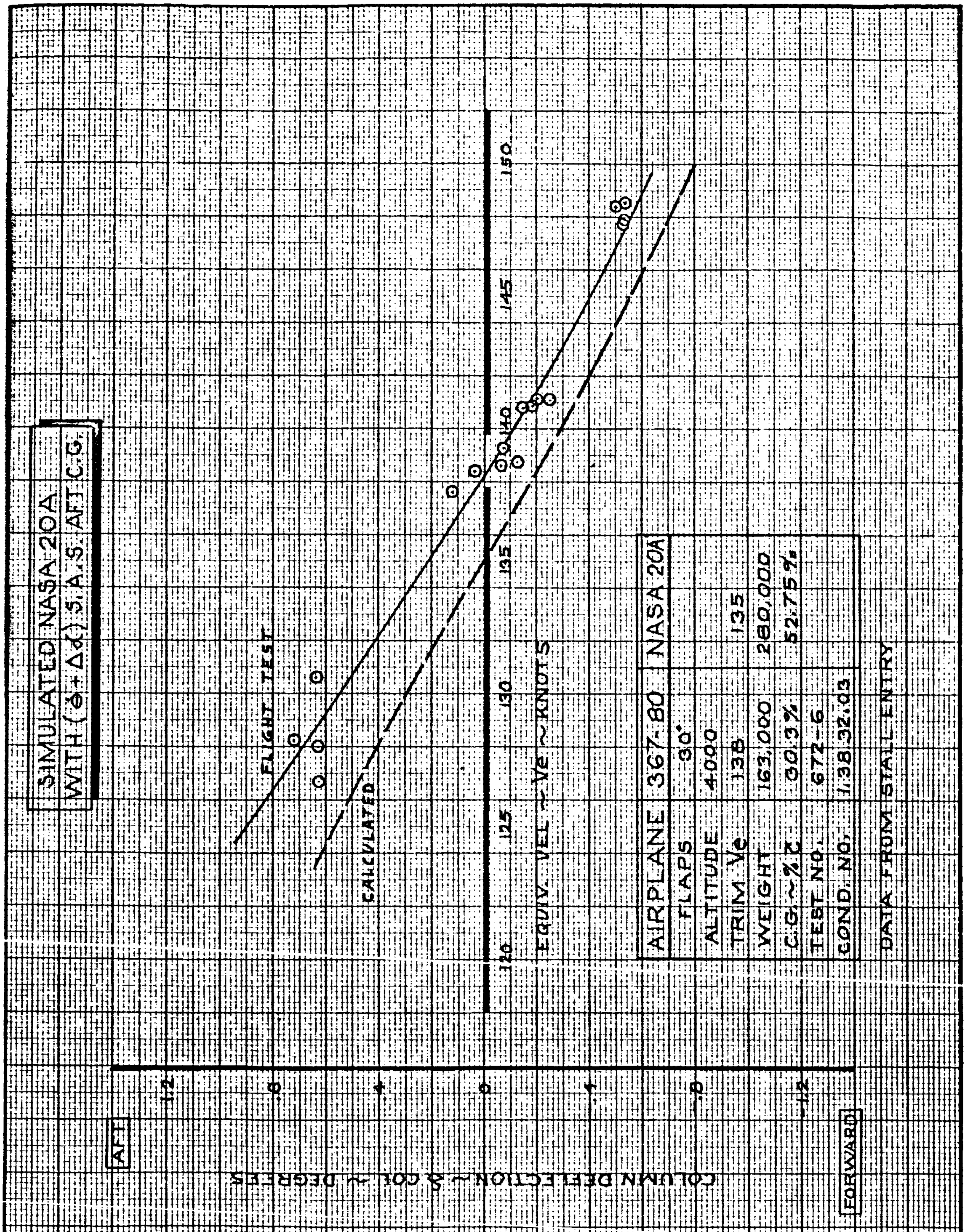

FIG. 47

CALC	TAYLOR	REVISED	DATE	COLUMN Vs. SPEED CHARACTERISTICS	NASA 20A AFT. C.G.
CHECK		R S	2-10-66		D6-10743
APR					
APR				THE BOEING COMPANY	PAGE 71B

TD 461 C-R4

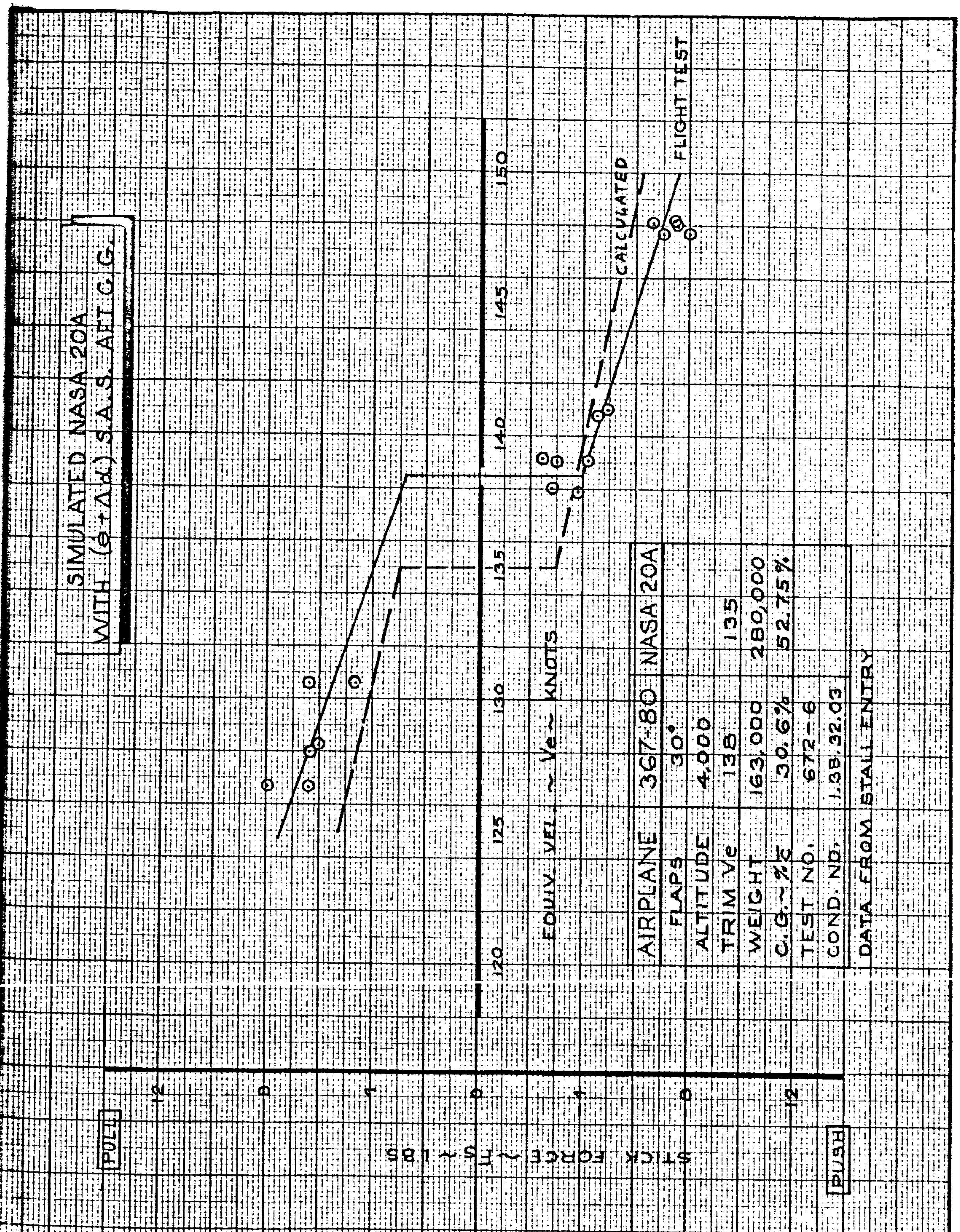

FIG. 50

CALC	TAYLOR		REVISED	DATE	SPEED STABILITY STICK FORCE Vs. SPEED	NASA 20A AFT. C.G.
CHECK			STEMWELL	1-31-66		D6-10743
APR					THE BOEING COMPANY	PAGE 72B
APR						

TB 461 C-R4

SIMULATED NASA 20A
WITH $(\dot{\theta} + \Delta\alpha)$ S.A.S. AFT. C.G.

AIRPLANE	367-80	NASA
FLAPS	30°	
ALTITUDE	7,350	
TRIM Ve	137	135
WEIGHT	153,400	280,000
CG ~ % $\bar{c}$	28.7%	52.75%
TEST NO.	672-7	
COND. NO.	1.38.32.02.2	

DATA FROM WIND-UP TURN

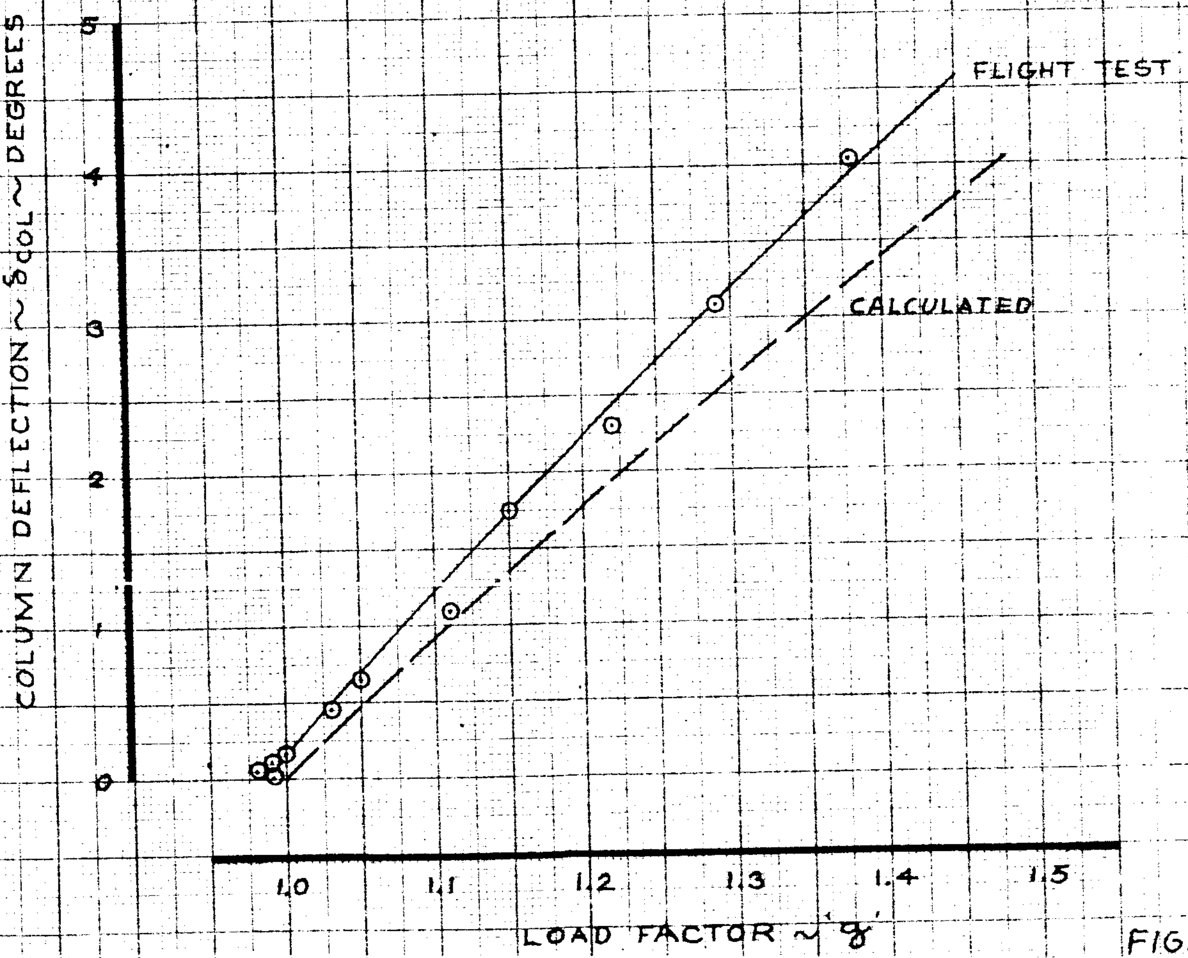

FIG. 51

CALC	TAYLOR	REVISED	DATE	NORMAL ACCELERATION VS. COLUMN CHARACTERISTICS	NASA 20A AFT. C.G.
CHECK		STEMWELL	1-31-66		D6-10743
APR				THE BOEING COMPANY	PAGE 73
APR					

SIMULATED NASA 20A
WITH AFT C.G. ($\dot{\theta} + \Delta\alpha$)

AIRPLANE	367-80	NASA 20
FLAPS	30°	
ALTITUDE	7,350	
TRIM Ve	137	135
WEIGHT	153,400	280,000
C.G. ~ % $\bar{c}$	28.7%	52.75%
TEST NO:	672-7	
COND NO.	1.38.32.02.2	

DATA FROM WIND-UP TURN

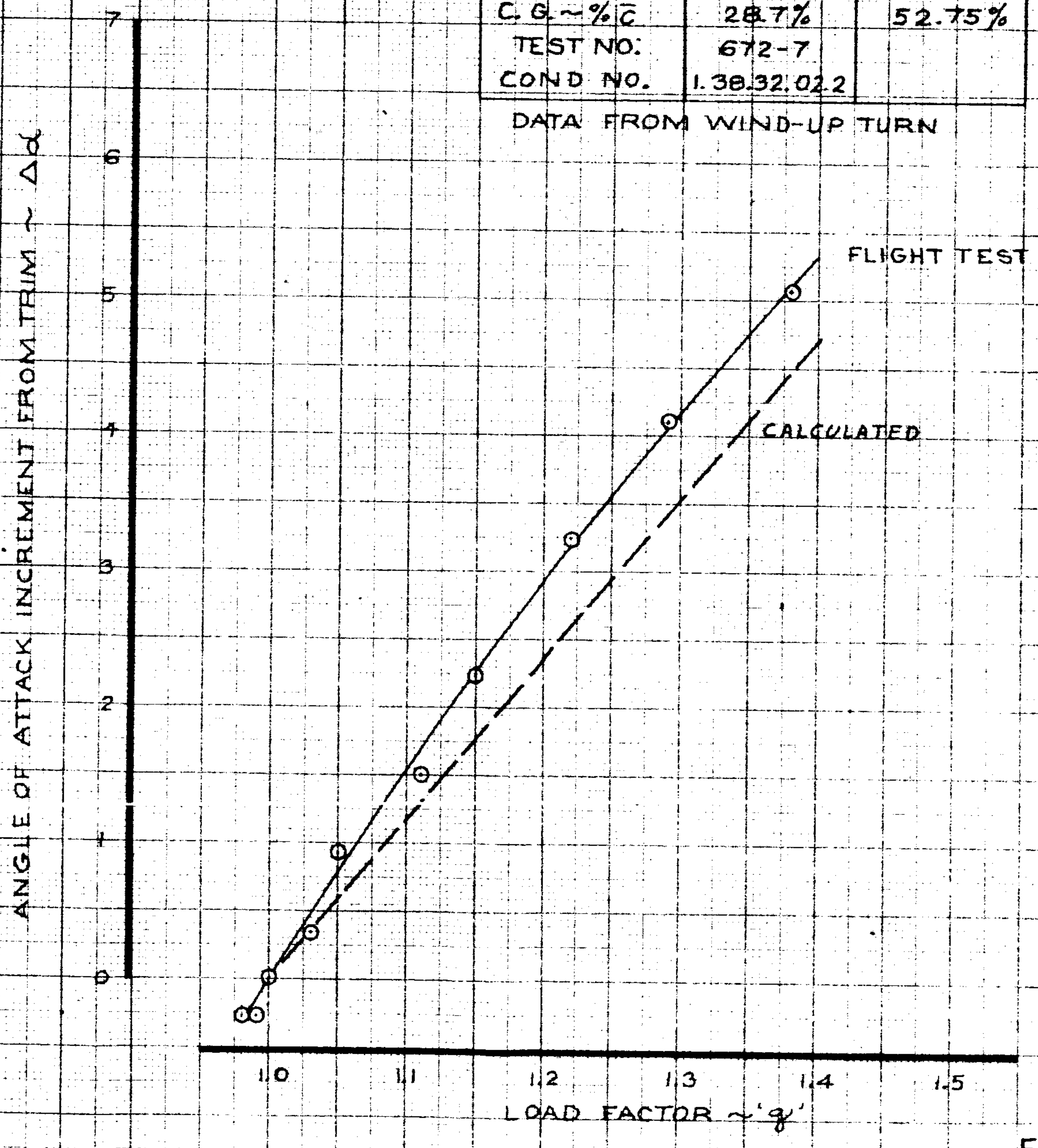

FIG. 52

CALC	TAYLOR	REVISED	DATE
CHECK		STEMWELL	1-31-66
APR			
APR			

NORMAL ACCELERATION
Vs
ANGLE OF ATTACK

THE BOEING COMPANY

NASA 20A AFT. C.G.

D6-10743

TD 461 C-R4

SIMULATED NASA 20
WITH $(\dot{\theta}+\Delta\alpha)$ S.A.S. AFT C.G.

AIRPLANE	367-80	NASA 20A
FLAPS	30°	
ALTITUDE	7,350	
TRIM Ve	137	135
WEIGHT	153,400	280,000
C.G. ~ % $\bar{c}$	28.7%	52.75%
TEST NO.	672-7	
COND. NO.	1.38.32.02.2	

DATA FROM WIND-UP TURN

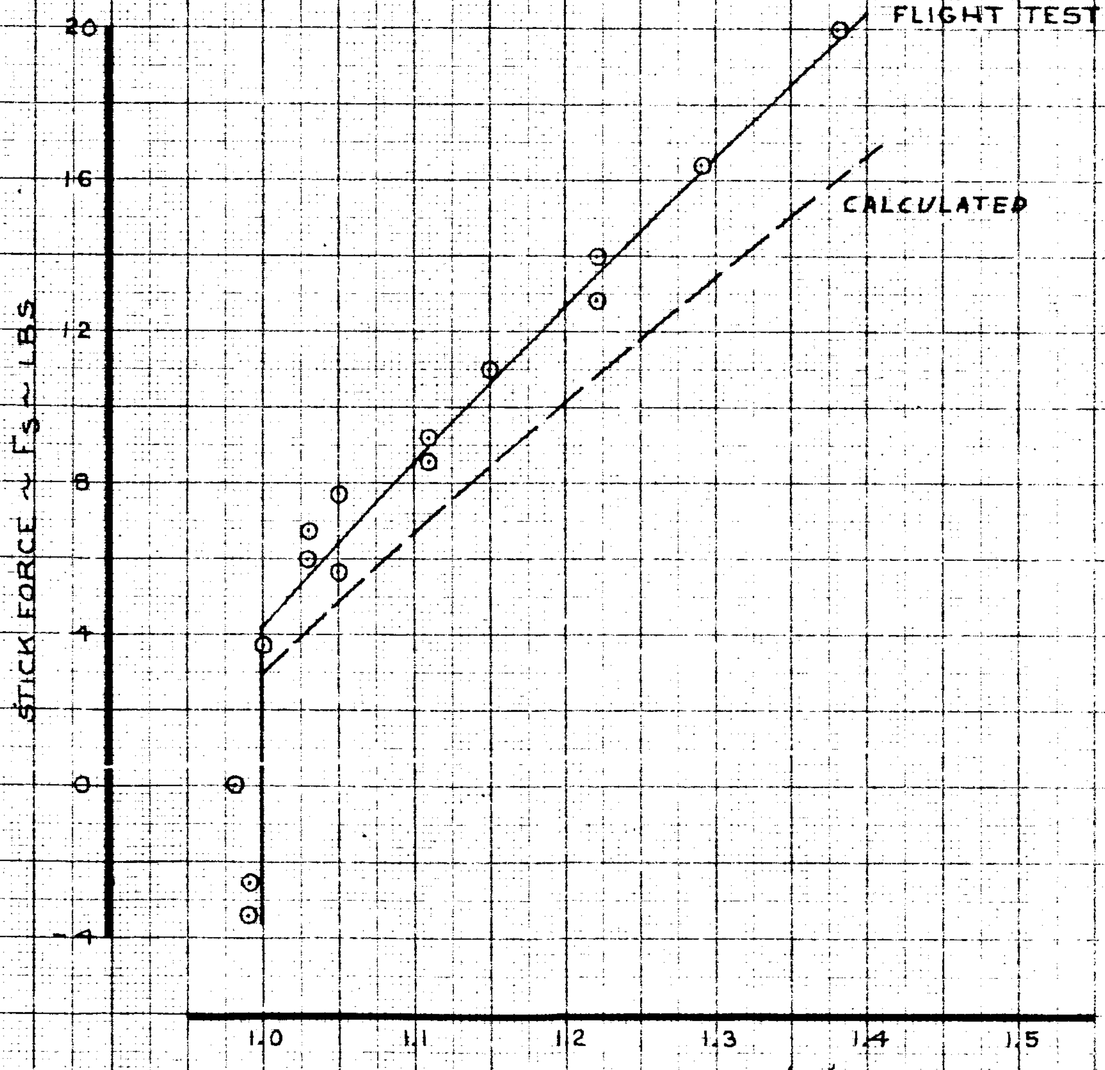

FIG. 53

CALC	TAYLOR		REVISED	DATE	NORMAL ACCELERATION Vs FORCE CHARACTERISTICS	NASA 20A AFT C.G.
CHECK			STEMWELL	1-31-66		D6-10743
APR					THE BOEING COMPANY	PAGE 75
APR						

TD 461 C-R4

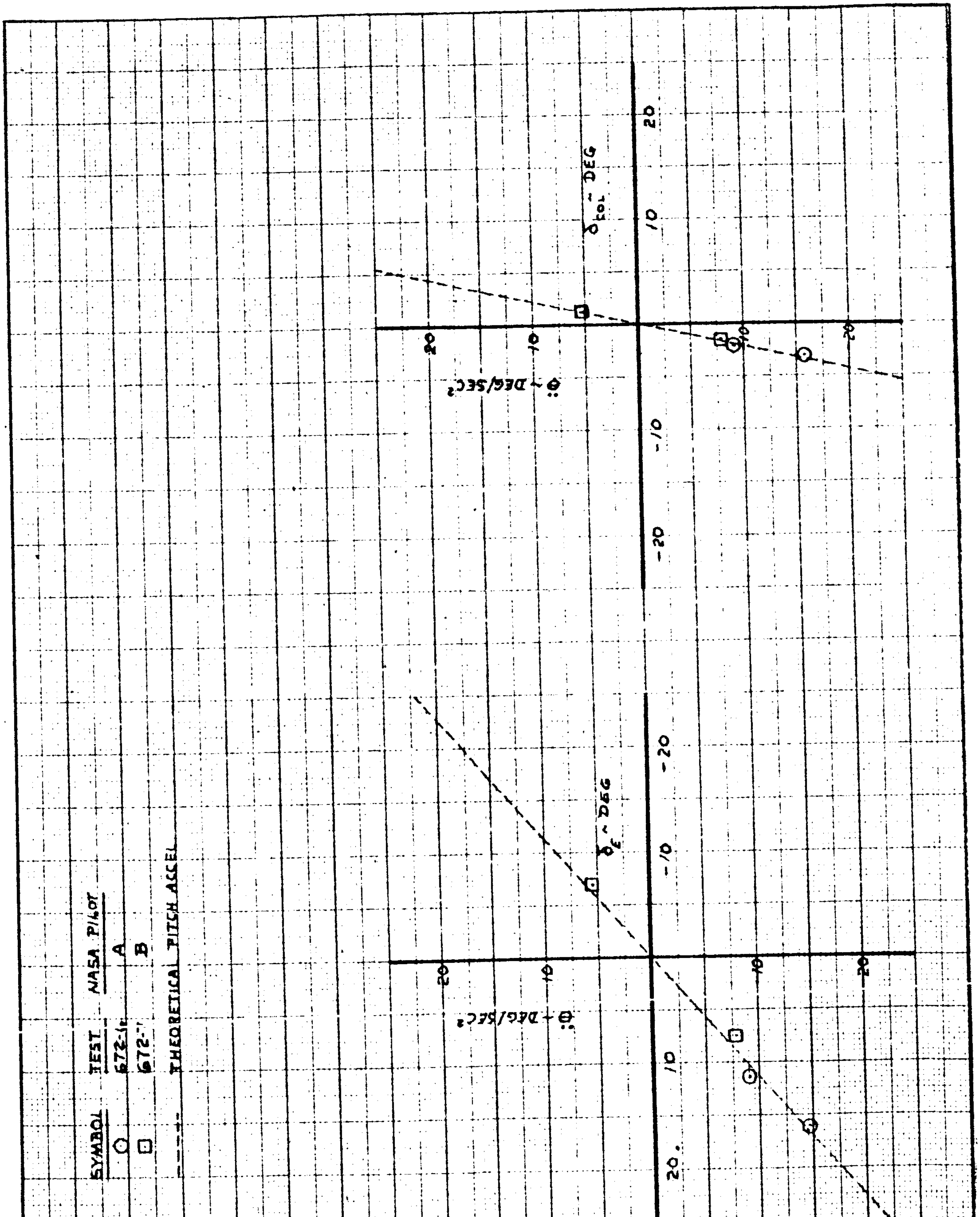

FIG. 54

CALC	D J BECK	11-18-65	REVISED	DATE	PITCH ACCELERATION OF THE NASA 20A SST (AFT CG ~ $\dot{\theta}$ + α SAS)	D6-10743
CHECK						
APR						PAGE 76
APR					THE BOEING COMPANY	

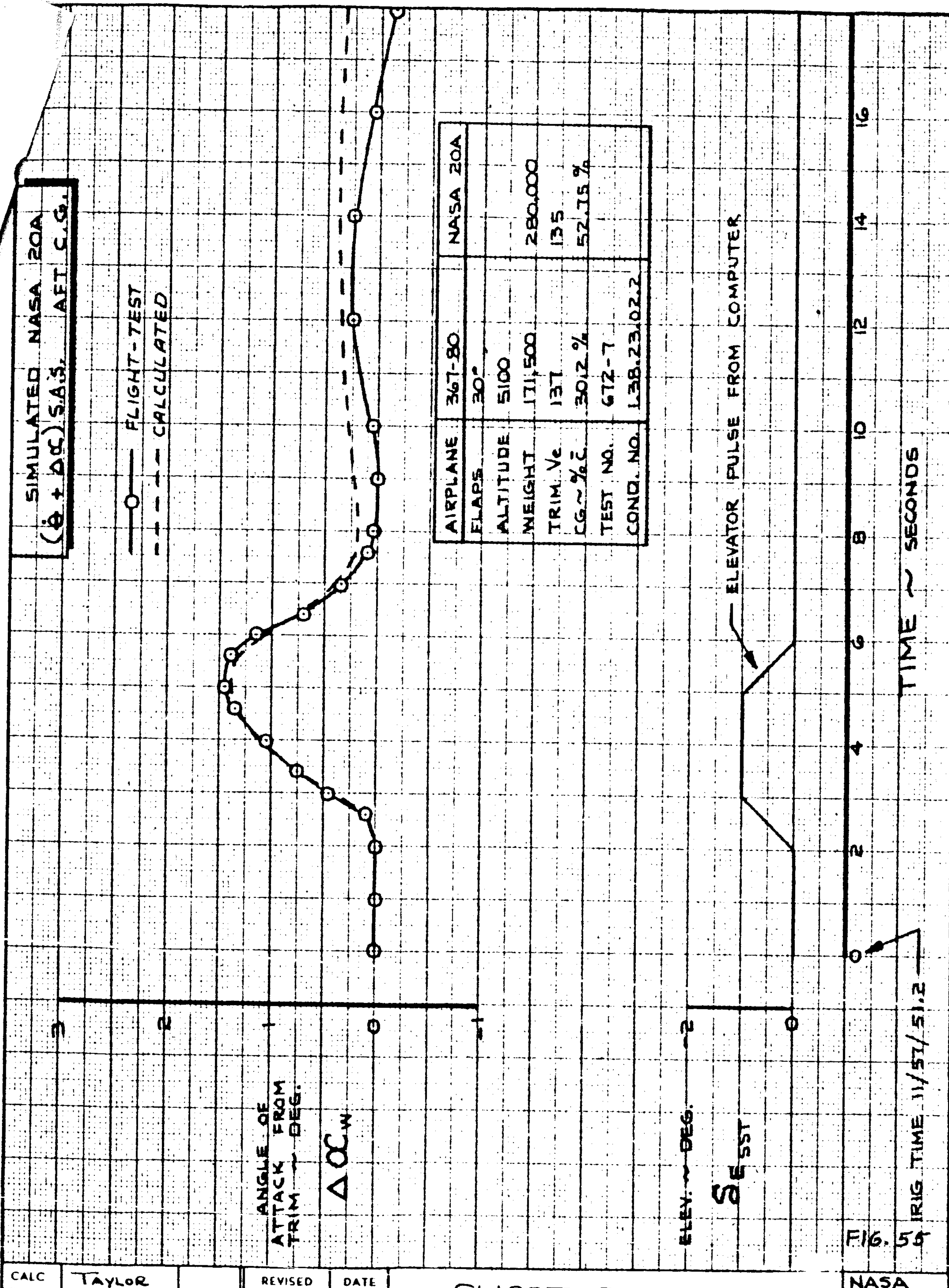

FIG. 55

CALC	TAYLOR		REVISED	DATE
CHECK				
APR				
APR				

SHORT PERIOD CHARACTERISTICS

NASA 20A AFT C.G.

D6-10743

THE BOEING COMPANY

TD 461 C R4

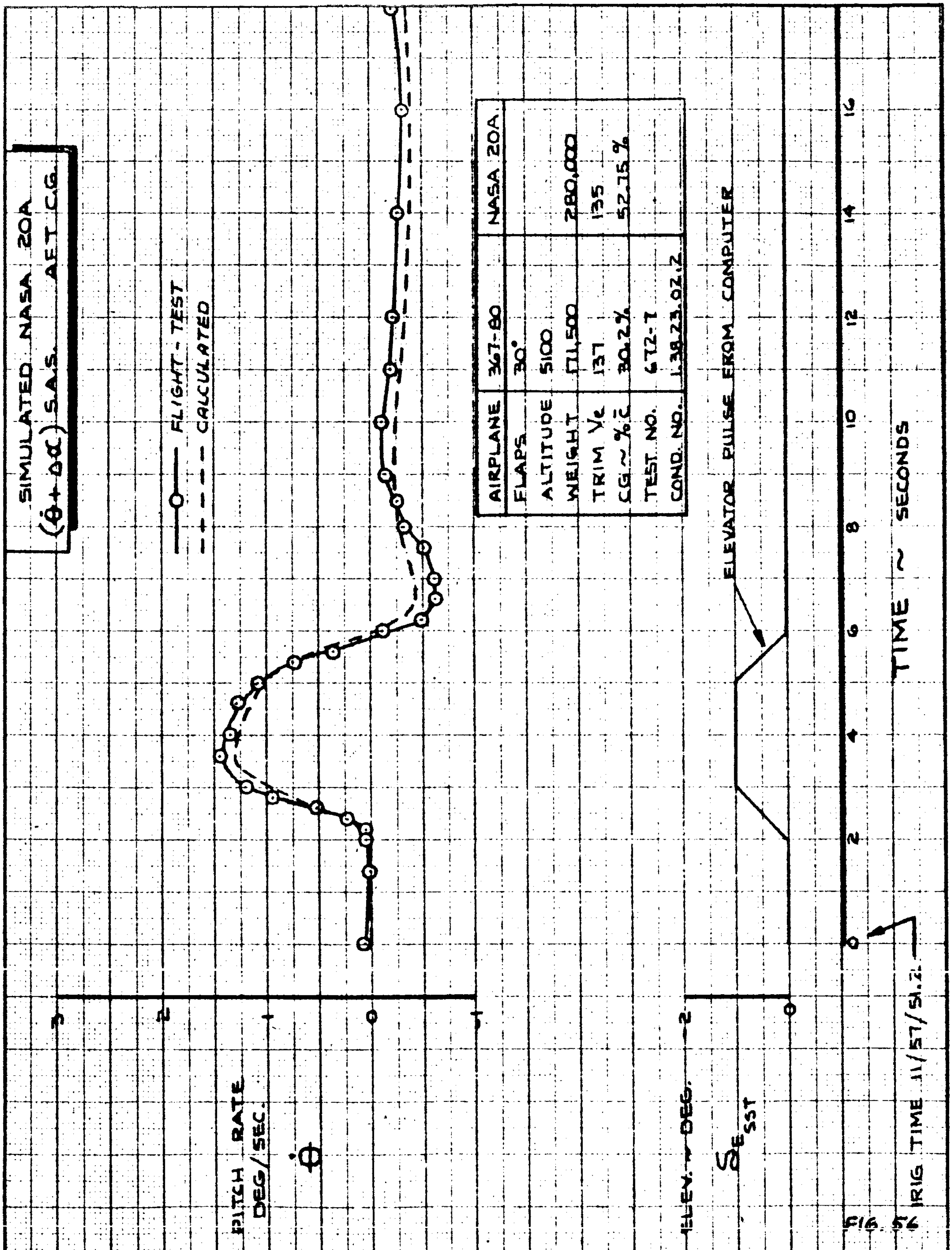

FIG. 56

CALC	TAYLOR		REVISED	DATE	SHORT PERIOD CHARACTERISTICS	NASA 20A AFT C.G.
CHECK						D6-10743
APR					THE BOEING COMPANY	PAGE 78
APR						

TD 461 C-R4

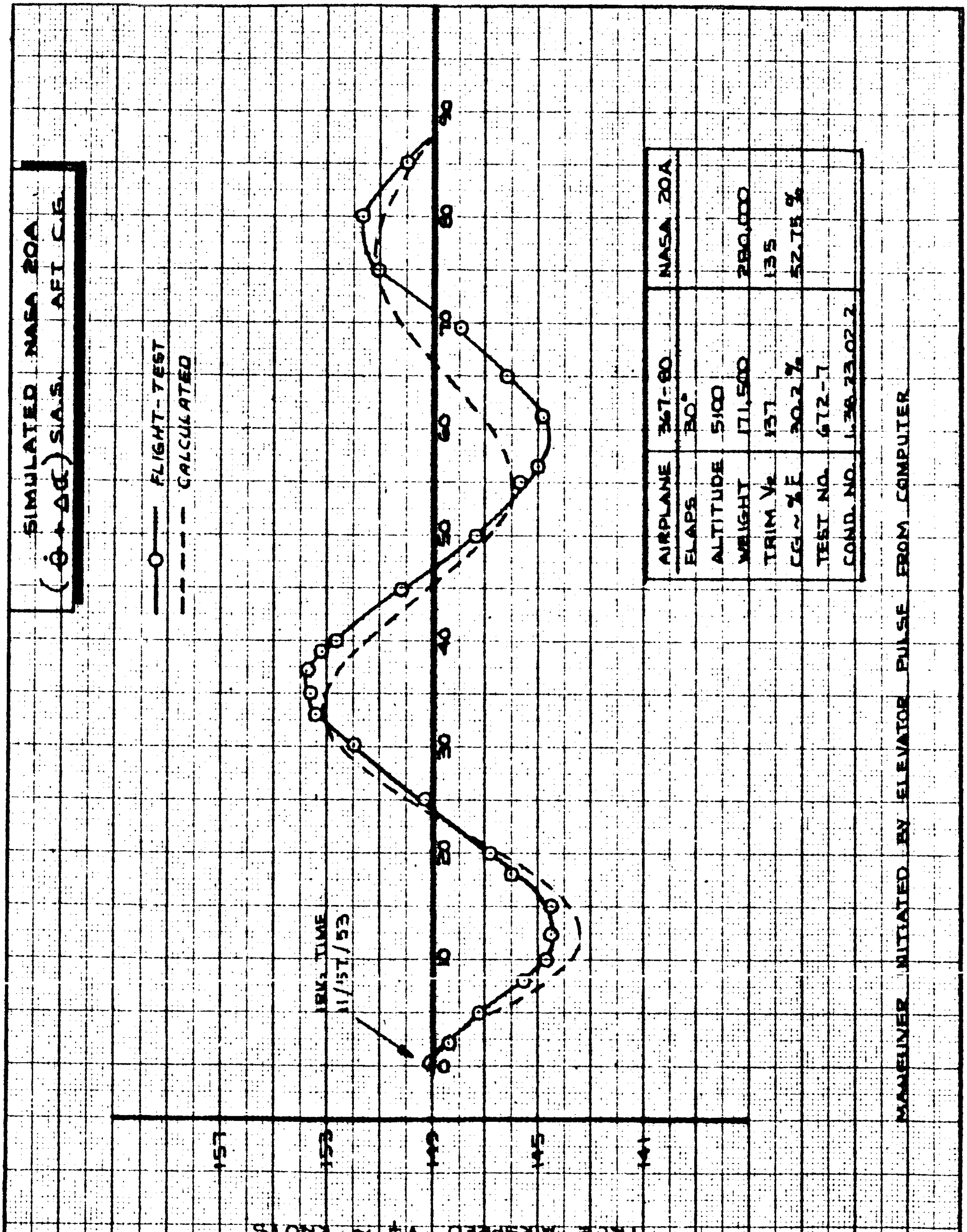

AIRPLANE	367-80	NASA 20A
FLAPS	30°	
ALTITUDE	5100	
WEIGHT	171,500	280,000
TRIM Ve	137	135
CG ~ %C	30.2 %	52.75 %
TEST NO.	672-7	
COND. NO.	1.38.23.02.2	

FIG. 57

CALC	Taylor		REVISED	DATE
CHECK				
APR				
APR				

PHUGOID CHARACTERISTICS

NASA 20A AFT C.G.

D6-10743

THE BOEING COMPANY

D 461 C-R4

Degraded Lateral - Directional

Because the stability derivatives used in the NASA-20 configuration are only theoretical and give excellent lateral-directional flying qualities, a degraded configuration was tested. This configuration was chosen to bracket the range of any computation error and the degradation that might be caused by any future configuration changes. An adverse yaw due to roll rate was introduced by changing the value of $C_{n_{\dot{\phi}}}$ from -.0223 to -.076. This gives a value of $N_{\dot{\phi}} = C_{n_{\dot{\phi}}} \cdot \frac{\bar{q} S b}{I_z}$ of -.1, which is representative of current jet transports in the landing approach configuration. The value of $C_{n_{\dot{\beta}}}$ was increased from 0 to -.1204 to destabilize the Dutch roll to .05 damping ratio, which is also representative of current jet transports with no yaw damper.

The $(\dot{\theta} + \Delta\alpha)$ longitudinal augmentation was used throughough these tests to help the pilots to evaluate only the lateral-directional characteristics. The combination of degraded lateral and basic longitudinal was evaluated by one pilot, but no documentation was done for these tests.

The flight test data from the documentation maneuvers of the degraded lateral NASA 20 (NASA 20B) are shown in Figs. 58 to 60. No longitudinal documentation was performed because this configuration was identical to the NASA 20 with $(\dot{\theta} + \Delta\alpha)$ augmentation. There was no cross-control sideslip, because none of the static derivatives were changed. The data from the wheel steps and reversals are shown in Figs. 58 and 59. The steady-state roll rate characteristics were simulated very accurately. There is a slight error in the lateral control sensitivity, of about the same magnitude as the basic NASA 20 configuration. The response to a rudder pulse is shown in Fig. 60.

The corresponding theoretical response was not calculated, but this response shows that the theoretical Dutch roll period and damping were matched well.

	367-80	NASA 20B
FLAPS	30°	
SPEED BRAKES	6°	
V_e	135 KTS	135 KTS
H_p	7500 FT	
GW	144,400 LBS	280,000 LBS
CG	29.1% MAC	46.0% MAC
TEST NO.	⊙ ~ 672-7	
	⊡ ~ 672-9	

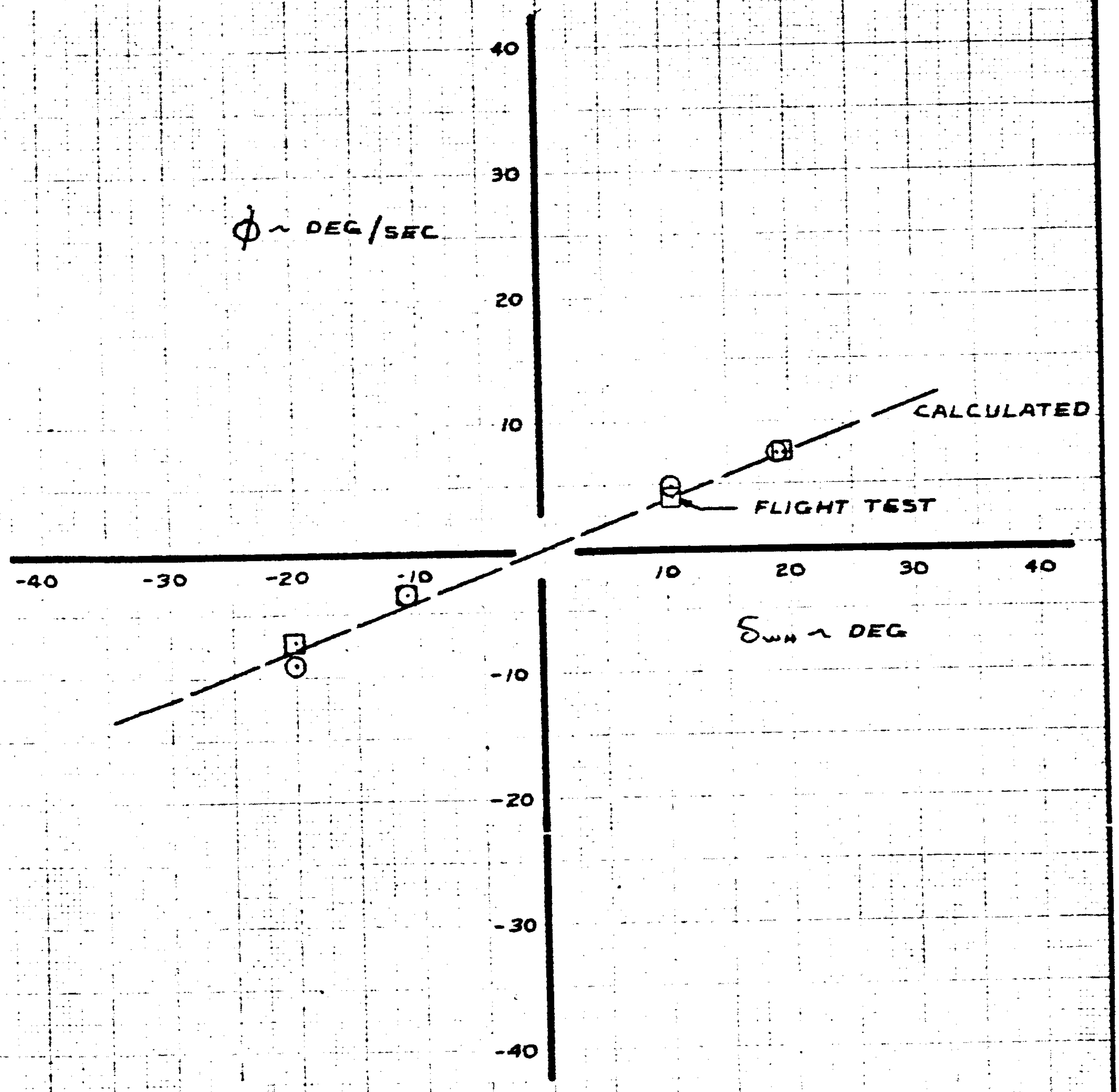

FIG. 58

CALC	RC	9/21/65	REVISED	DATE	LATERAL CONTROL RESPONSE STEADY STATE ROLL RATES	SIMULATED NASA 20B
CHECK						D6-10743
APR					THE BOEING COMPANY	PAGE 82
APR						

TD 461 C-R4

	367-80	NASA 208
FLAPS	30°	
SPEED BRAKES	6°	
V_e	135 KTS	135 KTS
H_p	2700 FT	
GW	149,100 LBS	280,000 LBS
CG	28.9% MAC	46.0% MAC
TEST NO.	⊙ ~ 672-7	
	⊡ ~ 672-9	

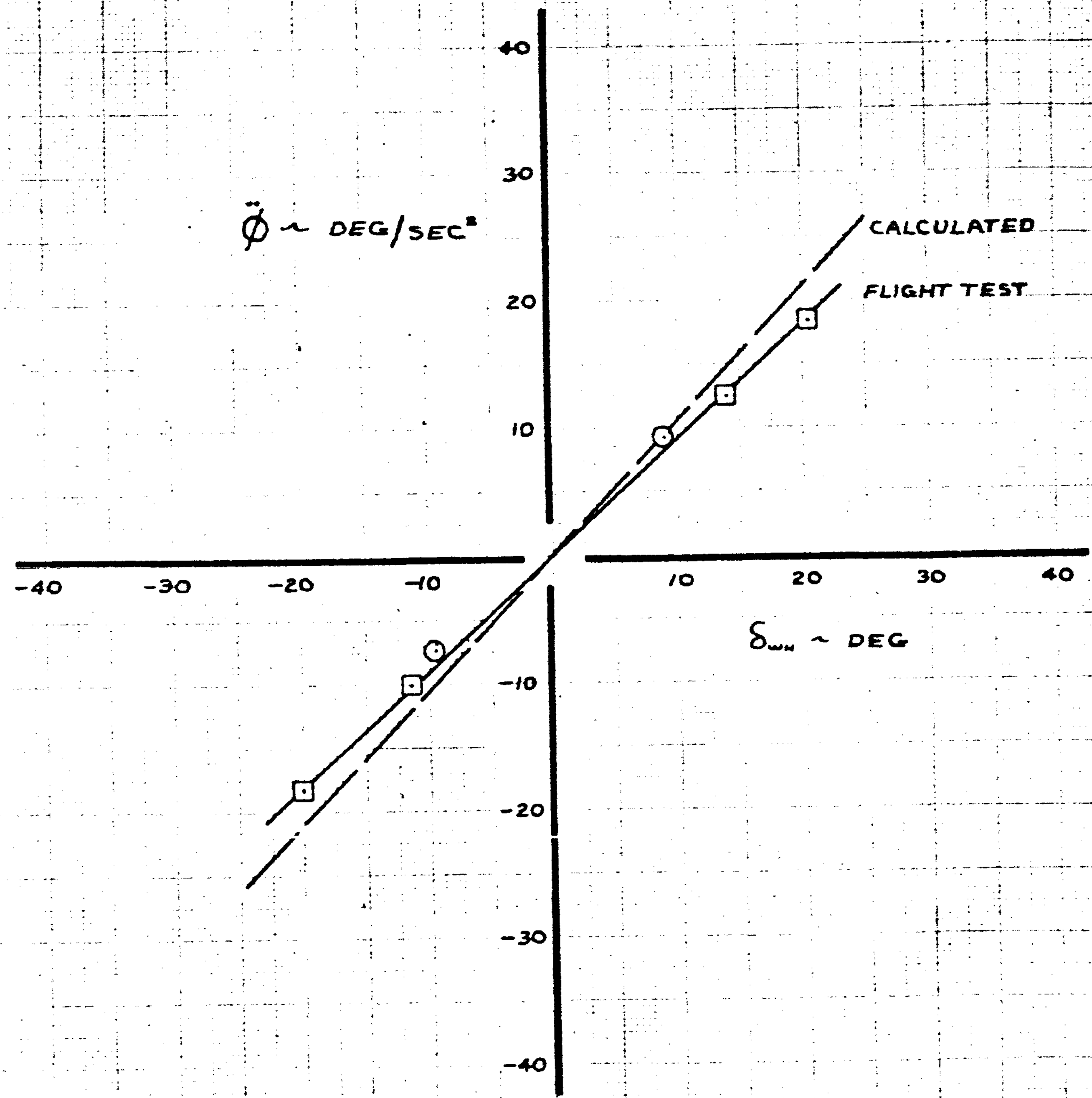

FIG. 59

CALC	RCJ	7/21/65	REVISED	DATE	ROLL ACCELERATION CHARACTERISTICS	SIMULATED NASA 208
CHECK						D6-10743
APR					THE BOEING COMPANY	PAGE 83
APR						

DUTCH ROLL NASA 208

$C_{n_p} = -0.0760$ /RAD/SEC
$C_{n_{\dot\beta}} = -0.1204$ /RAD/SEC
LONG. SAS : $\dot\theta + \Delta\alpha$

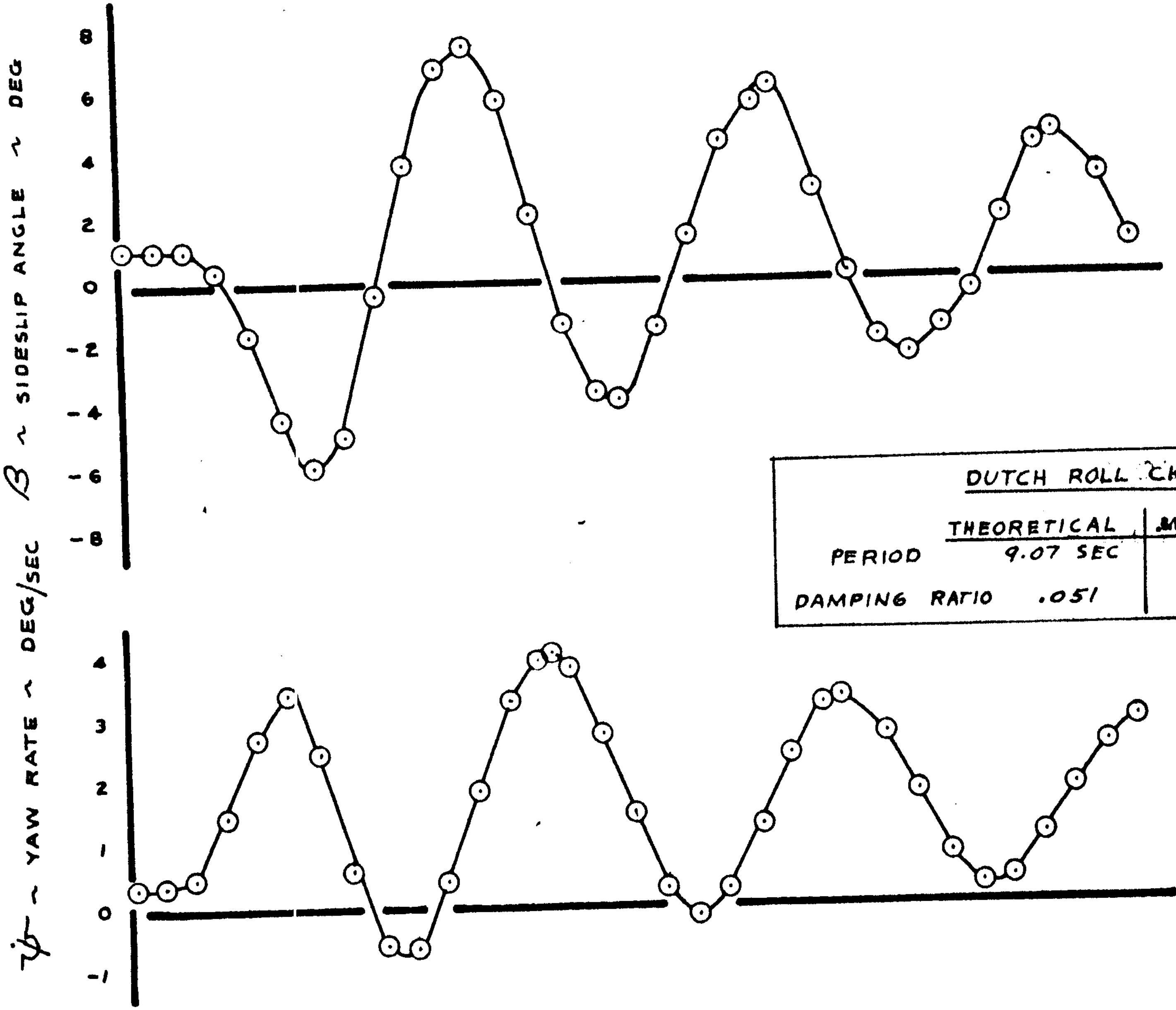

DUTCH ROLL CHARACTERISTICS

	THEORETICAL	MEASURED
PERIOD	9.07 SEC	9.33 SEC
DAMPING RATIO	.051	.05

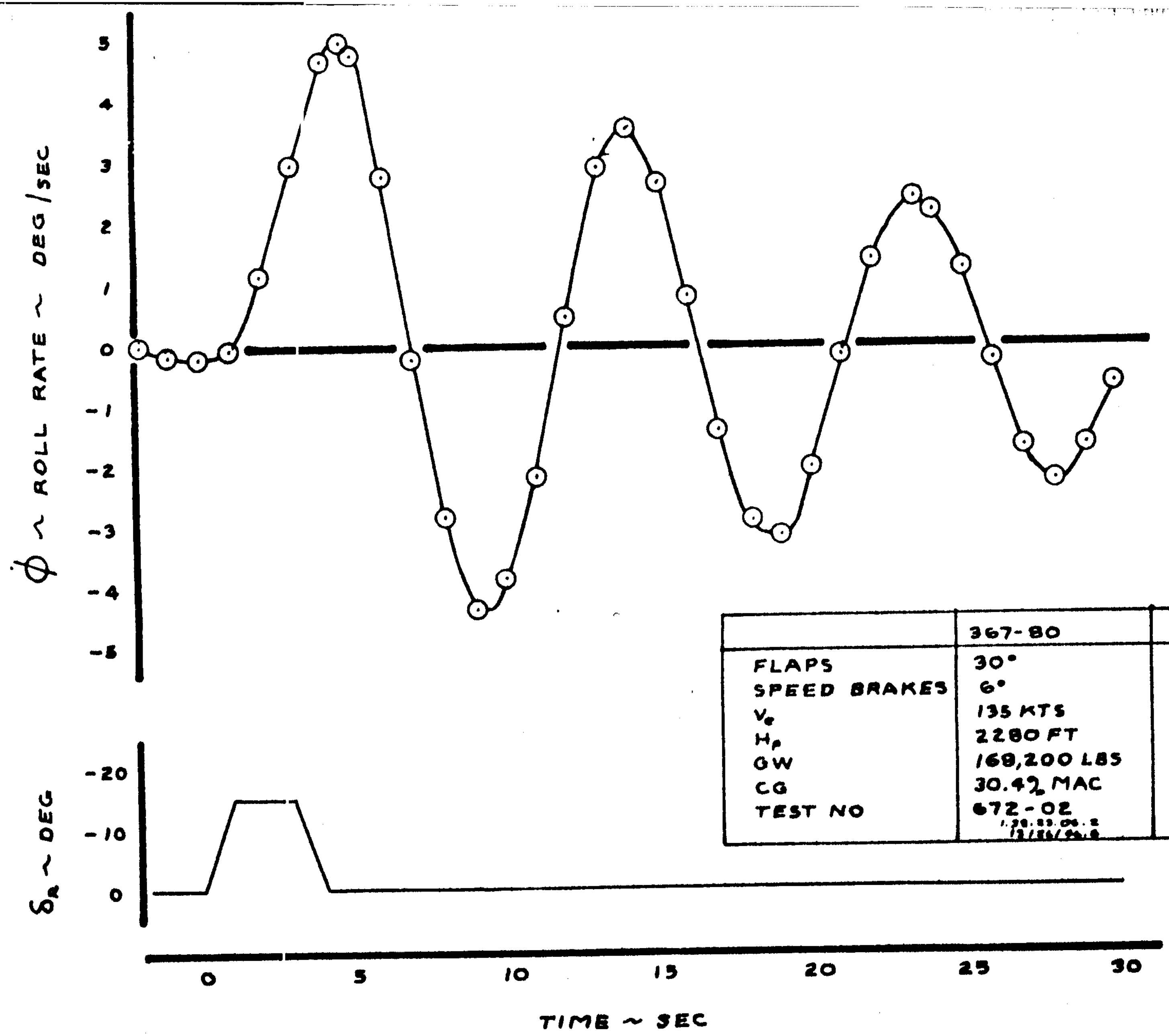

	367-80	NASA 20B
FLAPS	30°	
SPEED BRAKES	6°	
V_e	135 KTS	135 KTS
H_p	2280 FT	
GW	169,200 LBS	280,000 LBS
CG	30.4% MAC	46.0% MAC
TEST NO	672-02	

SAM 9/21/65
RCJ 9/28/65

FIG. 60

NASA DELTA

The basic configuration flown in the program was a representative delta wing supersonic transport. The geometry and stability derivatives are given in Appendix 2. As with the NASA 20 the approach speed was 135 kts indicated and the simulation was flown at this speed. There was no stability augmentation system (SAS) on the basic aircraft.

LONGITUDINAL DOCUMENTATION

Figs. 61 and 62 indicate an accurate simulation of the static longitudinal stability. Both the column deflection and stick force versus velocity show clost agreement with predicted values. The maneuver characteristics are documented in Figs. 63, 64 and 65 and show close agreement with calculated results. Data for these curves were obtained from a wind-up turn. Due to the large drag change with angle of attack (C_{D_α}) of the delta the pilots had difficulty holding speed in the wind-up turn which accounts for some of the scatter shown. The elevator response sensitivity is shown in the pitch reversal data of Fig. 66. Only one data point is shown, as the pilots had trouble with this maneuver and most of the data had large errors.

Dynamic response of the aircraft to an elevator input is shown in Figs. 67 to 69. The short period characteristics as shown in Figs. 67 and 68 indicate close agreement with the predicted response for the first six seconds of the motion. At this point the aircraft behaves as if the static stability were larger than predicted, i.e. the aircraft pitches nose down and the angle of attack returns toward equilibrium. This error was cause by the non-linear pitching moment of the -80 thrust reversers which are driven to change the drag equation terms. The unaccounted for pitch moment of the thrust reversers caused the aircraft to deviate from the predicted values of static stability. As the figures show, the motion is correct for a relatively long time period and the pilot will not be aware of the problem during active control of the aircraft. The matching of initial response and peak values was excellent.

Good phugoid data was difficult to obtain since any slight error in trimming the aircraft resulted in a velocity drift and gusts disturbed the motion. Fig.69 shows that the period is off by about 2.0 sec and the damping is essentially correct. The small error in period cannot be detected by the pilot as he is only mildly aware of the phugoid during active aircraft control and does not see the period at all.

LATERAL-DIRECTIONAL DOCUMENTATION

The static lateral-directional characteristics of the NASA Δ are shown in Fig. 70 . The data were obtained from steady sideslips and show good agreement with the predicted values . The error in δ_w vs. β indicates an error in C_{ℓ_β} which is due to inaccuracy in knowing C_{ℓ_β} of the basic -80. The roll rate, obtained as a function of wheel position is shown in Fig. 71 and the roll acceleration in Fig. 72 . Both of these curves indicate that the simulation was close to the predicted NASA Δ response in roll. The simulation limits are dictated by the maximum capability of the -80. Examination of pilot wheel inputs indicated that a maximum of 15° δ_w was used and the input rarely exceeded 10°. For this range of wheel, the simulation is excellent.

The dynamic response of the simulator to wheel and rudder pulses is shown in Figs. 73 to 78. The adverse yaw characteristic of the stability axis is shown in the $\dot{\psi}$ vs t plot. The flight test data falls very close to the predicted values for the first 9 seconds indicating good agreement. The portion of the curve after 10 seconds indicates a positive spiral stability, while the calculated values are divergent. It is dificult to determine whether this is a dynamic problem or a lateral mistrim. The spiral mode is very sensitive to trim, however the bulk of the flight test material indicates that the spiral was slightly convergent. This should not detract from the simulation during the active control, approach and flare situation since the pilot is interested in initial response to his control input.

The roll rate response for the wheel pulse looks good except for the same spiral convergence after six seconds. The sideslip response indicated the same trends with close initial agreement and then a departure from the predicted due to the spiral.

The dynamic response to rudder inputs shows excellent agreement in sideslip (note the slight mistrim), roll rate and yaw rate for the first five seconds. Following this period the trace exhibits the same spiral convergence noted in the wheel pulses and a lower dutch roll damping than predicted. These two results indicate that the value of C_{ℓ_β} is higher than predicted in the steady sideslip. High C_{ℓ_β} would result in lower Dutch roll damping and higher spiral stability.

For both the longitudinal and lateral directional dynamics, the response to control appears to be excellent. There are some errors in the free airplane dynamics in both cases, but since the aircraft was to be evaluated under active control, it is the controlled aircraft response that is important.

<u>ADDITIONAL PROBLEMS</u>

Since the Delta operates at a low static margin it is necessary to subtract out 92% of the basic -80 static stability. As a result, a 1% error in the -80 C_{m_α} appears as a 12.5% error in the Delta C_{M_α}. It was determined during early Delta work that the movement of flight personnel longitudinally in the aircraft was sufficient to produce a very measurable change in the Delta pitch response. Care was taken to maintain the c.g. position and personnel movements controlled to maintain correct response.

The non-linear pitching moment characteristics of the thrust reversers caused problems in early Delta work. A computer input to the SST throttle should produce a nose down pitch for decreased thrust. Flight work was not consistent, with a pitch up for certain runs and a pitch down for other runs. Once this problem was understood, care was taken to operate as much as possible in the linear area of the curve.

The Delta flies at a high trim angle of attack in the landing approach condition. It is impossible for the -80 to fly the same pitch altitude so that in the simulation the pilot is lower than he would be in the actual SST. This produces two problems. First, his position relative to the ground at touchdown is incorrect. There is little to be done to correct this problem and since the pilots felt that actual ground contact was an important evaluation point no attempt was made to flare at some point above the runway.

Second, the pilot sees certain motions differently due to his location and expressed in the following equations:

$$\dot{\phi}_{-80} = \dot{\phi}_{\Delta} \cos \alpha_c + \dot{\psi}_{\Delta} \sin \alpha_c$$

$$\dot{\psi}_{-80} = -\dot{\phi}_{\Delta} \sin \alpha_c + \dot{\psi}_{\Delta} \cos \alpha_c$$

where:

$$\alpha_c = \alpha_{\Delta} - \alpha_{-80}$$

TD 1546 L-R3

6-7000

This indicates a cross-feed of $\dot{\psi}_{\Delta}$ into $\dot{\phi}_{-80}$ and $\dot{\phi}_{\Delta}$ into $\dot{\psi}_{-80}$. The pilot sees this as adverse yaw for sharp roll inputs. Since this adverse yaw is a false cue due to pilot position it was partially removed from the simulation by using a rudder input with wheel (TCP). This technique does not change the free airplane dynamics and only slightly changes the static response. It serves to remove the false cue at the point where it is obvious to the pilot; at a sharp wheel input. This input also served to correct an apparent error in the $C_{n_{\delta w}}$ of the basic -80.

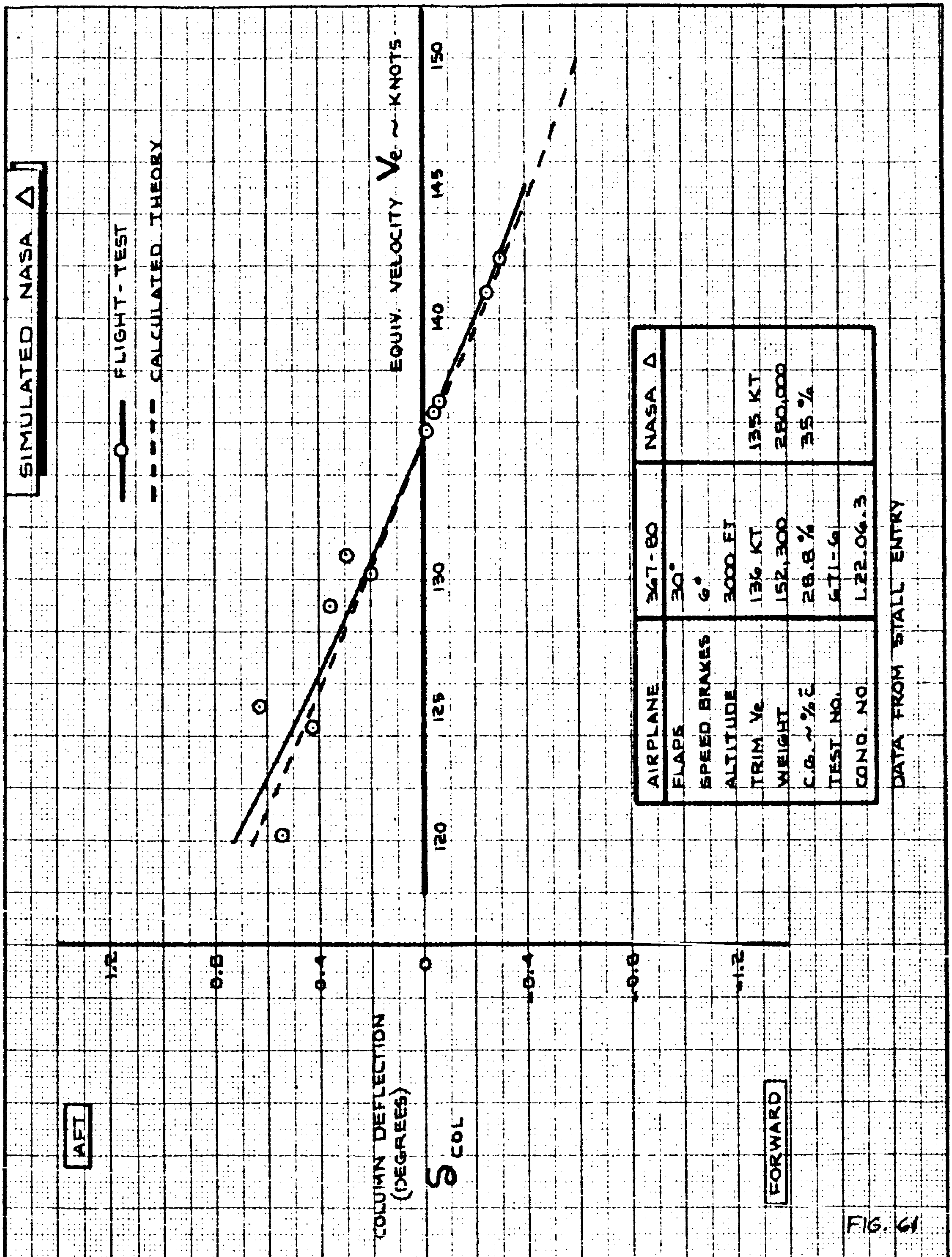

AIRPLANE	367-80	NASA Δ
FLAPS	30°	
SPEED BRAKES	6°	
ALTITUDE	3000 FT	
TRIM Ve	136 KT	135 KT
WEIGHT	152,300	280,000
C.G. ~ % c̄	28.8 %	35 %
TEST NO.	671-6	
COND. NO.	L22.06.3	

FIG. 61

CALC	TAYLOR		REVISED	DATE	COLUMN VS SPEED CHARACTERISTICS	BASIC NASA DELTA
CHECK						D6-10743
APR						
APR					THE BOEING COMPANY	PAGE 90

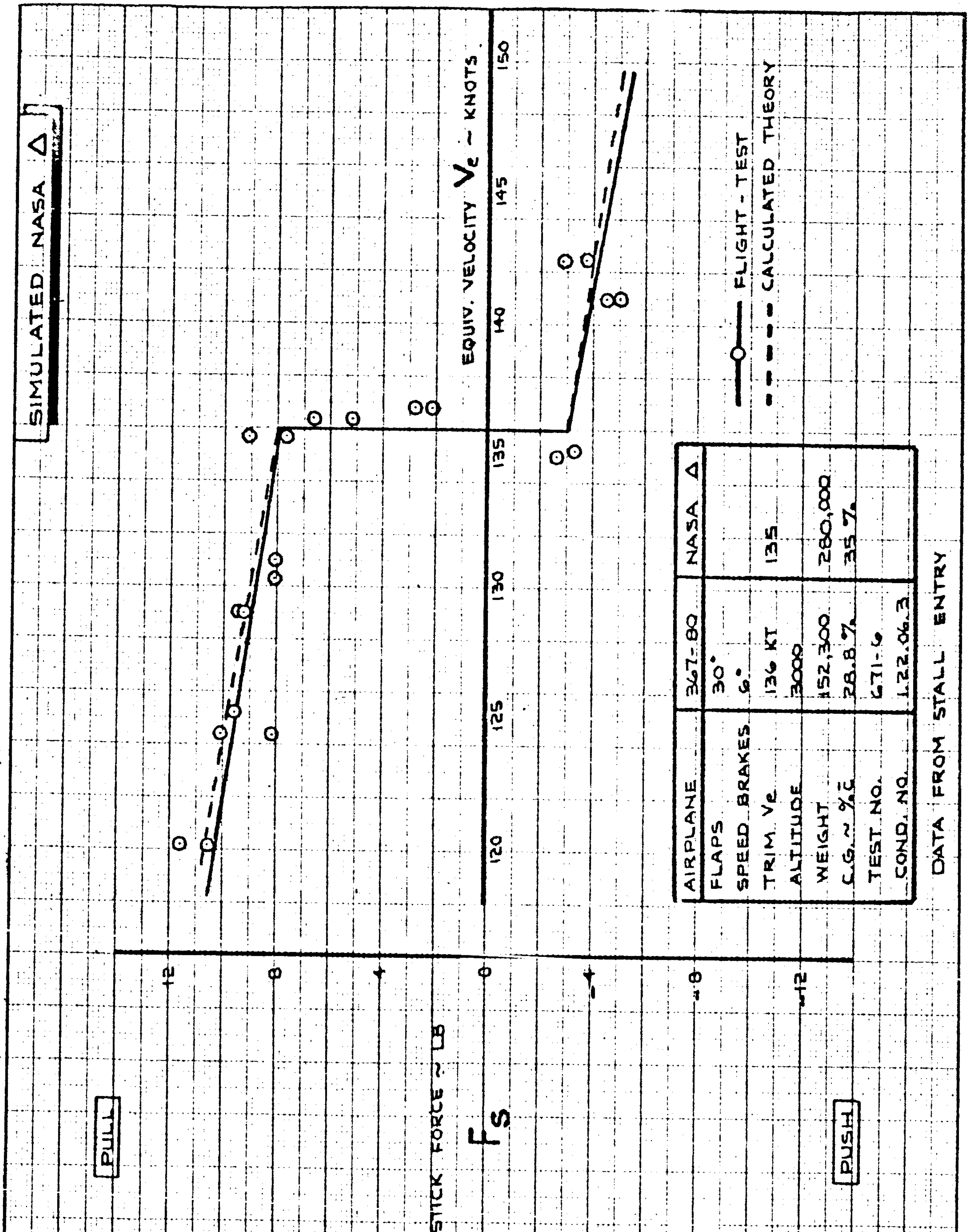

AIRPLANE	367-80	NASA Δ
FLAPS	30°	
SPEED BRAKES	6°	
TRIM Ve	136 KT	135
ALTITUDE	3000	
WEIGHT	152,300	280,000
C.G. ~ %c̄	28.8 %	35 %
TEST NO.	671-6	
COND. NO.	1.22.06.3	

FIG. 62

CALC	TAYLOR		REVISED	DATE	**SPEED STABILITY** STICK FORCE VS SPEED	BASIC NASA DELTA
CHECK						D6-10743
APR					THE BOEING COMPANY	PAGE 91
APR						

TD 441 C R4

SIMULATED NASA △

AIRPLANE	367-80	NASA △
FLAPS	30°	
SPEED BRAKES	6°	
ALTITUDE	3,000	
TRIM Ve	138	135
WEIGHT	167,000	280,000
C.G. ~ % $\bar{c}$	30.4%	35%
TEST NO.	671-6	
COND. NO.	1.22.06.02	& 02.1

DATA FROM WIND-UP TURN MANEUVER

$\delta_{E_{SST}} / \delta_{COL} = -1.0$

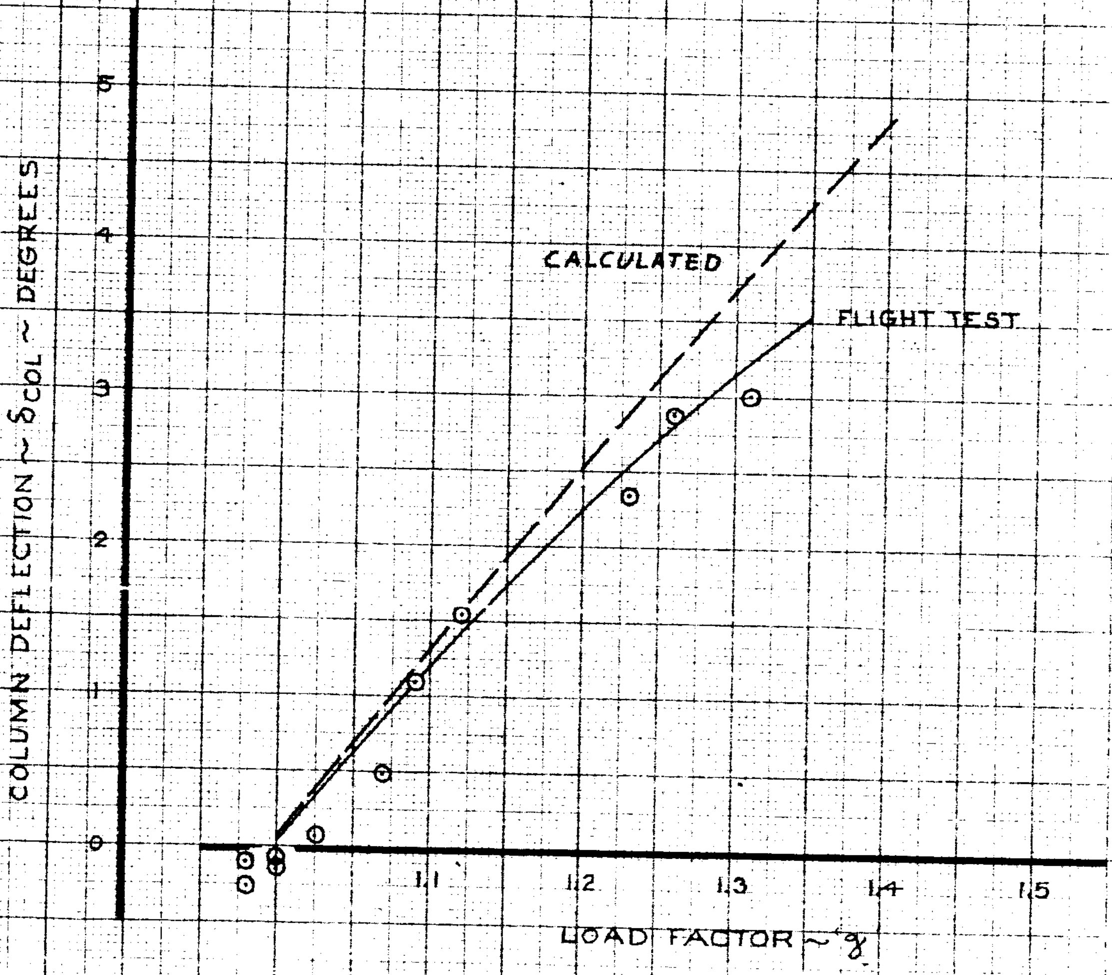

FIG. 63

CALC	TAYLOR		REVISED	DATE	NORMAL ACCELERATION Vs. COLUMN CHARACTERISTICS	BASIC NASA DELTA
CHECK			STEMWELL	1-31-66		D6-10743
APR					THE BOEING COMPANY	PAGE 92
APR						

TD 461 C-R4

SIMULATED NASA △

AIRPLANE	367-80	NASA △
FLAPS	30°	
SPEED BRAKES	6°	
ALTITUDE	3,000	
TRIM Ve	138	135
WEIGHT	167,000	280,000
C.G. ~ % $\bar{c}$	30.4%	35%
TEST NO.	671-6	
COND. NO.	1.22.06.02	8.02.1

DATA FROM WIND-UP TURN MANEUVER

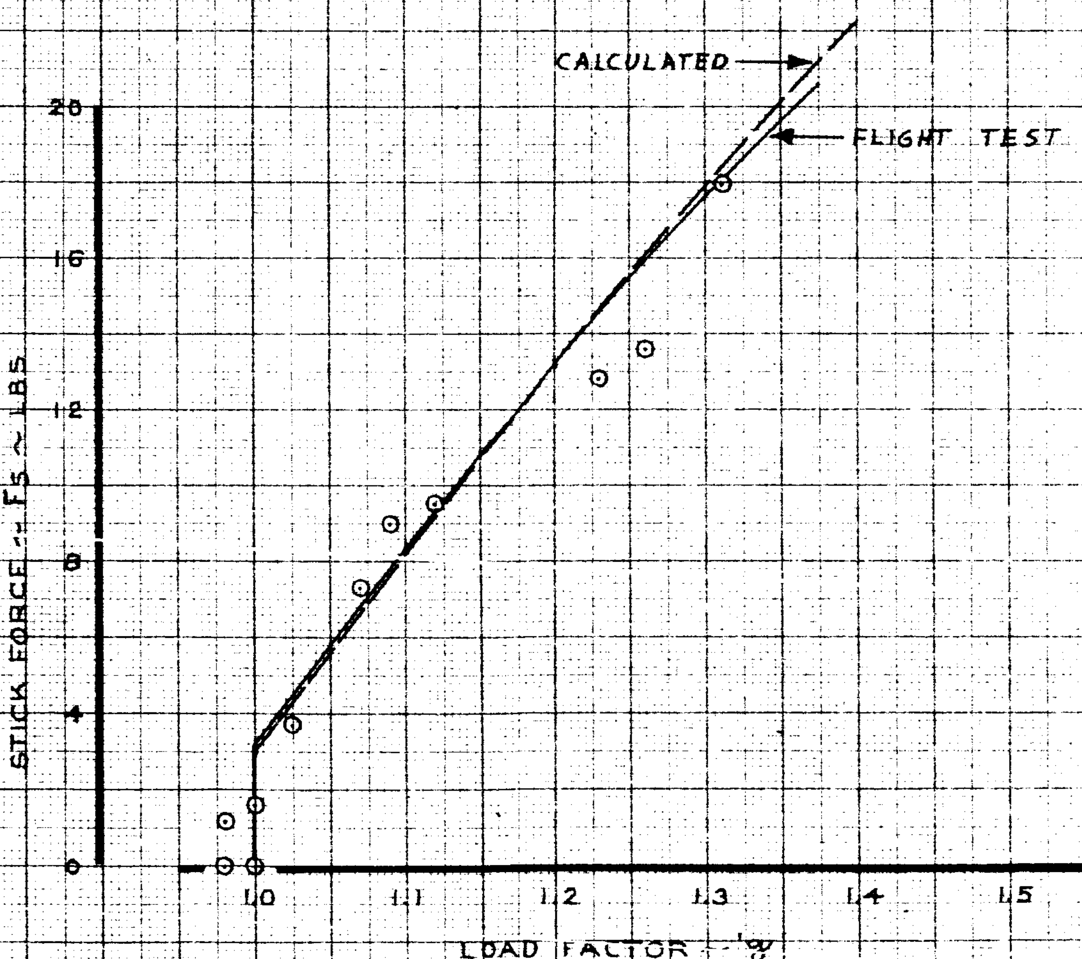

FIG. 64

CALC	TAYLOR	REVISED	DATE	NORMAL ACCELERATION Vs FORCE CHARACTERISTICS	BASIC NASA DELTA
CHECK		STEMWELL	2-1-66		D6-10743
APR				THE BOEING COMPANY	PAGE 93
APR					

SIMULATED NASA Δ

AIRPLANE	367-80	NASA Δ
FLAPS	30°	
ALTITUDE	3000	
TRIM Ve	138	135
WEIGHT	167,000	280,000
CG ~ % $\bar{c}$	30.4 %	35 %
TEST NO.	671-6	
COND. NO	1.22.06.02	

DATA FROM WIND-UP TURN

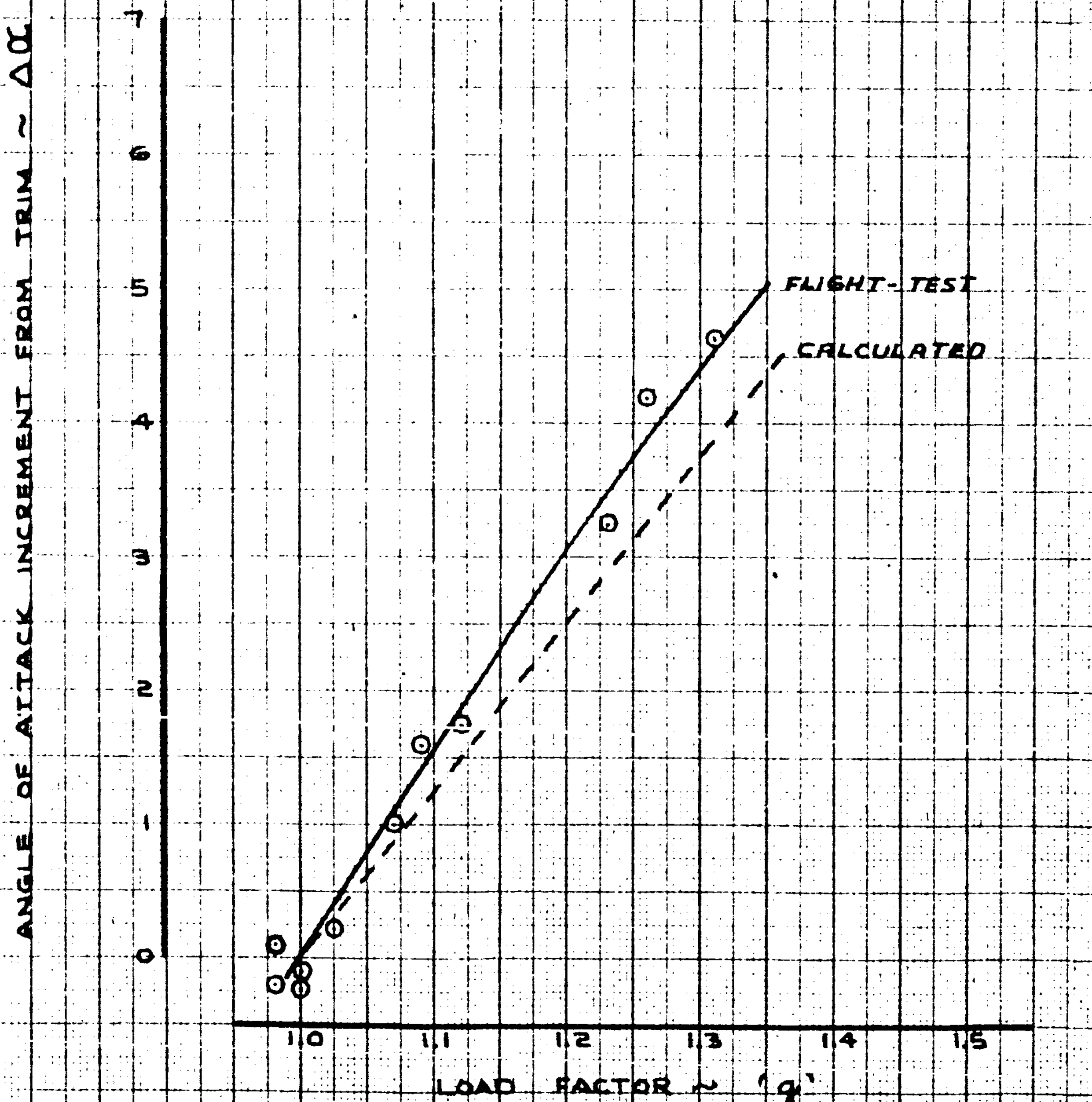

FIG. 65

CALC	TAYLOR		REVISED	DATE	NORMAL ACCELERATION VS. ANGLE OF ATTACK	BASIC NASA Δ
CHECK						D6-10743
APR					THE BOEING COMPANY	PAGE 94
APR						

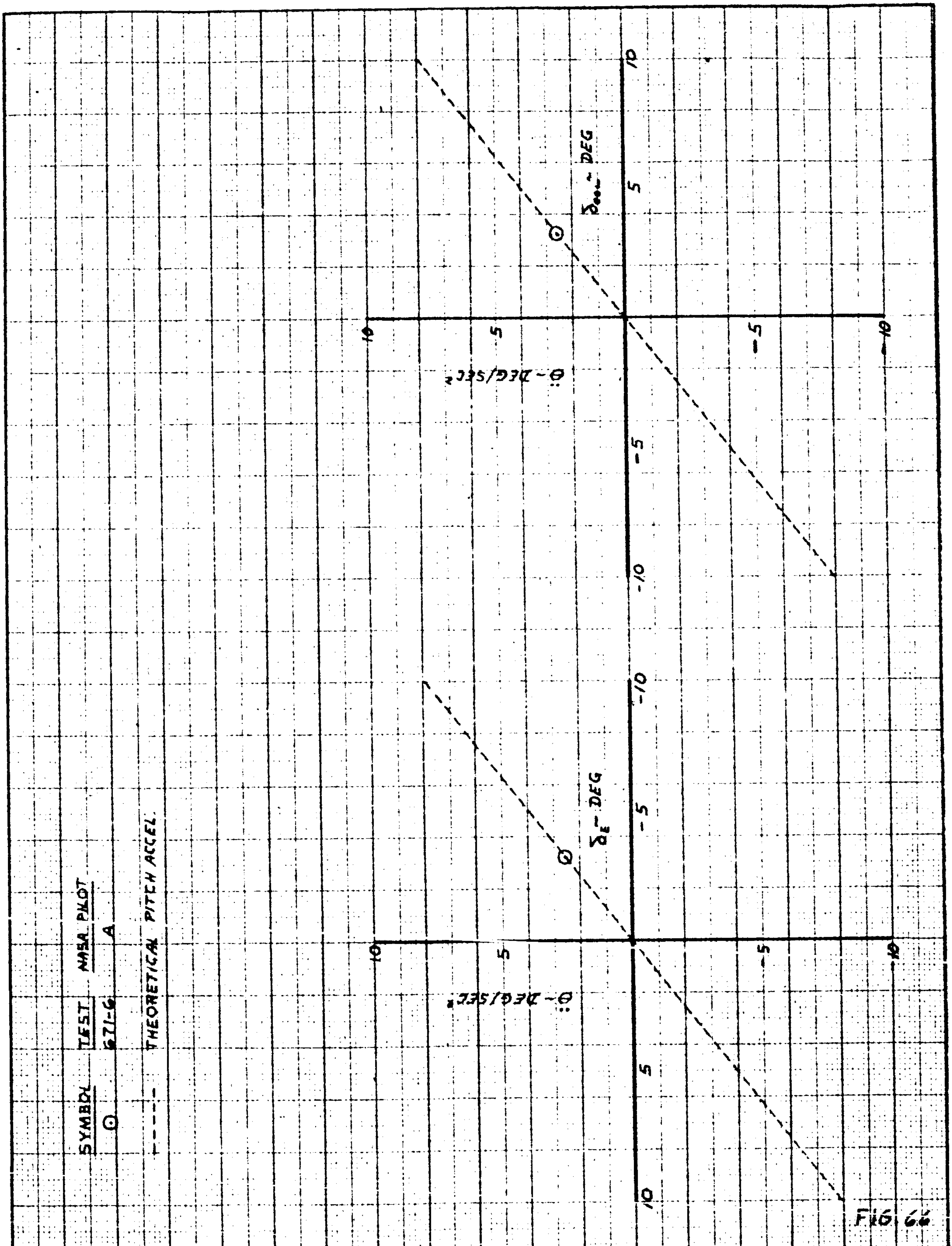

FIG. 66

CALC	D J BECK	11-18-65	REVISED	DATE
CHECK				
APR				
APR				

PITCH ACCELERATION OF THE NASA Δ SST (BASIC CG ~ NO SAS)

D6-10743

THE BOEING COMPANY

TD 441 C R4

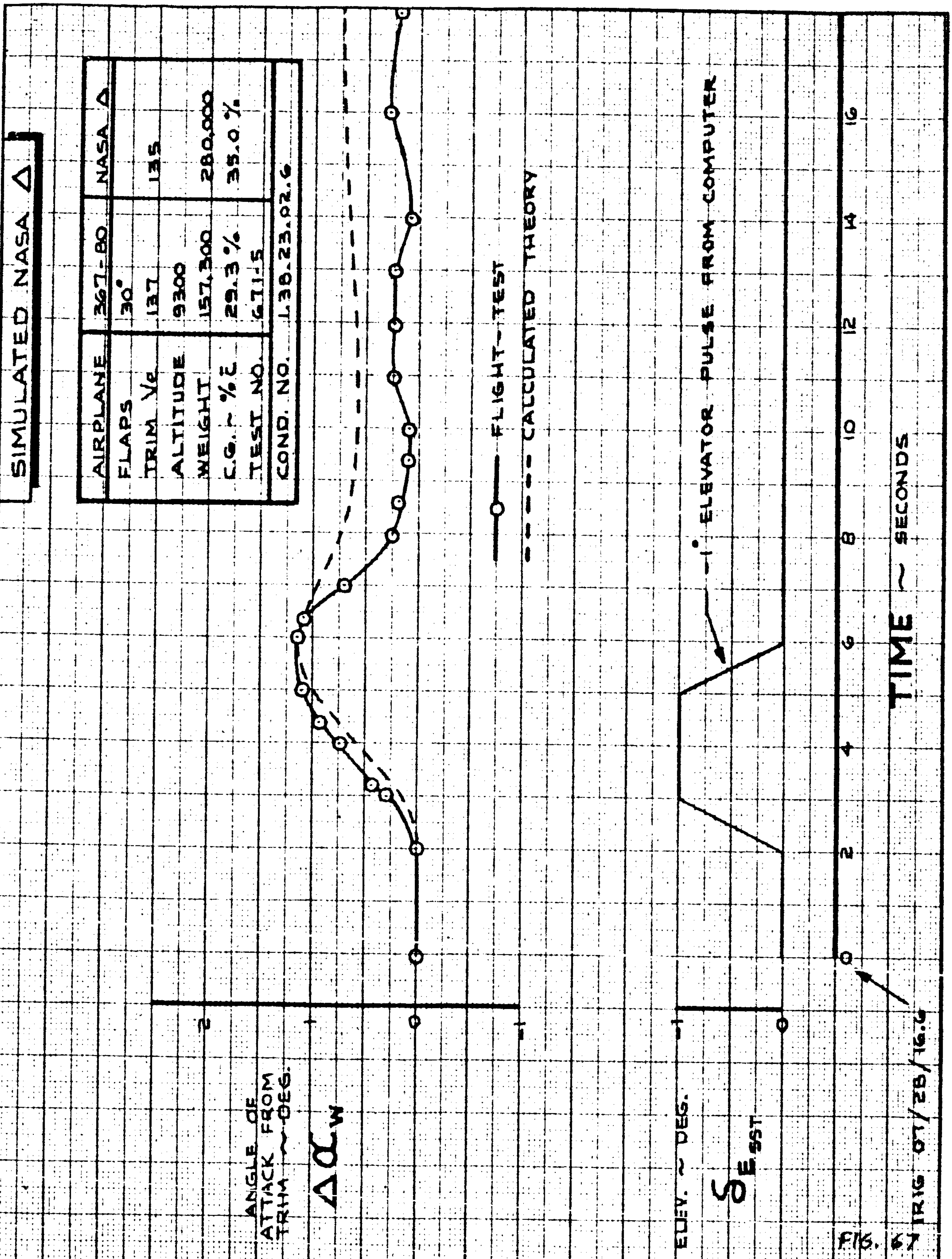

FIG. 67

CALC	TAYLOR		REVISED	DATE	SHORT PERIOD CHARACTERISTICS
CHECK					
APR					
APR					THE BOEING COMPANY

BASIC NASA DELTA

D6-10743

TD 441 C-R4

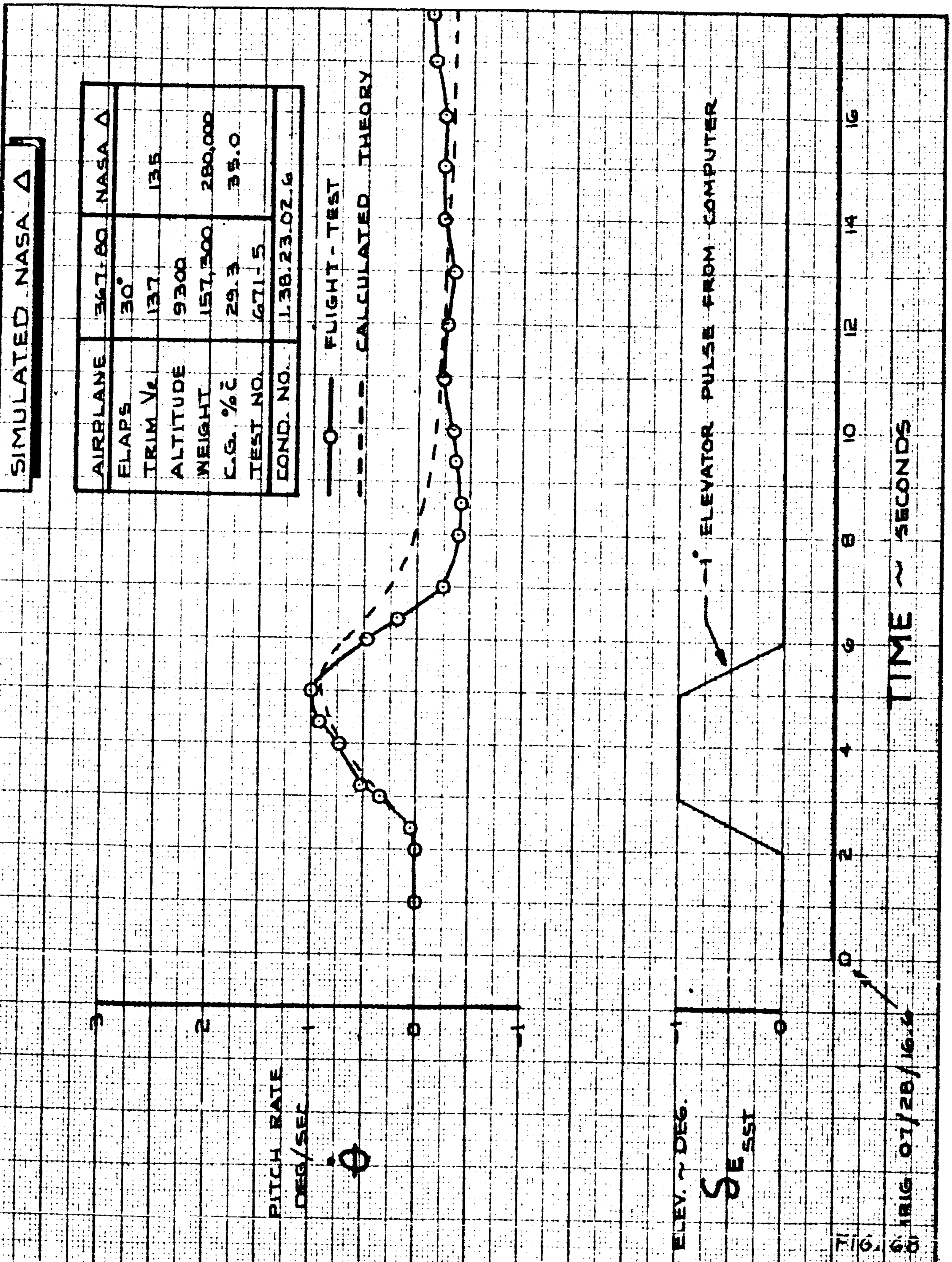

FIG. 68

CALC	TAYLOR		REVISED	DATE	SHORT PERIOD CHARACTERISTICS	BASIC NASA DELTA
CHECK						
APR						D6-10743
APR					THE BOEING COMPANY	PAGE 97

TD 461 C-R4

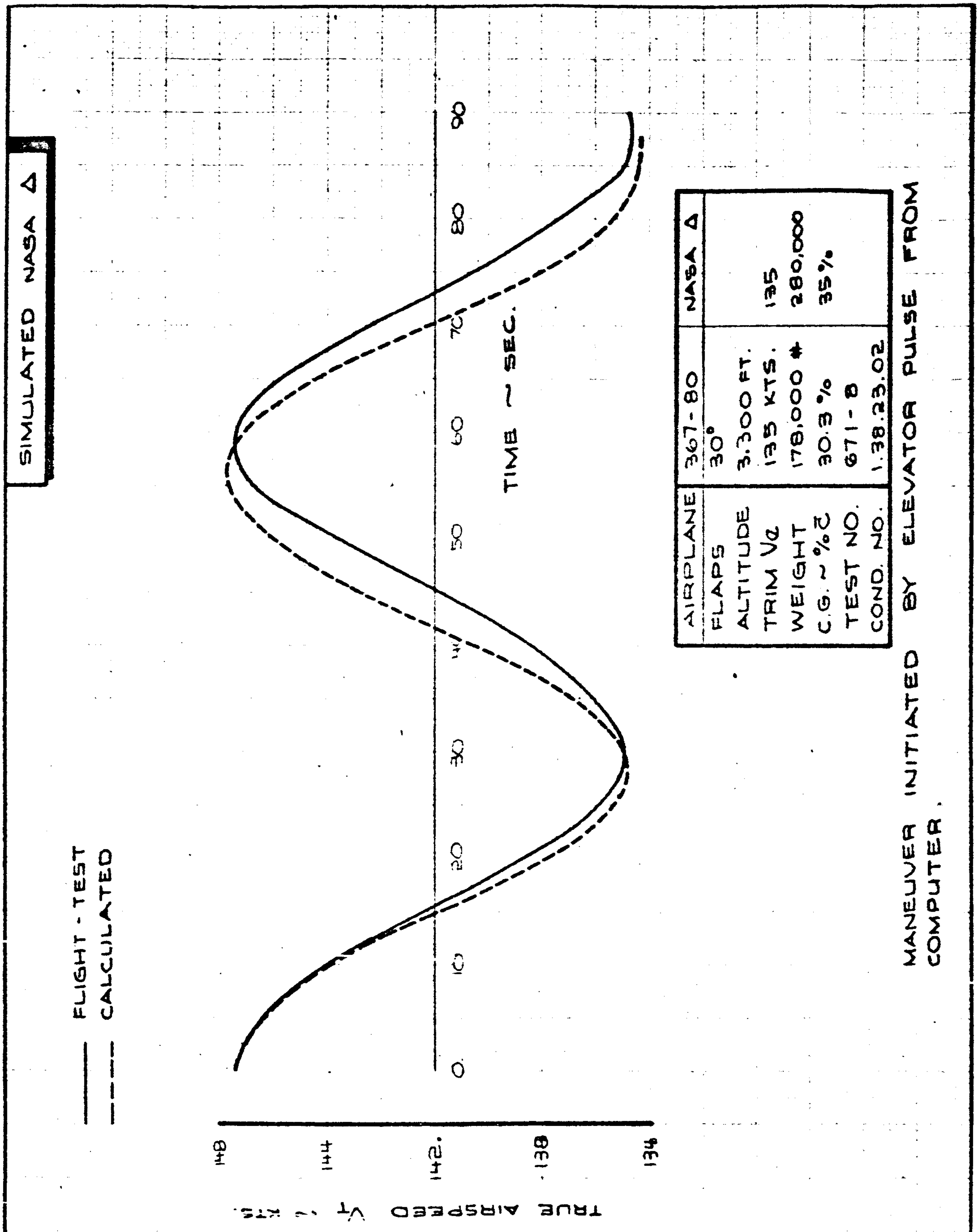

FIG. 69

CALC			REVISED	DATE	PHUGOID CHARACTERISTICS.	BASIC NASA DELTA
CHECK						
APR						D6-10743
APR					THE BOEING COMPANY	PAGE 98

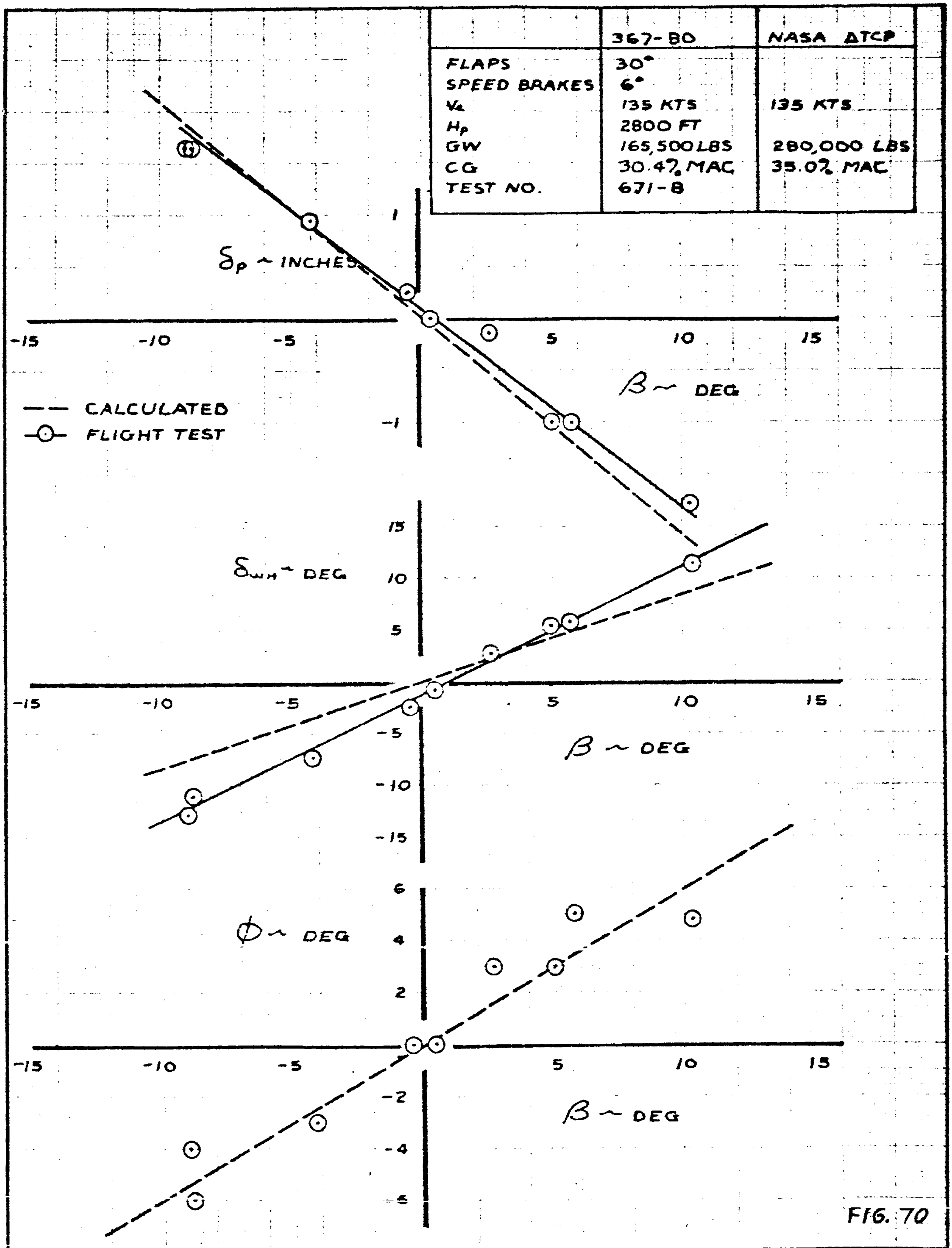

FIG. 70

CALC	RCS	9/3/65	REVISED	DATE
CHECK			RCS	12/2/65
APR				
APR				

LATERAL - DIRECTIONAL STATIC STABILITY

THE BOEING COMPANY

SIMULATED NASA ATCP

D6-10743

TD 461 C-R4

	367-80	NASA ΔTCP
FLAPS	30°	
SPEED BRAKES	6°	
V_e	135 KTS	135 KTS
H_p	3100 FT	
GW	160,700 LBS	280,000 LBS
CG	30.4 % MAC	35.0 % MAC
TEST NO.	671-8	

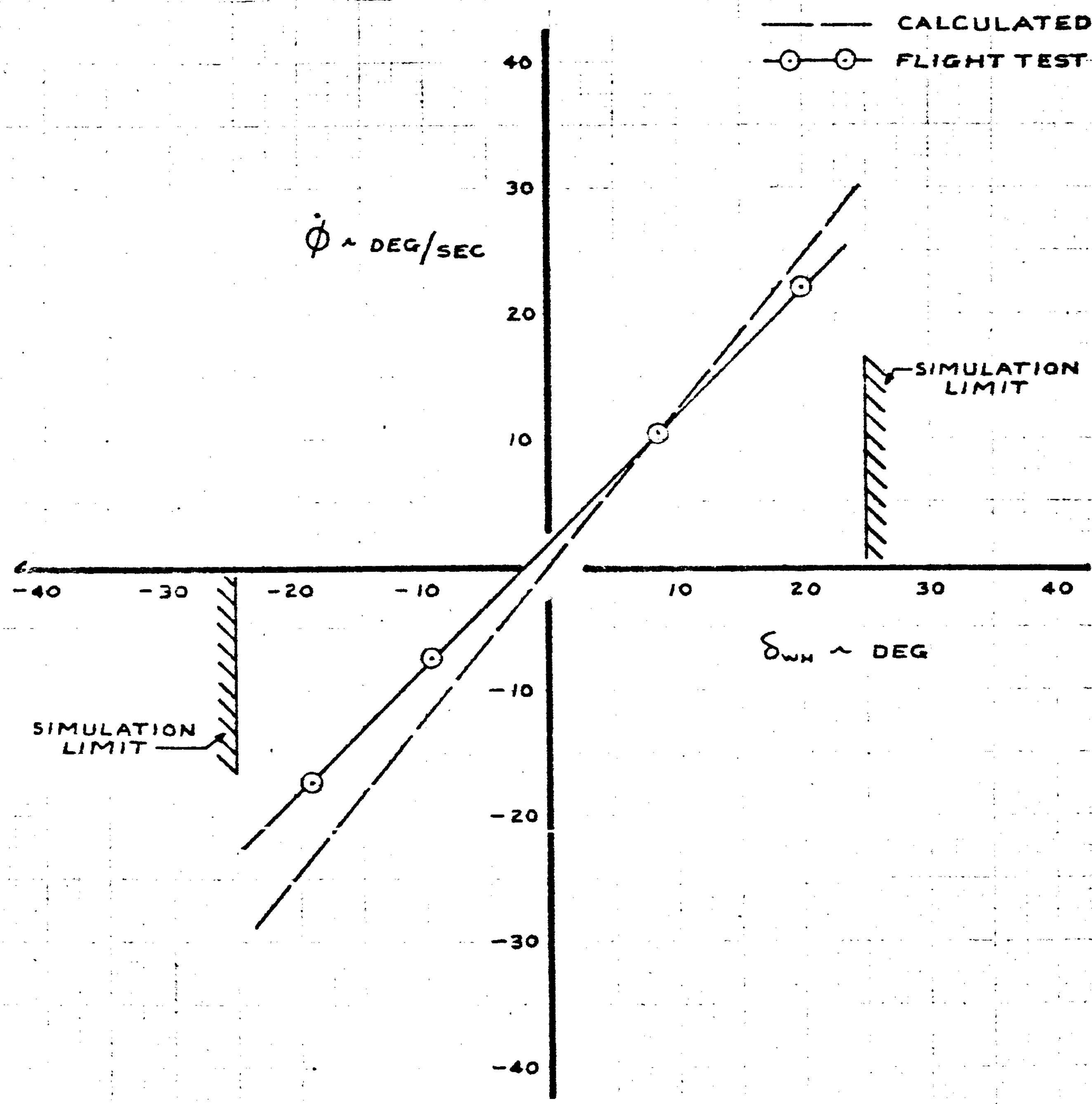

FIG. 71

CALC	SAM	10/22/65	REVISED	DATE	LATERAL CONTROL RESPONSE
CHECK	RCS	10/23/65	RCS	12/2/65	STEADY STATE ROLL RATE
APR					1 DEGREE OF FREEDOM
APR					THE BOEING COMPANY

SIMULATED NASA ΔTCP

D6-10743

TD 461 C-R4

	367-80	NASA ΔTCP
FLAPS	30°	
SPEED BRAKES	6°	
V_e	135 KTS	135 KTS
H_p	7470 FT.	
GW	147,900 LBS	280,000 LBS
CG	29.0 % MAC	35.0 % MAC
TEST NO.	⊙ ~ 671-B	
	⊡ ~ 674-2	

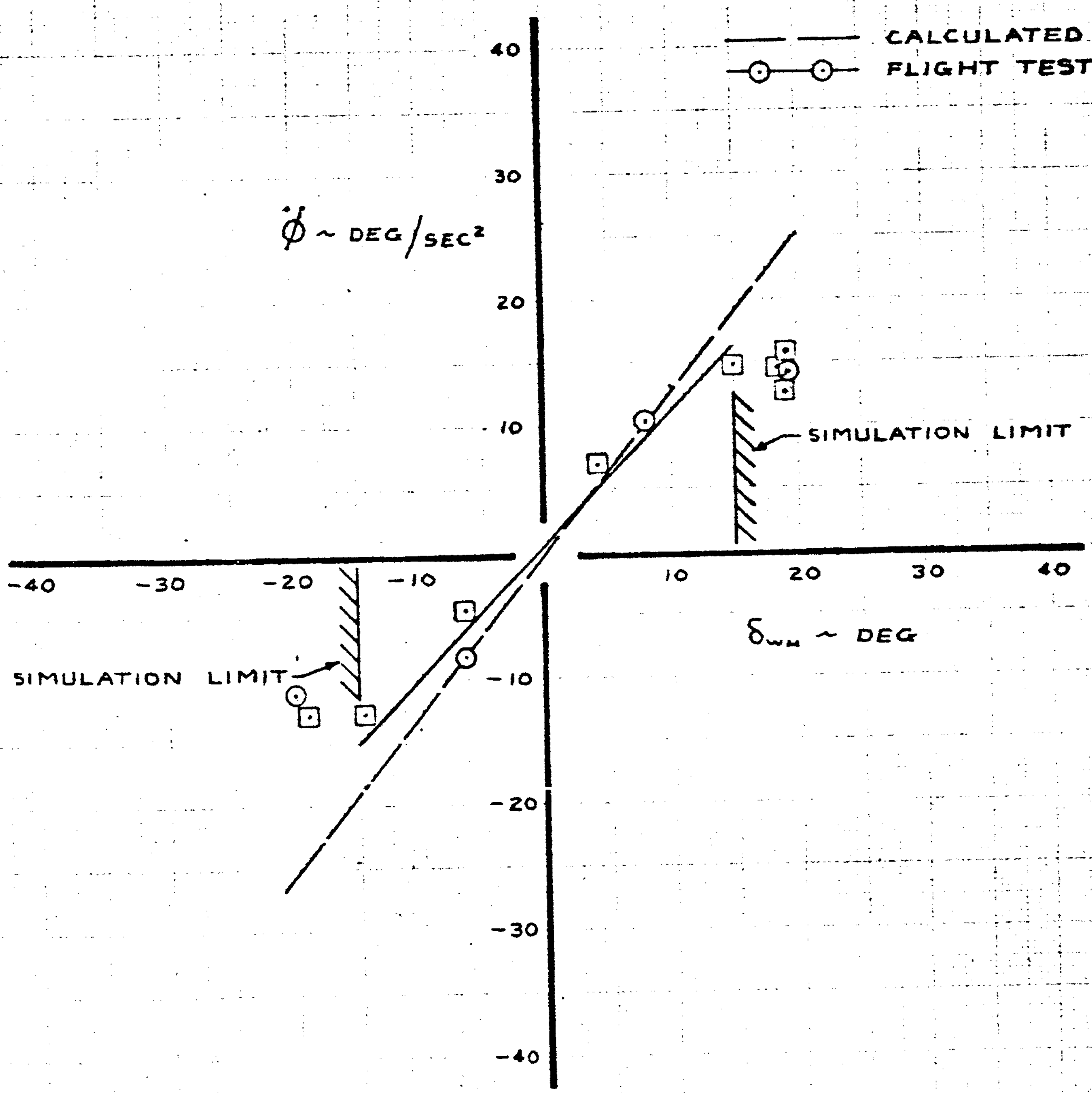

FIG. 72

CALC			REVISED	DATE	ROLL ACCELERATION CHARACTERISTICS 1 DEGREE OF FREEDOM	SIMULATED NASA ΔTCP
CHECK			RCS	12/2/65		D6-10743
APR						PAGE 101
APR					THE BOEING COMPANY	

	367-80	NASA ΔTCP
FLAPS	30°	
SPEED BRAKES	6°	
V_e	135 KTS	135 KTS
H_p	2750 FT	
GW	167,700 LBS	280,000 LBS
CG	30.3% MAC	35.0% MAC
TEST NO.	671-8	

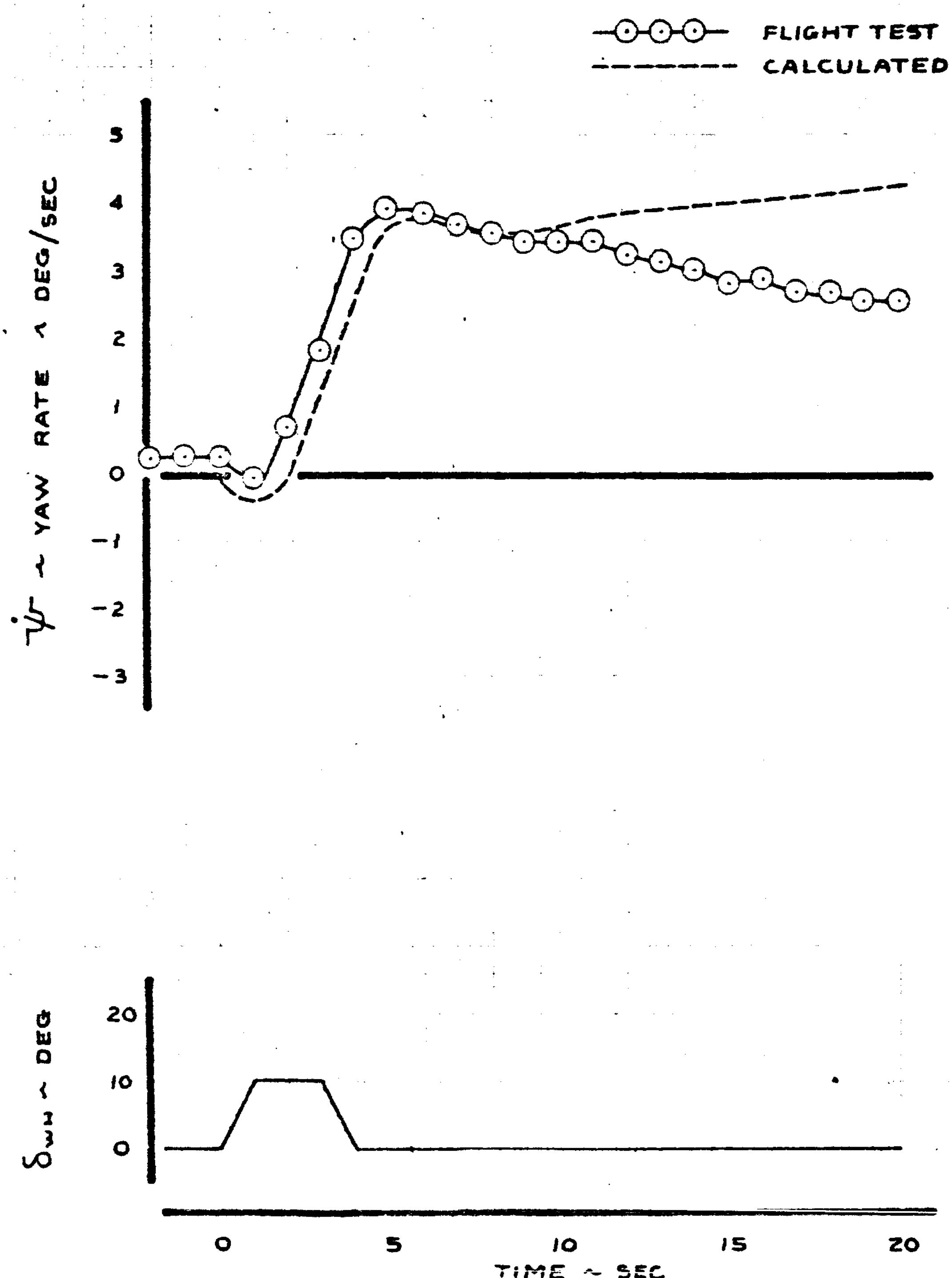

FIG. 73

CALC	RC?	10/10/65	REVISED	DATE
CHECK				
APR				
APR				

LATERAL CONTROL RESPONSE
COMPUTER WHEEL PULSE

1.38 27.01 9/19/18 8

THE BOEING COMPANY

SIMULATED NASA ΔTCP

D6-10743

TD 441 C-R4

	367-80	NASA ΔTCP
FLAPS	30°	
SPEED BRAKES	6°	
V_e	135 KTS	135 KTS
H_p	2750 FT	
GW	167,700 LBS	280,000 LBS
CG	30.3 % MAC	35.0 % MAC
TEST NO.	671-B	

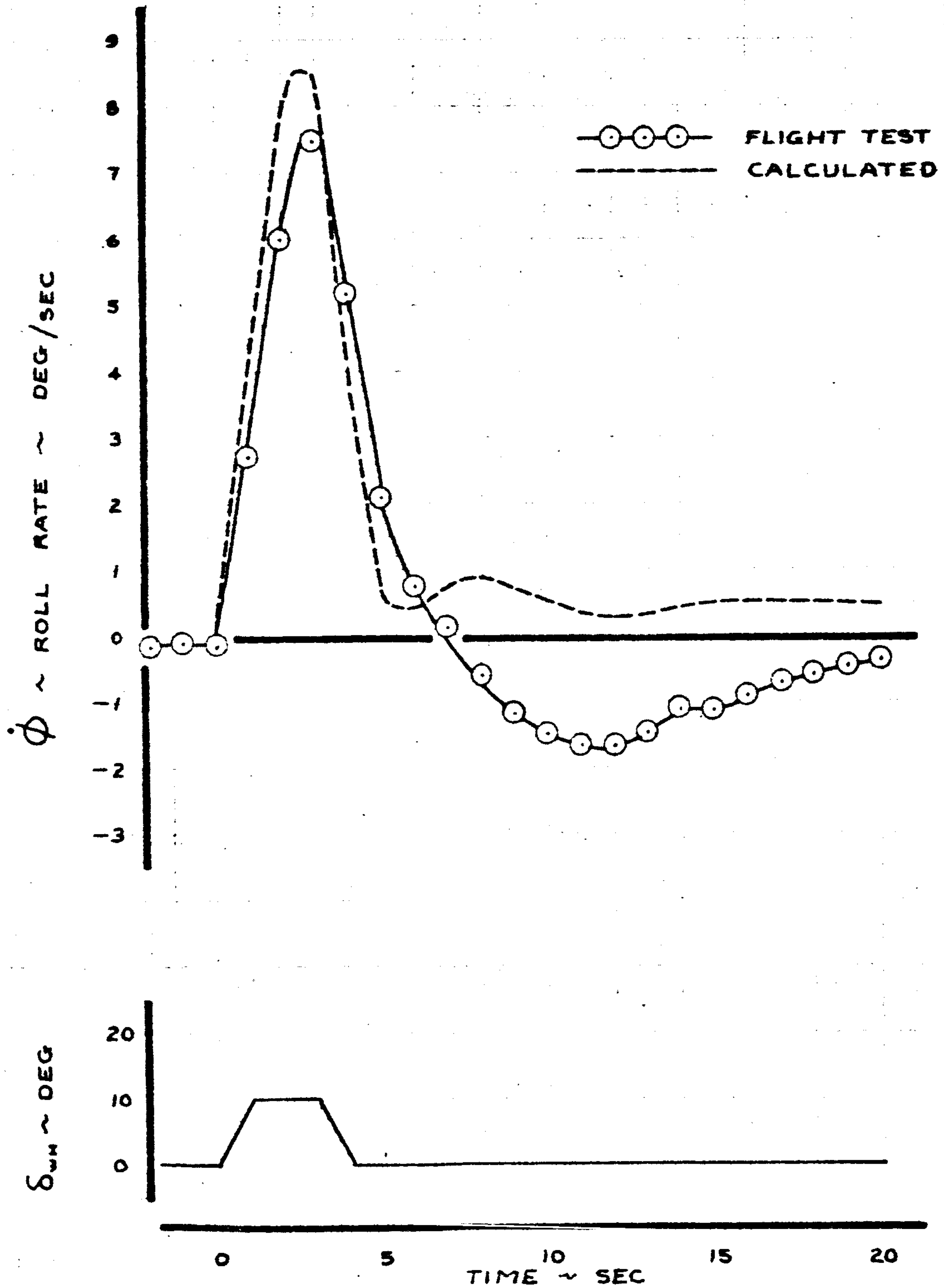

FIG. 74

CALC	RCJ	10/10/65	REVISED	DATE	LATERAL CONTROL RESPONSE COMPUTER WHEEL PULSE	SIMULATED NASA ΔTCP
CHECK						D6-10743
APR					THE BOEING COMPANY	PAGE 103
APR						

TD 461 C-R4

	367-80	NASA ΔTCP
FLAPS	30°	
SPEED BRAKES	6°	
V_e	135 KTS	135 KTS
H_p	2750 FT	
GW	167,700 LBS	280,000 LBS
CG	30.37% MAC	35.0% MAC
TEST NO.	671-8	

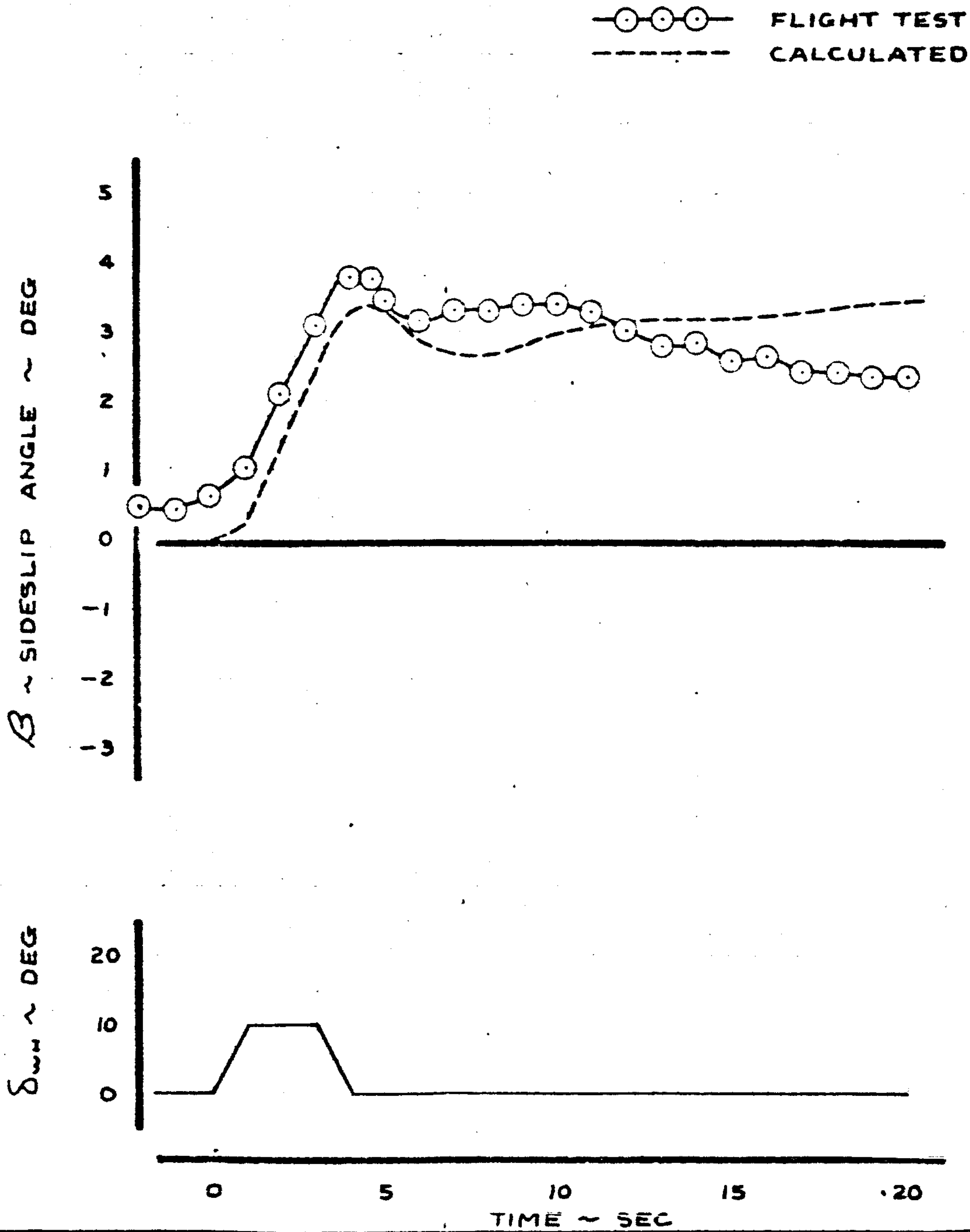

FIG. 75

CALC	RC	12/2/65	REVISED	DATE
CHECK				
APR				
APR				

LATERAL CONTROL RESPONSE
COMPUTER WHEEL PULSE

SIMULATED NASA ΔTCP

D6-10743

THE BOEING COMPANY

TD 461 C-R4

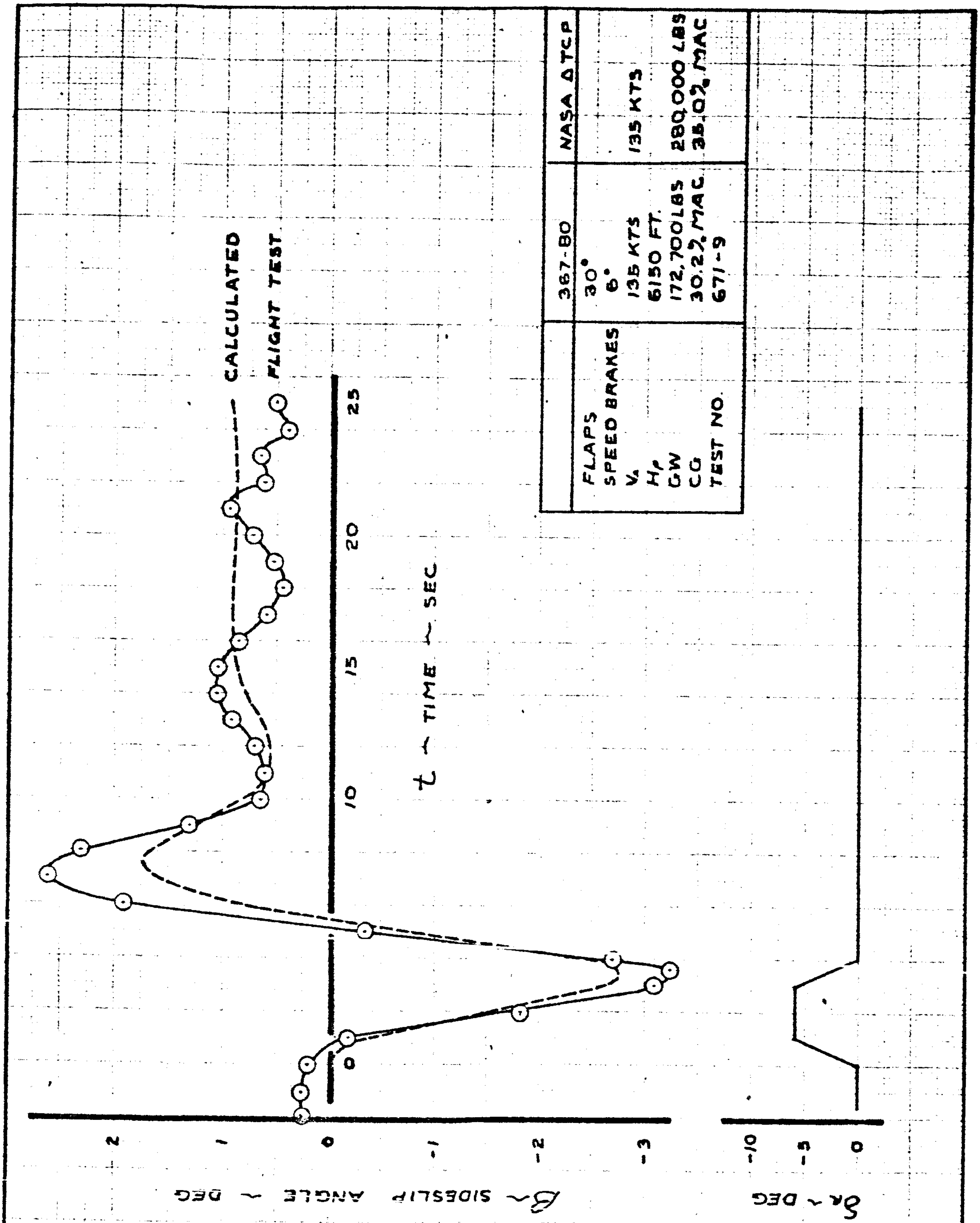

FIG. 76

CALC	RCD	9/2/65	REVISED	DATE	LATERAL — DIRECTIONAL DYNAMICS	SIMULATED NASA ΔTCP
CHECK	SAM	9/2/65				
APR					1-38.23.06	D6-10743
APR					THE BOEING COMPANY	PAGE 105

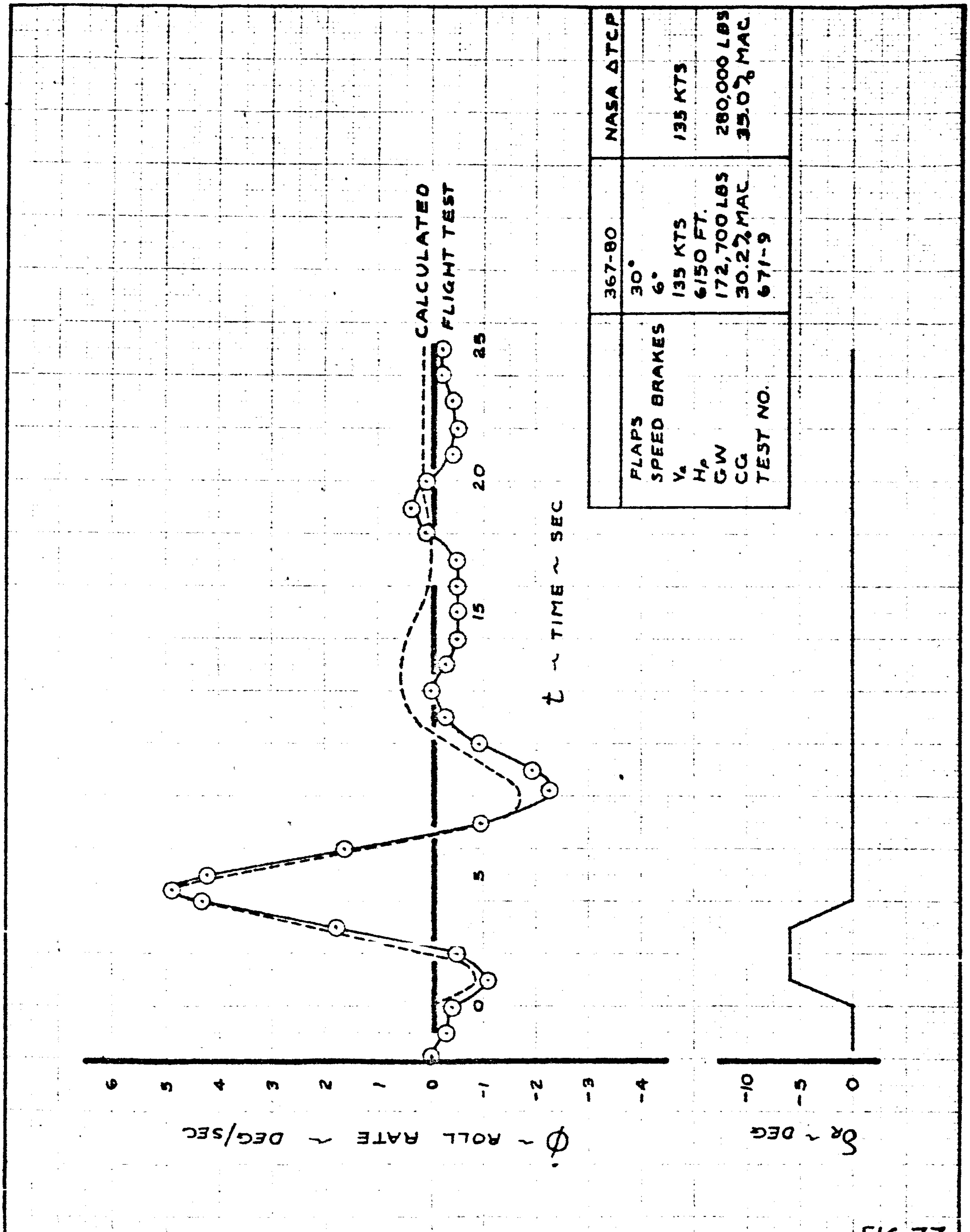

FIG. 77

CALC	RCJ	9/2/65	REVISED	DATE	LATERAL — DIRECTIONAL DYNAMICS	SIMULATED NASA ΔTCP
CHECK						D6-10743
APR					1.38.23.06	
APR					THE BOEING COMPANY	PAGE 106

TD 461 C-R4

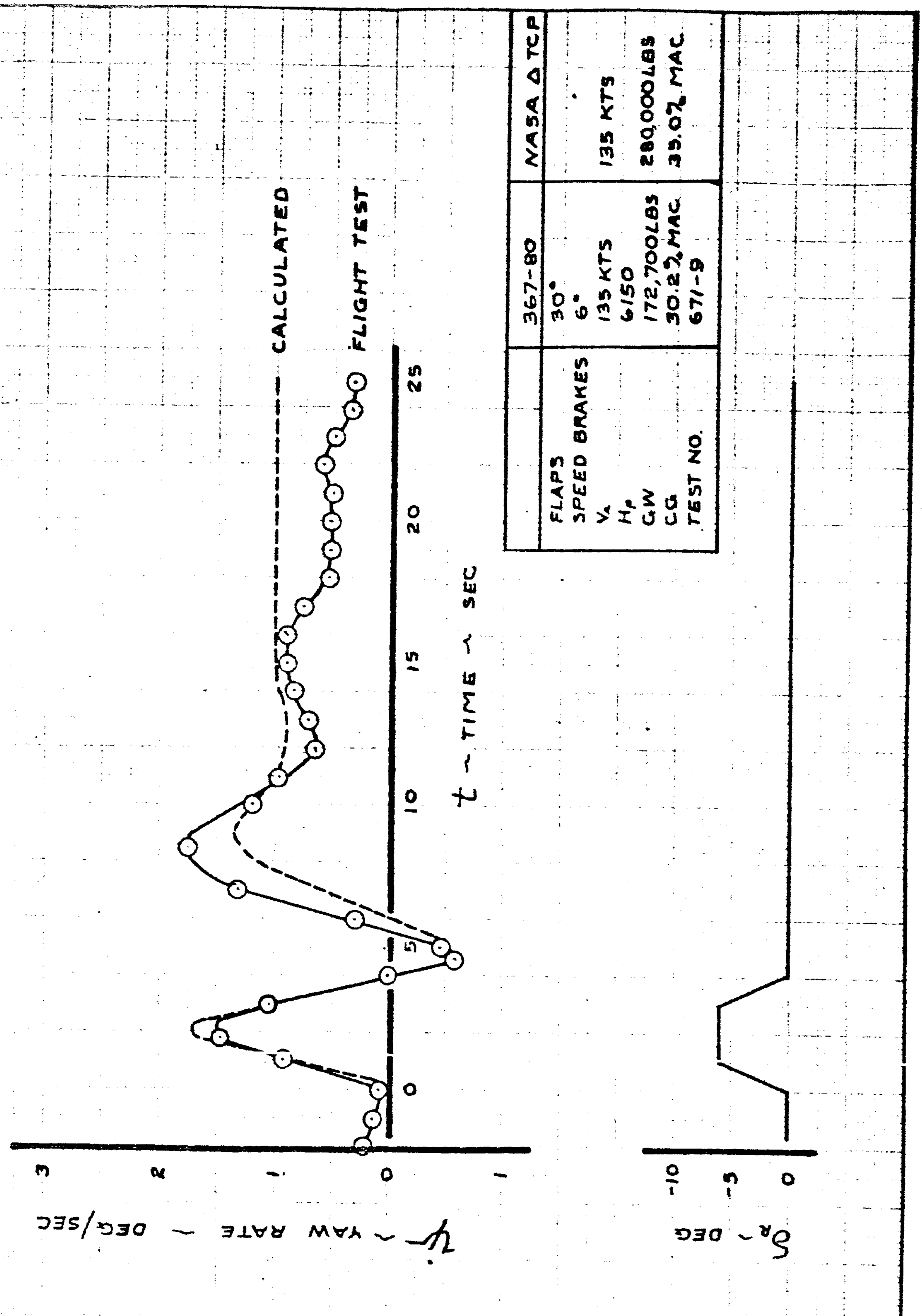

FIG. 78

CALC	RCB	9/2/65	REVISED	DATE	LATERAL - DIRECTIONAL DYNAMICS	SIMULATED NASA ΔTCP
CHECK						
APR					1.38.23.06	D6-10743
APR						
					THE BOEING COMPANY	PAGE 107

TD 461 C-R4

NASA DELTA AUGMENTED

The augmented version of the Delta contained both longitudinal stability augmentation and lateral-directional augmentation. The longitudinal SAS consisted of pitch rate and angle of attack feedbacks and a column to elevator gearing change to maintain the stick force per "g" constant. The elevator was driven according to the following expression:

$$\delta E = \left[\frac{\delta E}{\delta C}\right]_{BASIC} \times 4\,\delta C + 1.46\,\dot{\theta} + 1\,\Delta\alpha$$

This system is designed to increase the short period frequency while leaving the damping ratio approximately constant. In this case the natural frequency goes from 0.75 to 1.46 rad/sec while the damping ratio goes from 0.867 to 0.793.

The lateral-directional augmentation consisted of a roll damper which was implemented according to the following relation:

$$\delta_w = \delta_{w_p} - 0.45\dot{\phi}$$

where δ_{w_p} is the pilot wheel input. The lateral-directional augmentation is designed to decrease the rolling mode time constant from the basic value of 0.80 to the augmented value of 0.575.

LONGITUDINAL DOCUMENTATION

The static longitudinal characteristics of the NASA ΔA are shown in Figs. 79 to 80. The agreement with the predicted curves is excellent although there is considerable scatter and there was insufficient data for speeds above trim. Based upon the information shown in the column deflection vs. velocity curve and the accurate force vs. deflection characteristics of the stick, it is safe to assume that the static calibration should be equally good at higher speeds.

Figs. 81, 82, and 83 indicate a reasonably good match of the Delta Augmented maneuver characteristics. There is some error apparent, especially at the higher load factors. There is also an error apparent in the lift-curve slope (α_W vs. load factor) simulation. Data reduction of the wind-up turn is difficult and there is considerable error introduced by the manner in which the maneuver was performed. The aircraft was difficult to fly in the wind-up turn and the high C_{D_α} resulted in high rates of sink to maintain velocity.

Pitch acceleration data indicates excellent simulation of the elevator control power and sensitivity. The documentation shown here when used in conjunction with the Basic NASA Delta documentation indicated that the longitudinal characteristics were simulated correctly.

The lateral-directional documentation was limited since the only change was the inclusion of the roll damper. Both the 1 degree of freedom roll rates show that the change in roll damping was correctly simulated.

Fig. 87 shows a typical rudder pulse response to demonstrate the Dutch roll characteristics of the augmented version of the Delta. As with the longitudinal documentation, the data shown here in conjunction with the Basic NASA Delta shows that correct simulation was achieved.

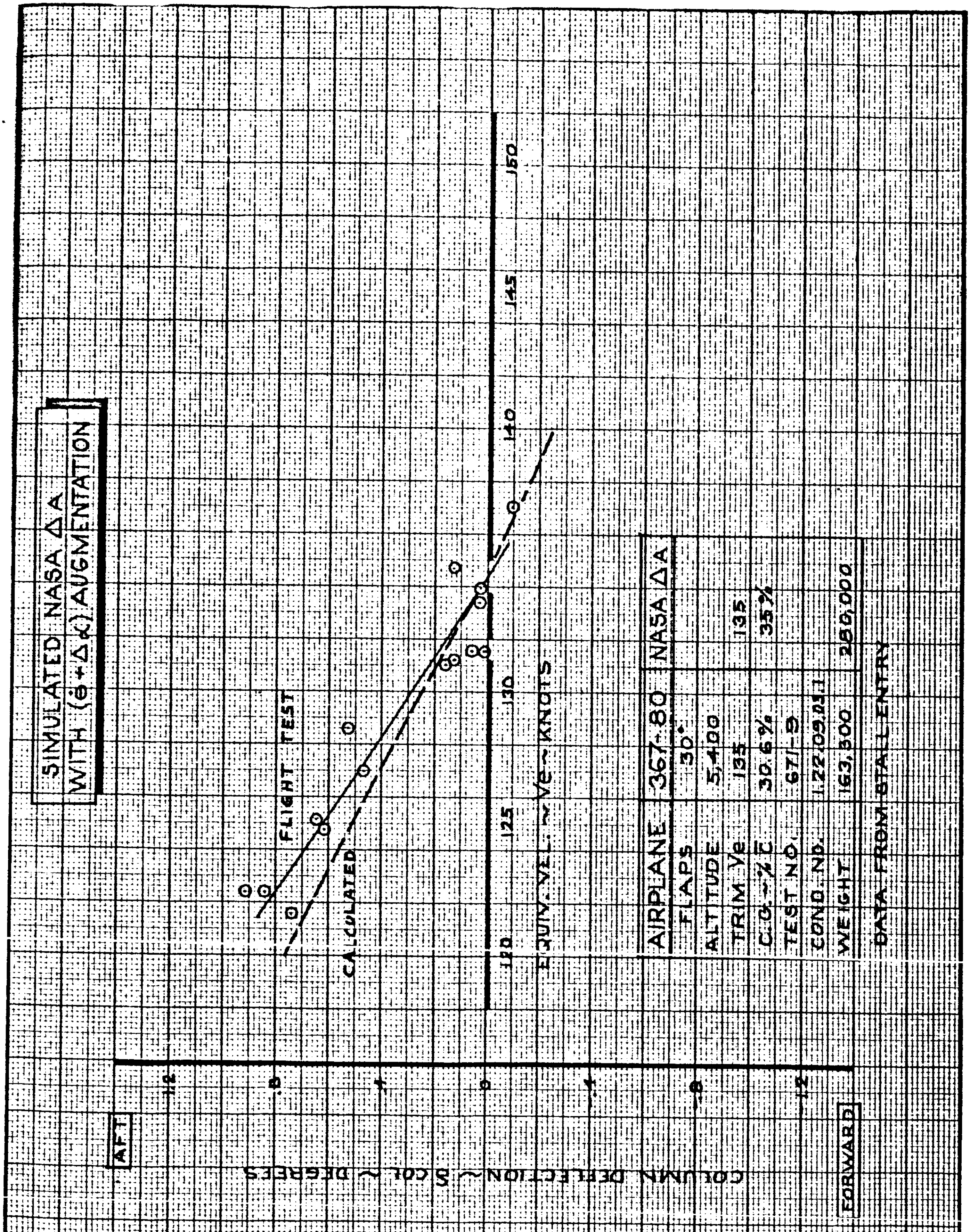

FIG. 79

			REVISED	DATE		
CALC	TAYLOR				COLUMN Vs SPEED CHARACTERISTICS	NASA ΔA
CHECK			R S	2-10-66		D6-10743
APR					THE BOEING COMPANY	PAGE 110 B
APR						

TD 461 C-R4

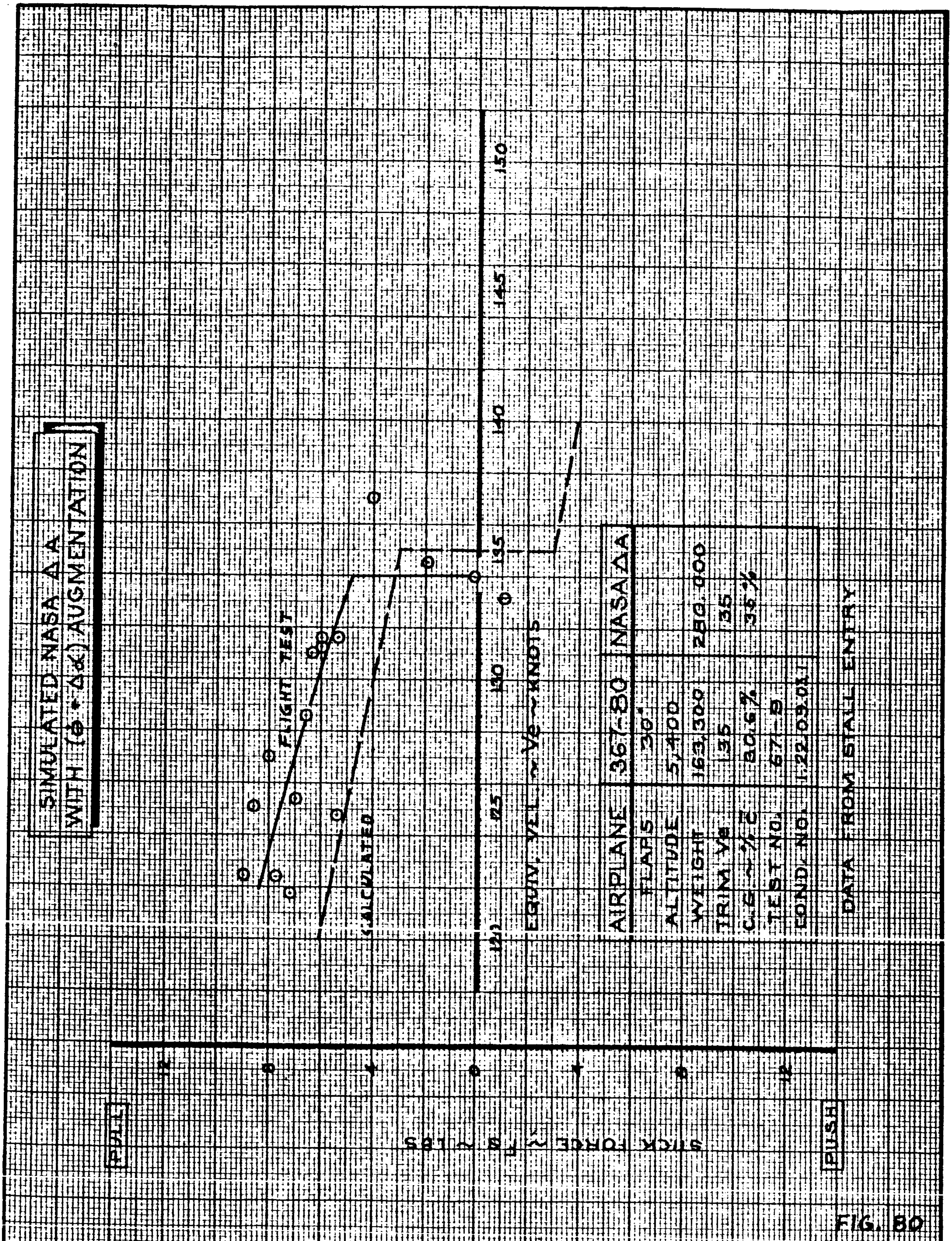

FIG. 80

CALC	TAYLOR	REVISED	DATE	SPEED STABILITY STICK FORCE Vs. SPEED	NASA ΔA
CHECK		STEMWELL	2-10-66		D6-10743
APR				THE BOEING COMPANY	PAGE 111 B
APR					

TD 461 C-R4

SIMULATED NASA ΔA
WITH ($\dot{\theta}$ + Δα) AUGMENTATION

AIRPLANE	367-80	NASA ΔA
FLAPS	30°	
ALTITUDE	8,000	
TRIM V_e	139	135
WEIGHT	168,800	280,000
C. G. ~ % $\bar{c}$	30.3%	35%
TEST NO.	671-8	-
COND. NO.	1.22.09.2	

DATA FROM WIND-UP TURN

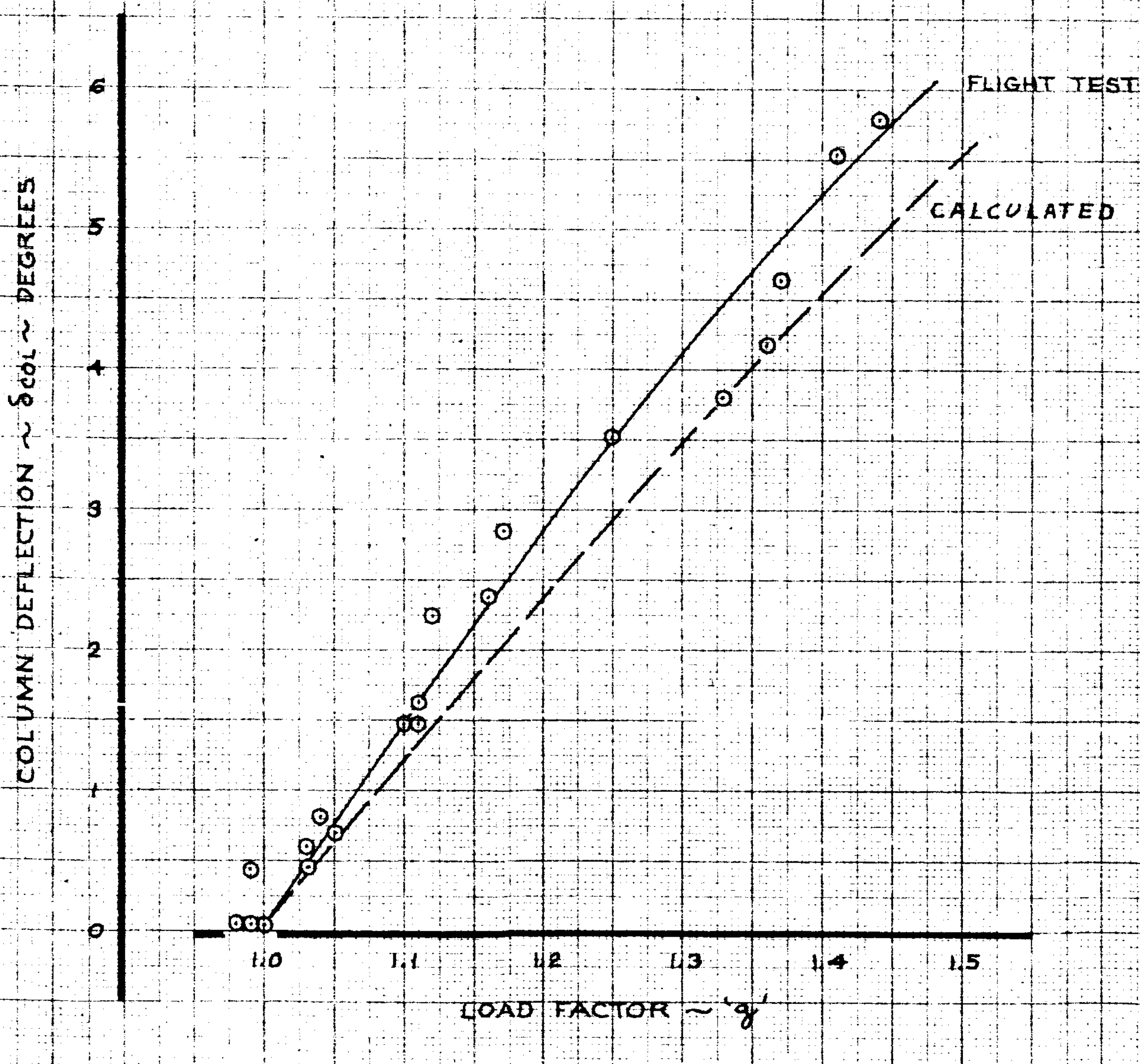

FIG. 81

CALC	TAYLOR		REVISED	DATE	NORMAL ACCELERATION Vs. COLUMN CHARACTERISTICS	NASA ΔA
CHECK			STEMWELL	1-2-66		D6-10743
APR					THE BOEING COMPANY	PAGE 112
APR						

TD 461 C-R4

SIMULATED NASA ΔA WITH ($\dot{\theta}$ + Δα) AUGMENTATION

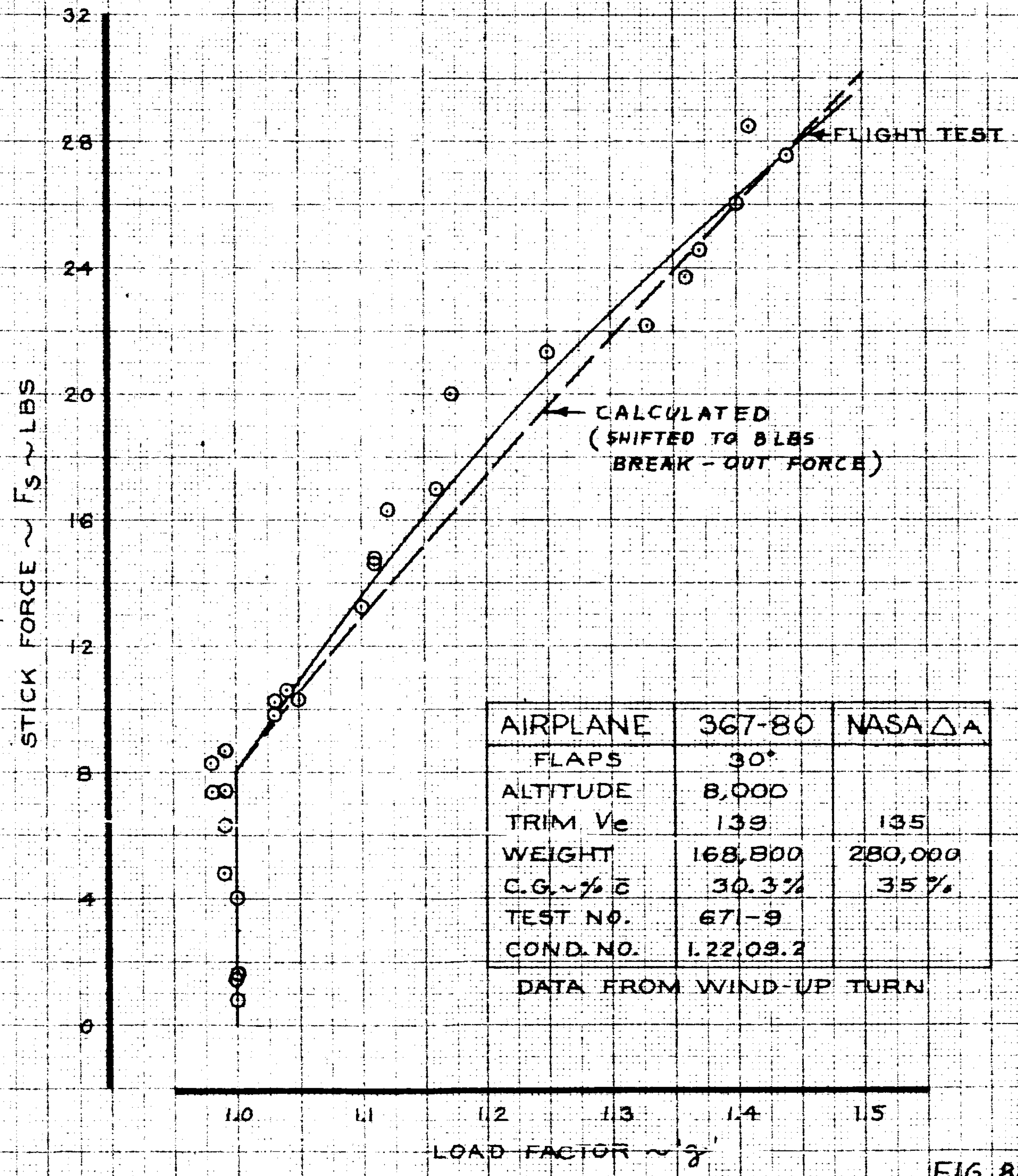

AIRPLANE	367-80	NASA ΔA
FLAPS	30°	
ALTITUDE	8,000	
TRIM V_e	139	135
WEIGHT	168,800	280,000
C.G. ~ % $\bar{c}$	30.3%	35%
TEST NO.	671-9	
COND. NO.	1.22.09.2	

DATA FROM WIND-UP TURN

FIG. 82

CALC	TAYLOR	REVISED	DATE	NORMAL ACCELERATION Vs FORCE CHARACTERISTICS	NASA ΔA
CHECK		STEMWELL	2-1-66		D6-10743
APR				THE BOEING COMPANY	PAGE 113
APR					

SIMULATED NASA ΔA
WITH ($\dot{\theta} + \Delta\alpha$) AUGMENTATION

AIRPLANE	367-80	NASA ΔA
FLAPS	30°	
ALTITUDE	8,000	
TRIM Ve	139	135
WEIGHT	168,800	280,000
C.G. ~ % $\bar{c}$	30.3%	35%
TEST NO.	671-9	
COND. NO.	1.22.09.2	

DATA FROM WIND-UP TURN

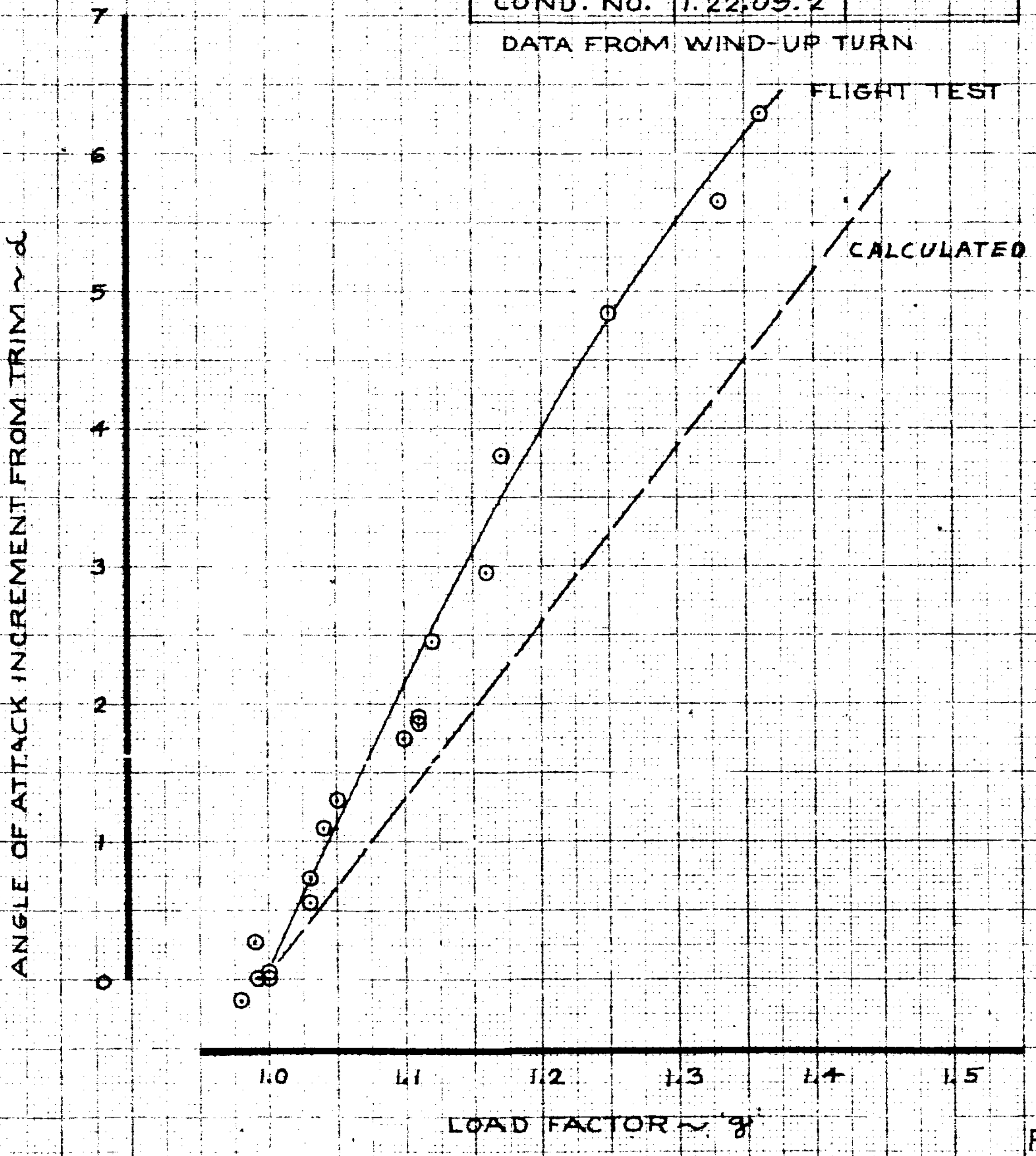

FIG. 83

CALC	TAYLOR	REVISED	DATE	NORMAL ACCELERATION Vs ANGLE OF ATTACK	NASA ΔA
CHECK		STEMWELL	2-1-66		D6-10743
APR					
APR				THE BOEING COMPANY	PAGE 114

TD 451 C-R4

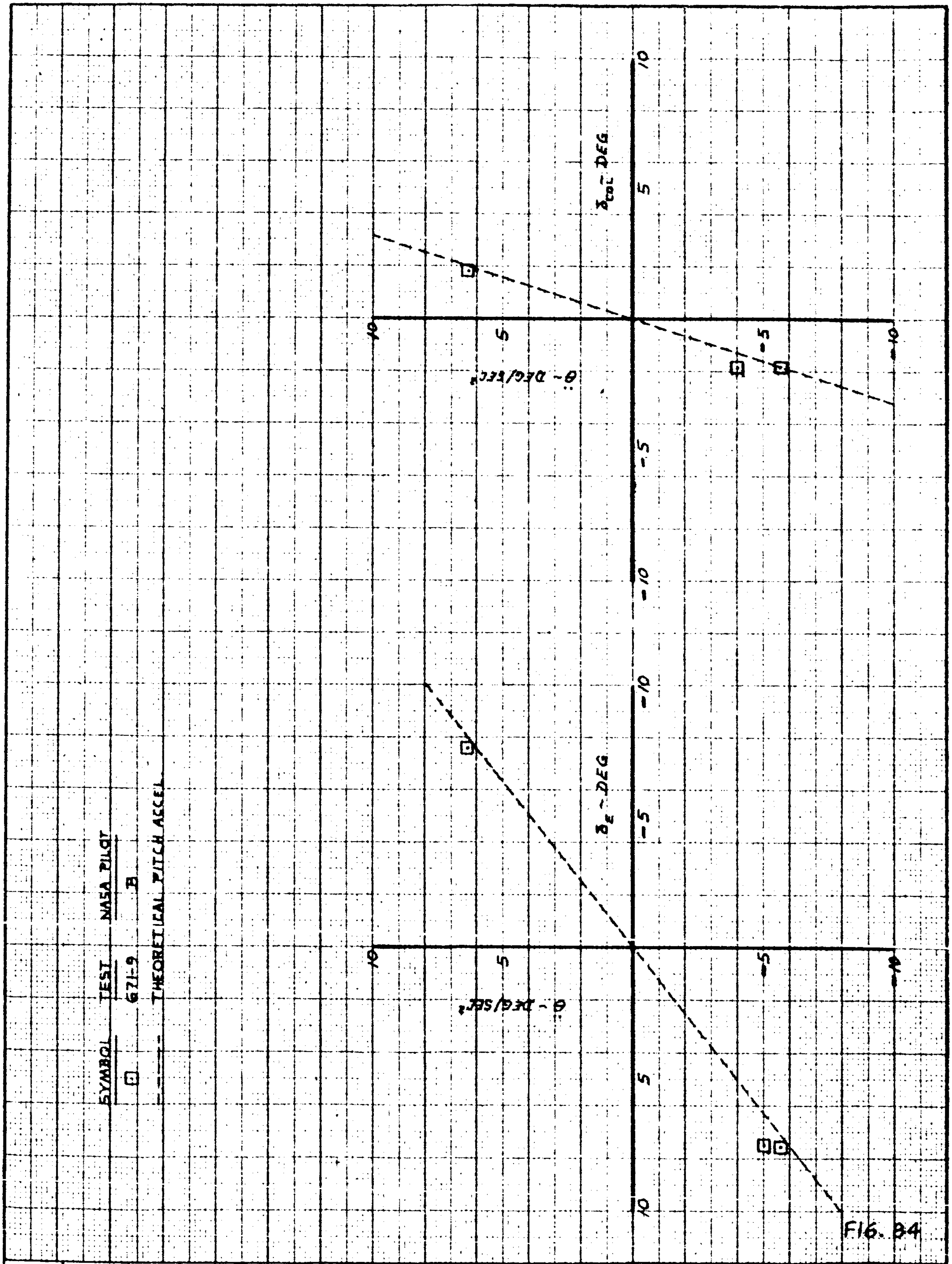

FIG. 84

CALC	D J BECK	11-18-65	REVISED	DATE
CHECK				
APR				
APR				

PITCH ACCELERATION OF THE NASA ΔA SST (BASIC CG ~ θ̇+α SAS)

D6-10743

THE BOEING COMPANY

TD 461 C R4

	367-80	NASA ΔA
FLAPS	30°	
SPEED BRAKES	6°	
V_e	135 KTS	135 KTS
H_p	3950 FT	
GW	149,700 LBS	280,000 LBS
CG	28.0% MAC	35.0% MAC
TEST NO.	671-8	

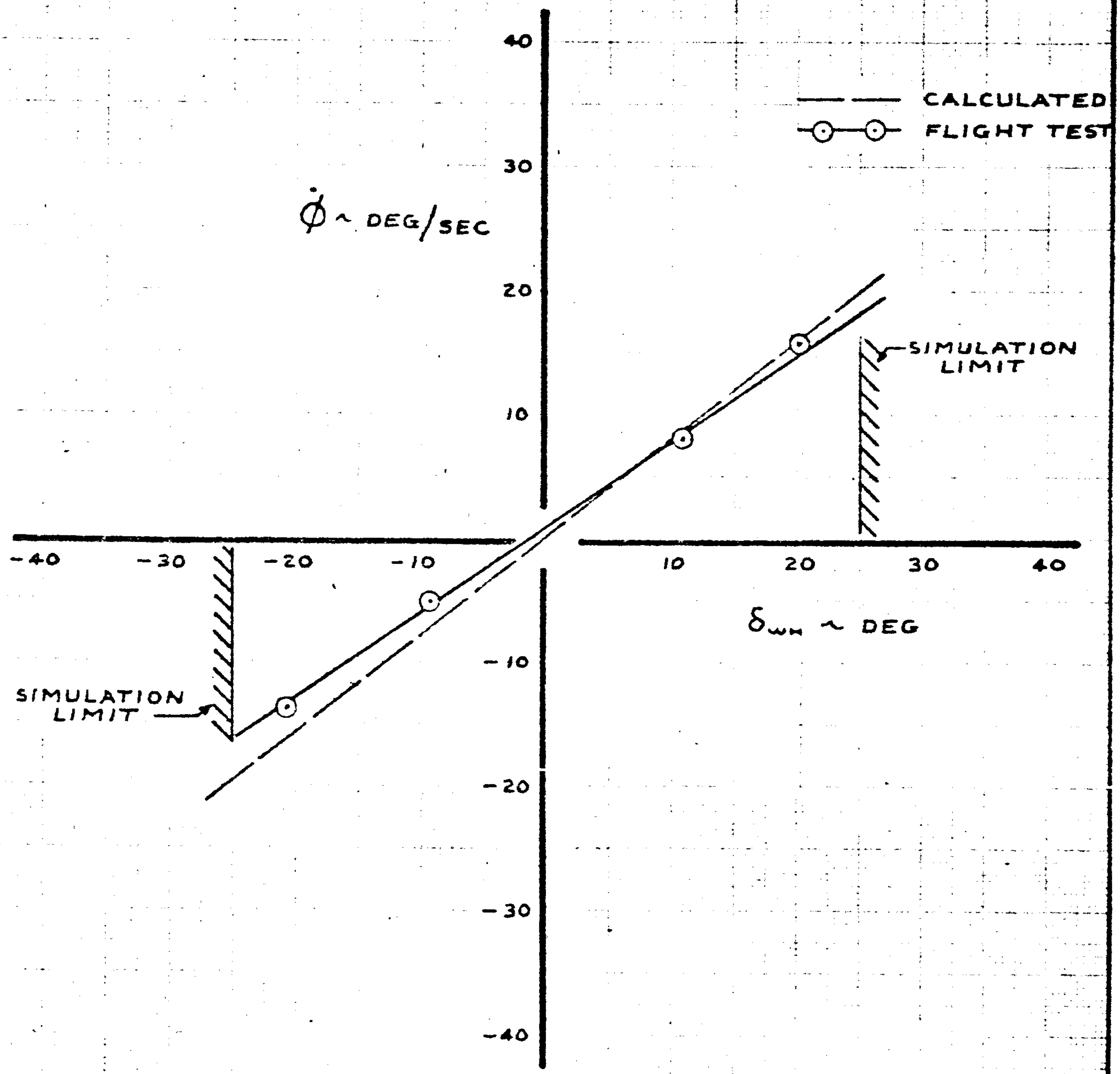

FIG. 85

CALC	SAM	10/22/65	REVISED	DATE
CHECK	RCJ	10/23/65		
APR				
APR				

LATERAL CONTROL RESPONSE
STEADY STATE ROLL RATE
1 DEGREE OF FREEDOM

SIMULATED NASA ΔA

D6-10743

THE BOEING COMPANY

TD 461 C-R4

	367-80	NASA ΔA
FLAPS	30°	
SPEED BRAKES	6°	
V_e	135 KTS	135 KTS
H_p	3950 FT	
GW	149,700 LBS	280,000 LBS
CG	28.0% MAC	35.0% MAC
TEST NO	671-8	

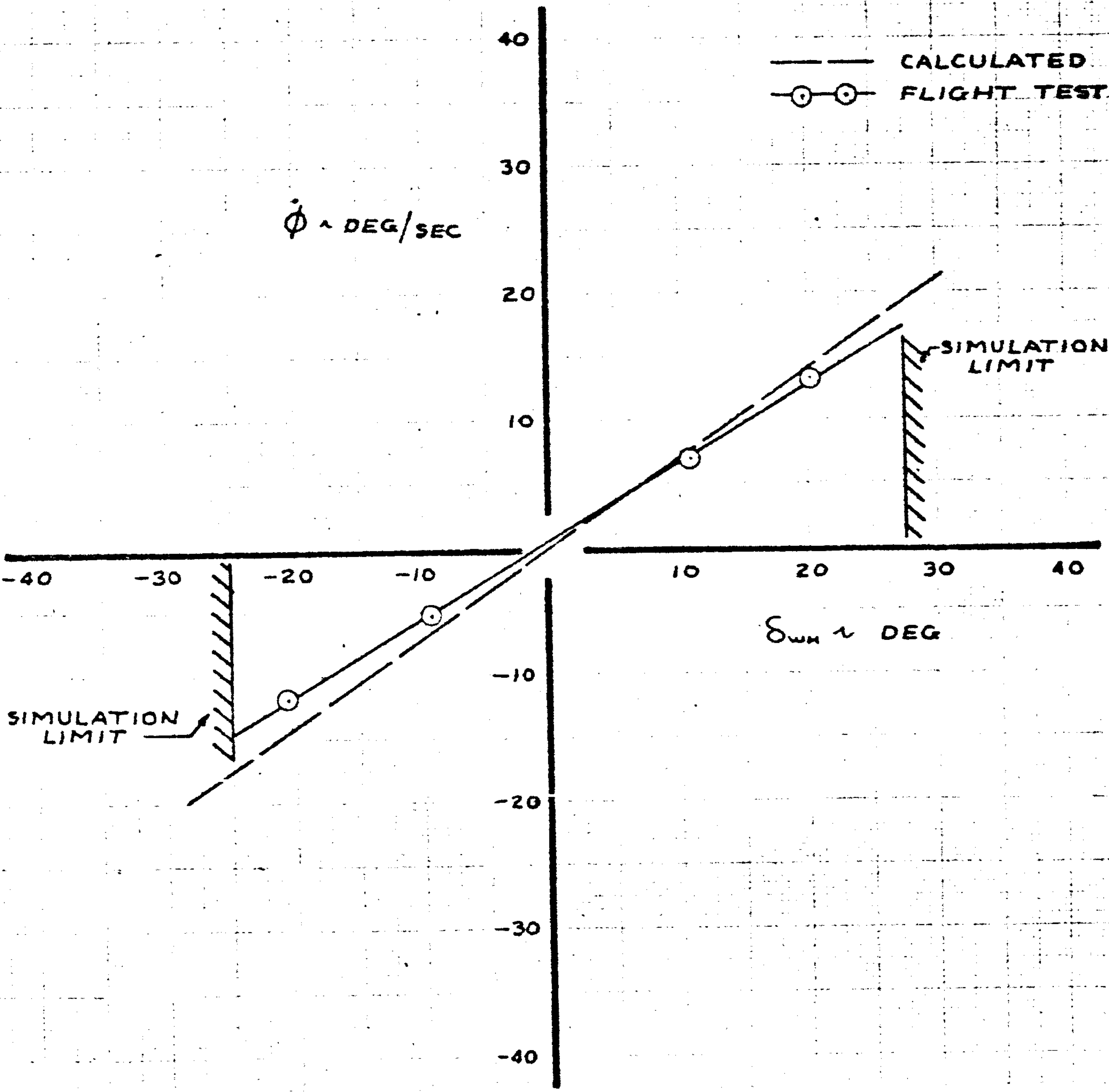

FIG. 86

CALC	RCS	8/27/65	REVISED	DATE	LATERAL CONTROL RESPONSE STEADY STATE ROLL RATE 3 DEGREE OF FREEDOM	SIMULATED NASA ΔA
CHECK	SAM	8/31/65	RCS	10/11/65		
APR						D6-10743
APR					THE BOEING COMPANY	PAGE 117

TD 461 C-R4

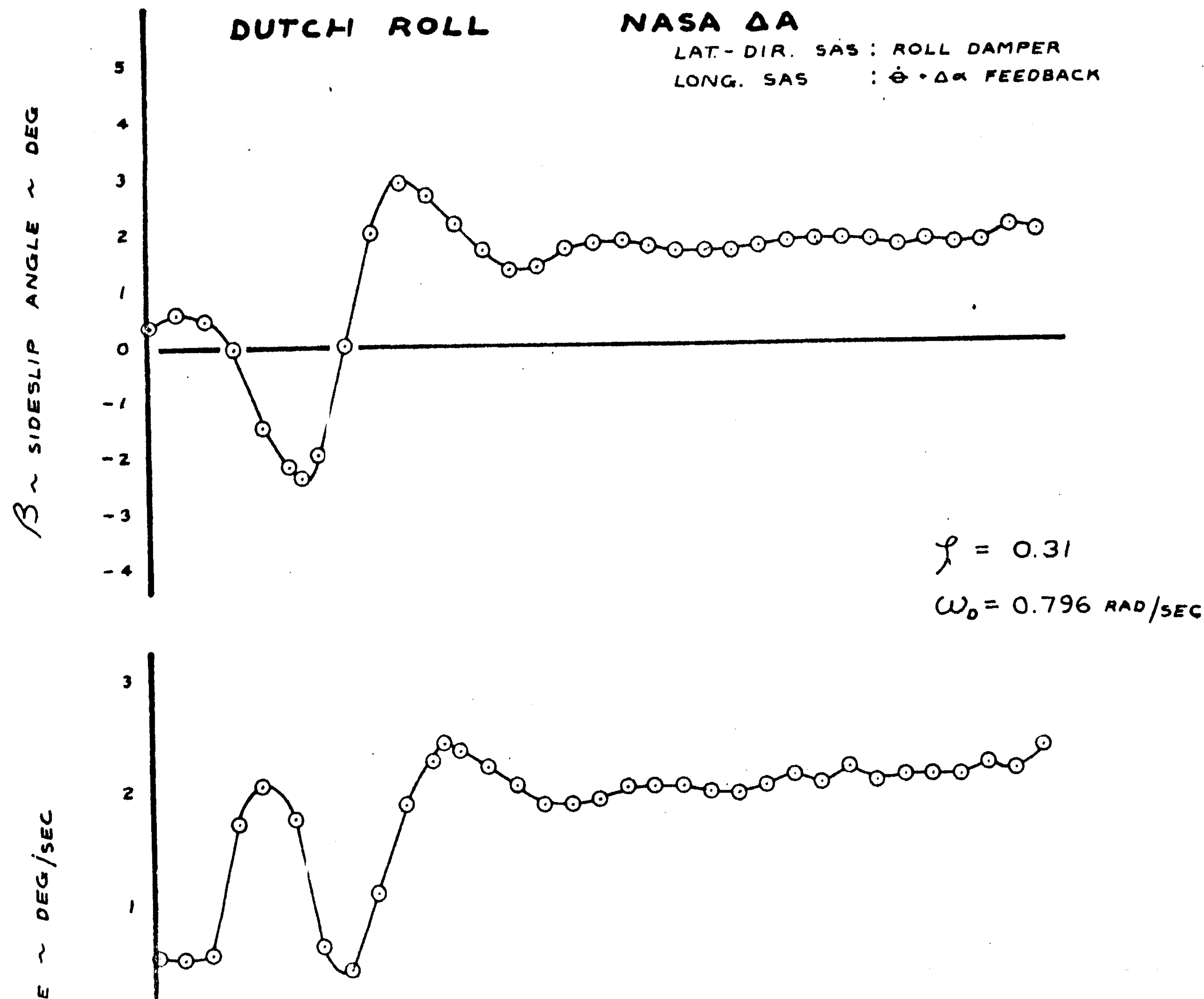
DUTCH ROLL
NASA ΔA
LAT.-DIR. SAS : ROLL DAMPER
LONG. SAS : $\dot{\theta} \cdot \Delta\alpha$ FEEDBACK
β ~ SIDESLIP ANGLE ~ DEG
5
4
3
2
1
0
-1
-2
-3
-4
$\zeta = 0.31$
$\omega_D = 0.796$ RAD/SEC
3
2
1
E ~ DEG/SEC

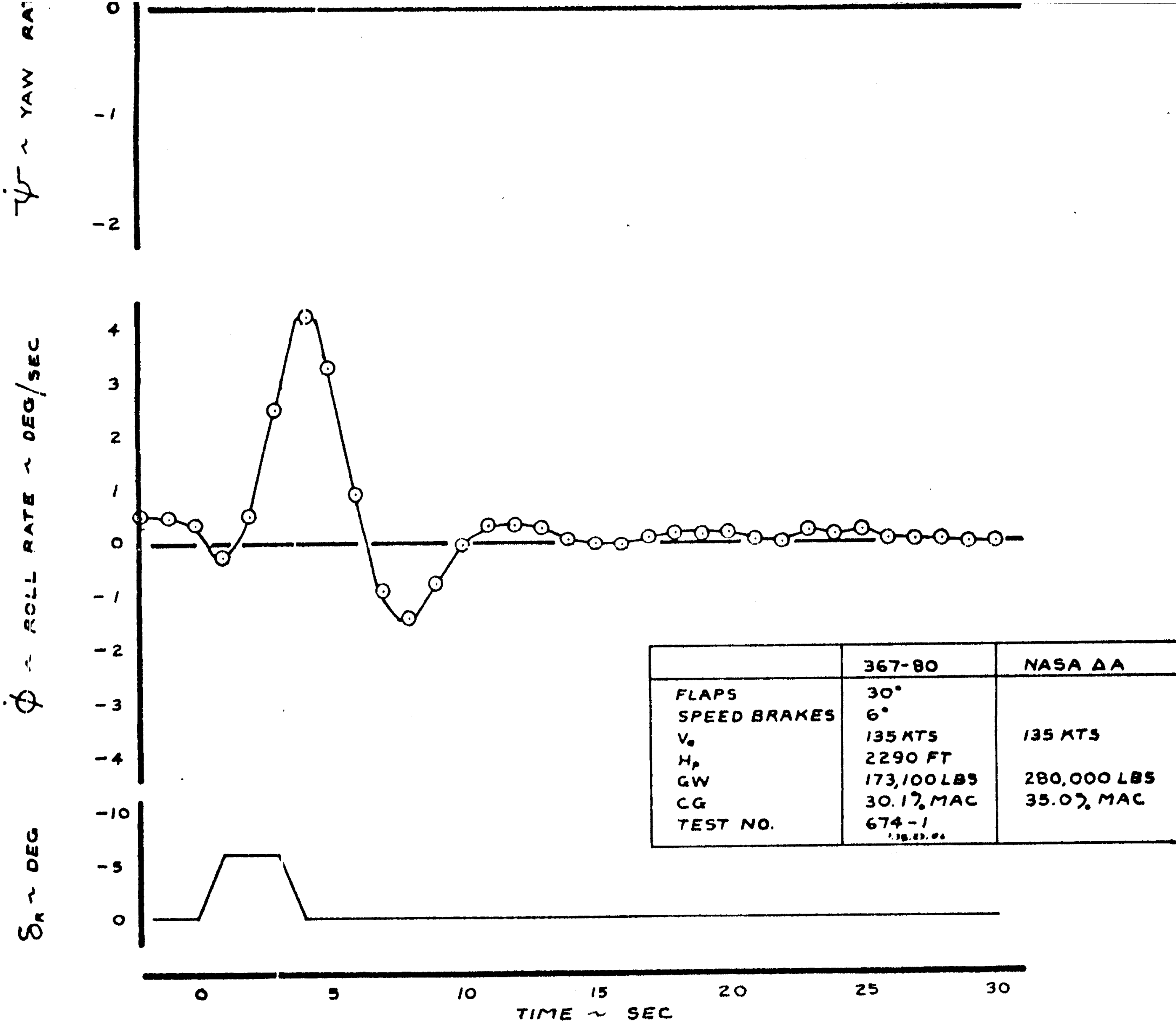

	367-80	NASA ΔA
FLAPS	30°	
SPEED BRAKES	6°	
V_e	135 KTS	135 KTS
H_p	2290 FT	
GW	173,100 LBS	280,000 LBS
CG	30.1% MAC	35.0% MAC
TEST NO.	674-1	

FIG. 87

FORWARD C. G.

The static margin of the basic delta configuration was 2.5%. In order to evaluate the effect of C. G. position on the delta control response, a forward C. G. configuration was selected at 7% static margin.

This configuration was set up and documented and received a short pilot evaluation. The testing of this configuration was discontinued because the pilots reported that the longitudinal control response amplitude was too small and that the forces were extremely high.

The data from the configuration documentation tests are shown in Figs. 88 to 93 The speed stability characteristics are shown in Figs. 88 and 89. The column deflection required to change airspeed is approximately twice the calculated value for this configuration. Calculations show that the static margin of the flight test configuration was 35%. It appears that this configuration was not set up correctly on the simulation computer. Figs. 90 to 92 show the wind-up turn data. The angle-of-attack to maneuver is simulated correctly, but the column deflection and stick force are higher than the predicted values. Data from the pitch reversals are shown in Fig. 93. These data indicate that the longitudinal control power was higher than calculated, which is contradictory to the low response in the speed stability tests.

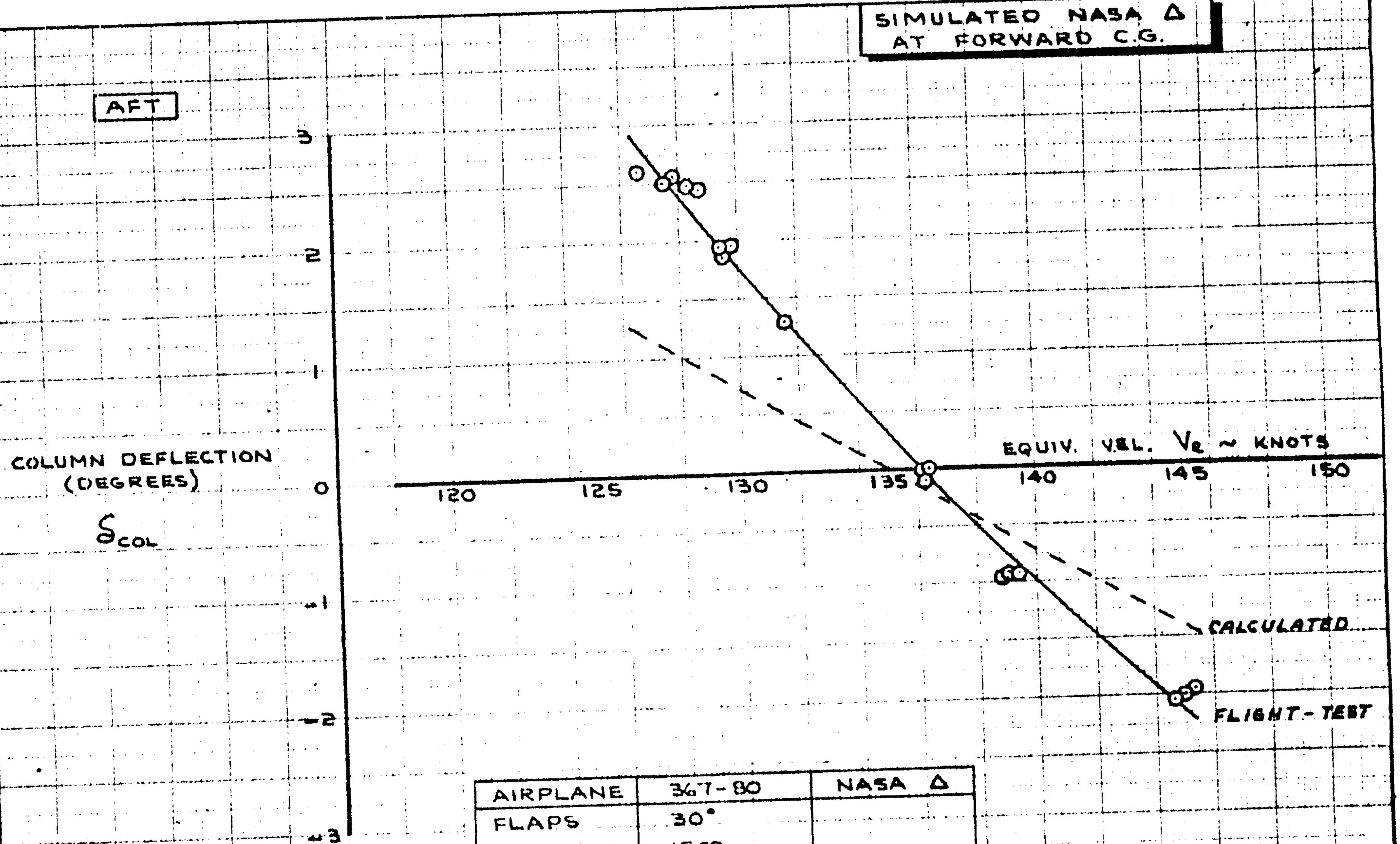

AIRPLANE	367-80	NASA Δ
FLAPS	30°	
ALTITUDE	1500	
TRIM. V_e	136	135
WEIGHT	152,500	280,000
C.G. ~ %$\bar{c}$	28.8 %	30.45 %
TEST NO.	676-1	
COND. NO.	1.38.41.03	

FIG. 88

CALC	TAYLOR	REVISED	DATE
CHECK			
APR			
APR			

COLUMN VS SPEED CHARACTERISTICS

NASA Δ FWD. C.G.

THE BOEING COMPANY

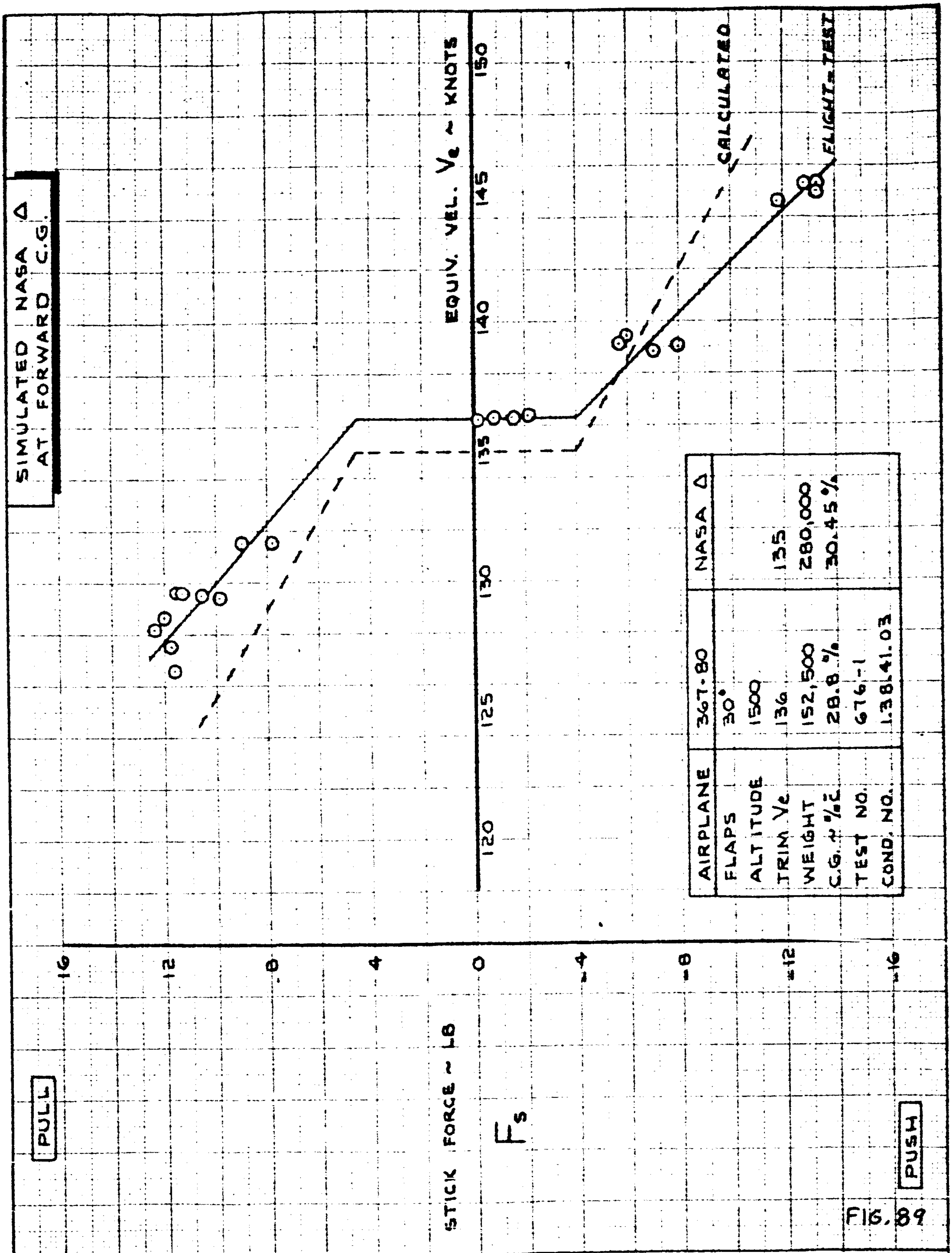

AIRPLANE	367-80	NASA Δ
FLAPS	30°	
ALTITUDE	1500	
TRIM V_e	136	135
WEIGHT	152,500	280,000
C.G. ~ %$\bar{c}$	28.8 %	30.45 %
TEST NO.	676-1	
COND. NO.	1.38 & 41.03	

FIG. 89

CALC	TAYLOR	REVISED	DATE	SPEED STABILITY STICK FORCE VS SPEED	NASA Δ FWD. C.G.
CHECK					D6-10743
APR				THE BOEING COMPANY	PAGE 121
APR					

SIMULATED NASA Δ
AT FORWARD C.G.

AIRPLANE	367-80	NASA Δ
FLAPS	30°	
ALTITUDE	1670	
TRIM Ve	135	135
WEIGHT	154,000	280,000
C.G. ~ %c̄	28.7 %	30.45 %
TEST NO.	676-1	
COND. NO.	1.38.41.02	

DATA FROM WIND-UP TURN

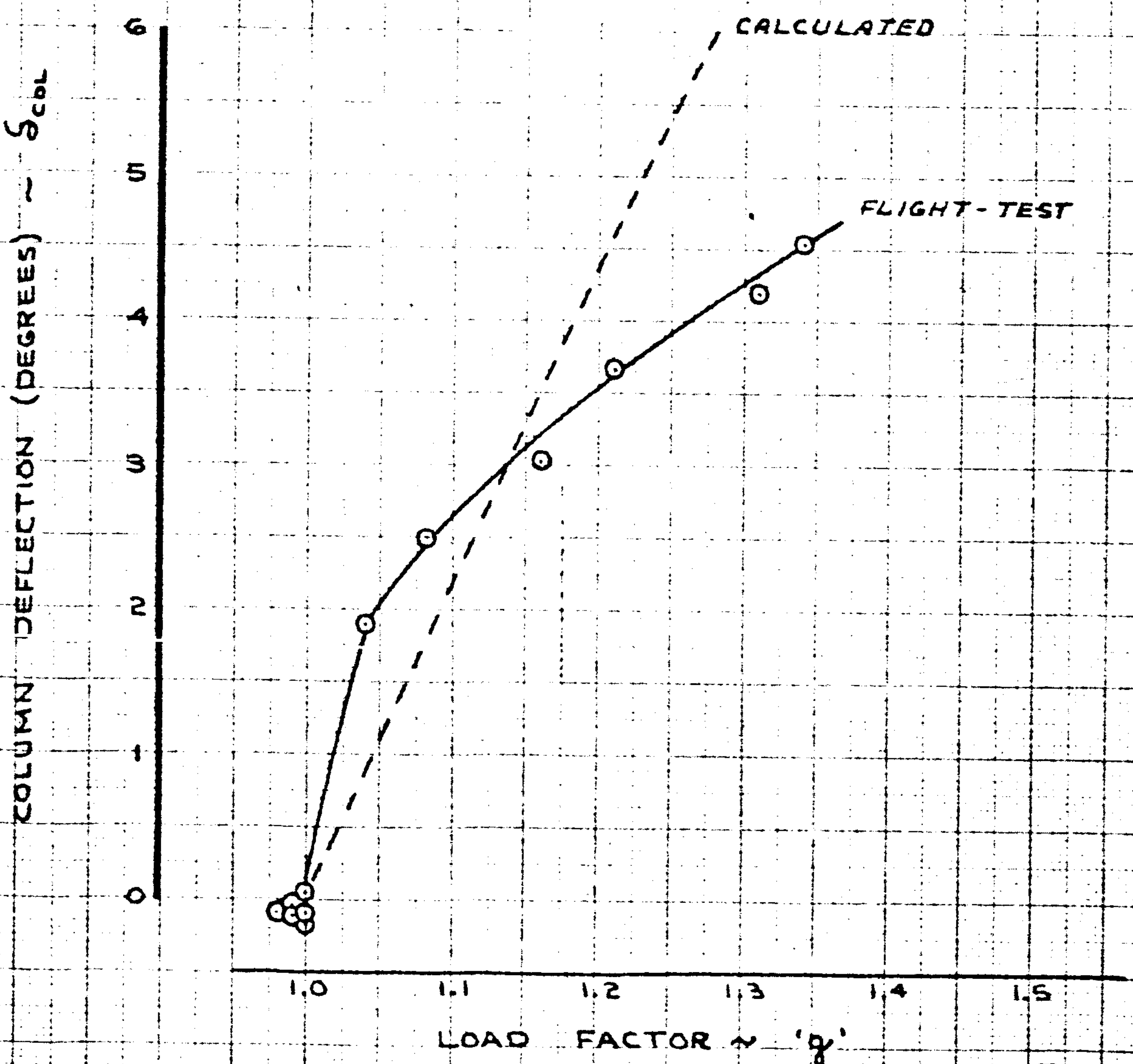

FIG. 90

CALC	TAYLOR	REVISED	DATE	NORMAL ACCELERATION VS. COLUMN CHARACTERISTICS	NASA Δ FWD C.G.
CHECK					D6-10743
APR				THE BOEING COMPANY	PAGE 122
APR					

TD 461 C-R4

SIMULATED Δ
AT FORWARD C.G.

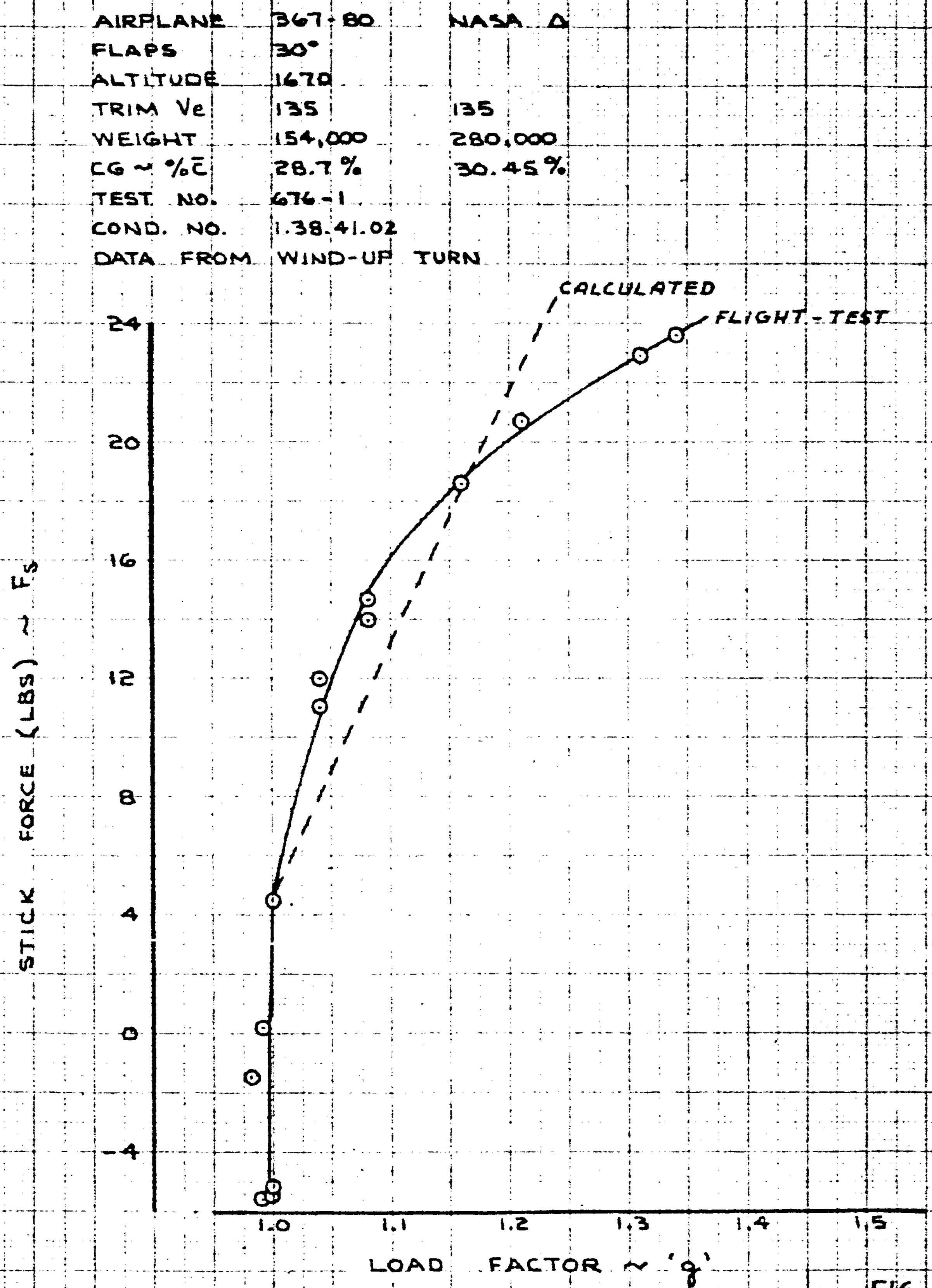

FIG. 91

CALC	TAYLOR	REVISED	DATE	NORMAL ACCELERATION VS. FORCE CHARACTERISTICS	NASA Δ FWD C.G.
CHECK					D6-10743
APR				THE BOEING COMPANY	PAGE 123
APR					

SIMULATED NASA Δ AT FORWARD C.G.

AIRPLANE	367-80	NASA Δ
FLAPS	30°	
ALTITUDE	1670	
TRIM Ve	135	135
WEIGHT	154,000	280,000
CG ~ % $\bar{c}$	28.7 %	30.45 %
TEST NO.	676-1	
COND. NO.	1.38.41.02	

DATA FROM WIND-UP TURN

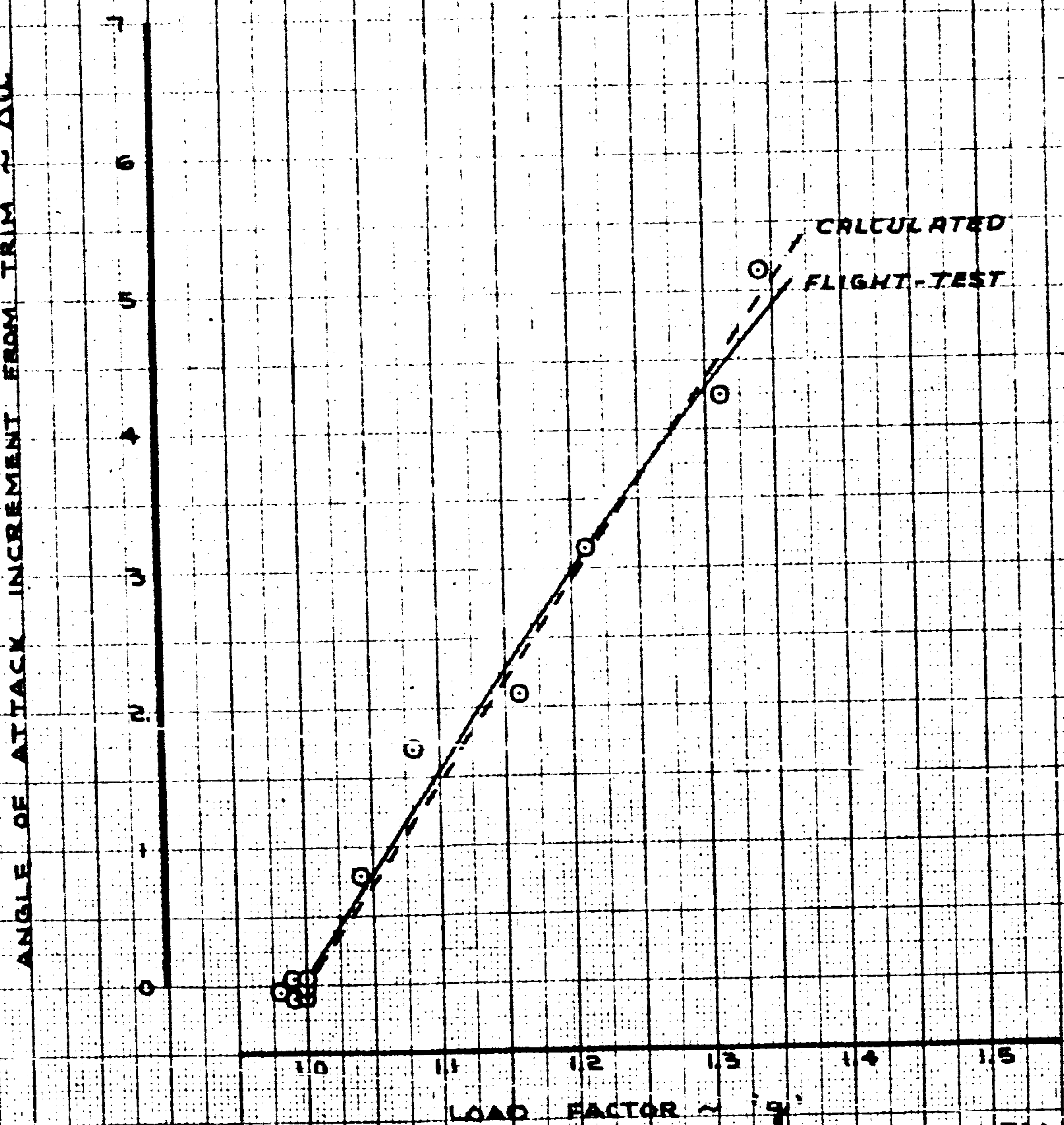

FIG. 92

		REVISED	DATE	
CALC	TAYLOR			NORMAL ACCELERATION VS. ANGLE OF ATTACK
CHECK				
APR				
APR				THE BOEING COMPANY

NASA Δ FWD C.G.

D6-10743

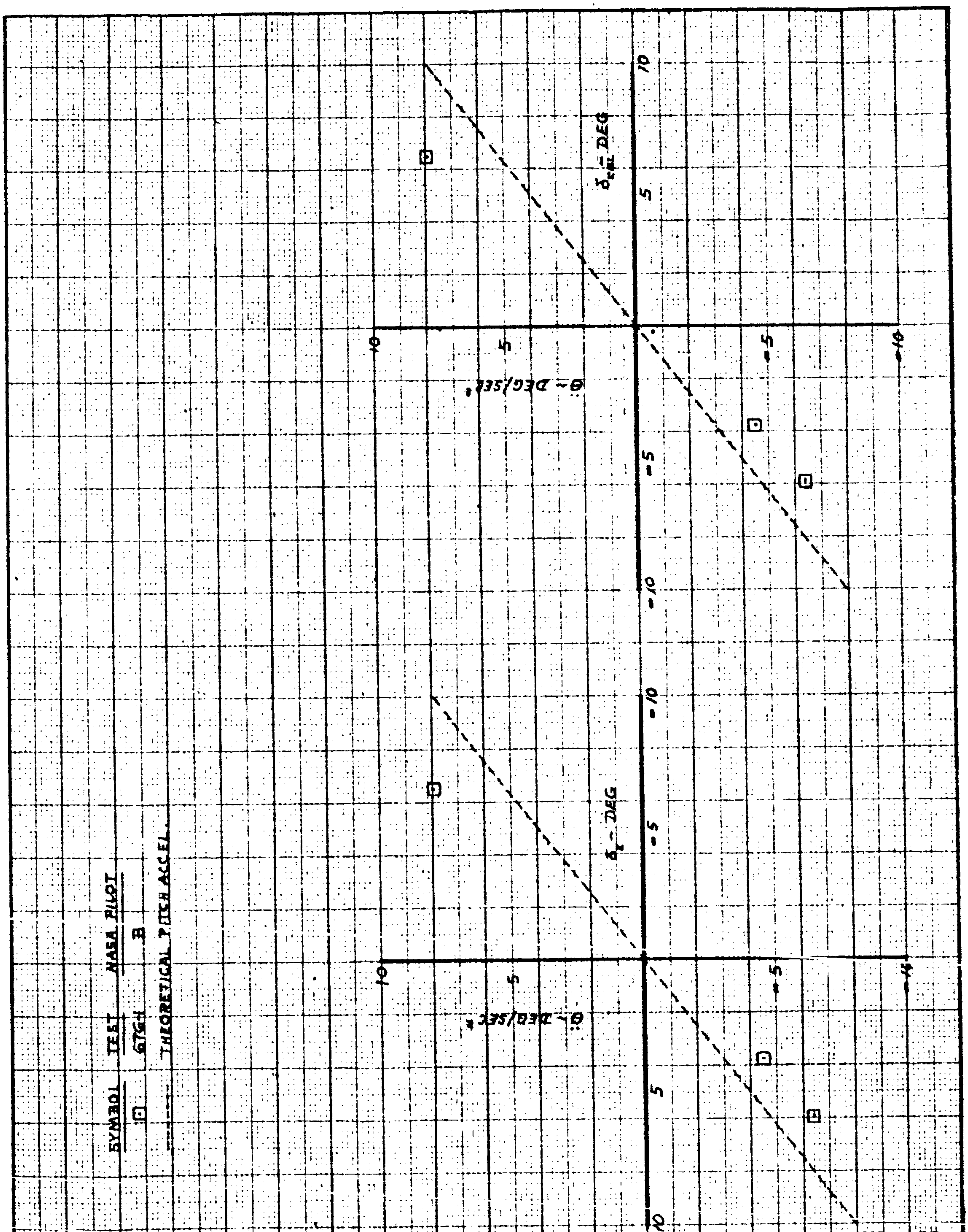

FIG. 93

CALC	DJ BECK	11-18-65	REVISED	DATE	PITCH ACCELERATION OF THE NASA Δ SST (FWD CG ~ NO SAS)
CHECK					
APR					D6-10743
APR					THE BOEING COMPANY

NASA △ B

The NASA Delta B is a variation on the basic Delta. This configuration had an adverse yaw due to roll rate, $N_{\dot{\phi}} = -.1$, and .05 Dutch roll damping ratio. The value of $C_{n_{\dot{\phi}}}$ was increased from -.0049 to -.0352 and the value of $C_{n_{\dot{\beta}}}$ was increased from 0 to -.138. Since the longitudinal configuration was not changed, the documentation of the basic configuration holds.

The lateral-directional documentation is minimal consisting of the roll response data, and a Dutch roll response. Fig. 94 shows the roll acceleration, and indicates the $C_{\ell_{\delta w}}$ is slightly smaller than expected. However the peak roll rate shown in Fig. 95 indicates that the roll damping must be slightly low so that for a given wheel a correct roll response is obtained. Fig. 96 shows the Dutch roll response with the low damping. The measured Dutch roll frequency and damping are .996 rad/sec and .055 which compares well with the theoretical values of .982 rad/sec and .05.

	367-80	NASA ΔB
FLAPS	30°	
SPEED BRAKES	6°	
V	135 KTS	135 KTS
H	1400 FT	
GW	162,900 LBS	280,000 LBS
CG	30.6 % MAC	35.0 % MAC
TEST NO.	671-13	

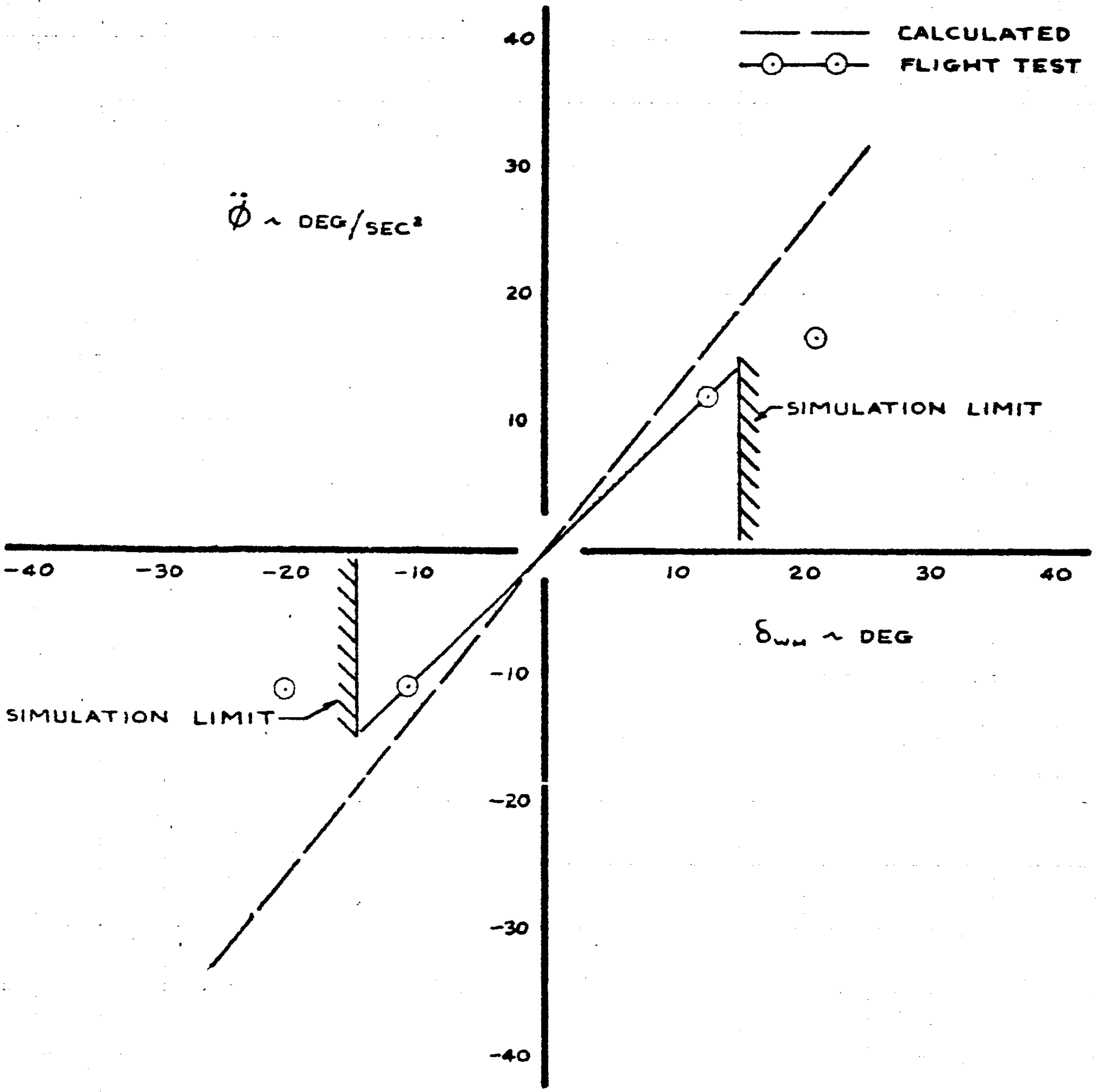

FIG. 94

CALC	RCS	12/3/65	REVISED	DATE
CHECK				
APR				
APR				

ROLL ACCELERATION CHARACTERISTICS
1 DEGREE OF FREEDOM

THE BOEING COMPANY

SIMULATED NASA ΔB

D6-10743

TD 461 C-R4

	367-80	NASA ΔB
FLAPS	30°	
SPEED BRAKES	6°	
V_e	135 KTS	135 KTS
H_p	1400 FT	
GW	163,700 LBS	280,000 LBS
CG	30.5% MAC	35.0% MAC
TEST NO.	671-13	

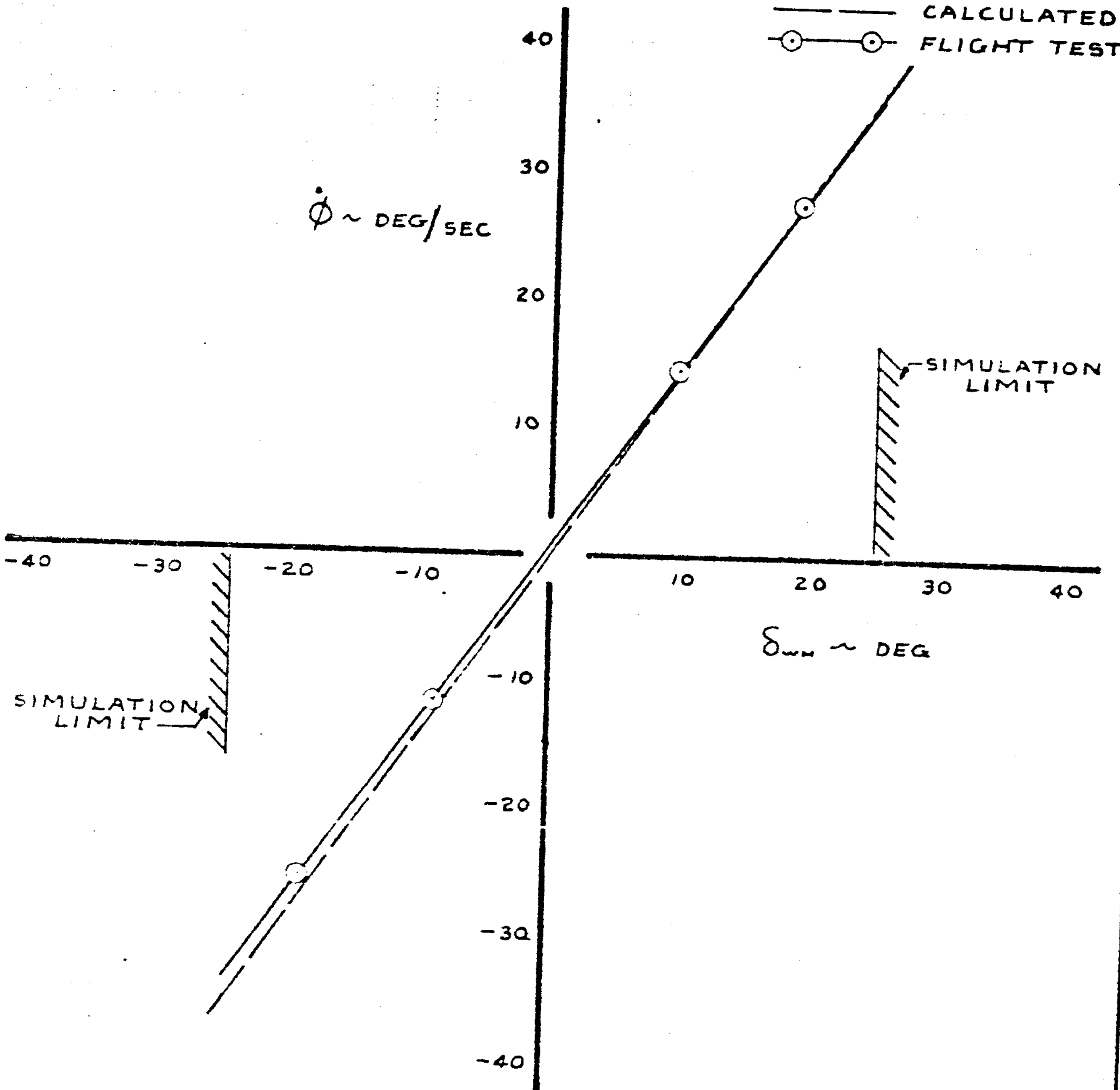

FIG. 95

CALC	RCJ	7/23/65	REVISED	DATE	LATERAL CONTROL RESPONSE	SIMULATED NASA ΔB
CHECK					STEADY STATE ROLL RATE 1 DEGREE OF FREEDOM	D6-10743
APR						
APR					THE BOEING COMPANY	PAGE 128

TD 461 C-R4

DUTCH ROLL NASA ΔB

$C_{n_p} = -0.0352$ / RAD/SEC
$C_{n_{\dot{p}}} = -0.168$ / RAD/SEC
LONG. SAS : $\dot{\theta} + \Delta\alpha$

$\zeta = 0.055$
$\omega_D = 0.996$ RAD/SEC

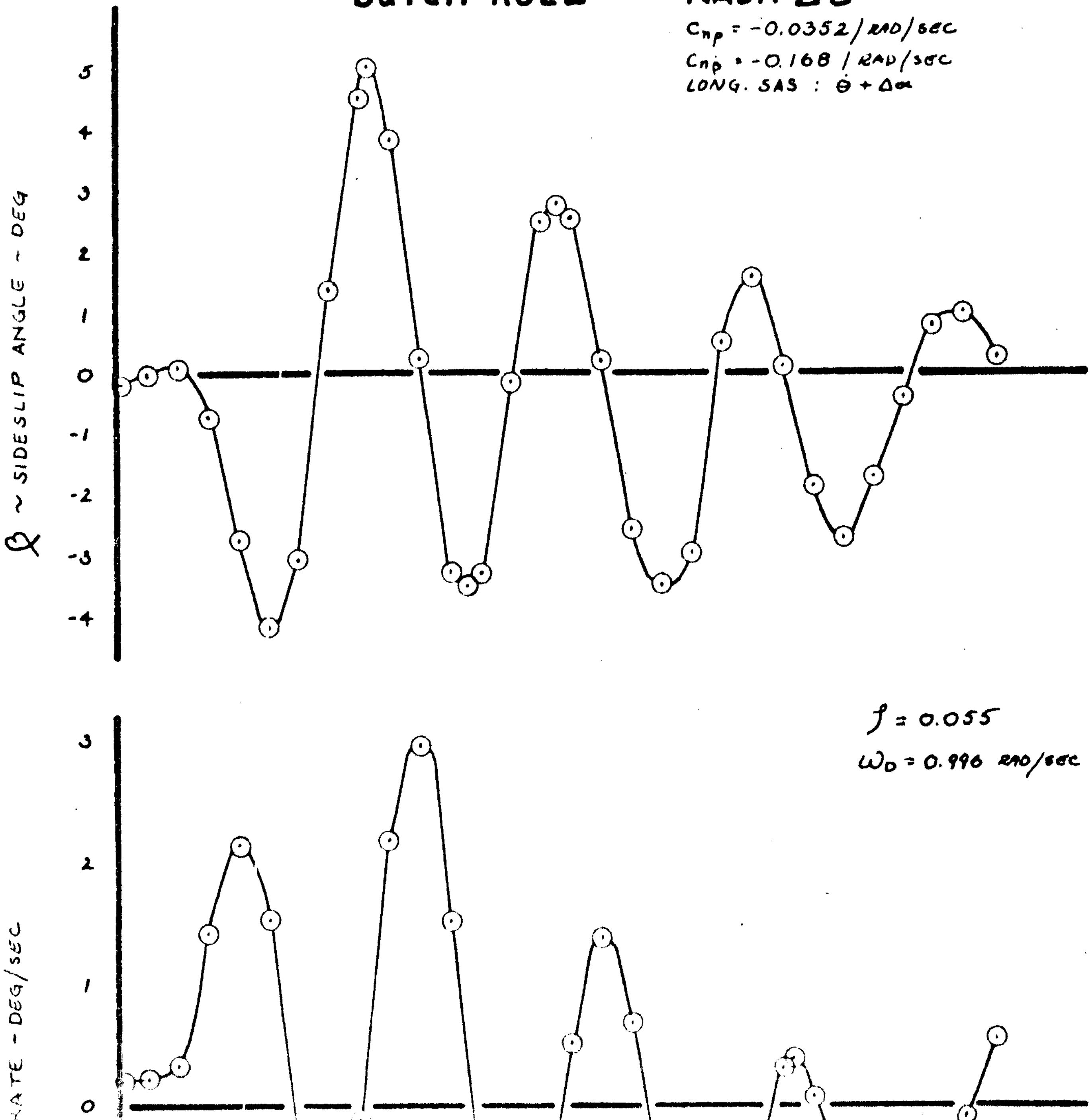

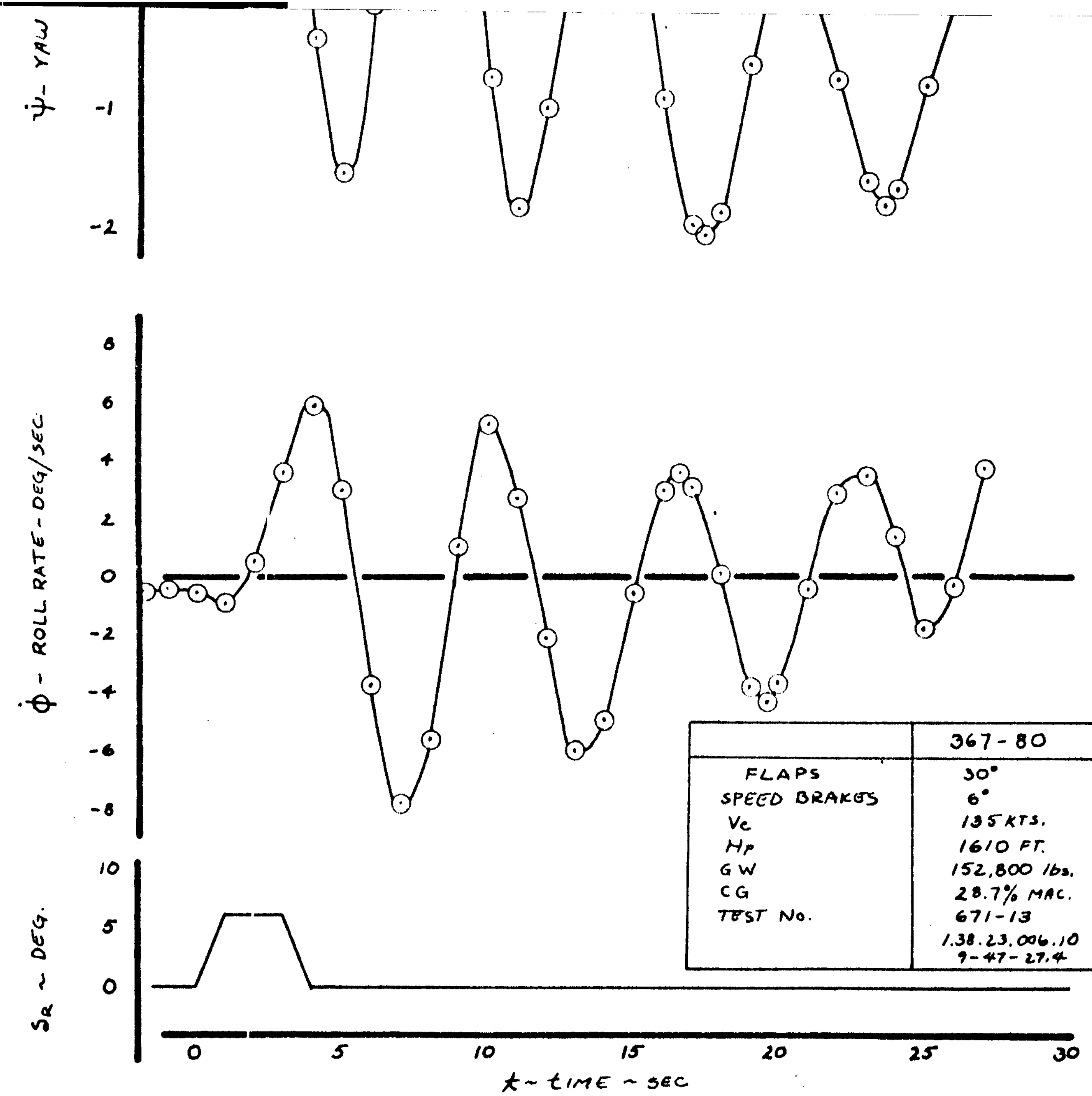

	367-80	NASA ΔB
FLAPS	30°	
SPEED BRAKES	6°	
Ve	135 KTS.	135 KTS.
Hp	1610 FT.	
GW	152,800 lbs.	280,000 lbs.
CG	28.7% MAC.	35.0% MAC
TEST No.	671-13 1.38.23.006.10 9-47-27.4	

SAM 9/23/65
RCJ 9/23/65

FIG. 96

NASA 72

The NASA 72 is a configuration representative of a variable sweep wing SST with the wings in the full aft position (72° leading edge sweep). The stability derivatives of this configuration are presented in Appendix 2. The actual aircraft has an approach speed of 180 kts indicated but the simulator was flown at 150 kts because of the 367-80 structural speed placards. The appropriate corrections were made to the equations of motion to account for the difference in speed.

The longitudinal characteristics of the NASA 72 configuration measured in flight did not agree well with the theoretical characteristics. The column deflection, stick force, and angle of attack in the wind-up turn were high and the column deflection and stick force required for airspeed changes were also high, although there was a good match of the elevator pulse response data.

These errors were caused by the mis-match between the flight speeds of the 367-80 and NASA 72. Also, since this configuration was evaluated only briefly, it was not checked-out and tailored as carefully as the others prior to pilot evaluation.

In order to correct these errors, the flight test data was used to calculate the actual NASA 72 configuration flown, using the equations and methods of appendix 2. This configuration is listed in Appendix 2.

The static longitudinal characteristics of the NASA 72 are shown in Fig. 97, 97A, and 97B. There are good matches of the column deflection, stick force, and angle of attack vs. speed. The maneuvering characteristics, measured in the wind-up-turn are shown in Fig. 98, 98A, and 98B. There are good matches of the column deflection, stick force, and angle of attack vs. "g" up to 1.4

load factor. The longitudinal control sensitivity, measured in the pitch reversal, is shown in Fig. 99. For the limited data available, there is good agreement with the theoretical characteristics.

The airplane response to an elevator pulse is shown in Fig. 100 and 101. The amplitude of the flight response is slightly higher than the theoretical characteristics, but there is good agreement in the shape of the responses.

The phugoid trace of airspeed, shown in Fig. 102, has good agreement in period (short by about 2 seconds) and lower damping than predicted. The actual value is difficult to determine due to a mistrim of the airplane and the sensitivity of the phugoid to gusts which disturb the motion).

The static lateral directional characteristics of the NASA 72 are shown in Fig. 103. The agreement of all three parameters vs. sideslip is good although there is a lateral mistrim as indicated by the bank angle vs. sideslip plot.

The lateral control power as represented by roll acceleration vs. wheel position is shown in Fig. 104. The mistrim is evident, however, the slopes are the same indicating a good simulation of control power. The steady state roll plots indicate that the roll damping is correct since Figs. 105 and 106 are a comparison between control power and roll damping and the previous figure showed good simulation of control power alone.

The dynamic response of the aircraft to a wheel pulse is shown in Figs. 107 to 109. The roll rate response show an error in the peak roll rate which is due to a -80 simulation limit. For NASA 72 wheel deflection above about 40° the rolling moment capability of the -80 drops off. Since most of the pilot inputs were limited to the area below this, the limit should not be a degradation of the simulation. The sideslip response is good for the first eight seconds. The Dutch roll frequency is off as shown in all three figures. The predicted damped frequency is 1.22 rad/sec while the flight test shows 1.36 rad/sec. The error in peak roll rate shifts the yaw rate response towards zero resulting in the curve shown in Fig. 109. The basic mode shape and magnitude are good.

The rudder inputs show the same basic trends as the wheel responses. Roll rate is slightly low at the peak (note that the high roll rate required is equivalent to about a 45° of wheel and is achieved by -80 aileron motion). The Dutch roll frequency is off as indicated above and the damping appears to be low. (The gust response of the aircraft tends to make the Dutch roll damping less than predicted). The sideslip response is good except for the mistrim shown. For a linear simulation this curve can be shifted so that the agreement is good. Yaw rate shows the same problems with a mistrim, and the low peak roll rate tending to separate the predicted and flight test results.

The basic response data of the NASA 72 shows good agreement with digital runs. Simulation limits in lateral control power show up in the wheel and rudder pulses, however, if this effect is removed and the mistrim corrected the response is excellent.

SIMULATED NASA 72

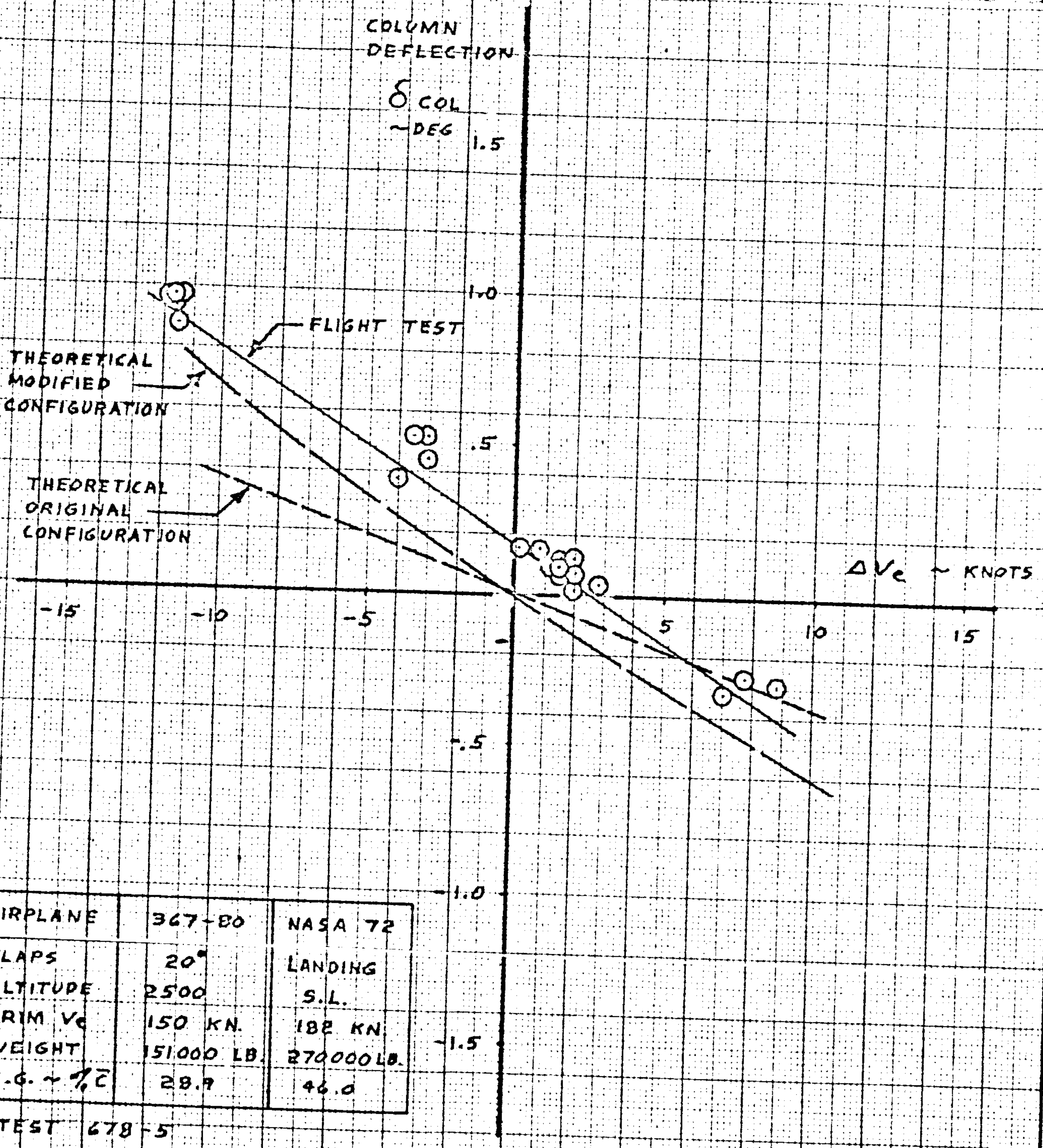

AIRPLANE	367-80	NASA 72
FLAPS	20°	LANDING
ALTITUDE	2500	S.L.
TRIM Ve	150 KN.	182 KN.
WEIGHT	151,000 LB.	270000 LB.
C.G. ~ %c̄	28.9	46.0

TEST 678-5
COND. 1.38.13.04

FIG. 97

CALC	TAYLOR		REVISED	DATE	COLUMN VS SPEED CHARACTERISTICS	NASA 72
CHECK			W.M.E	4-22-66		D6-10743
APR					THE BOEING COMPANY	PAGE 133
APR						

TD 461 C-R4

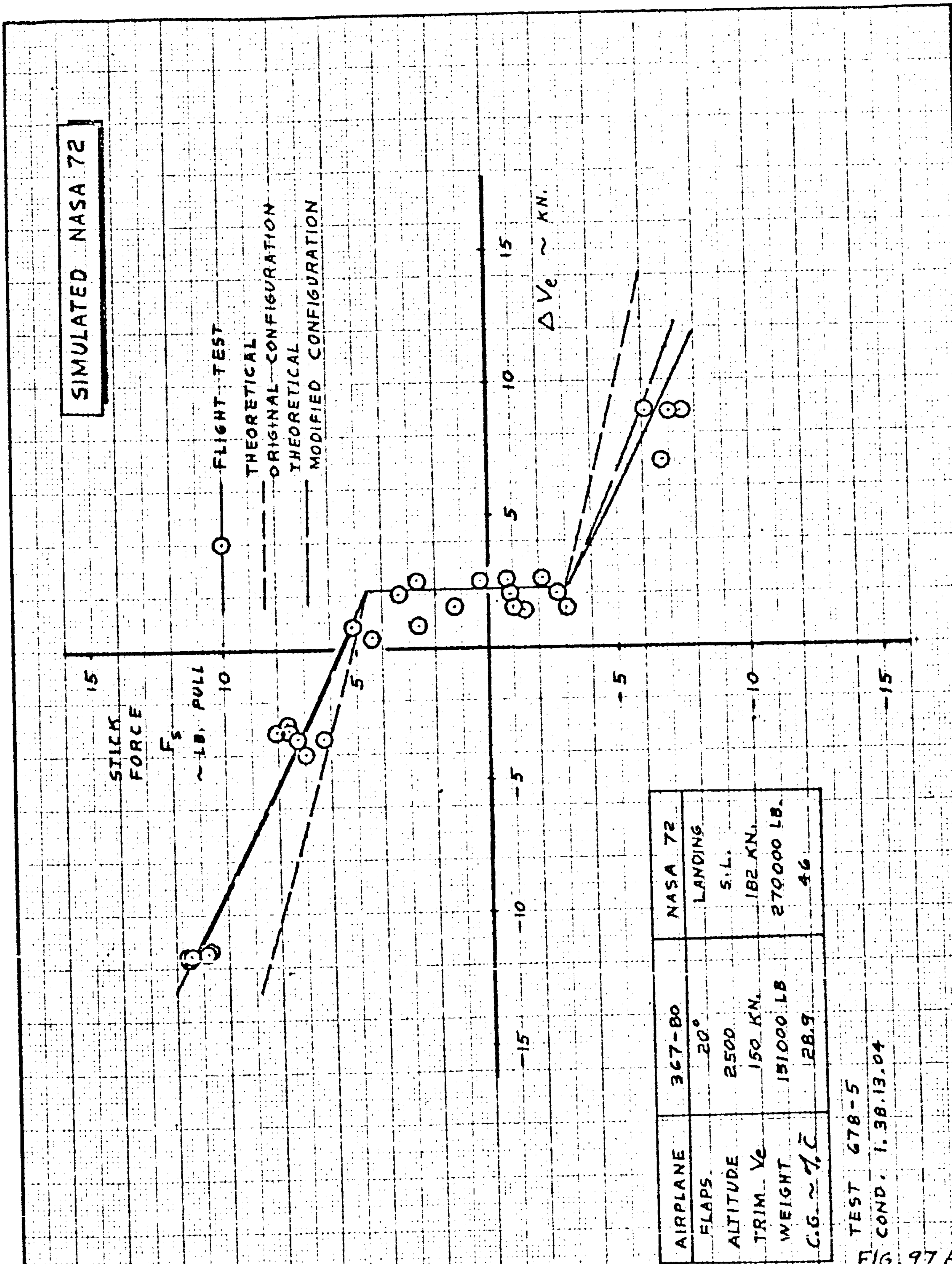

FIG. 97 A

CALC	TAYLOR		REVISED	DATE	SPEED STABILITY	NASA 72
CHECK			W.M.E.	4-22-66	STICK FORCE VS SPEED	D6-10743
APR						PAGE
APR					THE BOEING COMPANY	133A

TD 461 C-R4

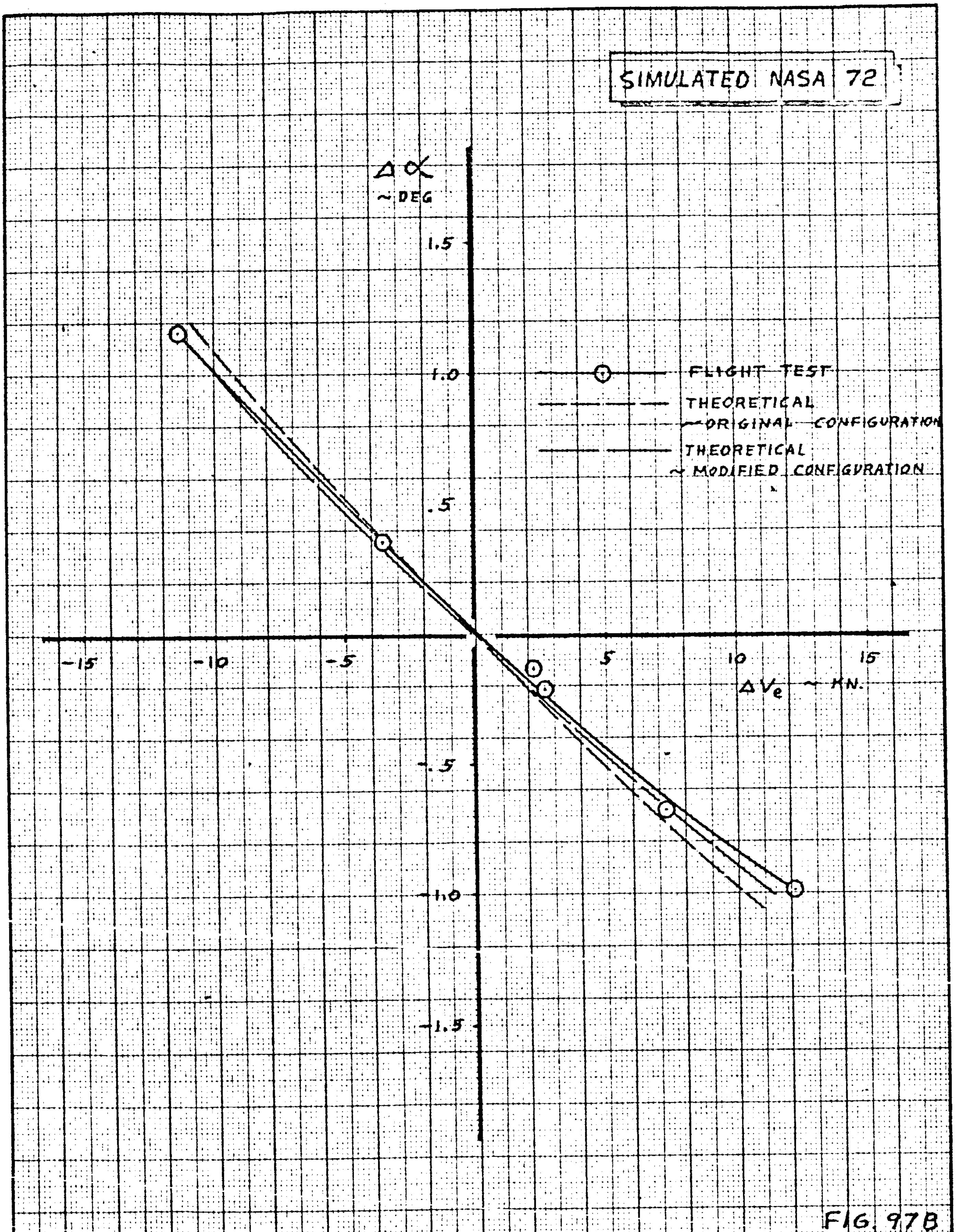

FIG. 97B

CALC	W.M.E	4-22-66	REVISED	DATE	SPEED STABILITY CHARACTERISTICS	NASA 72
CHECK						D6-10743
APR						
APR					THE BOEING COMPANY	PAGE 133 B

TD 461 C-R4

SIMULATED NASA 72

AIRPLANE	367-80	NASA 72
FLAPS	20°	
ALTITUDE	2200	
TRIM V_e	150	182
WEIGHT	167,500	270,000
CG ~ %$\bar{c}$	30.4 %	46 %
TEST NO.	678-5	
COND. NO.	1.22.05.02	

DATA FROM WIND-UP TURN

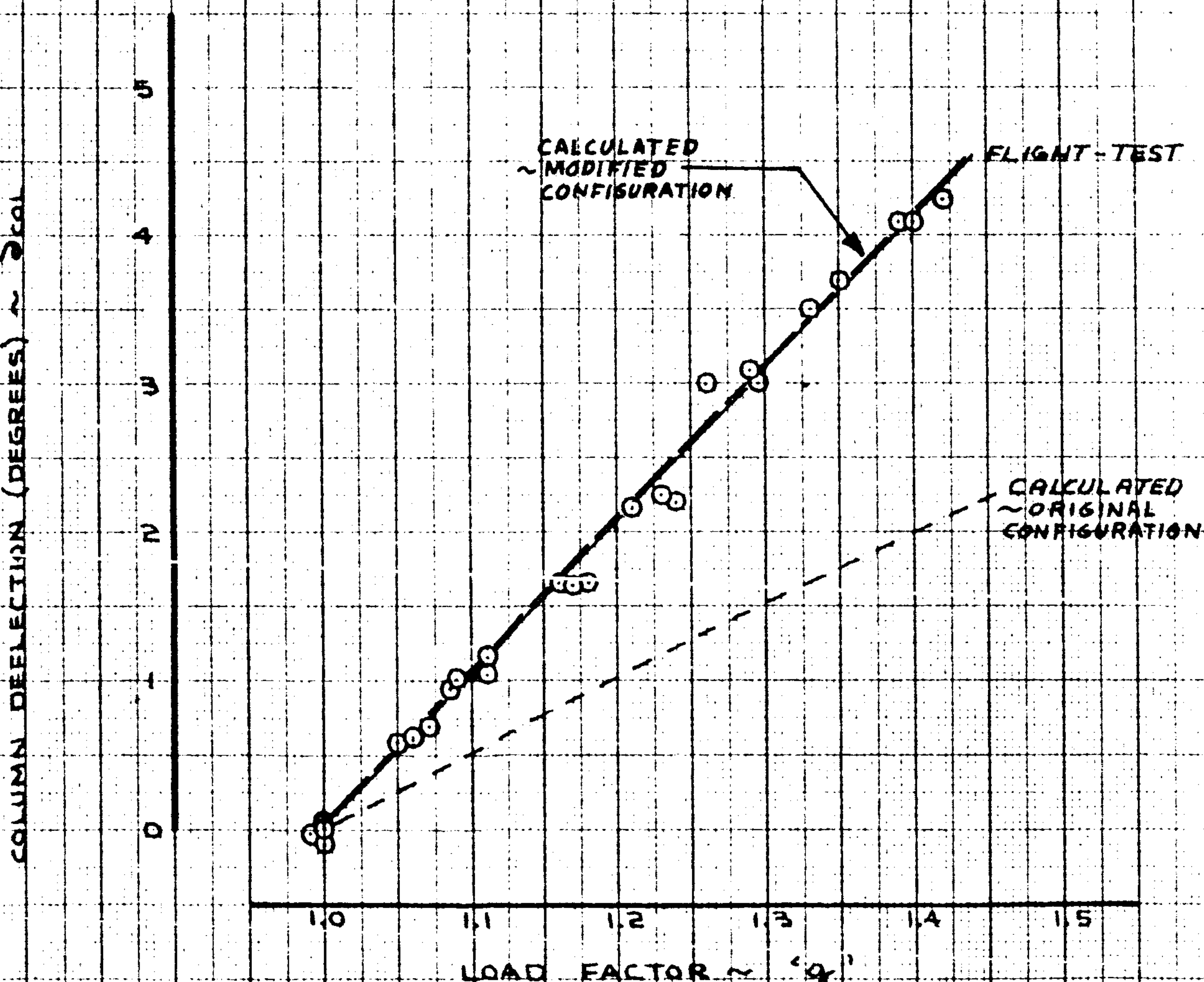

FIG. 98

CALC	TAYLOR	REVISED	DATE	NORMAL ACCELERATION VS COLUMN CHARACTERISTICS	NASA 72
CHECK		W.M.E	4-27-66		06-10743
APR					
APR				THE BOEING COMPANY	PAGE 134

SIMULATED NASA 72

AIRPLANE	367-80	NASA 72
FLAPS	20°	
ALTITUDE	2200	
TRIM Ve	150	182
WEIGHT	167,500	270,000
CG ~ %c̄	30.4 %	46 %
TEST NO.	678-5	
COND. NO.	1.22.05.2	

DATA FROM WIND-UP TURN

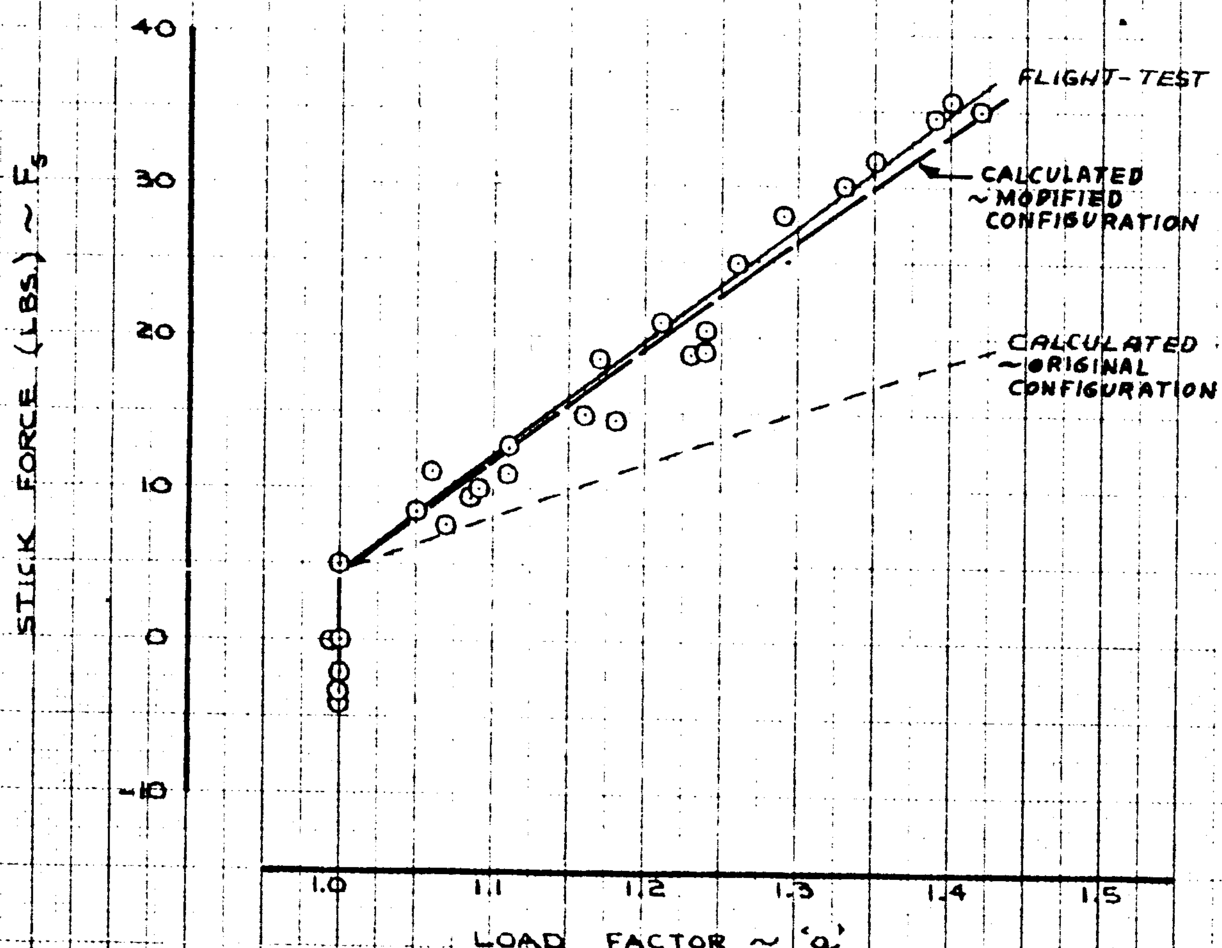

FIG. 98 A

CALC	TAYLOR		REVISED	DATE		
CHECK			W.M.E	4-27-66	NORMAL ACCELERATION VS. FORCE CHARACTERISTICS	NASA 72
APR						D6-10743
APR					THE BOEING COMPANY	PAGE 134 A

TD 461 C R4

SIMULATED NASA 72

AIRPLANE	367-80	NASA 72
FLAPS	20°	
ALTITUDE	2200	
TRIM Ve	150	182
WEIGHT	167,500	270,000
CG ~ %c̄	30.4 %	46.0 %
TEST No.	678-5	
COND. NO.	1.22.05.02	

DATA FROM WIND-UP TURN

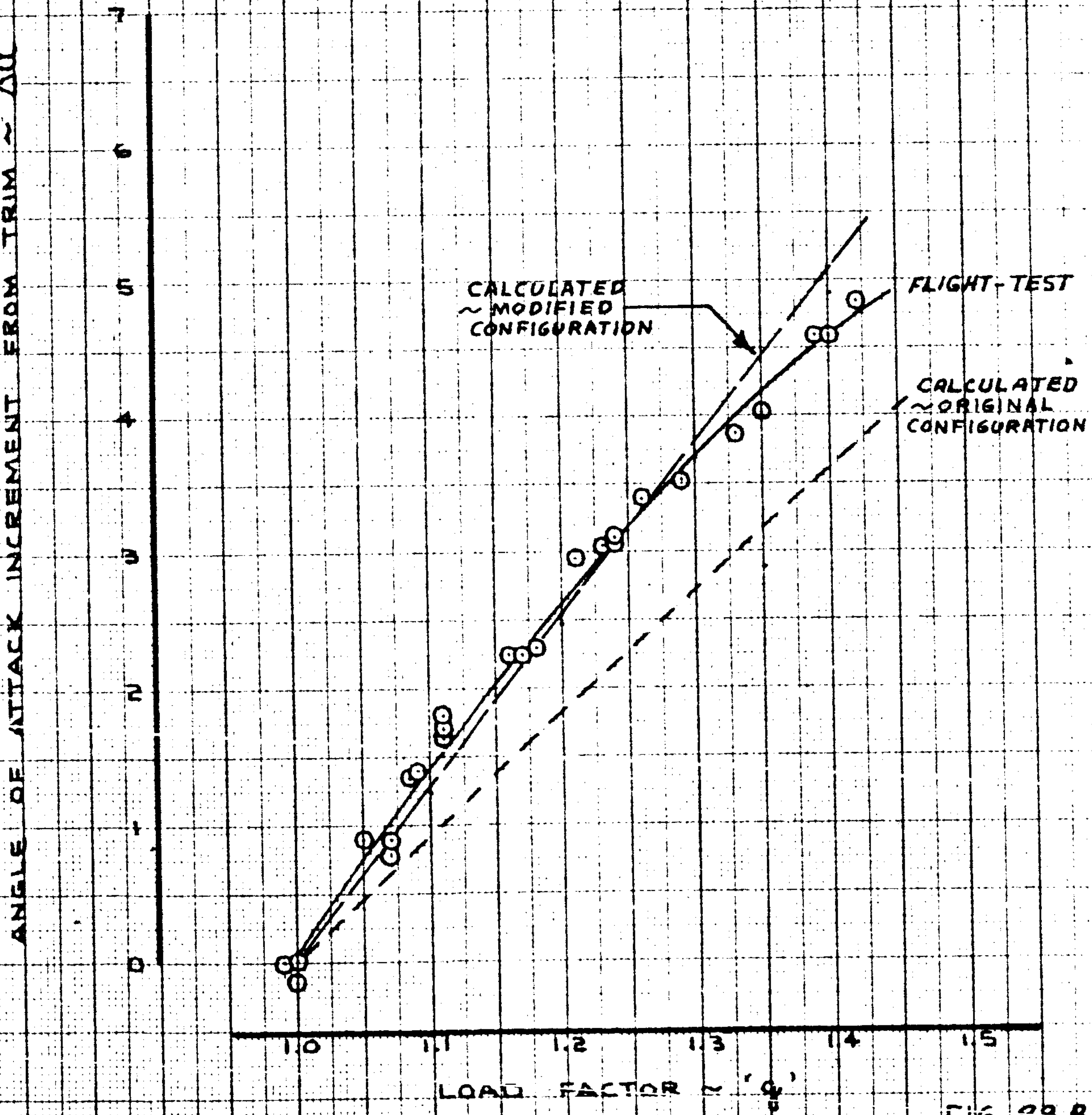

FIG. 98 B

CALC	TAYLOR		REVISED	DATE	NORMAL ACCELERATION VS. ANGLE OF ATTACK	NASA 72
CHECK			W.M.E	4-27-66		D6-10743
APR						
APR					THE BOEING COMPANY	PAGE 134 B

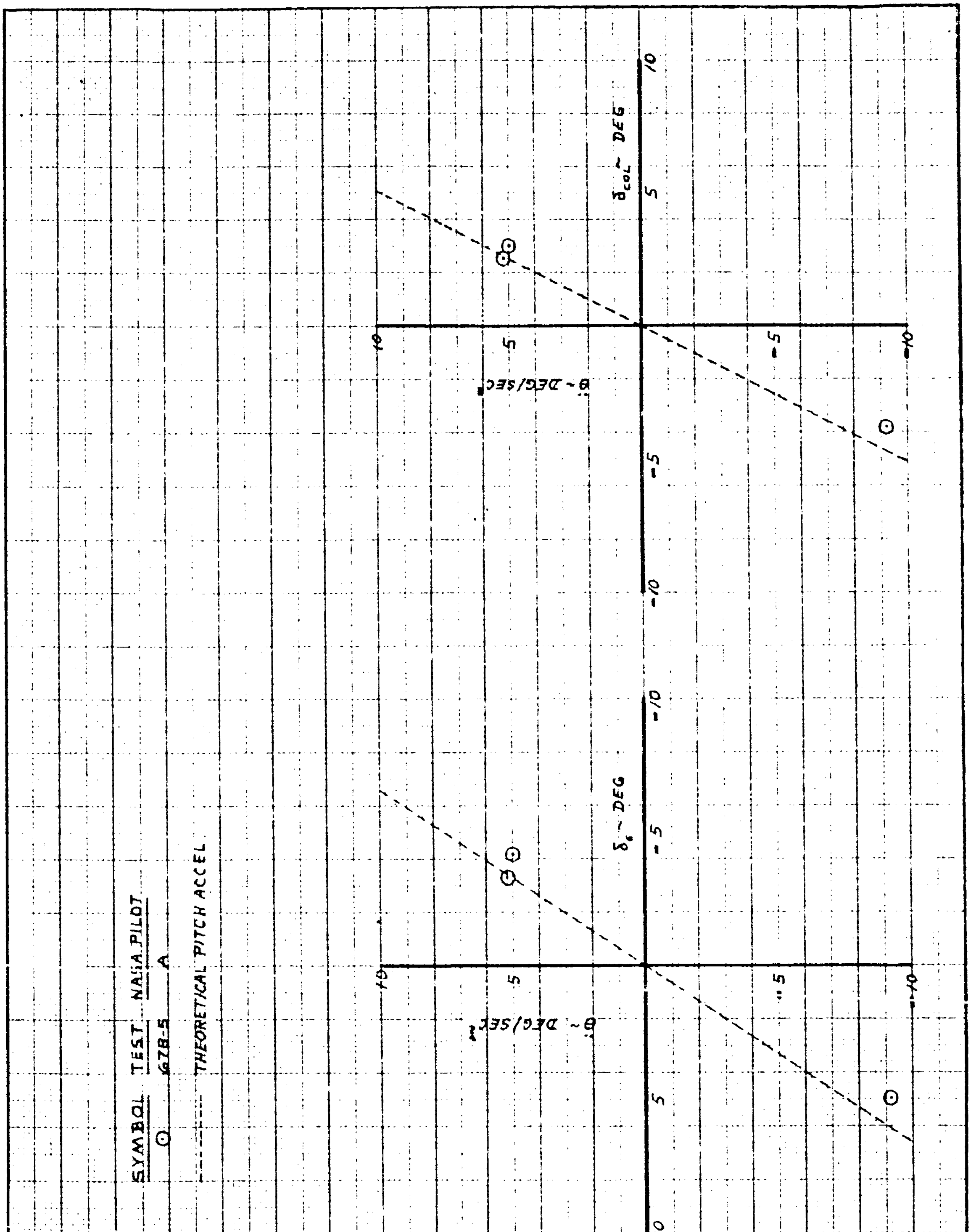

FIG. 99

CALC	DJ BECK	11-18-65	REVISED	DATE
CHECK				
APR				
APR				

PITCH ACCELERATION OF THE NASA 72 SST (BASIC CG ~ NO SAS)

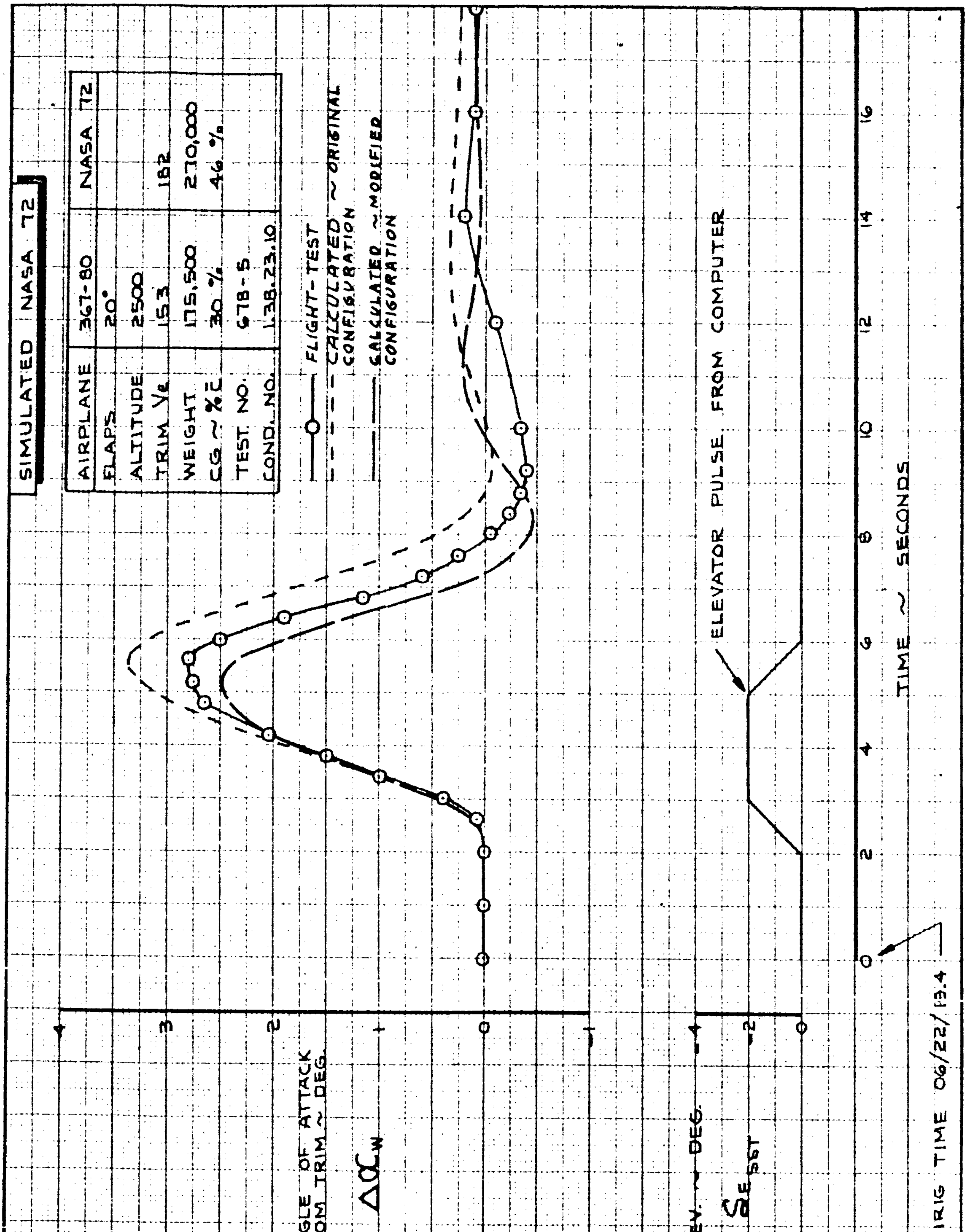

FIG. 100

CALC	TAYLOR	REVISED	DATE	SHORT PERIOD CHARACTERISTICS	NASA 72
CHECK		W.M.E	4-25-66		D6-10743
APR				THE BOEING COMPANY	PAGE 136
APR					

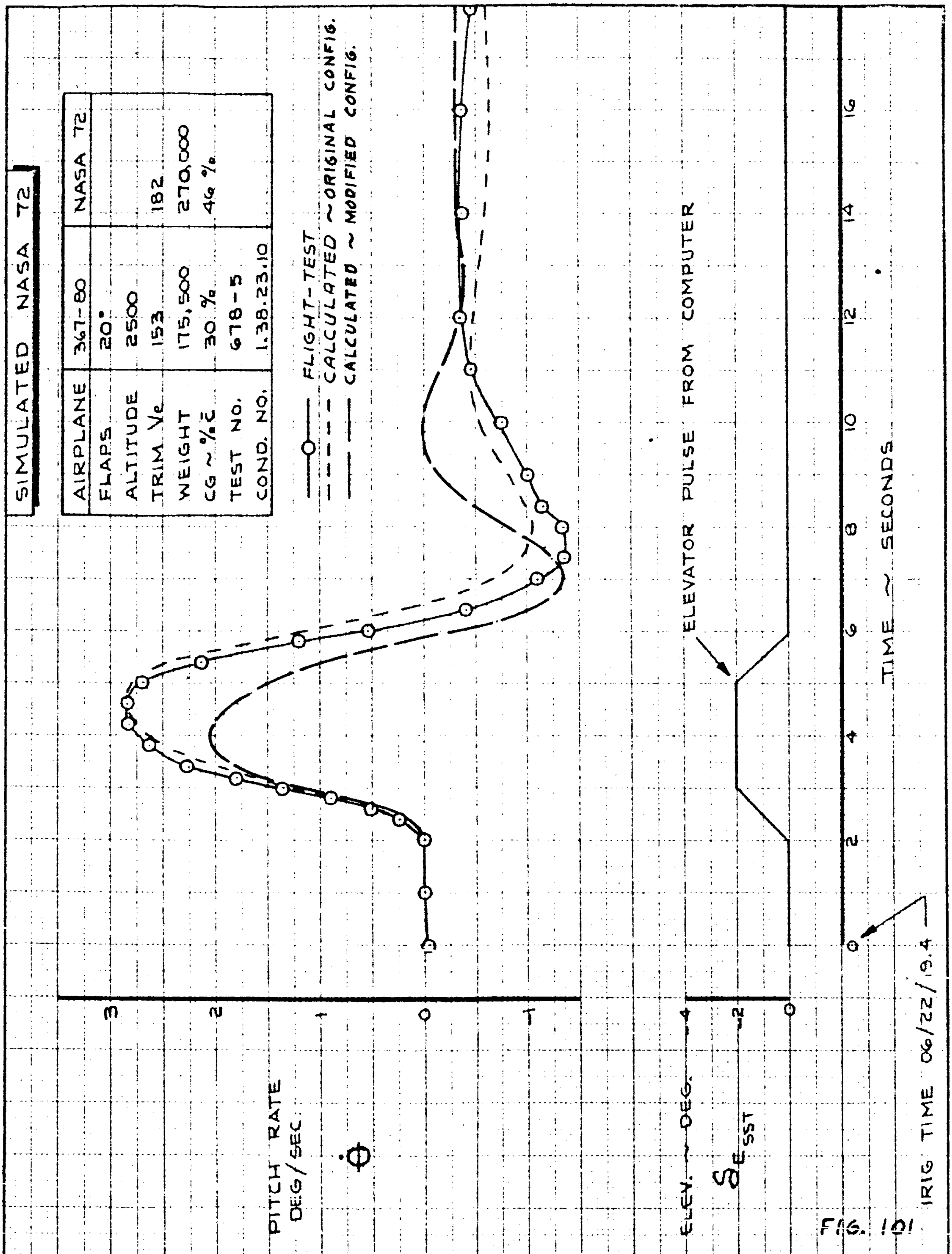

FIG. 101

CALC	TAYLOR		REVISED	DATE	SHORT PERIOD CHARACTERISTICS	NASA 72
CHECK			W.M.E	4-22-66		
APR						D6-10743
APR					THE BOEING COMPANY	PAGE 137

TD 461 C R4

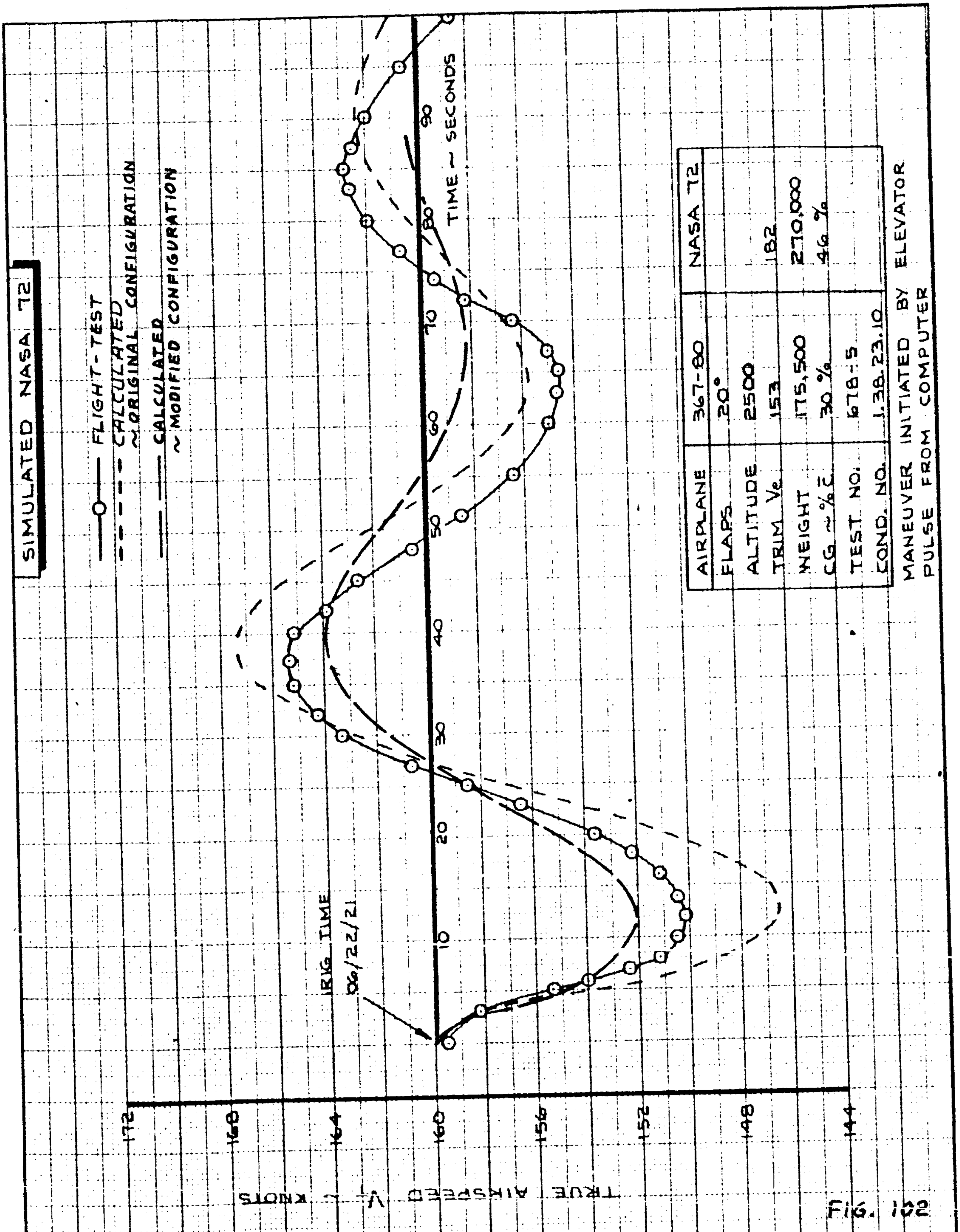

AIRPLANE	367-80	NASA 72
FLAPS	20°	
ALTITUDE	2500	
TRIM V_e	153	182
WEIGHT	175,500	270,000
CG ~ % $\bar{c}$	30 %	46 %
TEST NO.	678-5	
COND. NO.	1.38.23.10	

FIG. 102

CALC	TAYLOR	REVISED	DATE	PHUGOID CHARACTERISTICS	NASA 72
CHECK		W.M.E	4-27-66		D6-10743
APR					PAGE
APR				THE BOEING COMPANY	138

	367-80	NASA 72
FLAPS	20°	
SPEED BRAKES	6°	
V_e	150 KTS	182 KTS
H_p	1150 FT	
GW	156,300 LBS	270,000 LBS
CG	29.5% MAC	46.0% MAC
TEST NO.	678-5	

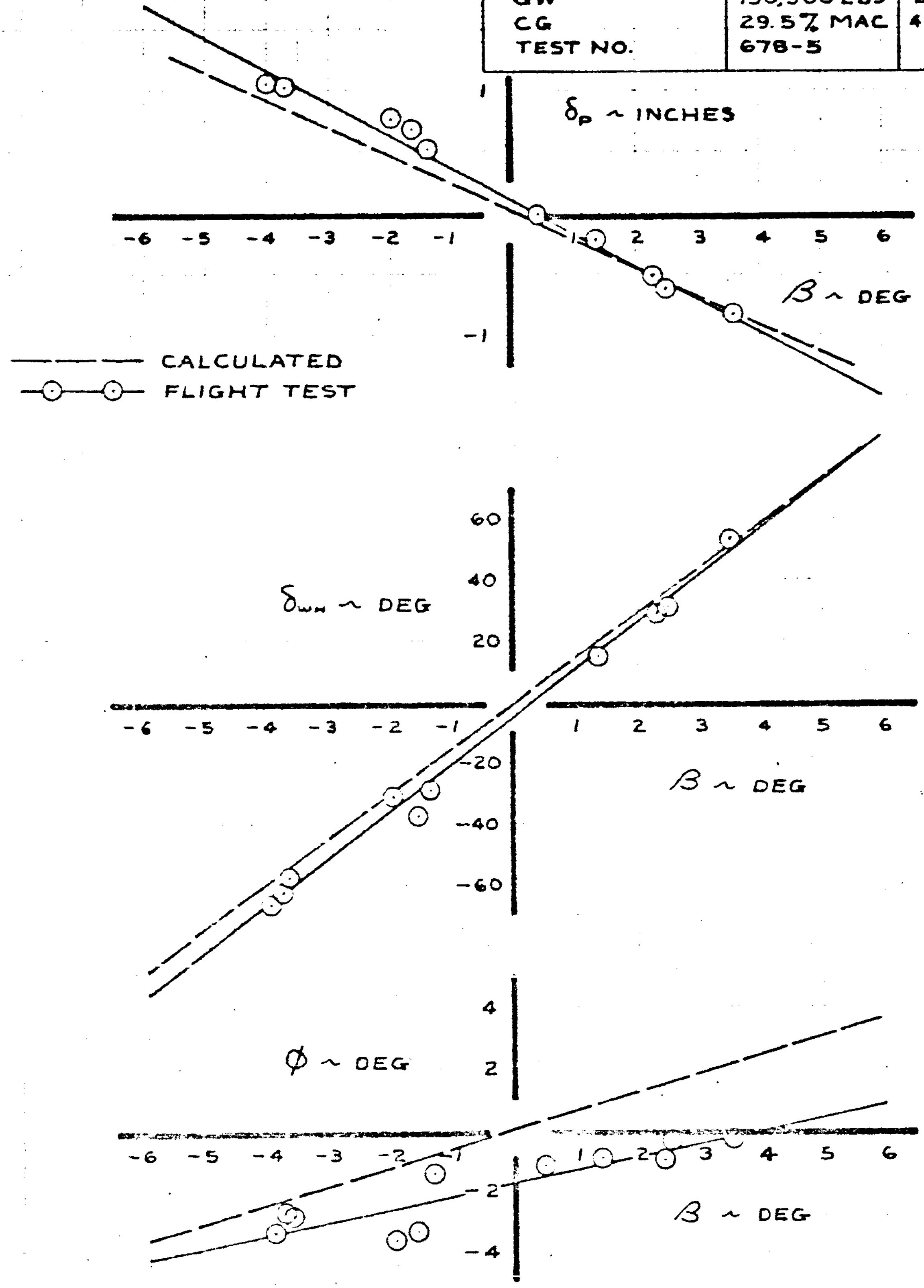

FIG. 103

CALC	SAM	11/1/65	REVISED	DATE	LATERAL - DIRECTIONAL STATIC STABILITY	SIMULATED NASA 72
CHECK	RCL	11/2/65				D6-10743
APR						PAGE 139
APR					THE BOEING COMPANY	

TD 461 C-R4

	367-80	NASA 72
FLAPS	20°	
SPEED BRAKES	6°	
V_e	150	182 KTS
H_p	1666 FT	
GW	161,000 LBS	270,000 LBS
CG	30.7 % MAC	46.0 % MAC
TEST NO.	678-5	

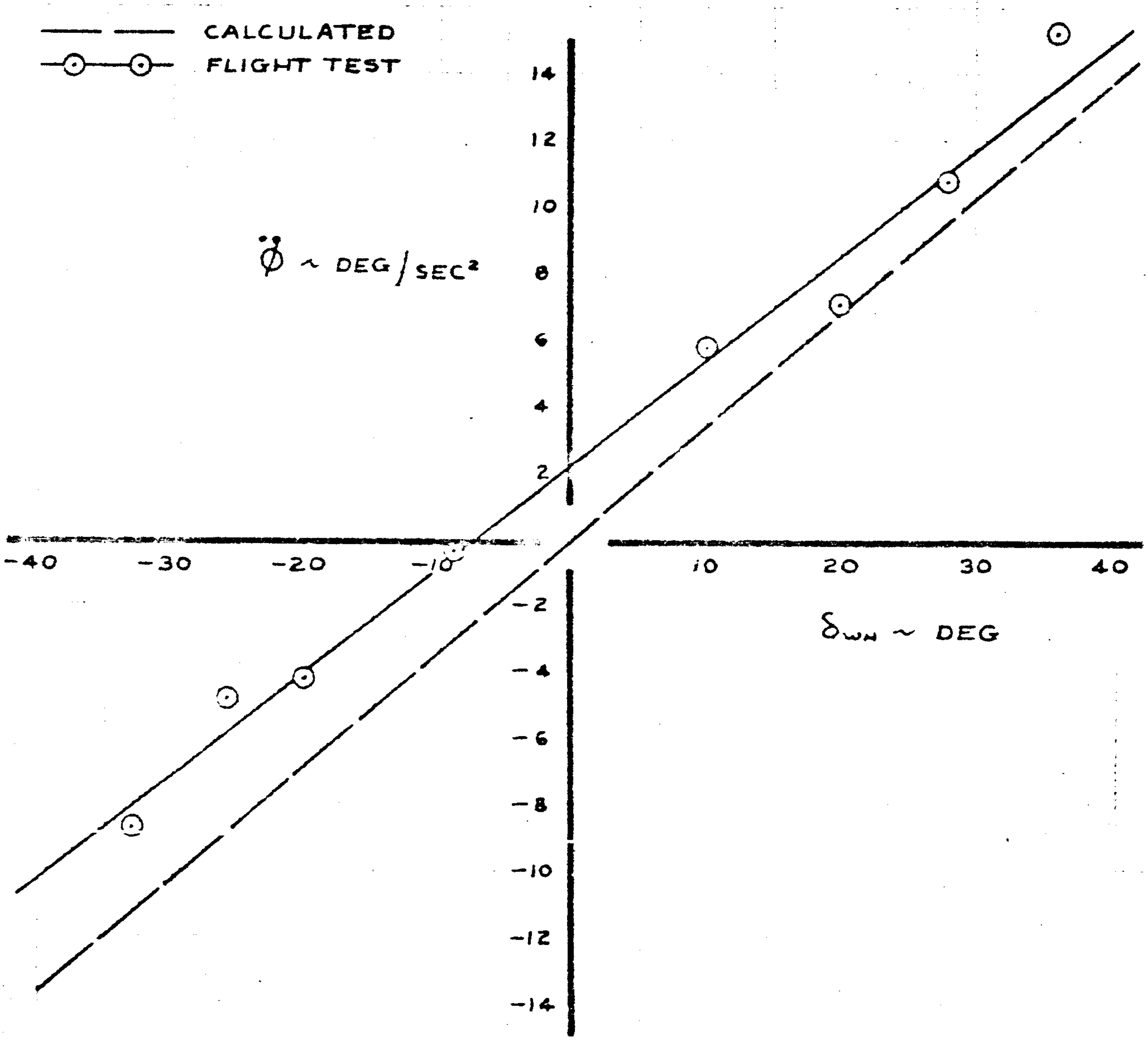

FIG. 104

CALC	SAM	11/1/65	REVISED	DATE	ROLL ACCELERATION CHARACTERISTICS 1 DEGREE OF FREEDOM	SIMULATED NASA 72
CHECK	RCL	11/2/65				D6-10743
APR					THE BOEING COMPANY	PAGE 140
APR						

TD 461 C-R4

	367-80	NASA 72
FLAPS	20°	
SPEED BRAKES	6°	
V_e	150 KTS	182 KTS
H_p	2150 FT	
GW	162,500 LBS	270,000 LBS
CG	30.6% MAC	46.0% MAC
TEST NO.	678-5	

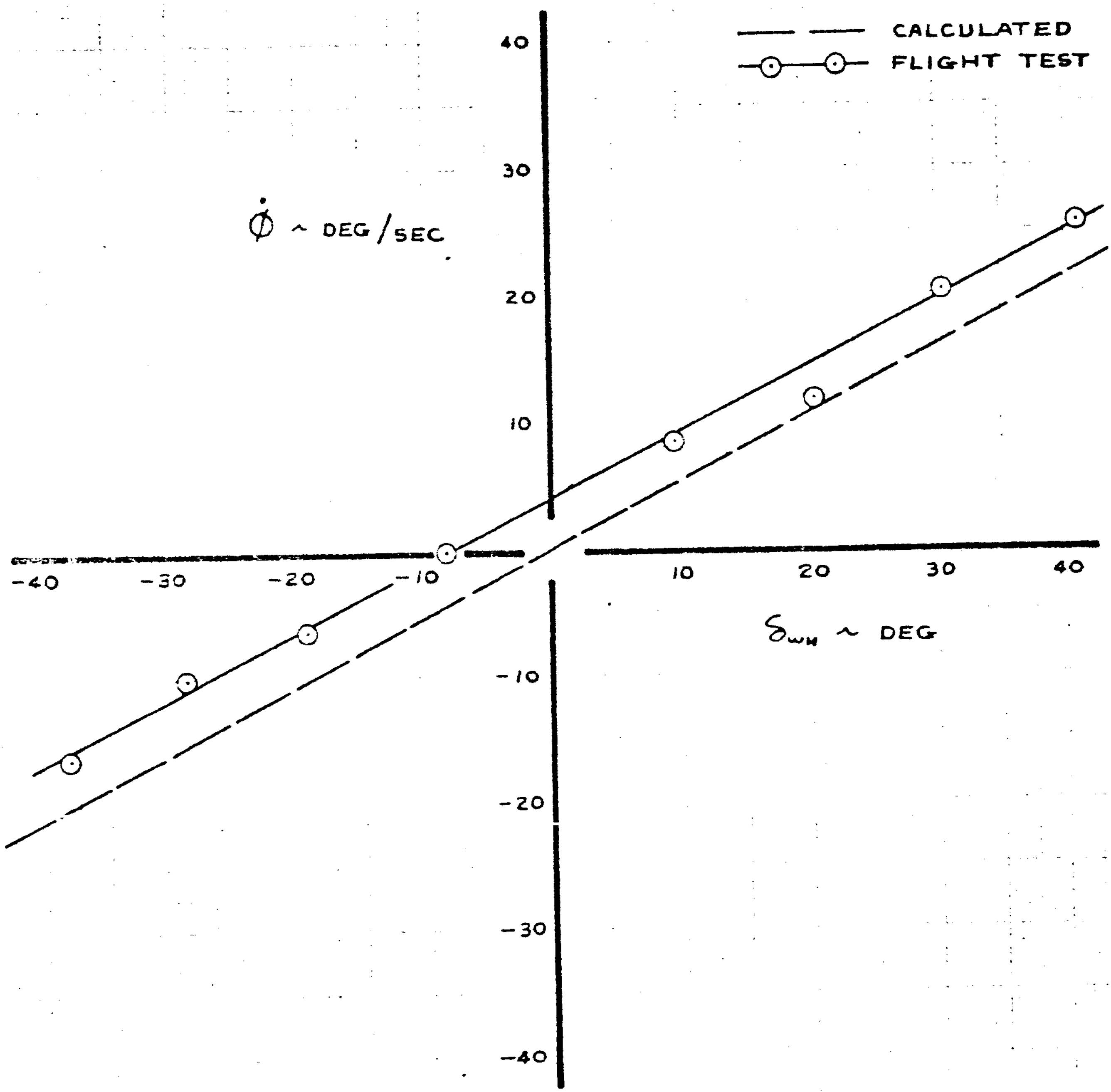

FIG. 105

CALC	RC	11/8/65	REVISED	DATE	LATERAL CONTROL RESPONSE STEADY STATE ROLL RATES 1 DEGREE OF FREEDOM	SIMULATED NASA 72
CHECK						D6-10743
APR						PAGE 141
APR					THE BOEING COMPANY	

	367-80	NASA 72
FLAPS	20°	
SPEED BRAKES	6°	
V_e	150 KTS	182 KTS
H_p	2150 FT	
GW	162,500 LBS	270,000 LBS
CG	30.6% MAC	46.0% MAC
TEST NO.	678-5	

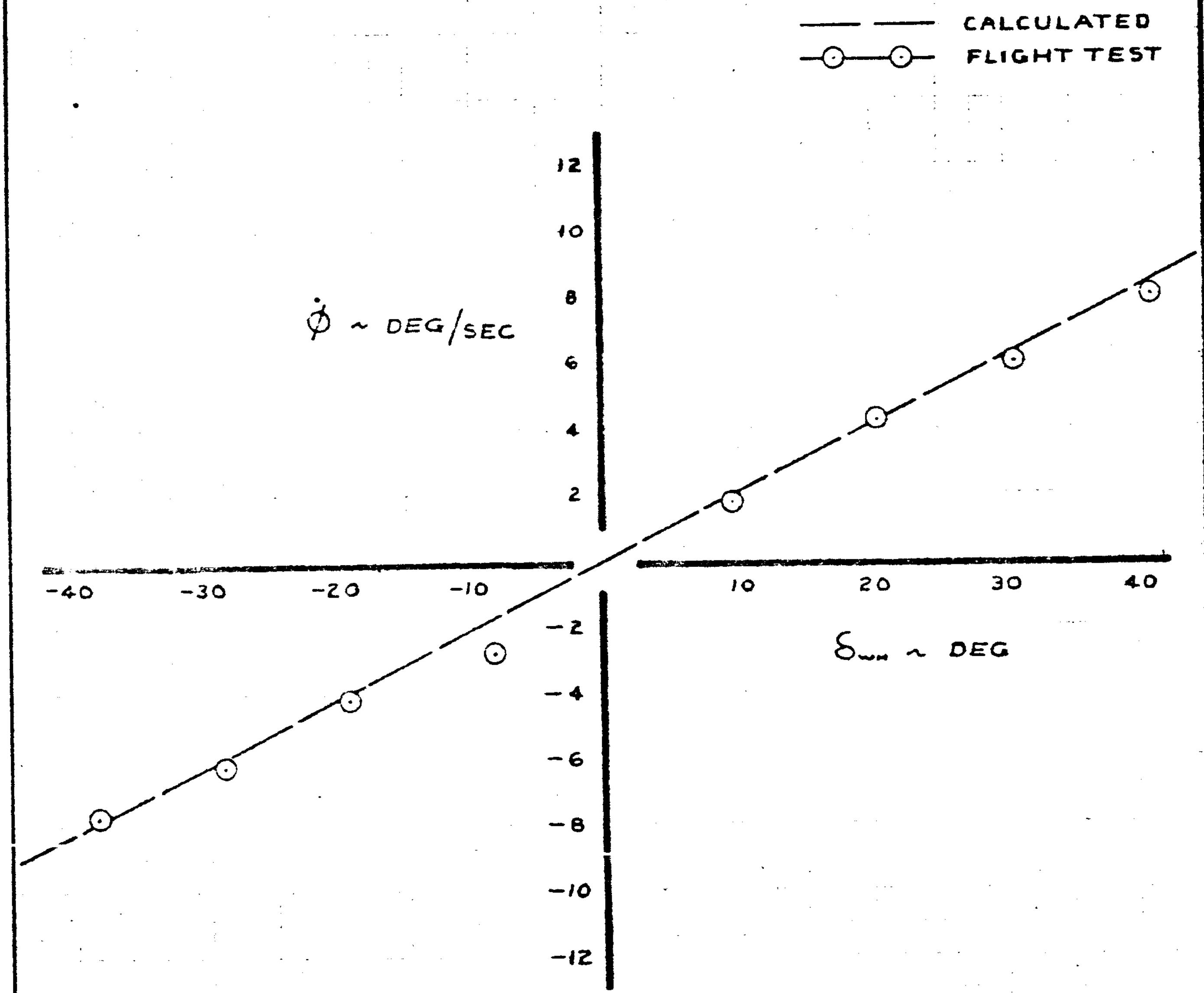

FIG. 106

CALC	SAM	10/27/65	REVISED	DATE	LATERAL CONTROL RESPONSE STEADY STATE ROLL RATES 3 DEGREE OF FREEDOM	SIMULATED NASA 72 D6-10743
CHECK	RCB	11/2/65				
APR						
APR					THE BOEING COMPANY	PAGE 142

TD 461 C-R4

	367-80	NASA 72
FLAPS	20°	
SPEED BRAKES	6°	
V_e	150 KTS	182 KTS
H_p	2100 FT	
GW	173,100 LBS	270,000 LBS
CG	30.1% MAC	46.0% MAC
TEST NO	678-5	

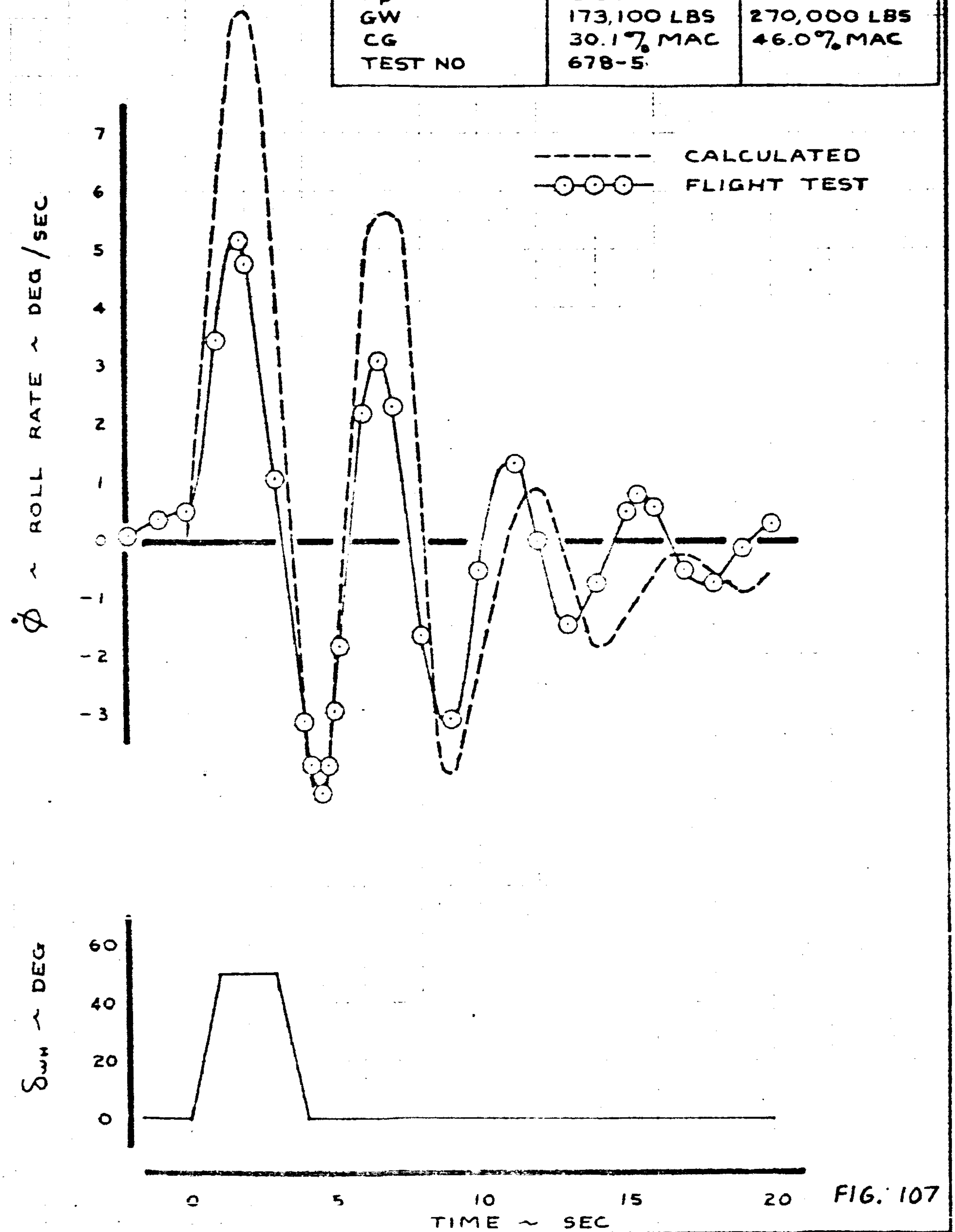

FIG. 107

CALC	SAM	10/29/65	REVISED	DATE	LATERAL CONTROL RESPONSE COMPUTER WHEEL PULSE	SIMULATED NASA 72
CHECK	RCS	11/5/65			678-5 1:30:23.16 6/20/20.4	D6-10743
APR					THE BOEING COMPANY	PAGE 143
APR						

TD 461 C-R4

	367-80	NASA 72
FLAPS	20°	
SPEED BRAKES	6°	
V_e	150 KTS	182 KTS
H_p	2100 FT	
GW	173,100 LBS	270,000 LBS
CG	30.1 % MAC	46.0 % MAC
TEST NO.	678 - 5	

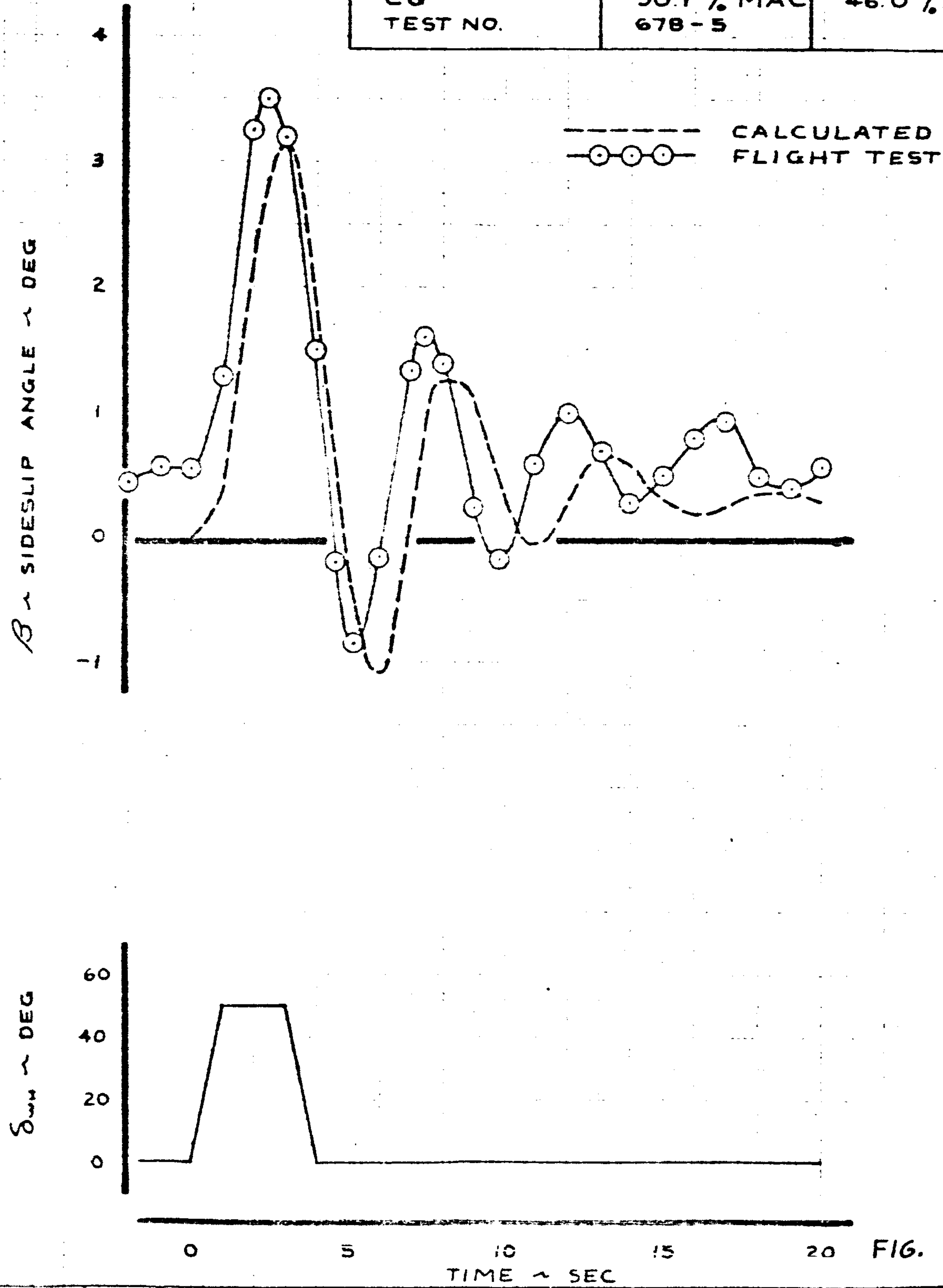

FIG. 108

CALC	JAM	10/27/65	REVISED	DATE	LATERAL CONTROL RESPONSE	SIMULATED NASA 72
CHECK	RCS	11/5/65			COMPUTER WHEEL PULSE	
APR					678-5 1.38.23.16 6/28/20.4	D6-10743
APR					THE BOEING COMPANY	PAGE 144

	367-80	NASA 72
FLAPS	20°	
SPEED BRAKES	6°	
V_e	150 KTS	182 KTS
H_p	2100 FT	
GW	173,100 LBS	270,000 LBS
CG	30.1 % MAC	46.0 % MAC
TEST NO.	678-5	

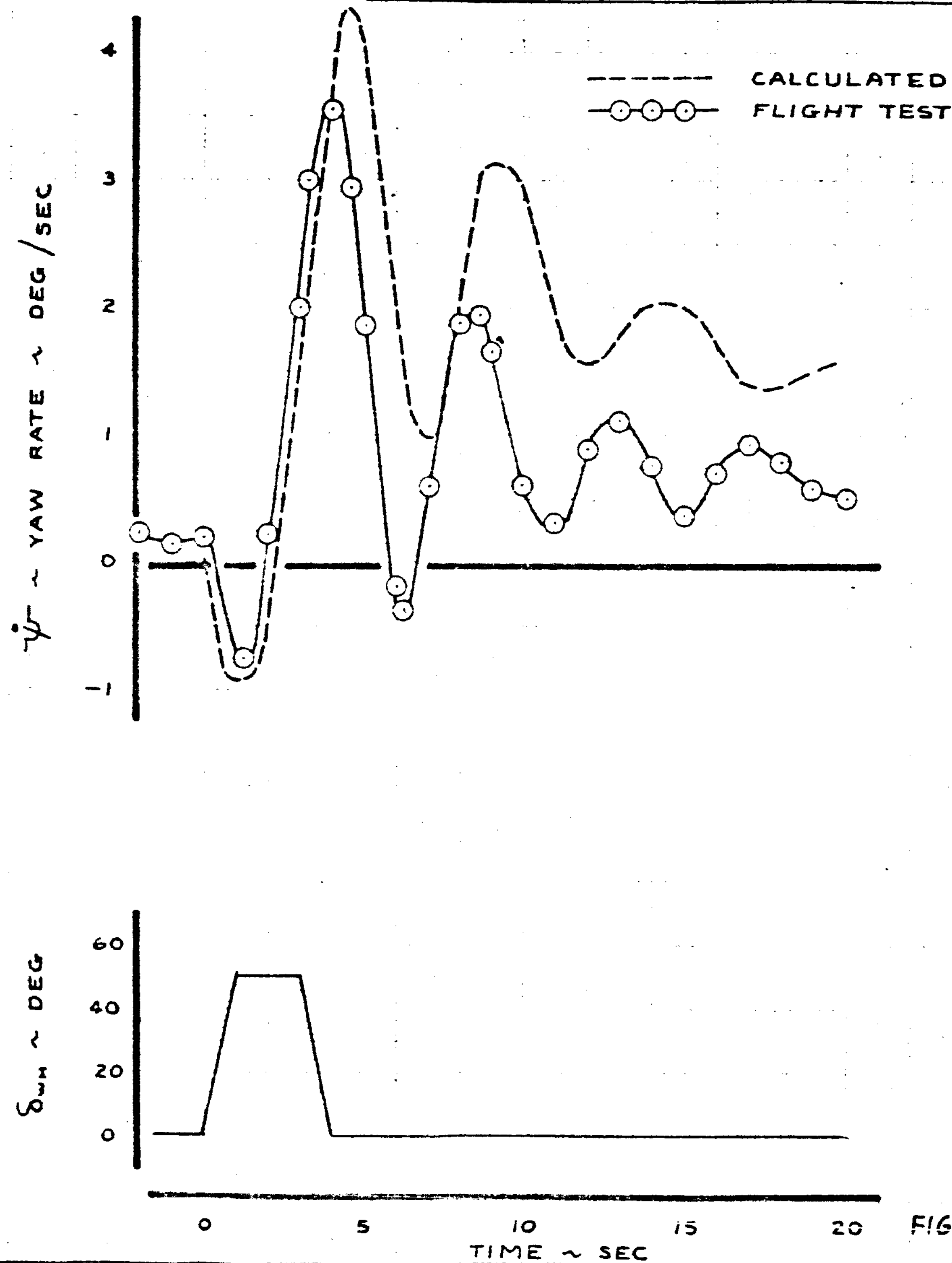

FIG. 109

CALC	SAM	10/28/65	REVISED	DATE	LATERAL CONTROL RESPONSE	SIMULATED
CHECK	RCL	11/5/65			COMPUTER WHEEL PULSE	NASA 72
APR					678-5 1 38.23.16 6/28/20.4	D6-10743
APR					THE BOEING COMPANY	PAGE 145

TD 461 C-R4

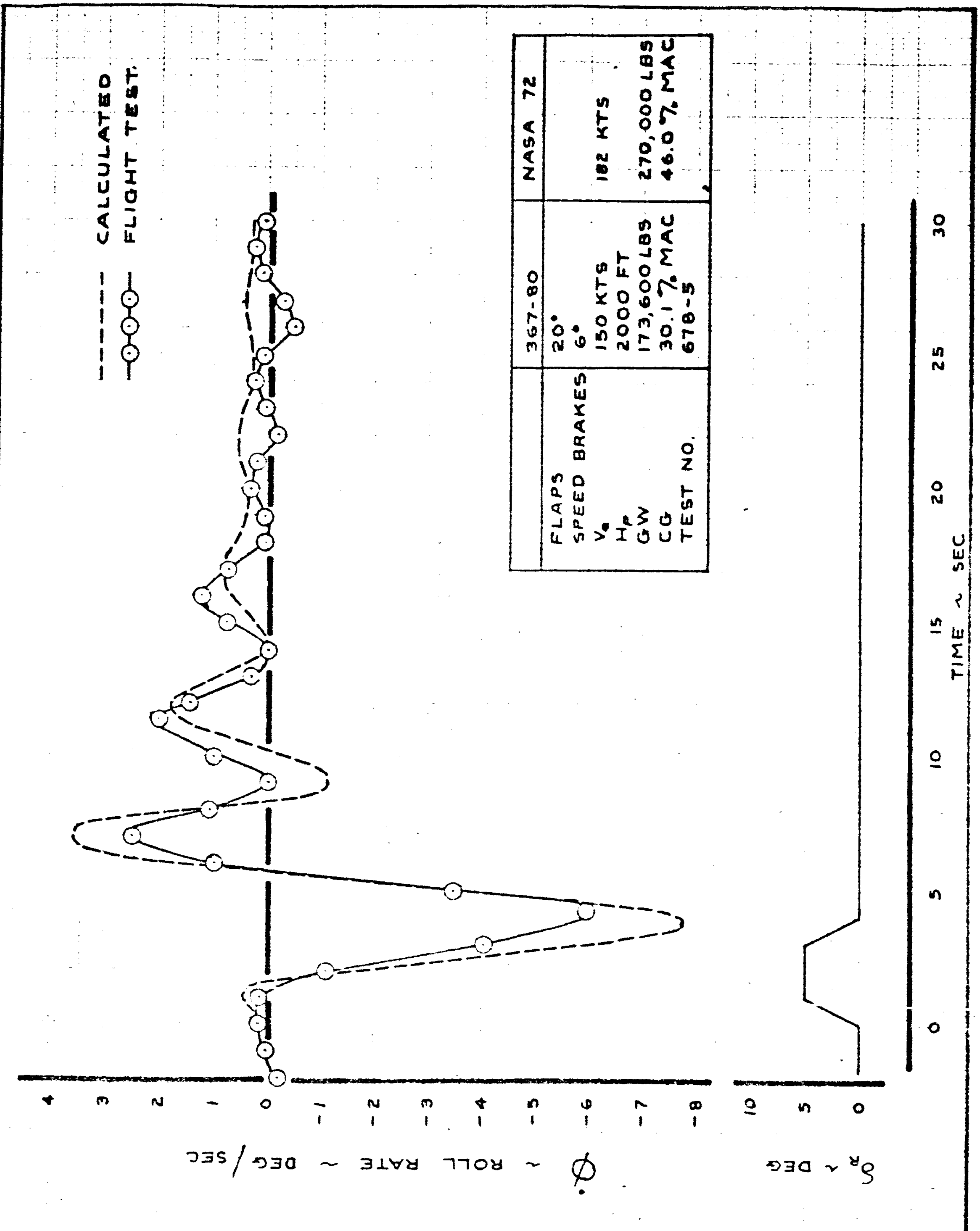

FIG. 110

CALC	RCS	11/2/65	REVISED	DATE	LATERAL - DIRECTIONAL DYNAMICS
CHECK	SAM	11/4/65			
APR					678-5 1.38.23.14 6/27/04.4
APR					THE BOEING COMPANY

SIMULATED NASA 72

D6-10743

TD 461 C-R4

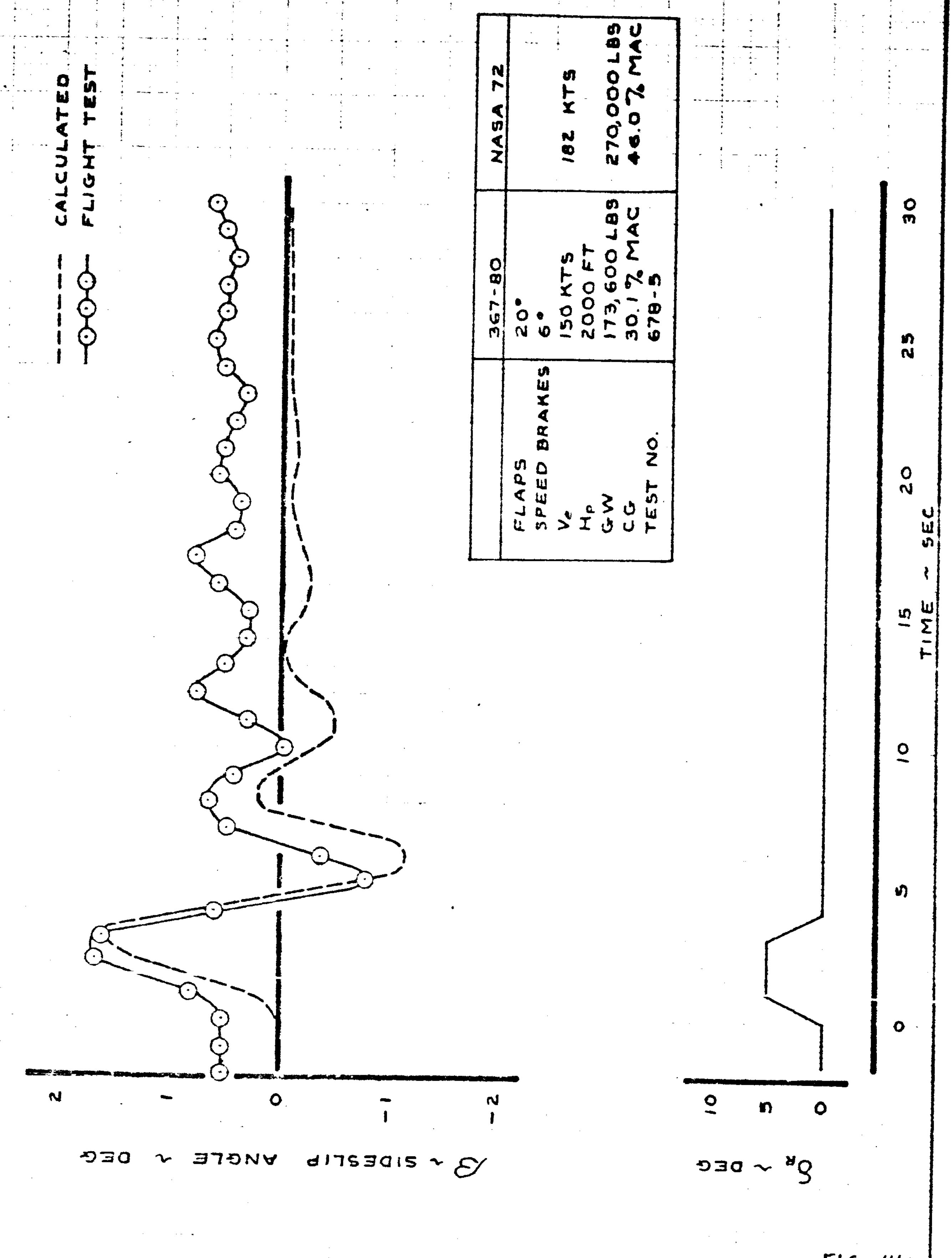

FIG. 111

			REVISED	DATE		
CALC	RC8	11/1/65			LATERAL - DIRECTIONAL DYNAMICS	SIMULATED NASA 72
CHECK	SAM	11/3/65				
APR					678-5 1 38.23.14 6/27/04.4	D6-10743
APR					THE BOEING COMPANY	PAGE 147

TD 461 C-R4

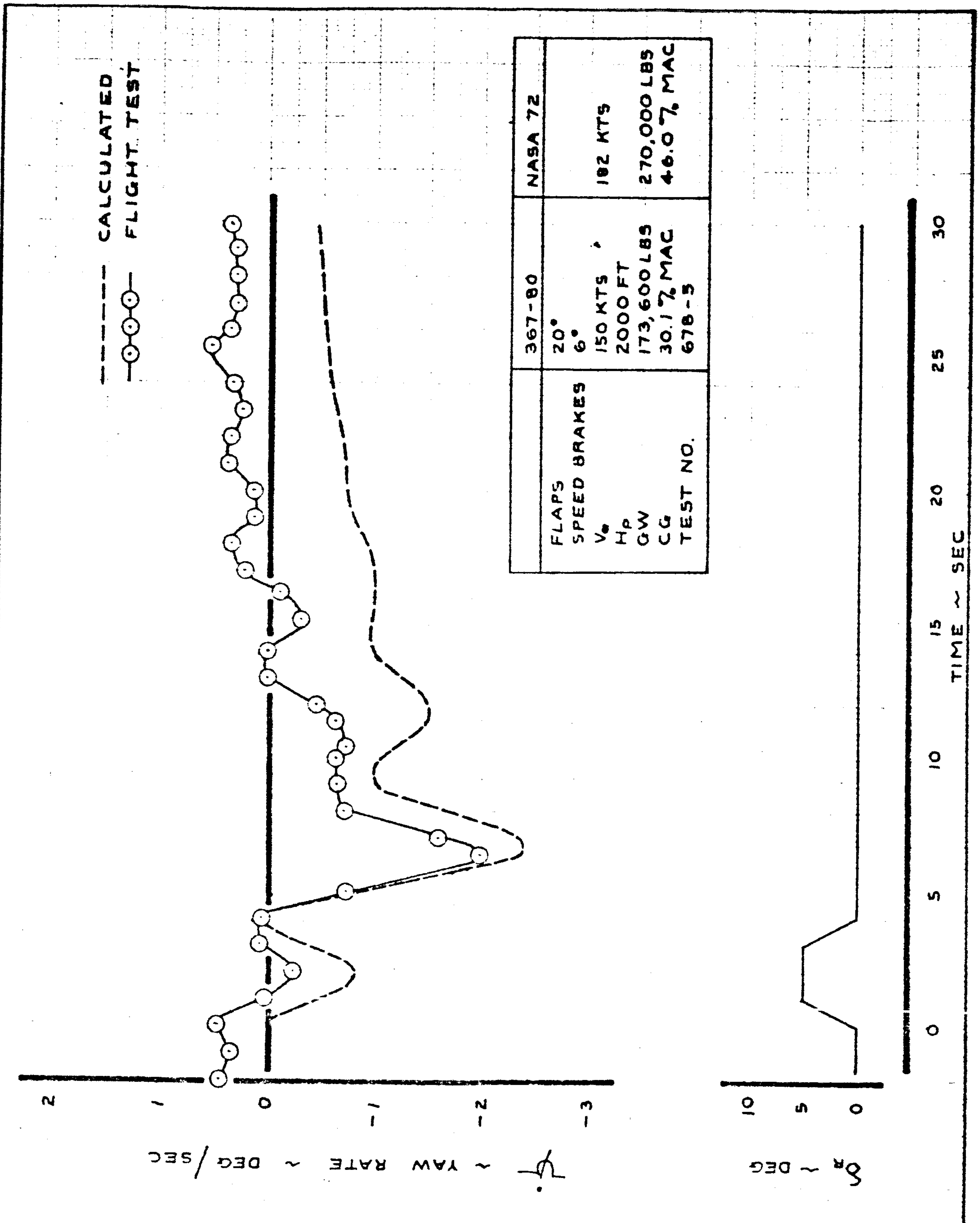

FIG. 112

CALC	RCJ	11/2/65	REVISED	DATE	LATERAL - DIRECTIONAL DYNAMICS	SIMULATED NASA 72
CHECK	SAM	11/4/65			678-5 1.38.23.14 6/27/04.4	D6-10743
APR					THE BOEING COMPANY	PAGE 148
APR						

TD 461 C-R4

APPENDIX I

367-80 Characteristics

367-80 Configuration Documentation

Flight tests were performed in August, 1964 (Boeing Test No. 643-1 to 643-4) to document the 367-80 flight configurations used for SST simulation. Speed stability tests were run to document the lift-drag characteristics and the effect of the spoilers. The thrust reversers were calibrated by holding constant speed and varying clamshell door angle. The lateral control static characteristics were measured by cross-control sideslips and the dynamic characteristics were documented by performing step wheel inputs. The airplane response to pulses of all the controls was documented for use in setting up the simulation computer.

Three configurations were documented in these tests: flaps 30°, BPR 1, flaps 30°, BPR 4 and flaps 20°, BPR 1. The configuration with BLC was not used for simulation, so only the data for the BPR 1 configurations are presented here.

The lift and drag characteristics at a number of speed brake deflections are shown in Figs. 113 to 111. The elevator-static stability relationships measured in these tests are shown in Figs. 117 and 118. Figs. 119 to 122 are cross-plots of the lift and drag curves which show the speed brake effectiveness. Fig. 123 is a cross-plot of the elevator curve to show the spoiler pitching moment. Fig. 124 is a correction of fig. 123 to show the spoiler pitching moment at constant airplane angle-of-attack. Figs. 125 and 126 show the thrust reverser calibration. The thrust curve has been normalized as the ratio of actual thrust to the thrust at 30° clamshell door angle. In the elevator curve, the airplane was initially trimmed at 0° clamshell with 0° elevator. The rudder and control wheel required in the cross-control sideslips with speed brakes up and down are shown in Figs. 127 to 130. The roll rate response to wheel step inputs is shown in Figs. 131 and 132.

Following these tests, the 367-80 was modified from servo tab operated aileron and elevator controls to powered hydraulic controls. This modification changed the effectiveness of the elevator and lateral controls. For small deflections (to 15°), the elevator effectiveness was increased by a factor of 1.26 over the tab elevator. The modified lateral control characteristics are shown in Fig. 133. This is shown for a trim condition with the speed brakes at 0° which was used for SST simulation.

Later flight testing also showed that the 367-80 had a moderate tail buffet when the inboard speed brakes were deflected above 10°. In order to prevent this buffet from degrading the simulation quality, the inboard speed brake deflection was limited at 10° by the computer while the outboard speed brakes operated to 16° for maximum lift modulation. The effectiveness of the inboard and outboard speed brakes, measured by wind tunnel testing and corrected by flight test data is shown in Figs. 134 and 135.

367-80 Stability Derivatives

The 367-80 stability derivatives and dynamic stability characteristics used for simulation of the NASA 20, NASA Δ, and NASA 72 SST configurations are tabulated on pages 176 to 179. These derivatives have been updated from the initial theoretical values by flight testing with the simulation system.

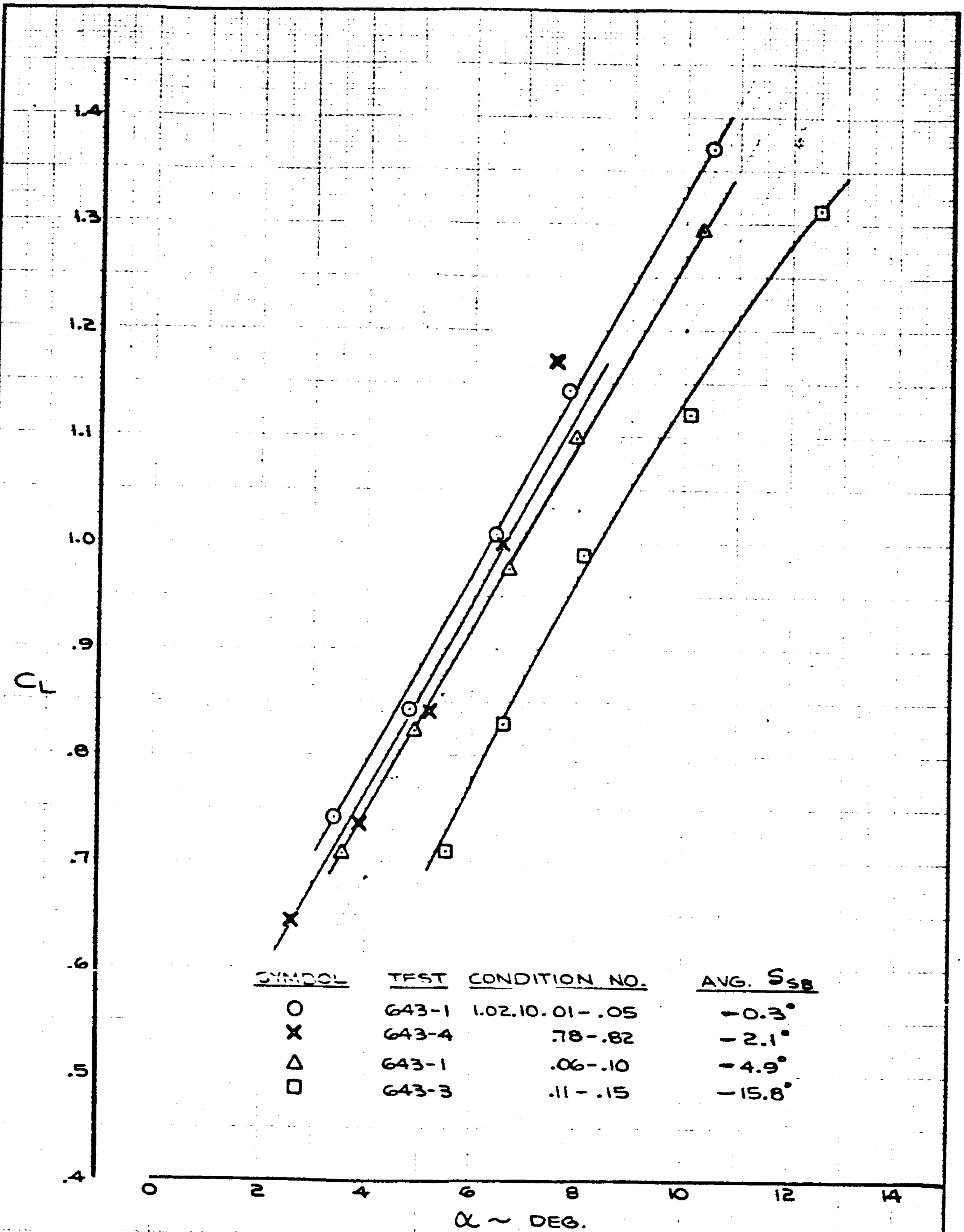

FIG. 113

CALC	TAYLOR	9.23.4	REVISED	DATE		367-80B BLC
CHECK					C_L VS α	
APR					FLAPS 30° BLOWING OFF	D6-10743
APR					THE BOEING COMPANY	PAGE 153

TD No. C-R4

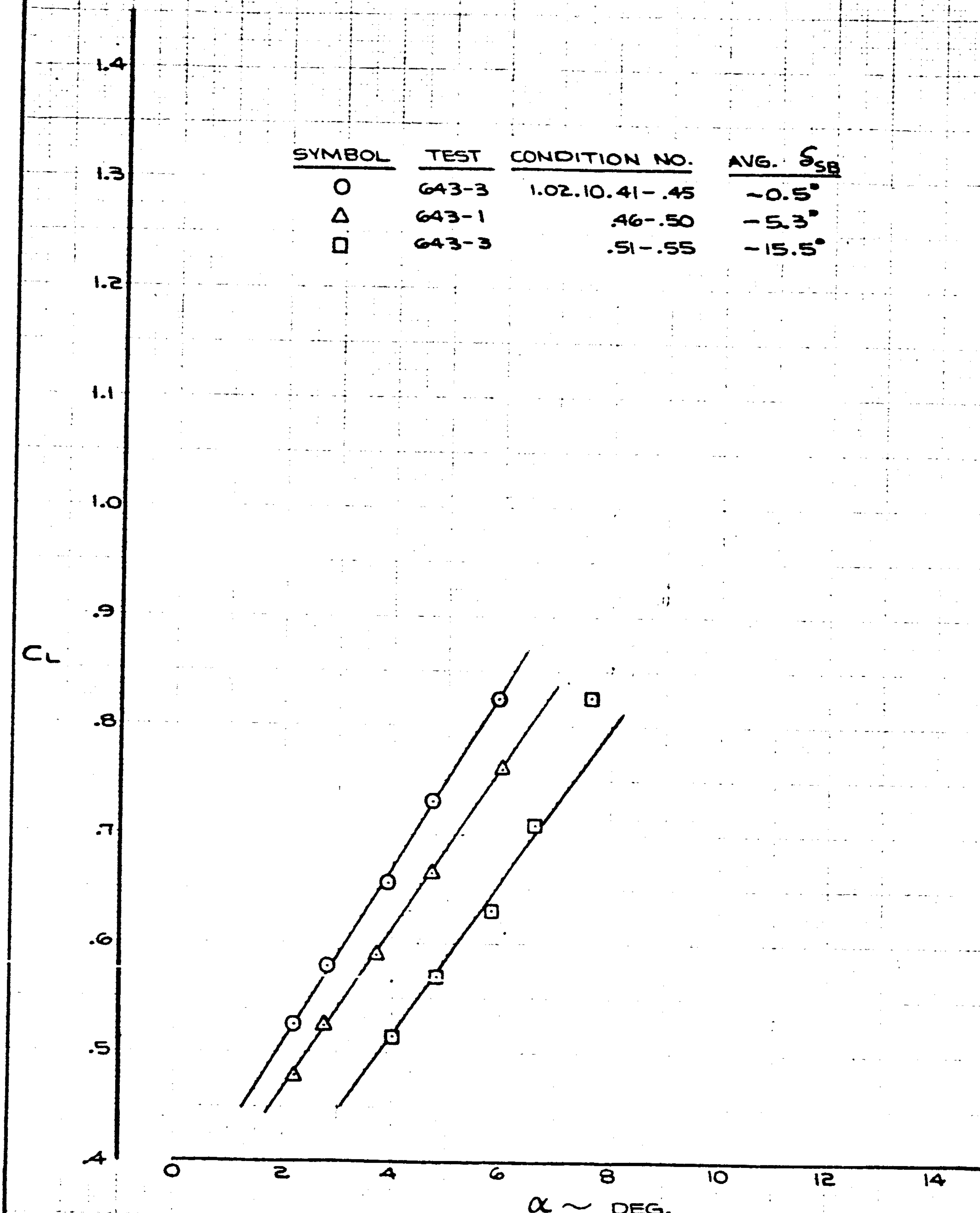

FIG. 114

CALC	TAYLOR	9-23-4	REVISED	DATE	C_L VS α	367-80B BLC
CHECK						
APR					FLAPS 20° BLOWING OFF	D6-10743
APR						
					THE BOEING COMPANY	PAGE 154

TD 461 C-R4

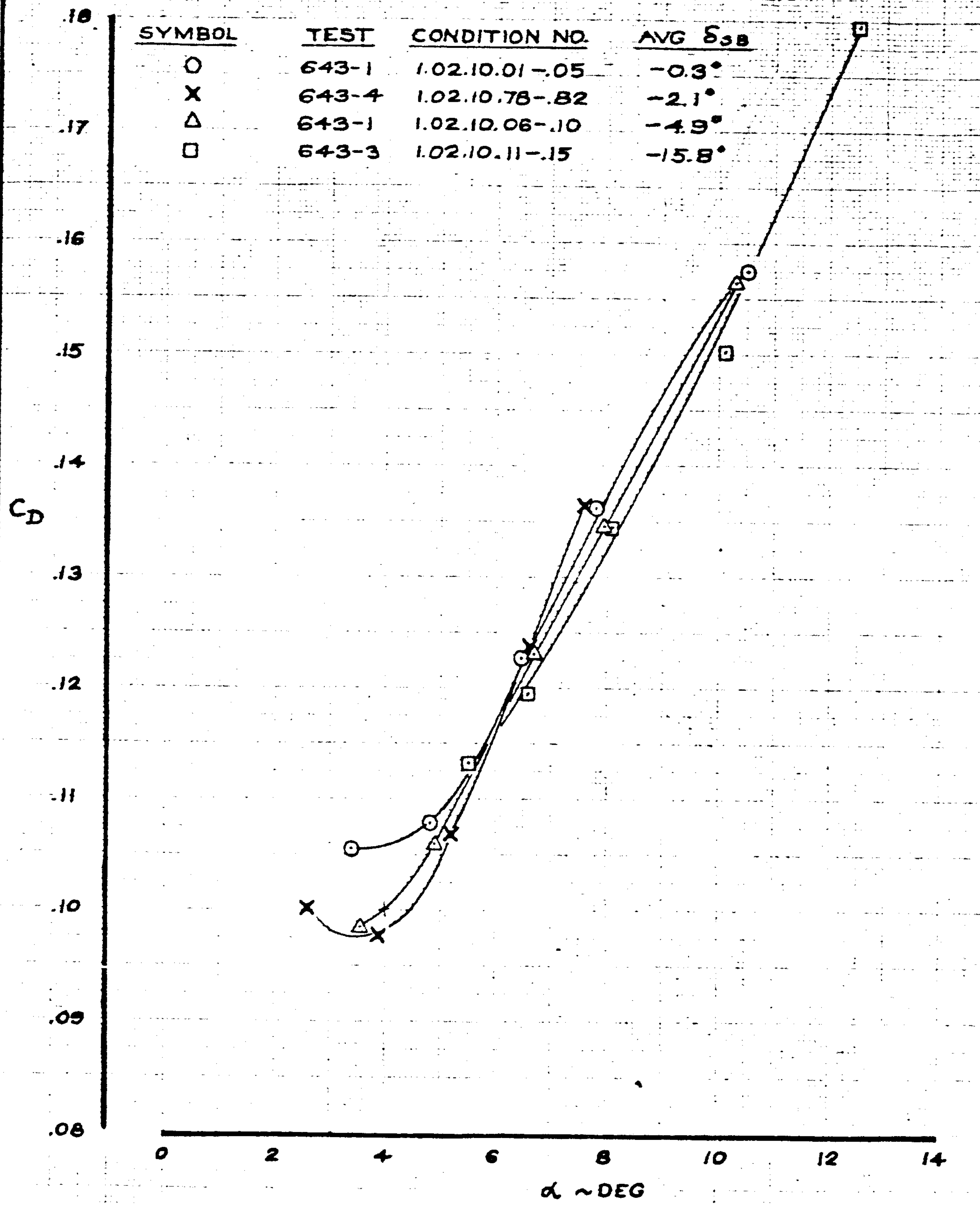

FIG. 115

CALC	STEMWELL	9-24-64	REVISED	DATE	C_D VS α	367-80B BLC
CHECK					FLAPS 30° BLOWING OFF	D6-10743
APR					THE BOEING COMPANY	PAGE 155
APR						

TD 461 C-R4

K+E ALBANENE® TRACING PAPER

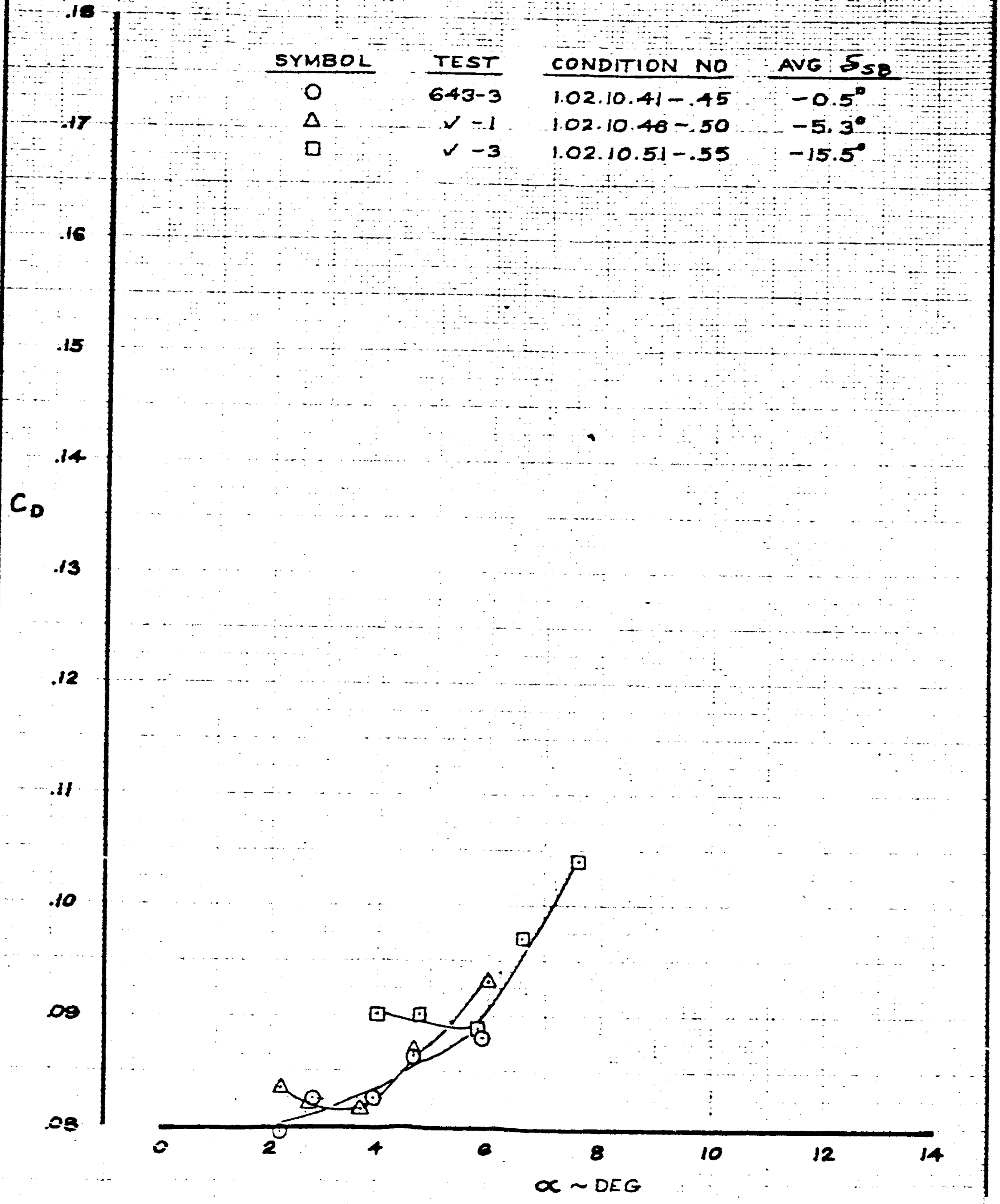

FIG. 116

CALC	STEMWELL	9-24-64	REVISED	DATE		367-80 BLC
CHECK					C_D VS α	
APR					FLAPS 20° BLOWING OFF	D6-1074
APR					THE BOEING COMPANY	PAGE 1

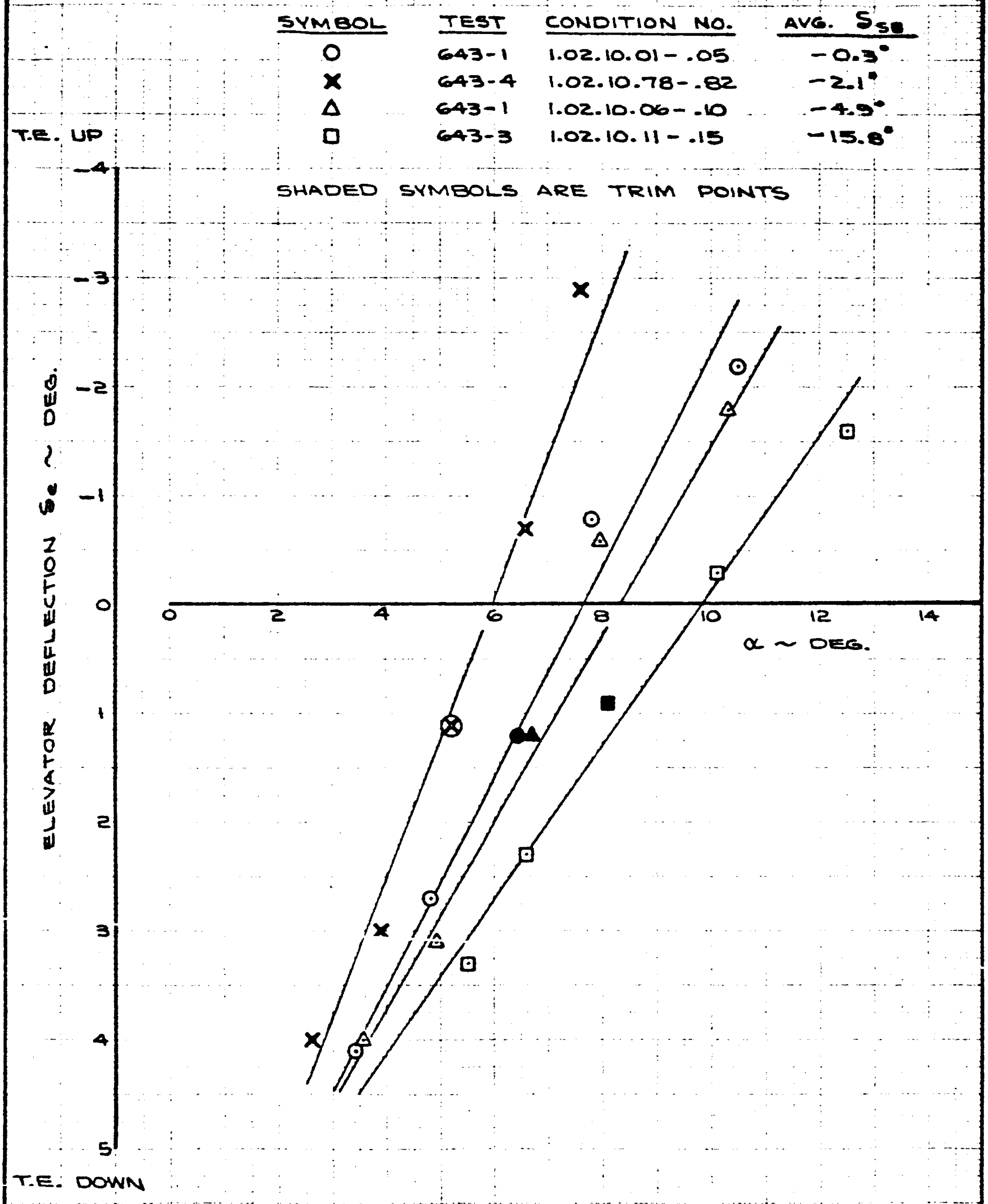

FIG. 117

CALC	TAYLOR	9-23-4	REVISED	DATE	δ_e VS α FLAPS 30° BLOWING OFF	367-80B BLC
CHECK						D6-10743
APR					THE BOEING COMPANY	PAGE 157
APR						

TD 461 C-R4

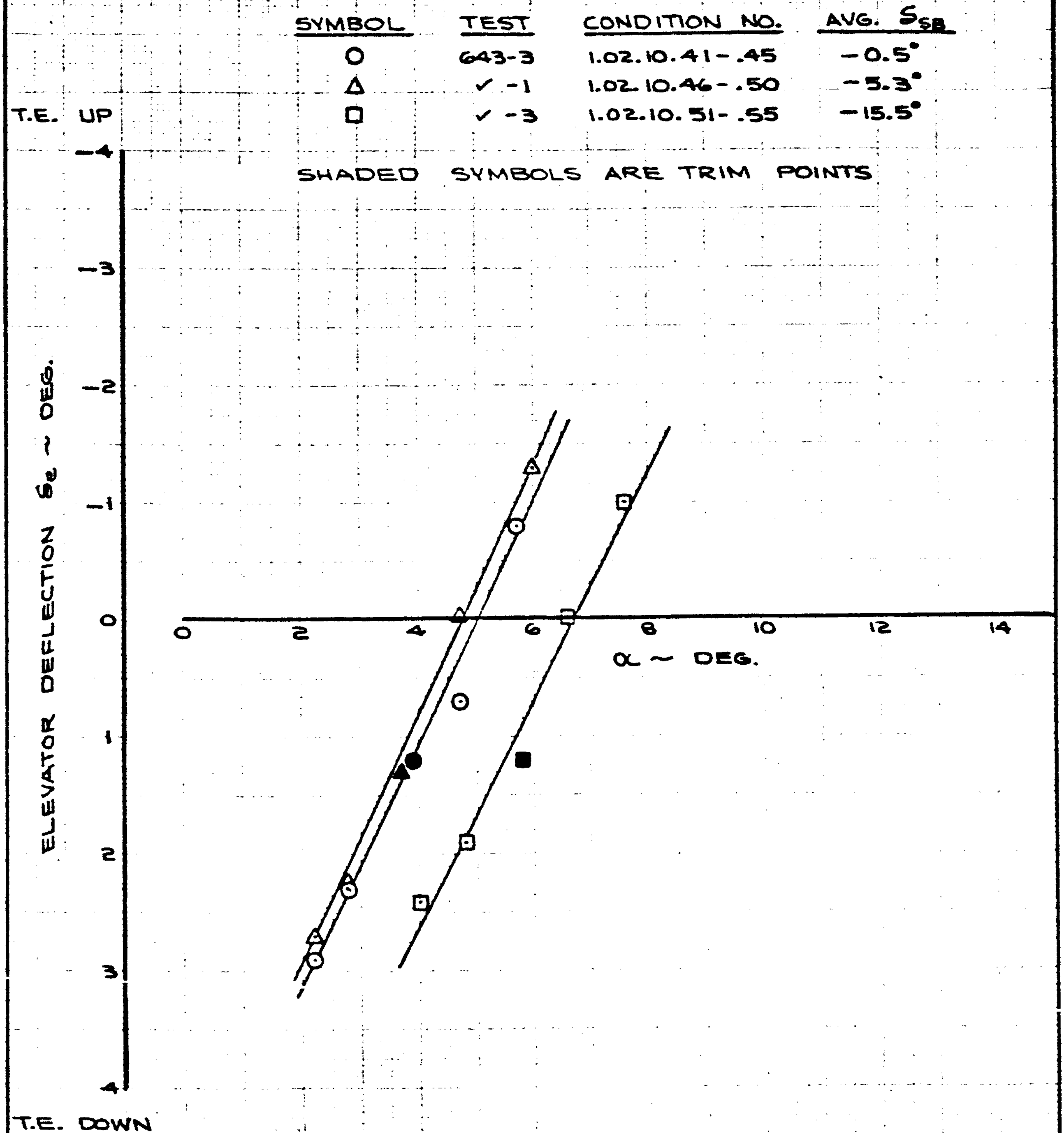

FIG. 118

CALC	TAYLOR	9.23.4	REVISED	DATE	δ_e VS α FLAPS 20° BLOWING OFF	367-80B BLC
CHECK						D6-10743
APR					THE BOEING COMPANY	PAGE 158
APR						

TD 461 C-R4

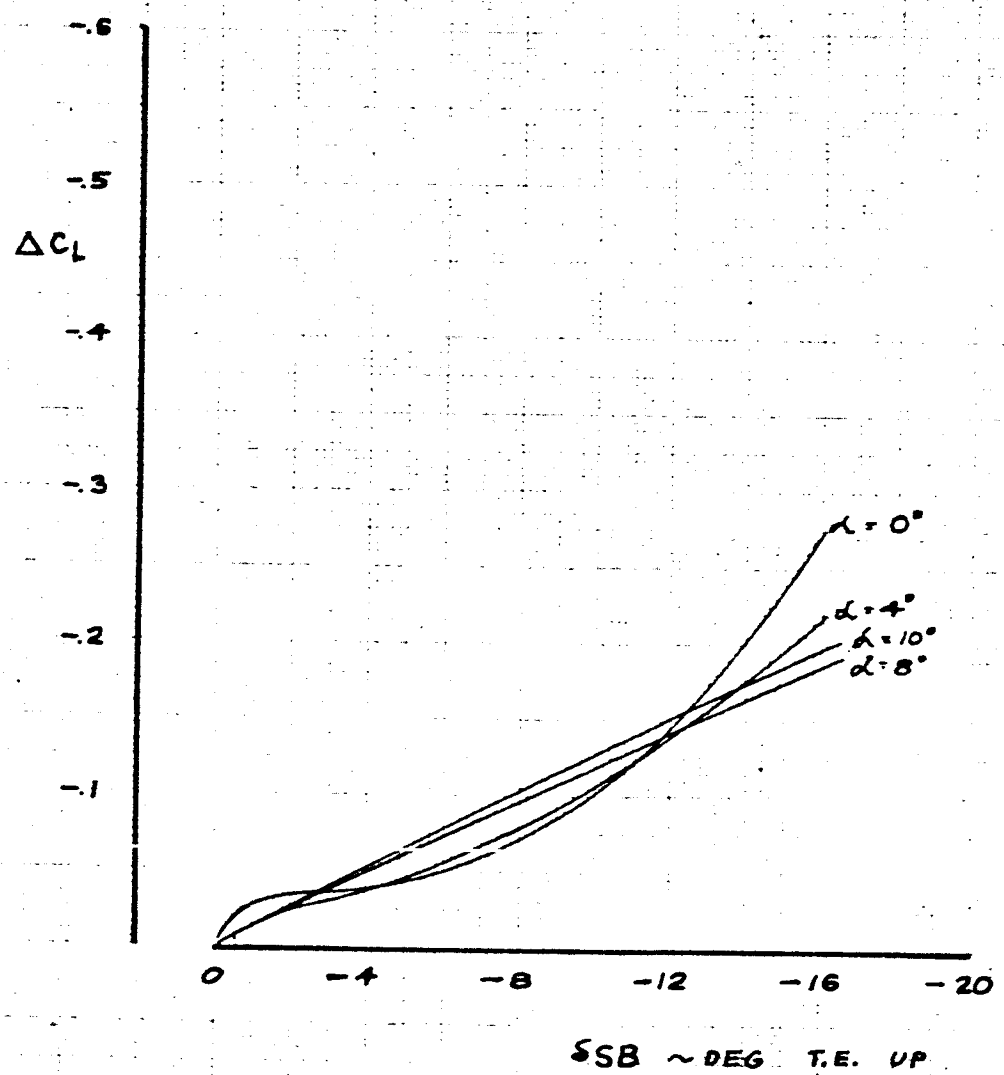

FIG. 119

CALC	STEMWELL	9-25-64	REVISED	DATE		367-80B BLC
CHECK					ΔCL VS δSB	
APR					FLAPS 30° BLOWING OFF	D6-10743
APR					THE BOEING COMPANY	PAGE 159

TD 461 C-R4

K·E ALBANENE® TRACING PAPER

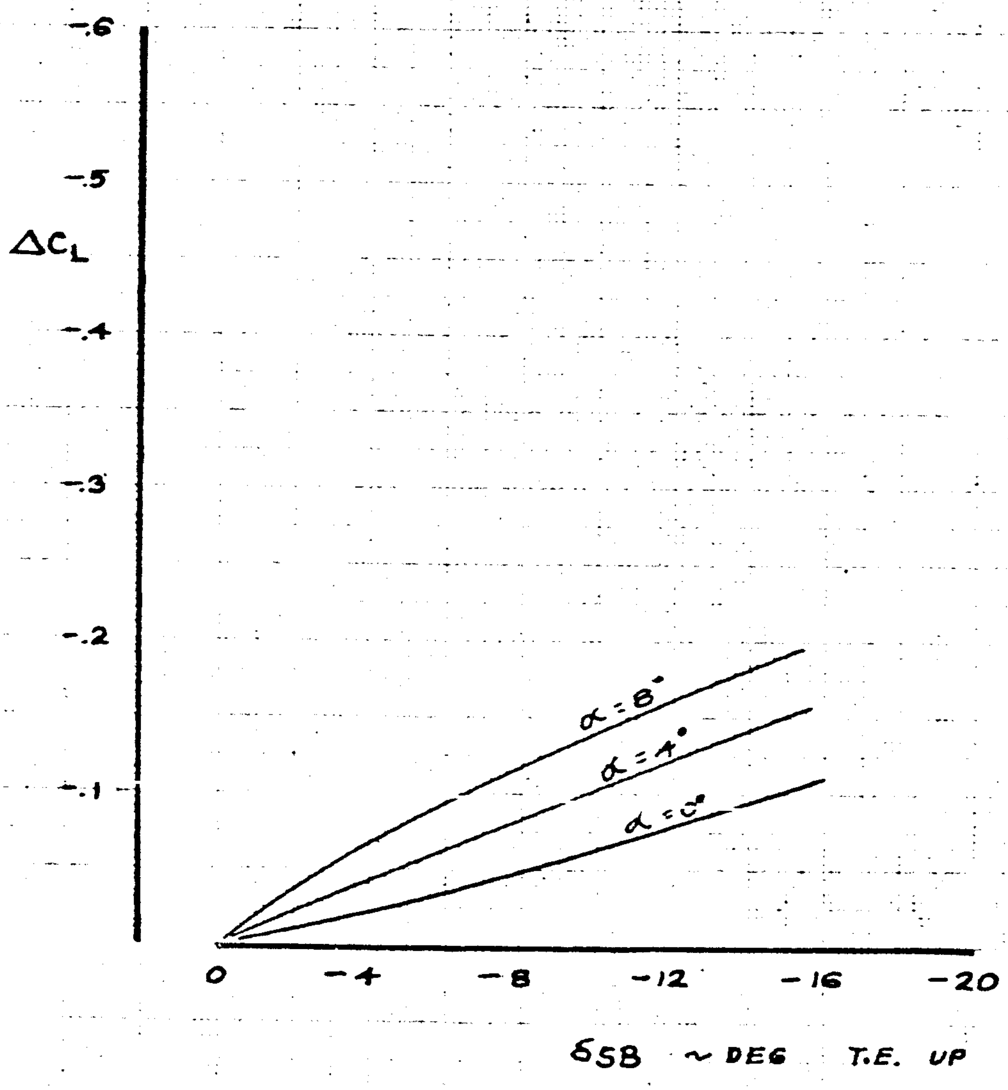

FIG. 120

CALC	STEMWELL	9-25-64	REVISED	DATE	ΔC_L VS δ_{SB}	367-80B BLC
CHECK					FLAPS 20° BLOWING OFF	D6-10743
APR					THE BOEING COMPANY	PAGE 160
APR						

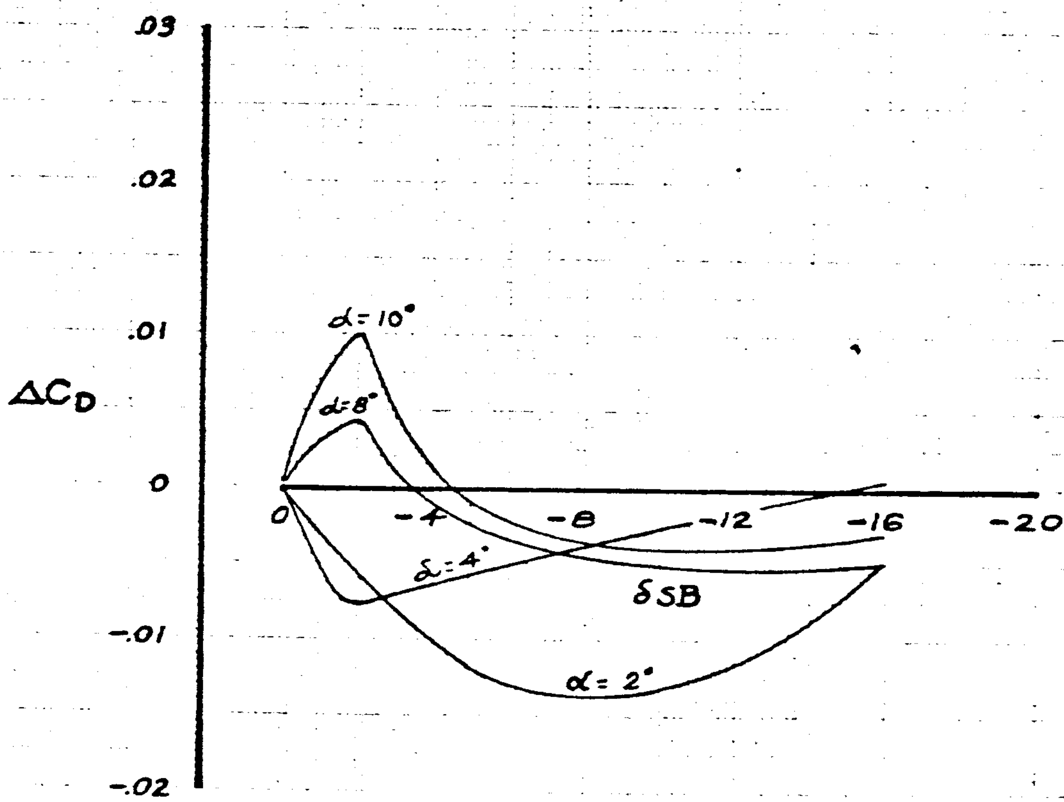

FIG. 121

CALC	STEMWELL	9-25-64	REVISED	DATE	ΔC_D VS δ_{SB} FLAPS 30° BLOWING OFF	367-80B BLC
CHECK						D6-10743
APR					THE BOEING COMPANY	PAGE 161
APR						

TD 461 C-R4

K+E ALBANENE® TRACING PAPER

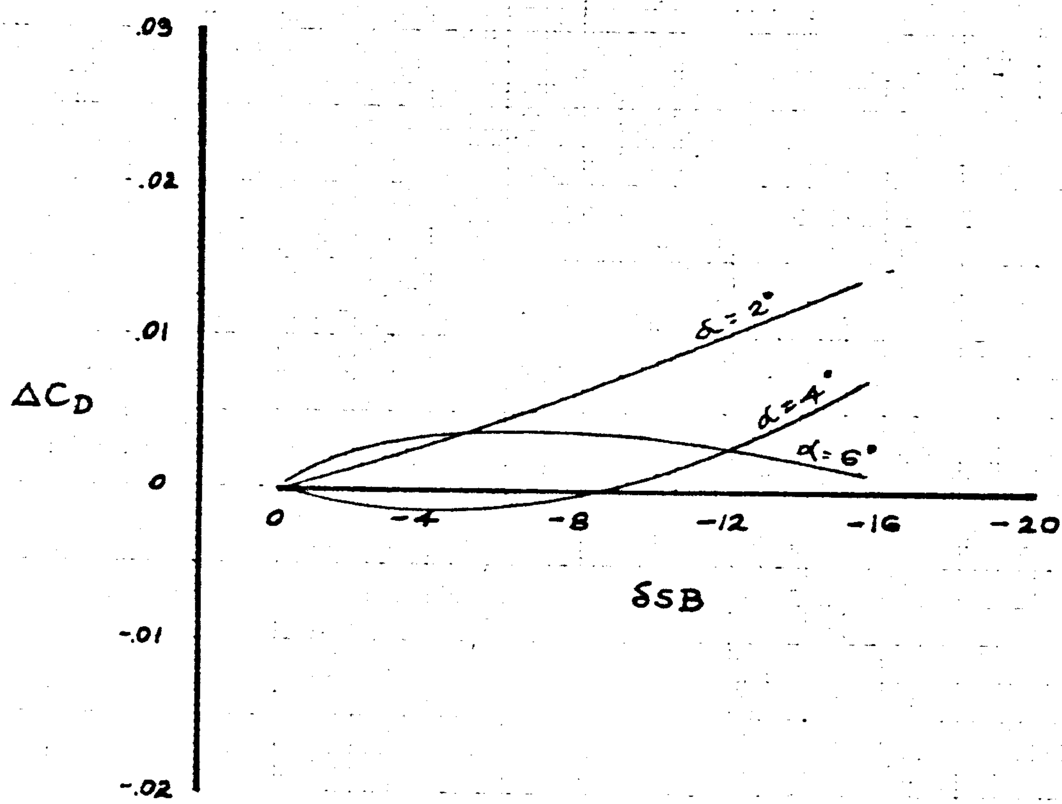

FIG. 122

CALC	STEMWELL	9-25-64	REVISED	DATE		367-80B BLC
CHECK					ΔC_D VS δ_{SB}	
APR					FLAPS 20° BLOWING OFF	D6-10743
APR					THE BOEING COMPANY	PAGE 162

TD 461 C-R4

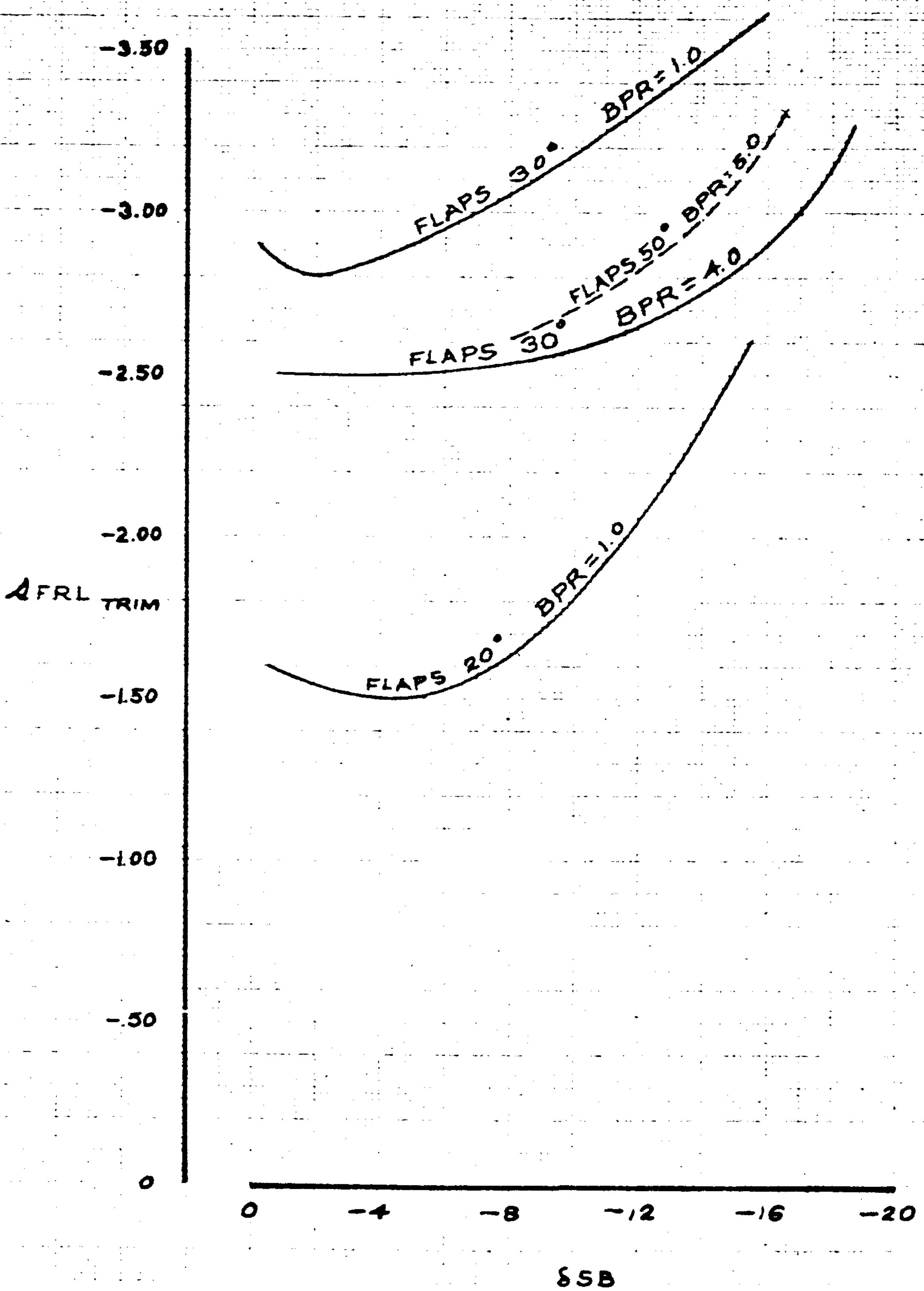

FIG. 123

CALC	STEMWELL	5-25-64	REVISED	DATE	$\alpha_{FRL\ TRIM}$ VS δ_{SB}	367-80B BLC
CHECK						D6-10743
APR					THE BOEING COMPANY	PAGE 163
APR						

TD 461 C-R4

K+E ALBANENE® TRACING PAPER

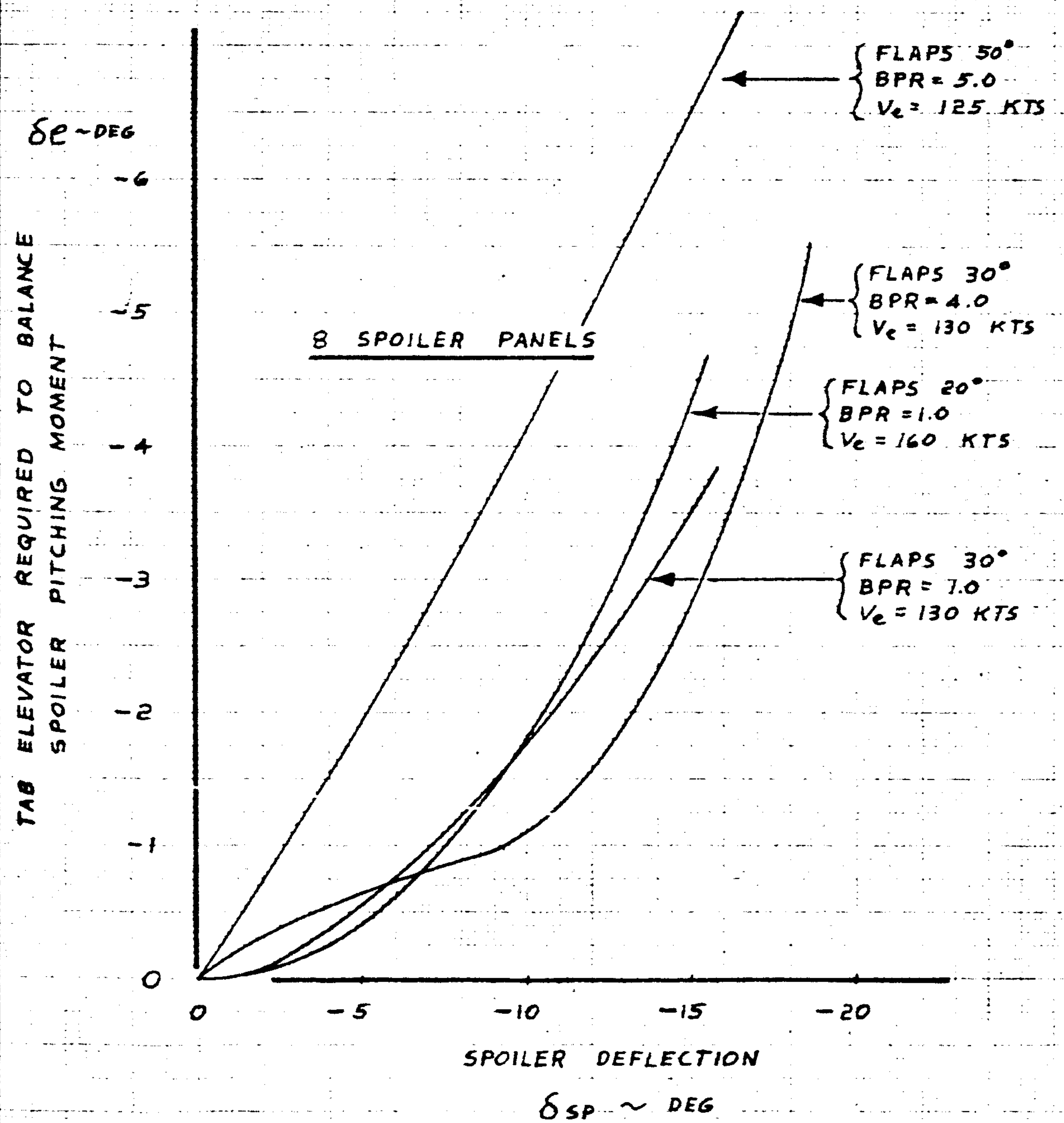

FIG. 124

CALC	W. M. E	9-30-64	REVISED	DATE	SPOILER PITCHING MOMENT	367-80 BLC
CHECK						D6-10743
APR					THE BOEING COMPANY	PAGE 164
APR						

TD 461 C-R4

K+E ALBANENE TRACING PAPER

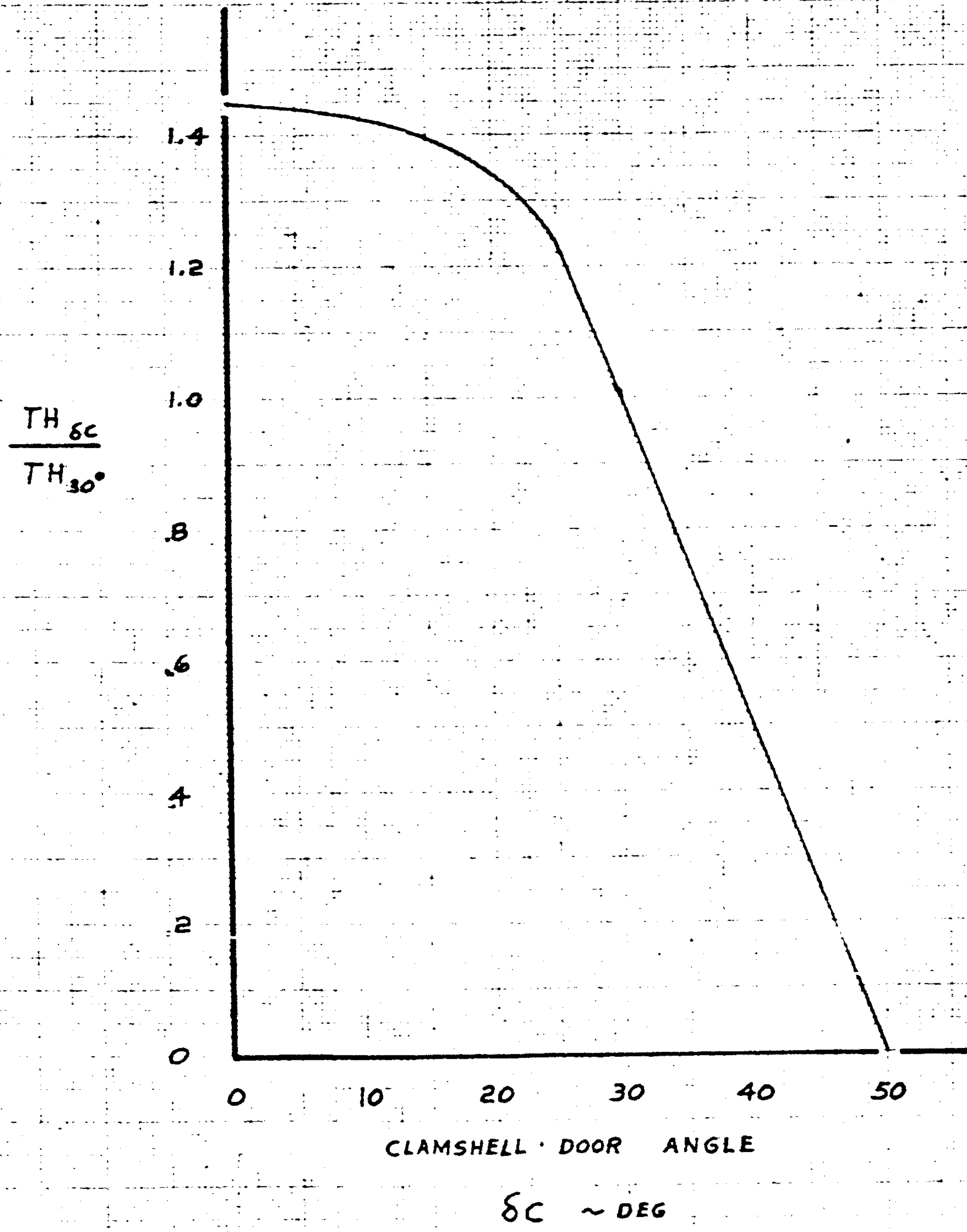

FIG. 125

CALC	W. M. E	3-30-65	REVISED	DATE	NORMALIZED THRUST	367-80 BLC
CHECK						D6-10743
APR						
APR					THE BOEING COMPANY	PAGE 165

SYM	BPR	δ_F DEG.	V_e KTS.	H_p FT.	W LB.	C.G. %$\bar{c}$
○	1	30	133.4	7300	146,800	30.4
□	1	20	164.1	7500	143,200	30.0
△	4	30	133.2	2600	151,600	29.5

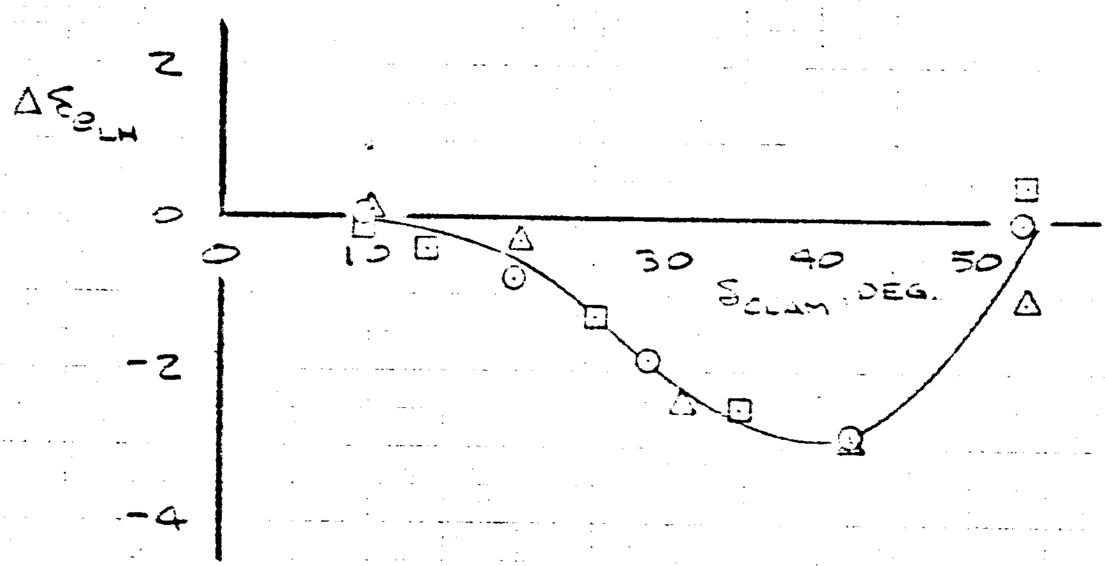

FIG. 126

CALC	D. C LEISY	10/7/4	REVISED	DATE
CHECK				
APR				
APR				

ELEVATOR BIAS REQUIRED TO BALANCE REVERSER MODULATION

THE BOEING COMPANY

367-80B BLC

FIG. 5

TD 461 C-R4

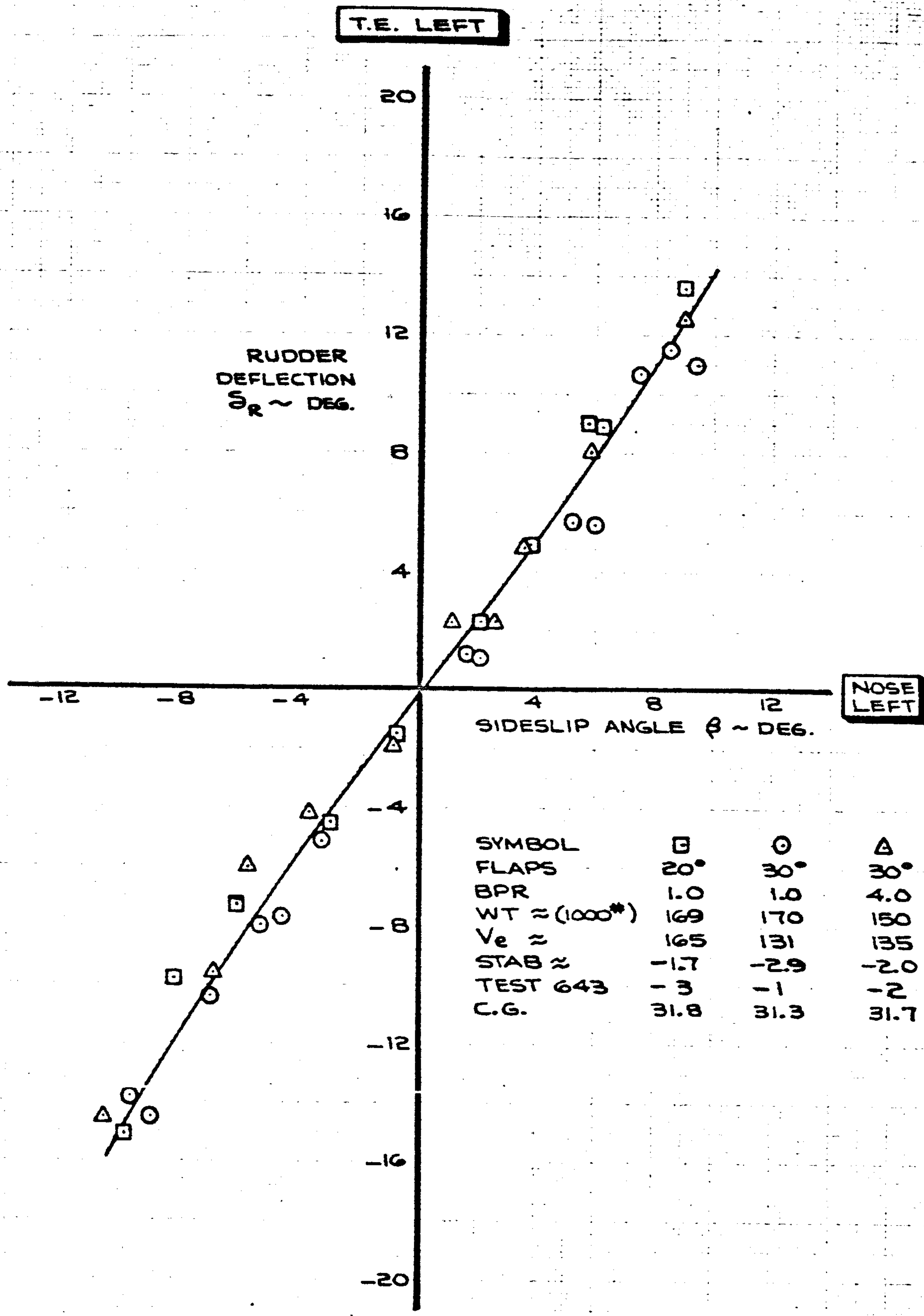

SYMBOL	⊡	⊙	△
FLAPS	20°	30°	30°
BPR	1.0	1.0	4.0
WT ≈ (1000#)	169	170	150
V_e ≈	165	131	135
STAB ≈	-1.7	-2.9	-2.0
TEST 643	- 3	-1	-2
C.G.	31.8	31.3	31.7

FIG. 127

CALC	TAYLOR	10-8-4	REVISED	DATE	RUDDER DEFLECTION VS SIDESLIP SPEED BRAKES = 0°	367-80B BLC
CHECK						D6-10743
APR					THE BOEING COMPANY	PAGE 167
APR						

TD 461 C-R4

K+E ALBANENE®

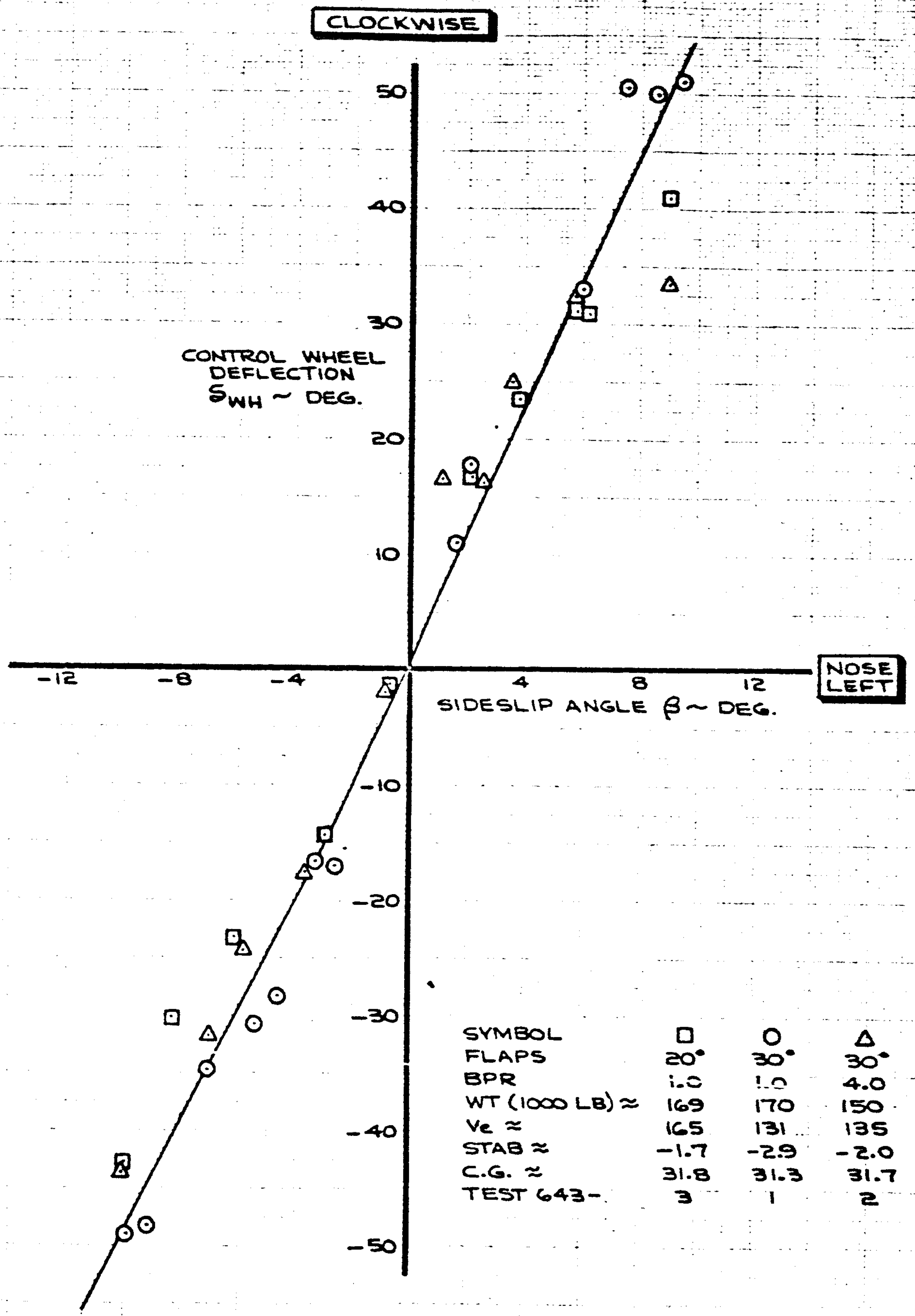

FIG. 128

CALC	TAYLOR	10-8-4	REVISED	DATE	δ_{WH} VS β SPEED BRAKES = 0°	367-80B BLC
CHECK						D6-10743
APR					THE BOEING COMPANY	PAGE 168
APR						

TD 461 C-R4

K+E ALBANENE TRACING PAPER

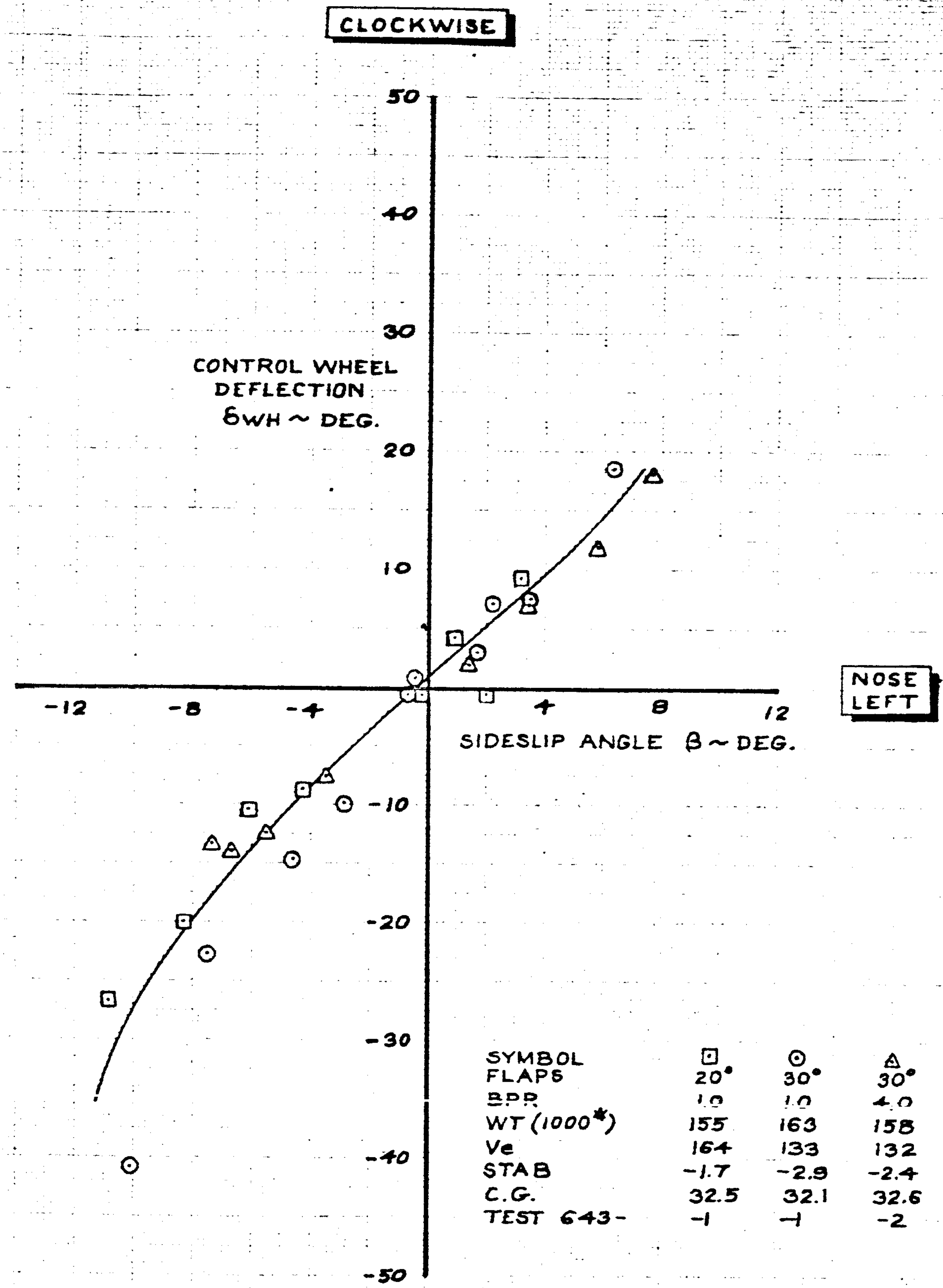

FIG. 129

CALC	STEMWELL	10-9-4	REVISED	DATE	δ_{WH} vs β SPEED BRAKES = 10°	367-80B BLC
CHECK						D6-10743
APR					THE BOEING COMPANY	PAGE
APR						169

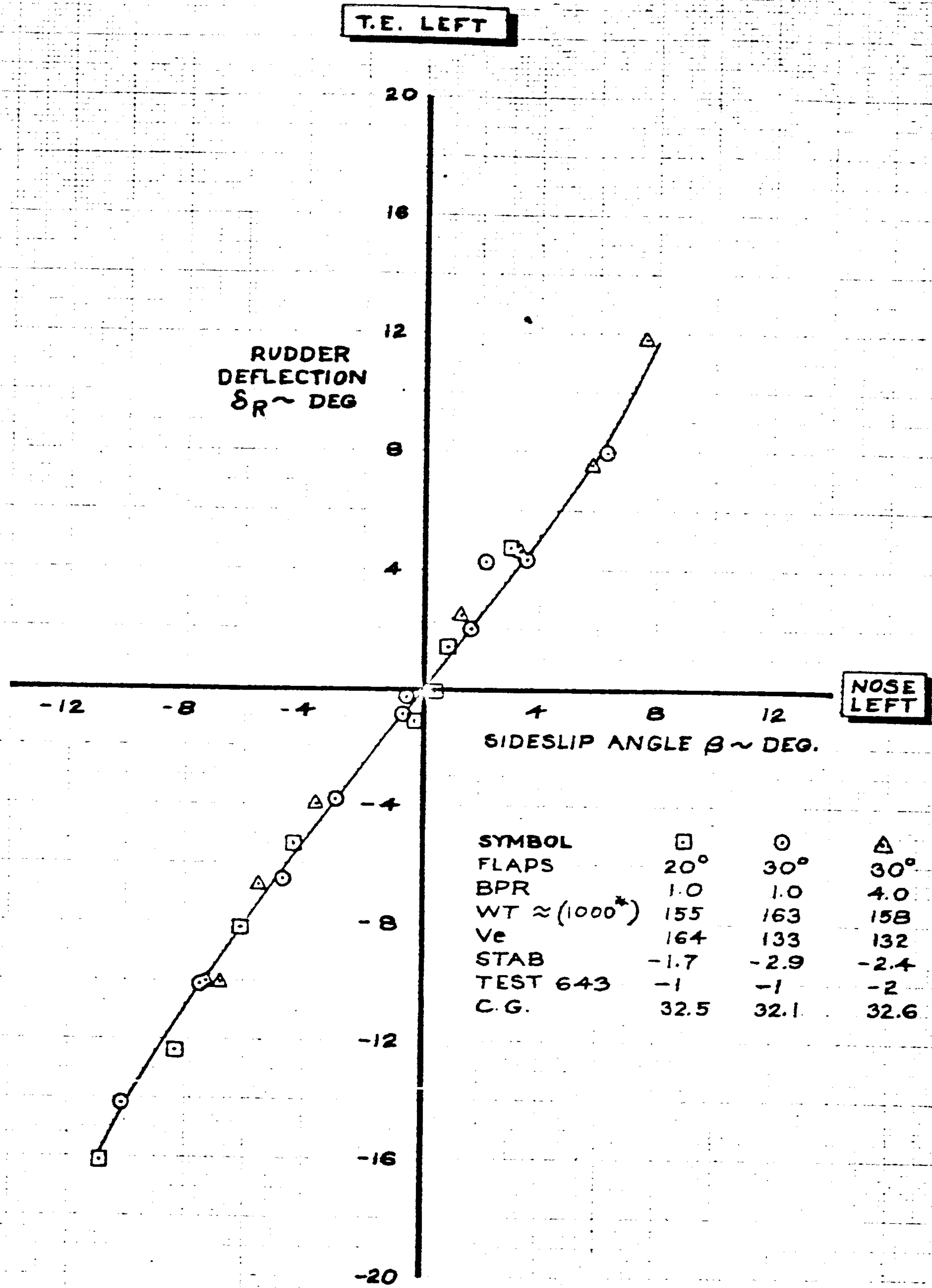

FIG. 130

CALC	STEMWELL	10-9-4	REVISED	DATE	367-80B BLC
CHECK					RUDDER DEFLECTION VS SIDESLIP
APR					SPEED BRAKES = 10°
APR					D6-10743
					THE BOEING COMPANY
					PAGE 170

TD 461 C-R4

K+E ALBANENE®

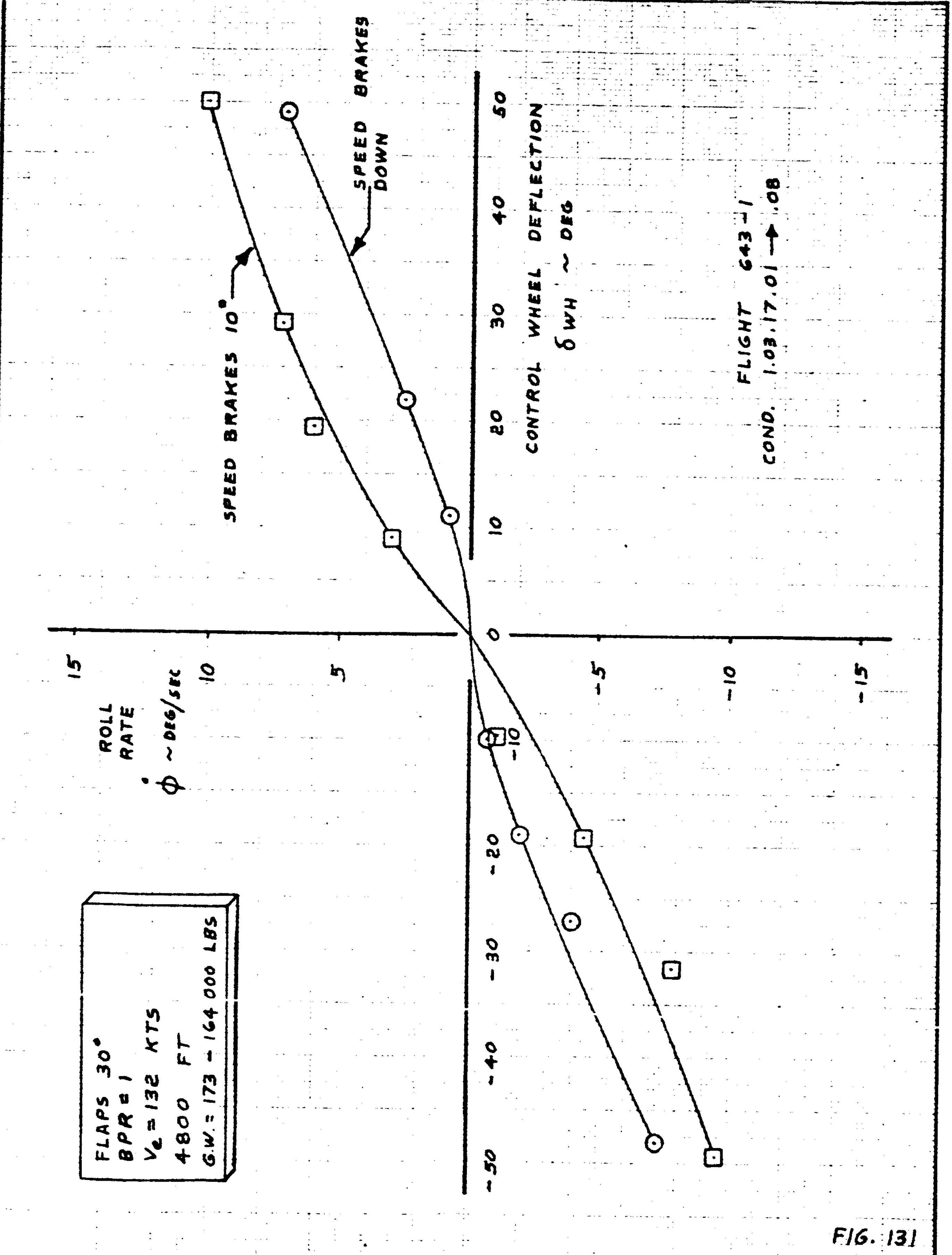

FIG. 131

CALC	W. M. E.	9-21-64	REVISED	DATE
CHECK				
APR				
APR				

LATERAL CONTROL RESPONSE
SST CONFIG. # 1

THE BOEING COMPANY

367-80 BLC

D6-10743

TD 461 C-R4

K+E ALBANENE® TRACING PAPER

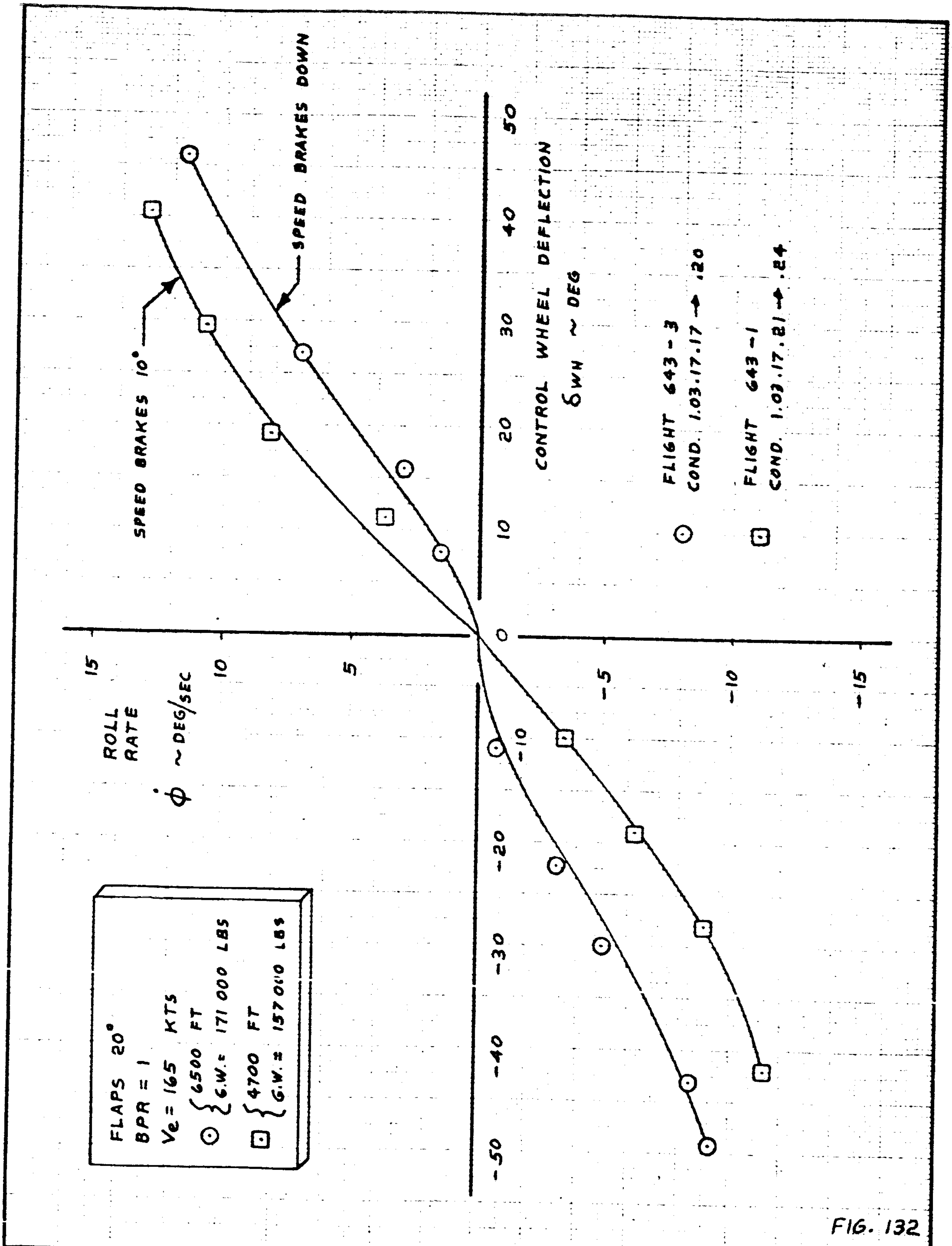

FIG. 132

CALC	W.M.E	9-22-64	REVISED	DATE
CHECK				
APR				
APR				

LATERAL CONTROL RESPONSE
SST CONFIG. # 3

THE BOEING COMPANY

367-80 BLC

D6-10743

TD 461 C-R4

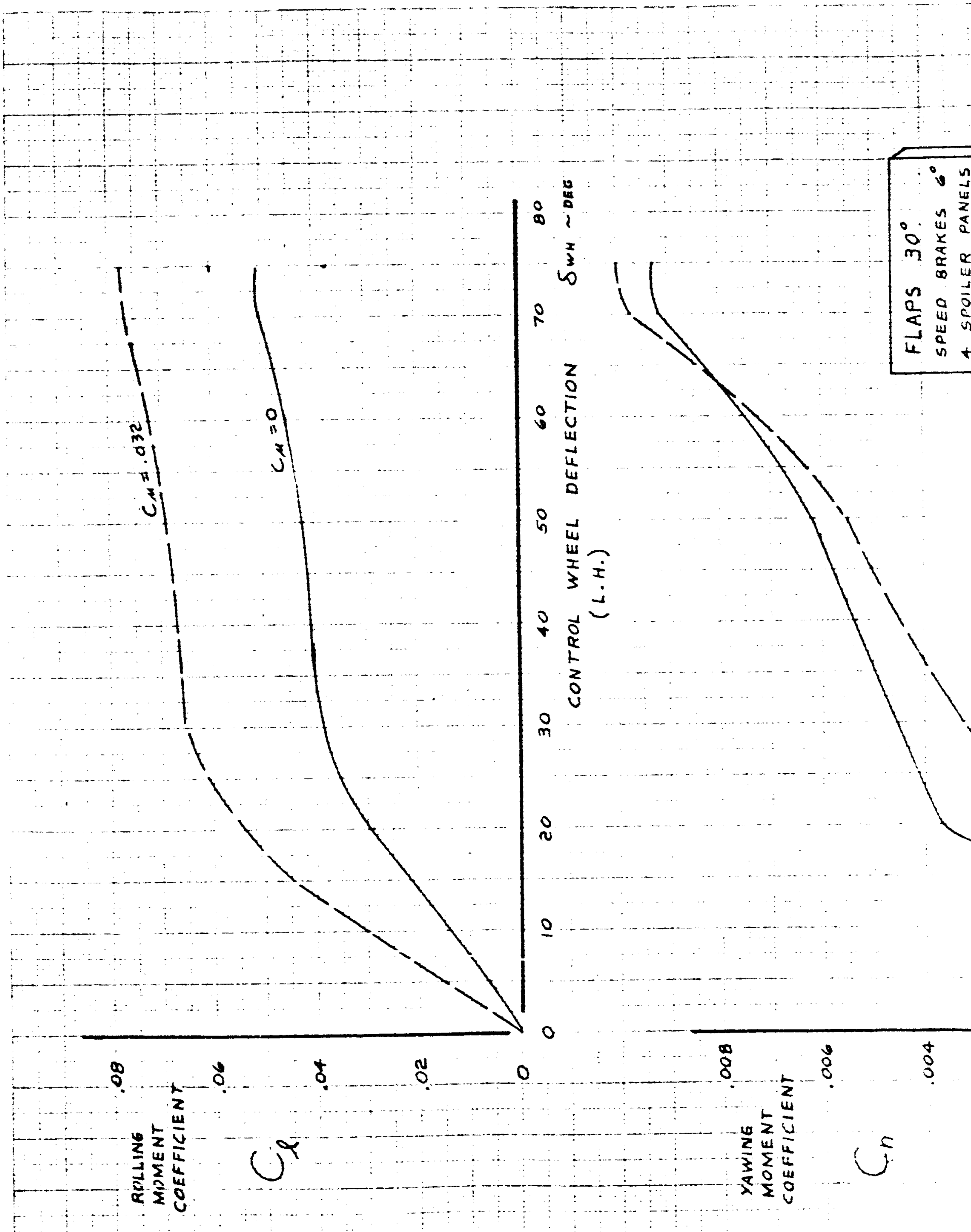

CALC	W. M. E	3-24-65	REVISED	DATE	LATERAL CONTROL SST SIMULATION	367-80 BLC
CHECK						
APPD.						
APPD.					THE BOEING COMPANY	PAGE

TD 1053-R5

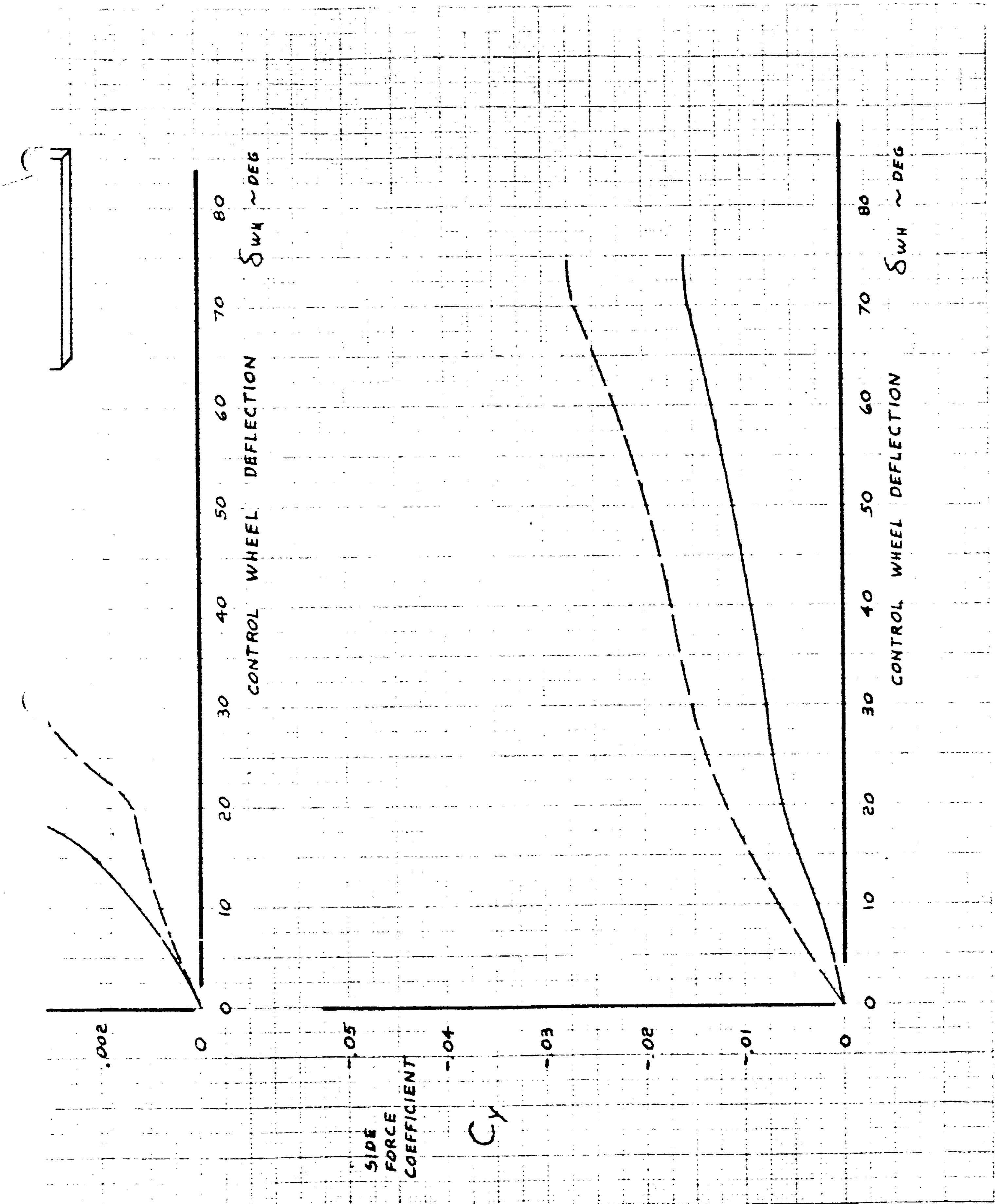
CONTROL WHEEL DEFLECTION δ_{WH} ~ DEG
0
10
20
30
40
50
60
70
80
SIDE FORCE COEFFICIENT
C_Y
0
-.01
-.02
-.03
-.04
-.05
.002

FIG. 133

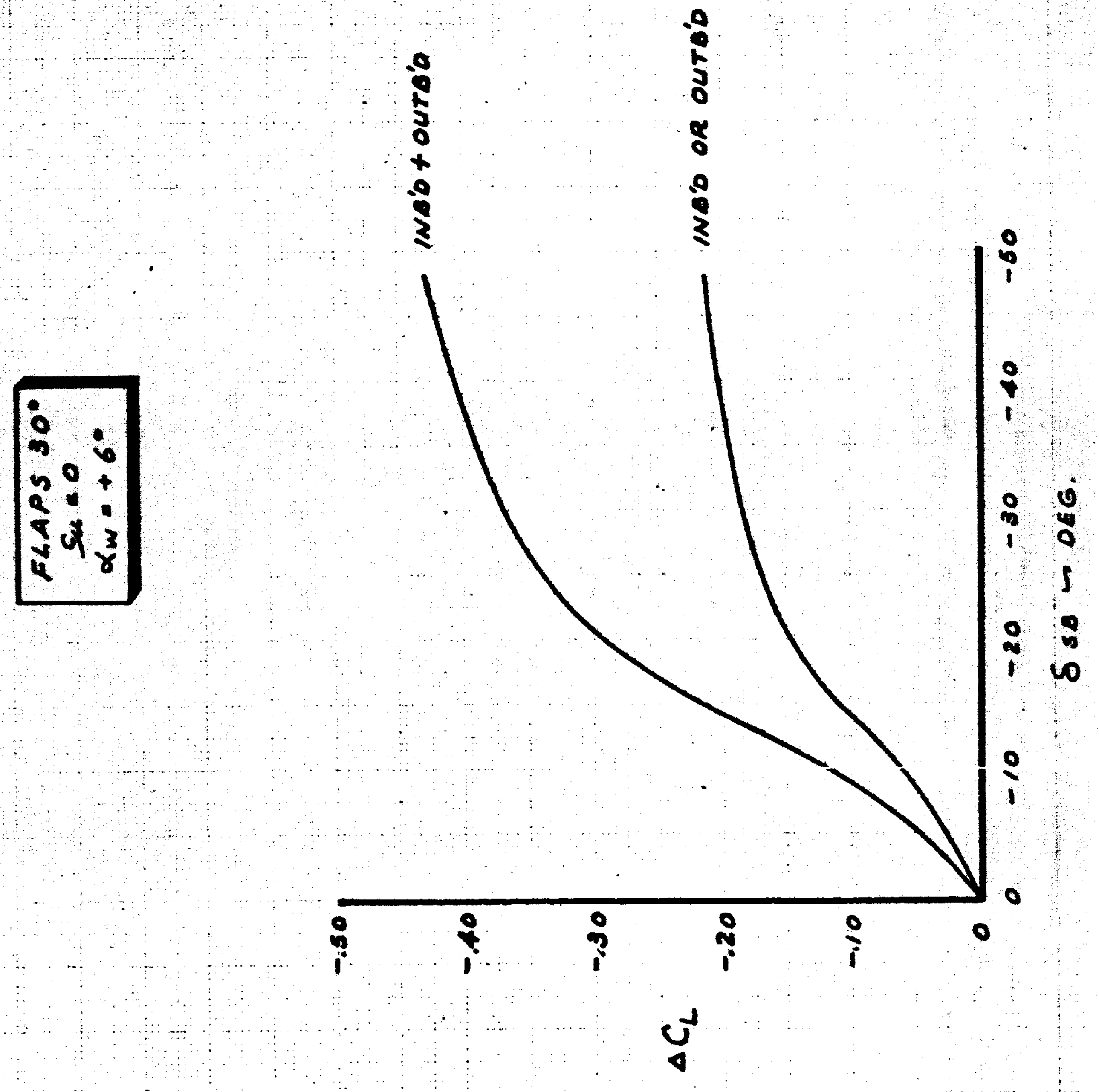

CALC	HUANG	3-1965	REVISED	DATE	SPEED BRAKE CHARACTERISTICS	367-80
CHECK						D6-10743
APR						
APR					174 THE BOEING COMPANY	PAGE 174

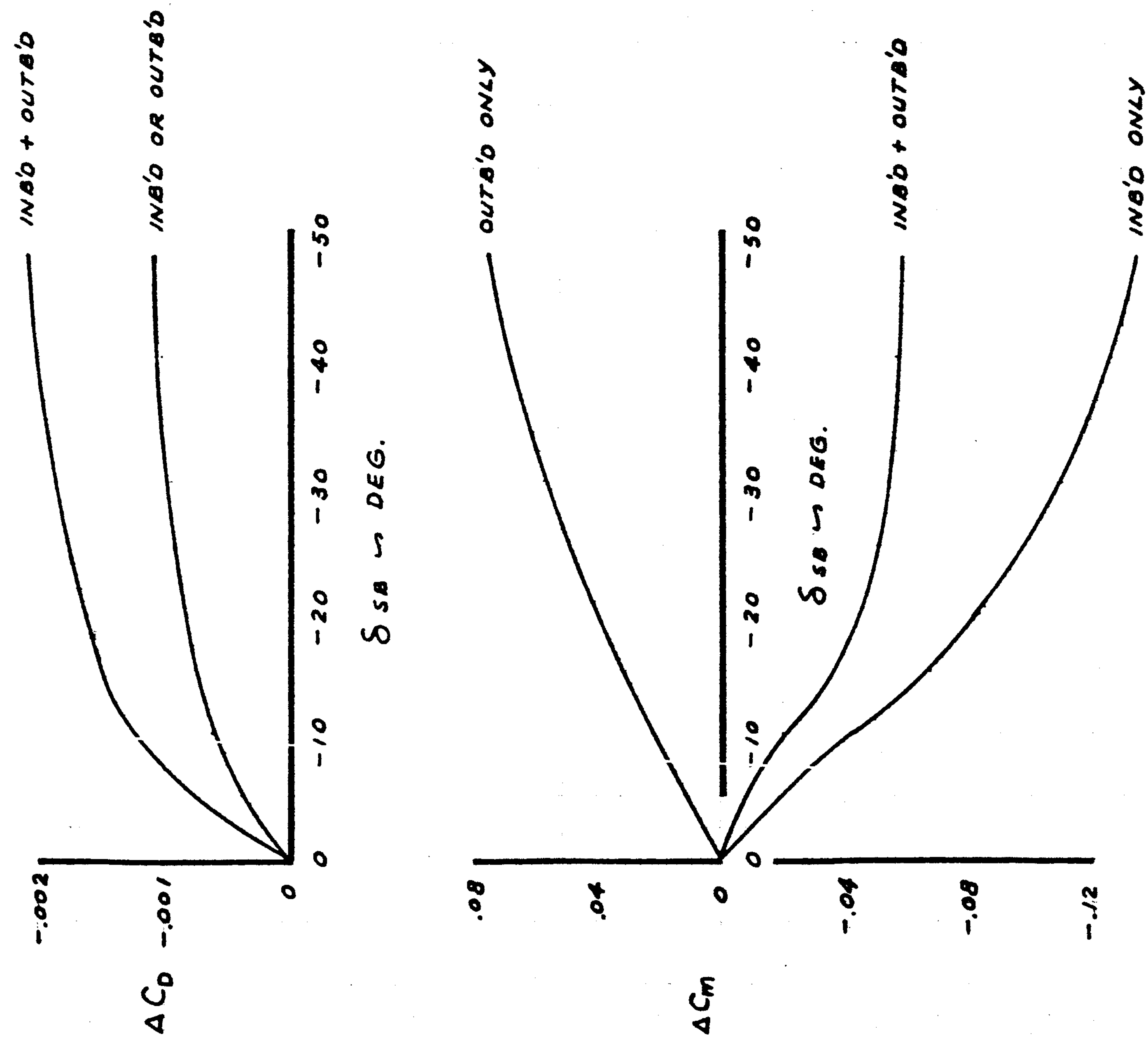
INB'D + OUTB'D
INB'D OR OUTB'D
OUTB'D ONLY
INB'D + OUTB'D
INB'D ONLY
-50
-40
-30
-20
-10
0
δ SB ~ DEG.
δ SB ~ DEG.
ΔC_D
-.002
-.001
0
ΔCm
.08
.04
0
-.04
-.08
-.12

FIG. 134

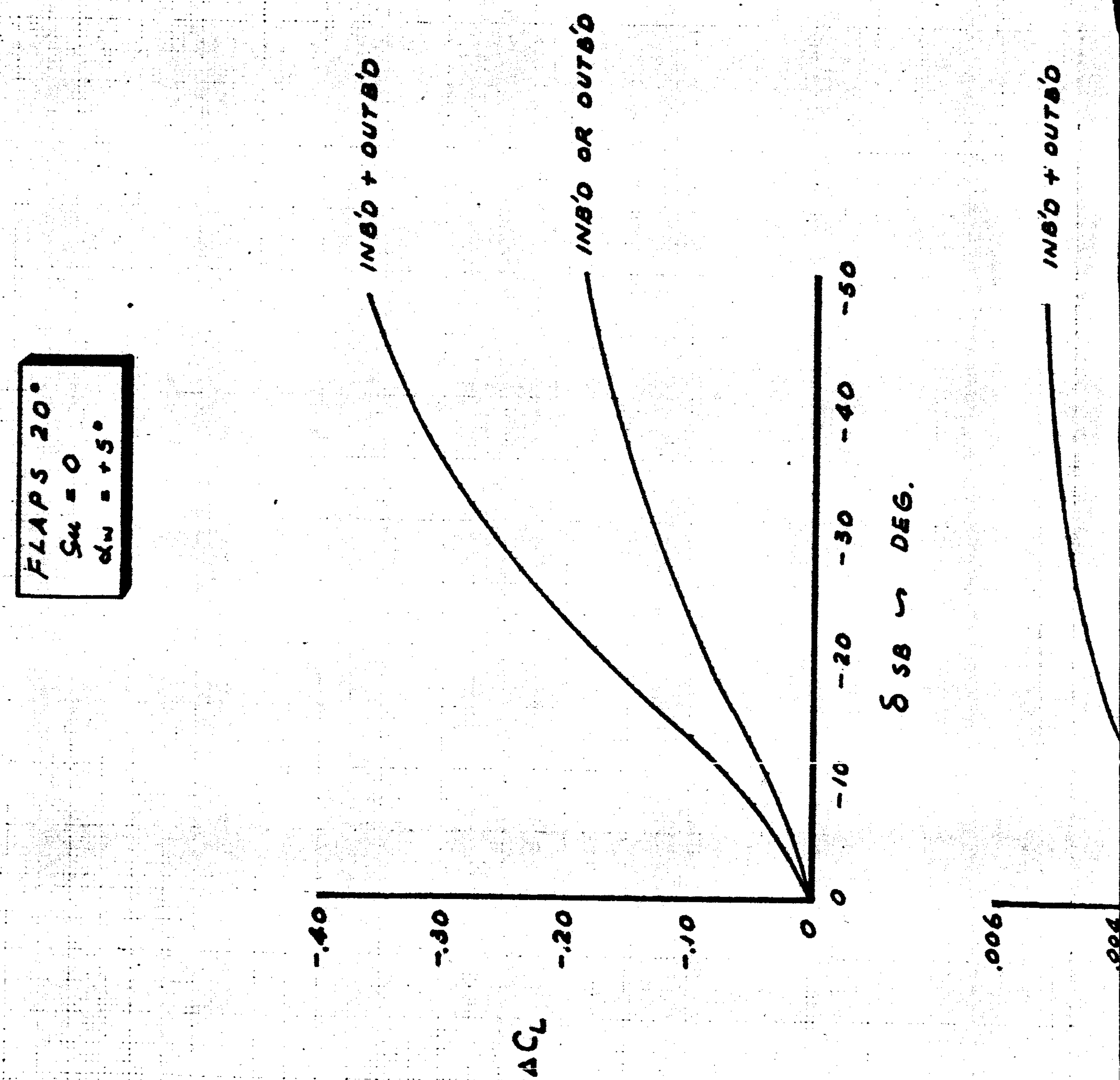

CALC	HUANG	3-22-65	REVISED	DATE	SPEED BRAKE CHARACTERISTICS	367-80
CHECK						D6-10743
APR					THE BOEING COMPANY	PAGE 175
APR						

175-1

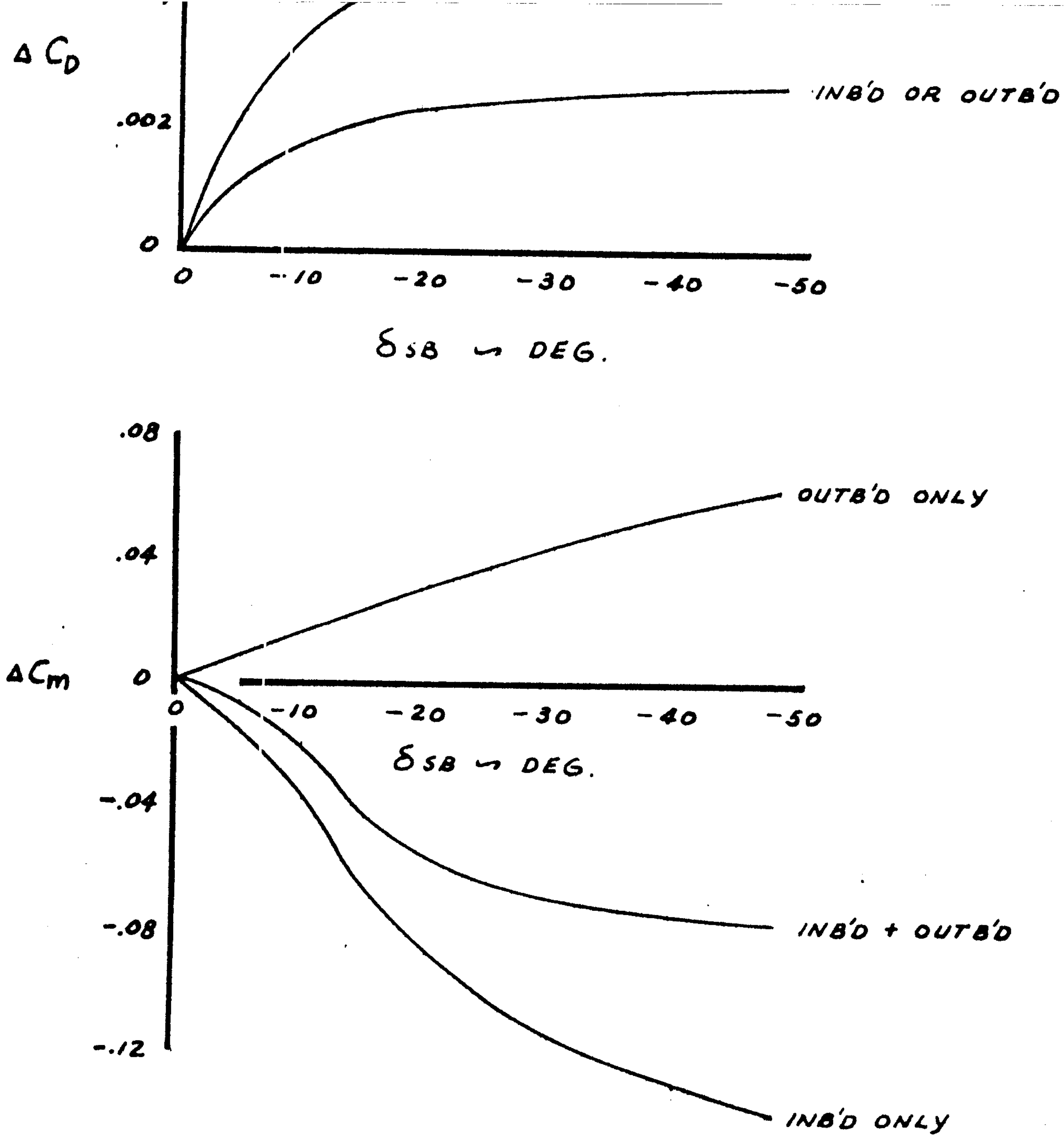

ΔCD
.002
0
0
-10
-20
-30
-40
-50
δSB ~ DEG.
INB'D OR OUTB'D
ΔCm
.08
.04
0
-.04
-.08
-.12
0
-10
-20
-30
-40
-50
δSB ~ DEG.
OUTB'D ONLY
INB'D + OUTB'D
INB'D ONLY

FIG. 135

LONGITUDINAL CHARACTERISTICS

367-80

Flight Condition	NASA-20 NASA-▲ SIMULATION	NASA-72 SIMULATION	
Ve	135	150	Kts
Flap Angle	30°	20°	
Weight	150,000	150,000	lbs
C. G. Location	30	30	$\%\bar{c}$
Speed Brake Trim Angle	-6°	-6°	
Lift Derivatives			
$C_{L_{TRIM}}$	.856	.6935	
C_{L_α}	4.9	4.55	/rad
$\alpha_{trim_{wcp}}$	5.45°	5.3°	
Drag Derivatives			
$C_{D\,trim}$	.1165	.0892	
C_{D_α}	.515	.327	/rad
Pitching Moment Derivatives			
$C_{\bar{m}_\alpha}$	-1.008	-1.11	/rad
$C_{m_{\dot{\alpha}}}$	-.261	-.361	/rad/sec
$C_{m_{\dot{\theta}}}$	-.594	-.425	/rad/sec
$C_{m_{\delta E}}$	-.85	-.9	/rad
Iy	2.25×10^6	2.25×10^6	Slug-Ft^2
$C_{m_{\delta V}}$	0	-.0003	/ft/sec

TD 1546 L-R3

6-7000

	NASA-20 NASA-Δ Simulation	NASA-72 Simulation	
Speed Brakes			
$C_{L_{\delta SB}}$	+.688	+.446	/rad
$C_{D_{\delta SB}}$	+.00573	-.0178	/rad
$Cm_{\delta SB}$	+.117	+.146	/rad
Airplane Dimensions			
Wing area	2821 Ft^2		
Wing Span	130.8 Ft		
MAC	20.1 Ft		
Longitudinal Dynamic Characteristics			
Short Period			
Undamped natural frequency	1.53	1.68	rad/sec
Damped natural frequency	1.09	1.38	rad/sec
Damping Ratio	.702	.698	
Undamped natural frequency	.134	.138	rad/sec
Damped natural frequency	.129	.137	rad/sec
Damping Ratio	.282	.096	

TD 1546 L-83

6-7000

367-80 Lateral-Directional Characteristics

Flight Condition	NASA-20 NASA-Δ Simulation	NASA-72 Simulation	
Ve	135	150	KTS
Flap Angle	30°	20°	
Weight	150,000	150,000	lbs
C. G. Location	30	30	%
Speed Brake Trim Angle	6°	6°	

Side Force Derivatives

Cy_{β}	-.931	-.825	/rad
$Cy_{\dot{\phi}}$	.1492	.0864	/rad/sec
$Cy_{\dot{\psi}}$	.0865	.0764	/rad/sec
$Cy_{\delta R}$	.1712	.0177	/rad
$Cy_{\delta A}$	0	0	
$Cy_{\delta SP}$	-.039	-.039	/rad
$Cy_{\delta WH}$	-.0128	-.0128	/rad

Rolling Moment Derivatives

$C_{\ell_{\beta}}$	-.1572	-.143	/rad
$C_{\ell_{\dot{\phi}}}$	-.1569	-.136	/rad/sec
$C_{\ell_{\dot{\psi}}}$	.0817	.0320	/rad/sec
$C_{\ell_{\delta R}}$	.0179	.0202	/rad
$C_{\ell_{\delta A}}$	.0809		/rad
$C_{\ell_{\delta SP}}$	.0468		/rad
$C_{\ell_{\delta WH}}$	.0653	.077	/rad
I_{x_B}	2.57×10^6	2.57×10^6	Slug-Ft²
$C_{\ell_{\dot{\beta}}}$	D	.0778	/rad/sec

	NASA-20 NASA-Δ Simulation	NASA-72 Simulation	
Yawing Moment Derivatives			
Cn_{β}	.0797	.1167	/rad
$Cn_{\dot{\beta}}$	-.043	-.027	/rad/sec
$Cn_{\dot{\phi}}$	-.0225	-.0166	/rad/sec
$Cn_{\dot{\psi}}$	-.0467	-.01[illegible]9	/rad/sec
$Cn_{\delta R}$	-.0725	-.068	/rad
$Cn_{\delta A}$	.0023		/rad
$Cn_{\delta SP}$	.0245		/rad
$Cn_{\delta WH}$	.0082	.0156	/rad
I_{zB}	4.73×10^6	4.73×10^6	Slug-Ft^2
J_{xz_b}	$.160 \times 10^6$	$.160 \times 10^6$	Slug-Ft^2
Lateral-Directional Dynamic Characteristics			
Spiral Divergence Time Constant	-188.8 (convergent)	127.	sec
Roll Convergence Time Constant	.665	.657	sec
Dutch Roll			
Undamped natural frequency	.799	.844	rad/sec
Damped natural frequency	.798	.843	rad/sec
Damping Ratio	.0419	.091	

TD 1546 L-R3

APPENDIX 2

SST Test Configurations

Theoretical Calculations

SST TEST CONFIGURATIONS

The theoretical SST stability derivatives and dynamic characteristics used in these tests are tabulated on pages 182 to 185 The supplemental longitudinal test configurations are summarized on page 186 and the lateral configurations on page 187.

The methods and equations used to calculate the theoretical SST longitudinal characteristics and the calculated values are shown on pages 188 to 197. The lateral-directional calculations are shown on pages 198 to 202.

SST LONGITUDINAL CHARACTERISTICS

Flight Condition	NASA-20	NASA-Δ	NASA-72	
Ve	135	135	182	KTS
Weight	280,000	280,000	270,000	
C.G. Location	46	35	36	% MAC
LIFT DERIVATIVES				
$C_{L_{trim}}$	.904	.565	.478	
$C_{L_{\alpha}}$	4.7	3.266	3.209	/rad
$C_{L_{\delta E}}$	.487	.3022	.487	/rad
α_{trim}	6.6°	12°	10.3°	
Drag Derivatives				
$C_{D_{trim}}$	.115	.125	.145	
$C_{D_{\alpha}}$	.418	1.203	.373	/rad
Pitching Moment Derivatives				
Cm_{α}	-.4584	-0.0802	-.3438	/rad
$Cm_{\dot{\alpha}}$	-.1335	0.	-.0288	/rad/sec
$Cm_{\dot{\theta}}$	-.2149	-.1757	-.1596	/rad/sec
$Cm_{\delta E}$	-.7163	-.287	-.7163	/rad
$Cm_{\delta th}$	.231X10-6	.045X10-6	.1225X10-6	/lb
Iy	$17.57X10^6$	$18.11X10^6$	$18.58X10^6$	slug-FT^2
Airplane Dimensions				
Wing Area	5000	8000	5000	FT^2
Wing Span	85	111	85	FT
MAC	70	89	70	FT

MODIFIED NASA 72 CONFIGURATION

(Corrected to Match Flight Data)

$C_{L_{\alpha}} = 2.78$ /rad

$C_{M_{\alpha}} = -.625$ /rad

$C_{L_{\delta v}} = -.000875$ /ft/sec

$C_{L_{\delta E}} = .585$ /rad

Short Period

Undamped Natural Frequency	1.232	rad/sec
Damped Natural Frequency	1.124	rad/sec
Damping Ratio	.411	

Phugoid

Undamped Natural Frequency	.1172	rad/sec
Damped Natural Frequency	.1141	rad/sec
Damping Ratio	.232	

TD 1646 L-R3

SST LATERAL - DIRECTIONAL CHARACTERISTICS

Flight Condition	NASA-20	NASA-6	NASA-72	
Ve	135	135	182	KTs
Weight	280,000	280,000	270,000	lbs
C. G. Location	46	35	46	% Mac
Side Force Derivatives				
C_{y_β}	-.573	-.5272	-.4928	/rad
$C_{y_{\dot\phi}}$	.0253	.0487	.0346	/rad/sec
$C_{y_{\dot\psi}}$	.093	.146	.0692	/rad/sec
$C_{y_{\delta R}}$	.1146	.1146	.1146	/rad
$C_{y_{\delta wh}}$	0.	0.	0.	/rad
Rolling Moment Derivatives				
C_{l_β}	-.1547	-.0825	-.1891	/rad
$C_{l_{\dot\phi}}$	-.2269	-.0438	-.0249	/rad/sec
$C_{l_{\dot\psi}}$	.0744	.073	.0208	/rad/sec
$C_{l_{\delta R}}$	0.	.0172	0.	
$C_{l_{\delta wh}}$	.1146	.0573	.0086	/rad
I_{X_B}	2.86×10^6	2.222×10^6	1.667×10^6	Slug-Ft^2

	NASA-20	NASA-Δ	NASA-72	
Yawing Moment Derivatives				
Cn_{β}	.2006	.131	.1604	/rad
$Cn_{\dot{\phi}}$	-.0223	-.0049	-.0067	/rad/sec
$Cn_{\dot{\psi}}$	-.0874	-.102	-.0554	/rad/sec
$Cn_{\delta R}$	-.086	-.0745	-.086	/rad
$Cn_{\delta wH}$	.0424	.0229	.002	/rad
I_{ZB}	$20x10^6$	$20x10^6$	$20x10^6$	Slug-Ft^2
J_{XZ_B}	0.	0.	0.	Slug-Ft^2
Lateral-Directional Dynamic Characteristics				
Spiral Divergence Time constant	349	74.9	-17.7 (convergent)	sec
Roll convergence Time Constant	.48	.802	1.7	sec
Dutch Roll				
Undamped natural frequency	.628	.811	1.24	rad/sec
Damped natural frequency	.618	.750	1.22	rad/sec
Damping Ratio	.186	.381	.169	

Modified NASA 72 Configuration

(Corrected to match flight data)

$F_{s/g}$ = 66 lbs

$\frac{\partial T/w}{\partial V}$ = .00116 / ft/sec

Short Period

ω_n = 1.232 rad/sec

ζ = .411

Phugoid

ω_n = .1172 rad/sec

ζ = .232

LATERAL TEST CONFIGURATIONS

Airplane	Configuration	Spiral Divergence τ ~ sec	Roll Convergence τ ~ sec	Dutch Roll ω_n rad/sec	ζ
NASA 20	Basic	349	.48	.628	.186
NASA 20A	$\dot{\beta}$ Damper, Pitch rate + Alpha Aug.	345	.478	.621	.282
NASA 20B	Deteriorated Lateral $N_{\dot{\phi}}$ = -.1, Pitch Rate + Alpha Aug.	397	.492	.642	.051
NASA 20B	Deteriorated Lateral Basic Longitudinal	397	.492	.692	.051
NASA Δ	Basic	74.9	.802	.811	.381
NASA Δ	Roll Damper Pitch Rate + Alpha Aug.	109.2	.573	.829	.379
NASA Δ	Deteriorated Lateral $N_{\dot{\phi}}$ = -.1 Pitch Rate + Alpha Aug.	99.6	.885	.982	.05
NASA 72	Basic	-17.6	1.7	1.24	.172

THEORETICAL CALCULATIONS
SPEED STABILITY EQUATIONS
ELEVATOR/VELOCITY
COLUMN/VELOCITY
STICK FORCE VELOCITY

DERIVATION OF EQUATIONS:

1.
$$C_L = C_{L_o} + C_{L_\alpha}\Delta\alpha + C_{L_{\delta E}}\delta E$$

2. Differentiating:
$$\frac{dC_L}{dV} = C_{L_\alpha}\frac{d\alpha}{dV} + C_{L_{\delta E}}\frac{d\delta E}{dV}$$

3. Rearranging Terms:
$$\frac{d\alpha}{dV} = \frac{-C_{L_{\delta E}}\frac{d\delta E}{dV} + \frac{dC_L}{dV}}{C_{L_\alpha}}$$

4. For Steady-State Pitching Moment (where $\dot{\theta}$ and $\dot{\alpha} = 0$):
$$C_m = C_{m_o} + C_{m_\alpha}\Delta\alpha + C_{m_V}\Delta V + C_{m_{\delta E}}\delta E$$

5. Differentiating:
$$\frac{dC_m}{dV} = C_{m_\alpha}\frac{d\alpha}{dV} + C_{m_V} + C_{m_{\delta E}}\frac{d\delta E}{dV}$$

6. Substituting Equation 3 into Equation 5 for $\frac{d\alpha}{dV}$:
$$\frac{C_{m_\alpha}}{C_{L_\alpha}}\left[-C_{L_{\delta E}}\frac{d\delta E}{dV} + \frac{dC_L}{dV}\right] + C_{m_{\delta E}}\frac{d\delta E}{dV} = 0$$

7. Rearranging Terms:
$$\frac{d\delta E}{dV} = \frac{-C_{m_\alpha}\frac{dC_L}{dV}}{C_{m_{\delta E}}C_{L_\alpha} - C_{m_\alpha}C_{L_{\delta E}}}$$

8. Now the lift equation is
$$L = \frac{\rho}{2}V^2 S C_L$$

9. Differentiating:
$$0 = \frac{\rho}{2}S\left(C_L 2V\,dV + V^2\,dC_L\right)$$

10. **Rearranging Terms:**

$$\frac{dC_L}{dV} = -\frac{2VC_L}{V^2} = -\frac{2C_L}{V}$$

11. **Rearranging and Substituting Equation 10 into Equation 7:**

$$\frac{d\delta E}{dV} = \frac{\frac{2C_L}{V} C_{m_\alpha}}{C_{m_{\delta E}} C_{L_\alpha} - C_{m_\alpha} C_{L_{\delta E}}}$$

Therefore:

$$\frac{\Delta \delta E}{\Delta V} = \frac{\frac{2C_L}{V} C_{m_\alpha}}{C_{m_{\delta E}} C_{L_\alpha} - C_{m_\alpha} C_{L_{\delta E}}}$$

$$\frac{\Delta \delta_{COL}}{\Delta V} = \frac{\Delta \delta E}{\Delta V} \times \frac{\delta_{COL}}{\delta E}$$

$$\frac{\Delta F_s}{\Delta V} = \frac{\Delta \delta_{COL}}{\Delta V} \times \frac{F_s}{\delta_{COL}}$$

For configurations with longitudinal augmentation, the value of $\frac{\Delta \delta E}{\Delta V}$ does not change. The pilot has an additional elevator input to equal to $-\frac{\delta E}{\Delta \alpha} \Delta \alpha$. The equivalent pilot elevator input is:

$$\frac{\Delta \delta E'}{\Delta V} = \left.\frac{\Delta \delta E}{\Delta V}\right]_{UNAUGMENTED} - \frac{\delta E}{\Delta \alpha} \cdot \frac{\Delta \alpha}{\Delta V}$$

$$= \frac{\frac{2C_L}{V} C_{m_\alpha}}{C_{m_{\delta E}} C_{L_\alpha} - C_{m_\alpha} C_{L_{\delta E}}} \left(1 + \frac{\delta E}{\Delta \alpha} \cdot \frac{C_{L_{\delta E}}}{C_{L_\alpha}}\right) + \frac{\delta E}{\Delta \alpha} \cdot \frac{\frac{2C_L}{V}}{C_{L_\alpha}}$$

THEORETICAL CALCULATIONS
WIND-UP TURN CHARACTERISTICS

ELEVATOR PER NORMAL ACCELERATION:

From Dynamics of Flight by Etkin (Page 301 - Equation 9.8, 6),

The Elevator Angle in the Turn, $\Delta \delta E$, is Given As

$$\Delta \delta E = (n-1) C_{L_0} \frac{C_{m_\alpha} + \frac{n+1}{2n} C_{L_\alpha} C_{m_{\dot{\theta}}}}{C_{L_{\delta E}} C_{m_\alpha} - C_{L_\alpha} C_{m_{\delta E}}}$$

Wind-up Turn

This was calculated by a digital computer

$$\frac{\delta_{COL}}{\Delta n} = \frac{\Delta \delta E}{\Delta n} \cdot \frac{\delta_{COL}}{\delta E}$$

$$\frac{\Delta F_s}{\Delta n} = \frac{\delta_{COL}}{\Delta n} \cdot \frac{F_s}{\delta_{COL}}$$

for configurations with longitudinal augmentation, the value of $\frac{\Delta \delta E}{\Delta n}$ does not change. For these configurations, an equivalent value of pilot elevator input, $\frac{\Delta \delta E'}{\Delta n}$, was calulated to obtain $\frac{\delta_{COL}}{\Delta n}$ and $\frac{\Delta F_s}{\Delta n}$

THEORETICAL CALCULATIONS

PULL-UP CHARACTERISTICS

ELEVATOR PER NORMAL ACCELERATION:

From Dynamics of Flight by Etkin (Page 56 - Equation 3.1, 7)

The Elevator Angle per "g" in a Steady Pull-up is Given as:

$$\frac{\Delta \delta E}{n-1} = \frac{\Delta \delta E}{\Delta n} = \frac{C_{L_0} C_{m_\alpha} + \frac{g}{V} C_{m_{\dot\theta}} C_{L_\alpha}}{C_{L_{\delta E}} C_{m_\alpha} - C_{L_\alpha} C_{m_{\delta E}}}$$

Pull-up

For configurations with longitudinal stability augmentation, an equivalent value of pilot elevator input is used:

$$\frac{\Delta \delta E'}{\Delta n} = \left.\frac{\Delta \delta E}{\Delta n}\right]_{UNAUGMENTED} - \frac{\delta E}{\Delta \alpha} \cdot \frac{\Delta \alpha}{\Delta n} - \frac{\delta E}{\dot\theta} \cdot \frac{\dot\theta}{\Delta n}$$

$$= \left.\frac{\Delta \delta E}{\Delta n}\right]_{UNAUGMENTED} - \frac{\delta E}{\Delta \alpha} \frac{\left(1 - \frac{C_{L_{\delta E}}}{C_{L_0}} \frac{\Delta \delta E}{\Delta n}\right)}{\frac{C_{L_\alpha}}{C_{L_0}}} - \frac{\delta E}{\dot\theta} \frac{g}{V}$$

COLUMN AND STICK FORCE PER NORMAL ACCELERATION:

Using the Above Equation for $\frac{\Delta \delta E}{\Delta n}$, the Column and Stick Force per "g" in a Steady Pull-up is

$$\frac{\Delta \delta_{COL}}{\Delta n} = \frac{\Delta \delta E}{\Delta n} \cdot \frac{\delta_{COL}}{\delta E}$$ Column

$$\frac{\Delta F_s}{\Delta n} = \frac{\Delta \delta_{COL}}{\Delta n} \cdot \frac{F_s}{\delta_{COL}}$$ Stick-Force

THEORETICAL CALCULATIONS
NORMAL ACCELERATION PER ANGLE OF ATTACK

The Normal Acceleration per Angle of Attack, n_z/α , is Usually Given as

$$\frac{n_z}{\alpha} = \frac{C_{L_\alpha}}{C_{L_o}} \quad \text{WHERE } C_{L_o} = C_{L_{TRIM}}$$

However, this Equation Neglects Lift Due to Elevator Deflection, Which can be Substantial at Times. To Compensate For the Elevator Lift, the C_{L_α} Term in the Above Equation May be Replaced by an Effective C_{L_α} Which Varies with Elevator Deflection.

$$C_{L_{\alpha_{EFF}}} = C_{L_\alpha} + \frac{\delta_E}{\Delta\alpha} C_{L_{\delta_E}} = C_{L_\alpha} + \frac{\delta_E}{n_z} \frac{n_z}{\alpha} C_{L_{\delta_E}}$$

Using this Term for C_{L_α} in the Top Equation Results in

$$\frac{n_z}{\alpha} = \frac{C_{L_{\alpha_{EFF}}}}{C_{L_o}} = \frac{C_{L_\alpha} + \frac{\delta_E}{n_z} \frac{n_z}{\alpha} C_{L_{\delta_E}}}{C_{L_o}}$$

Rearranging Terms:

$$\frac{n_z}{\alpha} = \frac{C_{L_\alpha}/C_{L_o}}{1 - \frac{\delta_E}{n_z} \frac{C_{L_{\delta_E}}}{C_{L_o}}} \quad \text{AT CONSTANT SPEED}$$

NOTE: n_z/α Will Vary for a Steady Pull-up and a Wind-up Turn Since it Includes the δ_E/n Term.

THEORETICAL CALCULATED VALUES FOR SPEED STABILITY DATA

CONFIGURATION	$\delta E/\delta_{COL}$	V_e	$\Delta\delta E/\Delta V$	$\Delta\delta_{COL}/\Delta V$	$\Delta F_s/\Delta V$
Basic NASA 20	-1.3	125	.119	-.092	-.364
		135	.110	-.085	-.340
		145	.103	-.079	-.317
NASA 20 + $\dot{\theta}$	-2.6	125	.119	-.046	-.184
		135	.110	-.043	-.170
		145	.103	-.040	-.159
NASA 20A + $(\dot{\theta} + \Delta\alpha)$	-5.2	125	.385*	-.074	-.296
		135	.372*	-.072	-.288
		145	.348*	-.067	-.268
NASA 20 AT AFT C.G.	-1.3	125	.035	-.027	-.108
		135	.032	-.025	-.100
		145	.030	-.023	-.093
NASA 20A + $(\dot{\theta} + \Delta\alpha)$ AT AFT C.G.	-5.2	125	.306*	-.059	-.246
		135	.282*	-.054	-.216
		145	.263*	-.051	-.204
	UNITS	KNOTS	DEG/KNOT	DEG/KNOT	LB/KNOT

STICK FORCE PER UNIT COLUMN DEFLECTION = 4 LBS/DEG. ON ALL ABOVE CONFIGS.

* Equivalent Pilot Elevator Input

THEORETICAL CALCULATED VALUES FOR SPEED STABILITY DATA

CONFIGURATION	$\delta E/\delta_{COL}$	V_e	$\Delta\delta E/\Delta V$	$\Delta\delta_{COL}/\Delta V$	$\Delta F_s/\Delta V$
BASIC NASA Δ	-1.0	125 135 145	.045 .042 .039	-.045 -.042 -.039	-.182 -.168 -.157
NASA ΔA + $(\dot{\theta}+\Delta\alpha)$	-4.0	125 135 145	.210* .194* .186*	*.053 -.049 -.046	-.212 -.196 -.184
NASA Δ AT FORWARD C.G.	-1.0	125 135 145	.155 .143 .133	-.155 -.143 -.133	-.618 -.572 -.532
NASA 72	-1.3	135 150 165	.062 .056 .051	-.048 -.043 -.039	-.333 -.299 -.272
	UNITS	KNOTS	DEG/KNOT	DEG/KNOT	LB/KNOT

STICK FORCE PER UNIT COLUMN DEFLECTION:

F_s/δ_{COL} = 4 LB/DEG FOR ALL NASA Δ CONFIGURATIONS

F_s/δ_{COL} = 7 LB/DEG FOR NASA 72 CONFIGURATION

* Equivalent Pilot Elevator Input

THEORETICAL CALCULATED VALUES FOR WIND-UP TURN MANEUVER

CONFIGURATION	$\delta E/\delta_{col}$	n_z	δE	δ_{col}	F_s	$\Delta\alpha$
BASIC NASA 20	-1.3	1.1	-1.25	.96	6.84	1.23
		1.2	-2.47	1.90	10.60	2.46
		1.3	-3.65	2.81	14.23	3.69
		1.4	-4.81	3.70	17.80	4.92
		1.5	-5.95	4.58	21.33	6.14
NASA 20 + $\dot{\theta}$	-2.6	1.1	-3.50*	1.35	8.4	1.23
		1.2	-6.79*	2.61	13.44	2.46
		1.3	-9.91*	3.81	18.25	3.69
		1.4	-12.90*	4.96	22.85	4.42
		1.5	-15.78*	6.06	27.25	6.14
NASA 20A + ($\dot{\theta} + \Delta\alpha$)	-5.2	1.1	-5.36*	1.03	7.12	1.23
		1.2	-10.49*	2.02	11.08	2.46
		1.3	-15.45*	2.97	14.88	3.69
		1.4	-20.27*	3.90	18.60	4.92
		1.5	-24.99	4.80	22.20	6.14
NASA 20 AT AFT C.G.	-1.3	1.1	-.69	.53	5.12	1.18
		1.2	-1.35	1.04	7.16	2.35
		1.3	-1.98	1.52	9.08	3.52
		1.4	-2.58	1.98	10.92	4.69
		1.5	-3.17	2.44	12.75	5.85
NASA 20A + ($\dot{\theta} + \Delta\alpha$) AT AFT C.G.	-5.2	1.1	-4.71*	.91	6.64	1.18
		1.2	-9.20*	1.77	10.08	2.35
		1.3	-13.52*	2.60	13.40	3.52
		1.4	-17.70*	3.40	16.60	4.69
		1.5	-21.78*	4.18	19.70	5.85
	UNITS	"g"	DEG	DEG	LBS	DEG

* Equivalent Pilot Elevator Input

STICK FORCE PER UNIT COLUMN DEFLECTION F_S/δ_{col} = 4 LB/DEG

STICK BREAK-OUT FORCE = 3 LBS.

THEORETICAL CALCULATED VALUES
FOR WIND-UP TURN MANEUVER

CONFIGURATION	$\delta E/\delta col$	n_z	δE	δcol	F_s	$\Delta\alpha$
BASIC NASA Δ	-1.0	1.1	-1.31	1.31	8.25	1.32
		1.2	-2.54	2.54	13.15	2.61
		1.3	-3.71	3.71	17.85	3.89
		1.4	-4.83	4.83	22.30	5.16
		1.5	-5.92	5.92	26.65	6.42
NASA Δ A + $(\dot{\theta}+\Delta\alpha)$	-4.0	1.1	-9.38*	1.22	7.38	1.32
		1.2	-9.48*	2.37	12.48	2.61
		1.3	-13.87*	3.46	16.87	3.89
		1.4	-18.08*	4.52	21.03	5.16
		1.5	-22.17*	5.53	25.17	6.42
NASA AT FORWARD C.G.	-1.0	1.1	-2.16	2.16	11.65	1.52
		1.2	-4.23	4.23	19.92	3.02
		1.3	-6.22	6.22	27.88	4.51
		1.4	-8.16	8.16	35.65	5.98
		1.5	-10.16	10.06	43.20	7.44
NASA 72	-1.3	1.1	-.72	.55	6.85	.97
		1.2	-1.42	1.09	10.63	1.93
		1.3	-2.10	1.62	13.13	2.89
		1.4	-2.76	2.12	17.32	3.85
		1.5	-3.42	2.63	21.40	4.81
	UNITS	"g"	DEG	DEG	LBS	DEG

STICK FORCE PER UNIT COLUMN DEFLECTION:

F_S/δ_{col} = 4 LB/DEG FOR ALL NASA Δ CONFIGURATIONS

F_S/δ_{col} = 7 LB/DEG FOR NASA 72

Column Break-Out Force = 3 LBS.

* Equivalent Pilot Elevator Input

MODIFIED NASA 72 CONFIGURATION

(Corrected to match flight data)

Speed Stability

$\delta E/\delta_{COL}$	V_e	$\Delta\delta E/\Delta V$	$\Delta\delta_{COL}/\Delta V$	$\Delta F_s/\Delta V$	
-1.3	177 182 137	.0501 .0487 .0474	.0385 .0375 .0365	.2695 .2625 .2558	
Units	Knots	Deg/Knot	Deg/Knot	Lb/Knot	

Wind-up Turn

$\delta E/\delta_{COL}$	n_z	δE	δ_{COL}	F_s	$\Delta\alpha$
-1.3	1.1 1.2 1.3 1.4 1.5	-1.37 -2.72 -4.04 -5.36 -6.66	1.06 2.09 3.11 4.12 5.12	11.92 19.12 26.30 33.32 40.3	1.28 2.55 3.82 5.09 6.35
Units	"g"	Deg	Deg	Lbs.	Deg

Steady Pull-up Maneuver

$\delta E/\delta_{COL}$	F_s/δ_{COL}	$\Delta\delta E/\Delta n$	$\Delta\delta_{COL}/\Delta n$	$\Delta F_s/\Delta n$	$n_{z\alpha}$
-1.3	7.0	-12.23	9.42	66	.1014
Units	Lb/Deg	Deg/g	Deg/g	Lb./g	g/Deg

THEORETICAL CALCULATIONS - STEADY SIDESLIP

Derivation of Equations:

Four degrees of freedom are used for analysis - only static terms are considered

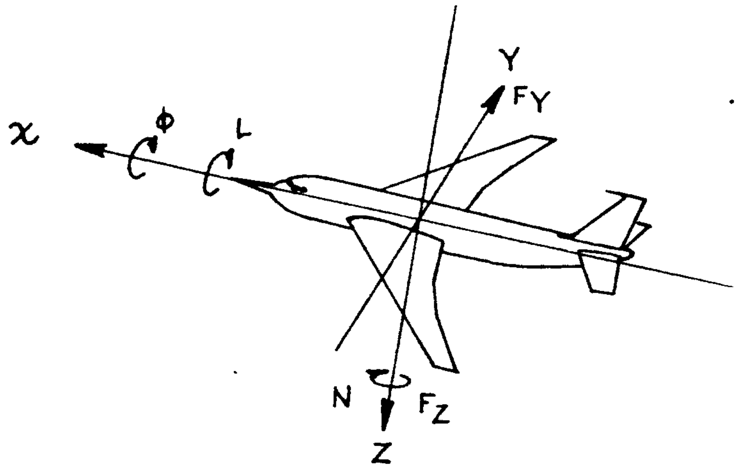

1. Yawing moment

$$\Sigma N = 0 = Cn_{\beta}\beta + Cn_{\delta R}\,\delta R + Cn_{\delta WH}\,\delta WH$$

2. Lift

$$\Sigma F_Z = 0 = \text{LIFT} - W \cos\phi$$

3. Side Force

$$\Sigma F_Y = 0 = C_{Y_\beta}\beta + C_{Y_{\delta R}}\,\delta R + \frac{W}{qS}\sin\phi$$

4. Rolling moment

$$\Sigma L = 0 = C_{\ell_\beta}\beta + C_{\ell_{\delta WH}}\,\delta WH + C_{\ell_{\delta R}}\,\delta R$$

Calculation of rudder and wheel required:

From 1 and 4,

$$C_{n_{\delta R}}\,\delta R + C_{n_{\delta WH}}\,\delta WH = -C_{n_\beta}\,\beta$$

$$C_{\ell_{\delta R}}\,\delta R + C_{\ell_{\delta WH}}\,\delta WH = -C_{\ell_\beta}\,\beta$$

$$\frac{\delta R}{\beta} = \frac{-C_{n_\beta} C_{\ell_{\delta WH}} + C_{\ell_\beta} C_{n_{\delta WH}}}{C_{n_{\delta R}} C_{\ell_{\delta WH}} - C_{n_{\delta WH}} C_{\ell_{\delta R}}}$$

$$\frac{\delta WH}{\beta} \quad \frac{-C_{n_{\delta R}} C_{\ell_\beta} + C_{n_\beta} C_{\ell_{\delta R}}}{C_{n_{\delta R}} C_{\ell_{\delta WH}} - C_{n_{\delta WH}} C_{\ell_{\delta R}}}$$

Calculation of bank angle:

From 3,

$$\frac{W}{qS} = C_{L_{1g}} \qquad \sin\phi \approx \phi$$

$$C_{Y_\beta}\,\beta + C_{Y_{\delta R}}\,\delta R + C_{L_{1g}}\,\phi = 0$$

$$\phi = -\frac{1}{C_{L_{1g}}}\left[C_{Y_\beta}\,\beta + C_{Y_{\delta R}}\,\delta R\right]$$

$$\left.\frac{\phi}{\beta}\right]_{CALC} = -\frac{1}{C_{L_{1g}}}\left[C_{Y_\beta} + C_{Y_{\delta R}} \cdot \frac{\delta R}{\beta}\right]$$

THEORETICAL CALCULATIONS - ROLL RATE

Rolling moment equation:

$$\frac{I_x}{qSb}\ddot{\phi} = C_{l_{\delta WH}}\delta WH + C_{l_\beta}\beta + C_{l_{\delta R}}\delta R + \frac{J_{xz}}{qSb}\ddot{\psi} + C_{l_{\dot{\phi}}}\dot{\phi} + C_{l_{\dot{\psi}}}\dot{\psi}$$

For steady state roll rate, $\ddot{\phi} = 0$

$$\dot{\phi}_{SS} = -\frac{1}{C_{l_{\dot{\phi}}}}\left[C_{l_{\delta WH}}\delta WH + C_{l_\beta}\beta + C_{l_{\delta R}}\delta R + C_{l_{\dot{\psi}}}\dot{\psi} + \frac{J_{xz}}{qSb}\ddot{\psi}\right]$$

The theoretical value of $\dot{\phi}_{SS}$ was calculated by an IBM program which computes the airplane response to a step wheel input in three-degrees-of-freedom.

On the NASA Δ and NASA 72 configurations, it was difficult to measure the steady-state roll rate correctly because of the high inertia cross-product term. On these configurations, a one-degree-of freedom roll rate was used. This was calculated from the roll and yaw equations, assuming that $\dot{\psi}$ and β are 0:

$$C_{l_{\dot{\phi}}}\dot{\phi} + \frac{J_{xz}}{qSb}\ddot{\psi} = -C_{l_{\delta WH}}\delta WH$$

$$C_{n_{\dot{\phi}}}\dot{\phi} - \frac{I_z}{qSb}\ddot{\psi} = -C_{n_{\delta WH}}\delta WH$$

$$\left.\frac{\dot{\phi}}{\delta WH}\right]_{\substack{1\ DEG\\CALC}} = \frac{C_{l_{\delta WH}}\frac{I_z}{qSb} + C_{n_{\delta WH}}\frac{J_{xz}}{qSb}}{-C_{l_{\dot{\phi}}}\frac{I_z}{qSb} - C_{n_{\dot{\phi}}}\cdot\frac{J_{xz}}{qSb}}$$

$$\boxed{\left.\frac{\dot{\phi}}{\delta WH}\right]_{\substack{1\ DEG\\CALC}} = -\frac{C_{l_{WH}} + C_{n_{\delta WH}}\frac{J_{xz}}{I_z}}{+C_{l_{\dot{\phi}}} + C_{n_{\dot{\phi}}}\frac{J_{xz}}{I_z}}}$$

In reducting the data, $\dot{\phi}$ was measured at a point where $\dot{\psi}$ was zero and the measured value of $\dot{\phi}$ was corrected for the measured sideslip:

$$\dot{\phi}_{\substack{FLIGHT\\TEST}} = \dot{\phi}_{MEAS} + \frac{C_{\ell_\beta} + \frac{J_{xz}}{I_z} C_{n_\beta}}{C_{\ell_{\dot{\phi}}} + \frac{J_{xz}}{I_z} C_{n_{\dot{\phi}}}} \cdot \beta$$

THEORETICAL CALCULATIONS - ROLL ACCELERATION

The roll reversal data was measured at a point where $\dot{\phi}, \dot{\psi}, \beta = 0$.

The roll and yaw equations become:

$$-\frac{I_x}{qSb}\ddot{\phi} + \frac{J_{xz}}{qSb}\ddot{\psi} = -C_{\ell_{\delta WH}}\delta_{WH}$$

$$\frac{J_{xz}}{qSb}\ddot{\phi} - \frac{I_z}{qSb}\ddot{\psi} = -C_{n_{\delta WH}}\delta_{WH}$$

$$\left.\frac{\ddot{\phi}}{\delta_{WH}}\right]_{CALC} = \frac{C_{\ell_{\delta WH}}\frac{I_z}{qSb} + C_{n_{\delta WH}}\frac{J_{xz}}{qSb}}{\frac{I_x I_z}{(qSb)^2} - \frac{J_{xz}^2}{(qSb)^2}}$$

$$\boxed{\left.\frac{\ddot{\phi}}{\delta_{WH}}\right]_{CALC} = \frac{C_{\ell_{\delta WH}} + C_{n_{\delta WH}}\frac{J_{xz}}{I_z}}{\frac{I_x}{qSb} - \frac{J_{xz}^2}{qSb}}}$$

If the maneuver was not performed correctly, the measured value of $\ddot{\phi}$ was corrected:

$$\ddot{\phi}_{\substack{FLIGHT\\TEST}} = \ddot{\phi}_{MEAS} - \frac{\left(C_{\ell_\beta} + \frac{J_{xz}}{I_z}C_{n_\beta}\right)\beta + \left(C_{\ell_{\dot{\psi}}} + \frac{J_{xz}}{I_z}C_{n_{\dot{\psi}}}\right)\dot{\psi}}{\frac{I_x}{qSb} - \frac{J_{xz}^2}{qSb}}$$

THEORETICAL LATERAL-DIRECTIONAL CHARACTERISTICS

CONFIGURATION	ϕ/β	$\delta P/\beta$ in/deg	δ_{WH}/β	$\dot{\phi}/\delta_{WH}$	$\ddot{\phi}/\delta_{WH}$
NASA 20	.343	-0.309	1.35	.439/sec	1.054/sec^{2}*
NASA 20A	↓	↓	↓	0.444/sec	↓
NASA 20B	↓	↓	↓	0.385/sec	↓
NASA △	.602	-0.209	.837	1.23/sec*	1.26/sec^{2}*
NASA △ A	↓	↓	↓	.795/sec*	↓
NASA △ B	↓	↓	↓	1.43 /sec*	↓
NASA 72	0.619	-0.228	14.66	0.530/sec*	0.343/sec^{2}

* $\dfrac{\dot{\phi}}{\delta_{WH}}$ corrected to 1 D value